CAPITAL UNIVERSITY OF SCIENCE AND
TECHNOLOGY, ISLAMABAD

The Impact of Cattaneo-Christov Double Diffusion and Energy Activation on a Flow of Casson Fluid over a Stretching Surface

by

Zameen Akhter

A thesis submitted in partial fulfillment for the
degree of Master of Philosophy

in the

Faculty of Computing
Department of Mathematics

2024

*I dedicate my dissertation work to my **family** and dignified **teachers**. A special feeling of gratitude to my loving parents who have supported me in my studies.*

CERTIFICATE OF APPROVAL

The Impact of Cattaneo-Christov Double Diffusion and Energy Activation on a Flow of Casson Fluid over a Stretching Surface

by

Zameen Akhter

(MMT203020)

THESIS EXAMINING COMMITTEE

(a)	External Examiner	Dr. Taimoor Salahuddin	MUST, Mirpur
(b)	Internal Examiner	Dr. Muhammad Sabeel Khan	CUST, Islamabad
(c)	Supervisor	Dr. Muhammad Sagheer	CUST, Islamabad

Dr. Muhammad Sagheer
Thesis Supervisor
August 2024

Dr. Muhammad Sagheer
Head
Department of Mathematics
August, 2024

Dr. M. Abdul Qadir
Dean
Faculty of Computing
August, 2024

Author's Declaration

I, **Zameen Akhter**, hereby state that my MPhil thesis titled "**The Impact of Cattaneo-Christov Double Diffusion and Energy Activation on a Flow of Casson Fluid over a Stretching Surface**" is my own work and has not been submitted previously by me for taking any degree from Capital University of Science and Technology, Islamabad or anywhere else in the country/abroad.

At any time if my statement is found to be incorrect even after my graduation, the University has the right to withdraw my MPhil Degree.

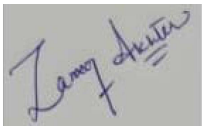

(Zameen Akhter)

Registration No: MMT203020

Plagiarism Undertaking

I solemnly declare that research work presented in this thesis titled "**The Impact of Cattaneo-Christov Double Diffusion and Energy Activation on a Flow of Casson Fluid over a Stretching Surface**" is solely my research work with no significant contribution from any other person. Small contribution/help wherever taken has been dully acknowledged and that complete thesis has been written by me.

I understand the zero tolerance policy of the HEC and Capital University of Science and Technology towards plagiarism. Therefore, I as an author of the above titled thesis declare that no portion of my thesis has been plagiarized and any material used as reference is properly referred/cited.

I undertake that if I am found guilty of any formal plagiarism in the above titled thesis even after award of MPhil Degree, the University reserves the right to withdraw my MPhil degree and that HEC and the University have the right to publish my name on the HEC/University website on which names of students are placed who submitted plagiarized work.

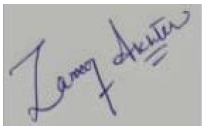

(Zameen Akhter)

Registration No: MMT203020

Acknowledgement

I got no words to articulate my cordial sense of gratitude to **Almighty Allah** who is the most merciful and most beneficent to his creation.

I also express my gratitude to the last prophet of **Almighty Allah, Prophet Muhammad (PBUH)** the supreme reformer of the world and knowledge for human being.

I am grateful to my parents, **Muhammad Irshad** and **Shaheen Akhter**, whose love and sacrifices have been the foundation of all my achievements. My heartfelt thanks go to my brothers (**Muhammad Bilal**, **Attiq-ur-Rehman**, **Faizan Ali**) and sister-in-laws for their unwavering support and encouragement. A special acknowledgment to my brother **Khaleeq ur Rehman** for his wise counsel and steadfast belief in my abilities.

I would like to be grateful to my thesis supervisor **Dr. Muhammad Sagheer**, the Head of the Department of Mathematics, for guiding and encouraging towards writing this thesis. It would have remained incomplete without his endeavours. Due to his efforts I was able to write and complete this dissertation.

Last but not the least, I am deeply thankful to my best friends, **Shamas un Nisa** and **Mehreen Fatima**, whose friendship have been a source of constant strength and joy throughout this journey. I would also like to extend my heartfelt gratitude to my fellow companions, **Abdul Rehman**, **Hajra Batool**, and **Muhammad Samiullah**, for their invaluable support.

(Zameen Akhter)

Registration No: MMT203020

Abstract

The theoretical investigation of Cattaneo-Christov double diffusion model and energy activation on Casson fluid flow over a stretching sheet has been carried out through the utilization of the shooting method. The primary objective of the current research is to comprehensively analyze the influence of Arrhenius energy activation, while incorporating the Cattaneo-Christov double diffusion model. Additionally, this study takes into account factors such as thermophoresis effects, Brownian diffusion, velocity slip, and chemical reaction, in the context of a Casson fluid flowing over an extensible sheet. The similarity transformations have been employed to convert the nonlinear partial differential equations into a set of ordinary differential equations. Tables and graphs vividly illustrate the impact of various parameters, including the magnetic field parameter, Casson fluid parameter, Prandtl number, thermophoresis parameter, Brownian motion parameter, and Eckert number. The findings indicate that as the chemical reaction parameter γ_1 increases, both the velocity and concentration profiles exhibit a decrement, while the temperature profile increases. As the Casson parameter β values increase, there is a downfall in the local Nusselt and Sherwood numbers, and a simultaneous increase in the skin friction.

Contents

List of Figures

List of Tables

Abbreviations

EMF	Electromotive force
IVPs	Initial value problems
MHD	Magnetohydrodynamics
ODEs	Ordineary differential equations
PDEs	Partial differential equations
RK	Runge-Kutta
UCM	Upper-converted Maxwell

Symbols

Ω	Angular velocity
T_∞	Ambient temperature of the nanofluid
C_∞	Ambient concentration of the nanofluid
k^*	Absorption coefficient
Nb	Brownian motion parameter
D_B	Brownian diffusion coefficient
C_w	Concentration of the wall
K_c	Chemical reaction parameter
C	Concentration
ρ_f	Density of the fluid
f	Dimensionless velocity
θ	Dimensionless temperature
ϕ	Dimensionless concentration
ρ	Density
ρ_{nf}	Density of the nanofluid
ρ_f	Density of the pure fluid
σ	Electrical conductivity
Ec	Eckert number
σ_f	Electrical conductivity of the fluid
q	Heat generation constant
$(\rho C_p)_f$	Heat capacitance of fluid
ν	Kinematic viscosity
ν_f	Kinematic viscosity of the base fluid
Nu_x	Local Nusselt number
Sh_x	Local Sherwood number

Re_x	Local Reynolds number
B_0	Magnetic field constant
M	Magnetic parameter
Nu	Nusselt number
Pr	Prandtl number
Re	Reynolds number
q_r	Radiative heat flux
K_c^*	Rate of chemical reaction
Γ_c	Relaxation time for mass flux
Γ_e	Relaxation time for heat flux
γ_1	Rotation parameter
λ_C	Relaxation time parameter of concentration
λ_E	Relaxation time parameter of temperature
Sc	Schmidt number
Sh	Sherwood number
σ^*	Stefan Boltzmann constant
ψ	Stream function
τ	Stress tensor
θ	Stream function
ϕ	Stream function
η	Similarity variable
C_{fx}	Skin friction coefficient along x direction
C_{fy}	Skin friction coefficient along y direction
a	Stretching constant
T_w	Temperature of the wall
T	Temperature
Nt	Thermophoresis parameter
k	Thermal conductivity
α	Thermal diffisuitivity
α_f	Thermal diffusivity
κ_f	Thermal conductivity of the fluid
D_T	Thermophortic diffusion coefficient
μ	Viscosity

μ_{nf}	Viscosity of the nanofluid
μ_f	Viscosity of the base fluid
μ_{nf}	Viscosity of the nanofluid
μ_f	Viscosity of the fluid
u	x-component of fluid velocity
v	y-component of fluid velocity

Chapter 1

Introduction

Fluids were early studied by Archimedes in ancient Greece era around $250BC$ and he established fluid buoyancy formulation known as Archimedes's principle. Fluid is basically a material or a substance that can flow or move. Fluids are further classified into two types which are Newtonian and non-Newtonian. A Newtonian fluid such as water has linear proportionality between its viscosity and the velocity gradient at the boundary surface. The non-Newtonian fluids such as honey, fruit juice, shampoo, paint, sanitizer, mud, and blood don't have the proportionality between viscosity and the velocity gradient at the boundary region. Casson fluid is one of the non- Newtonian fluids. Casson fluids which by nature are shear thining, were firstly presented by Casson in 1959.

Crane [1] initially studied the behavior of viscous and incompressible Newtonian fluids over a linearly stretching surface. He comprehended that the stretching velocity of the fluid is proportional to the distance from the slit. The manufacturing of plastic film is an example of this. Rajgopal [2] studied the two-dimensional flow of viscous and incompressible fluid over a moving sheet. Ishak et al. [3] examined the boundary layer of laminar magneto hydrodynamic, a viscous and incompressible fluid, over a moving wedge with effects of suction/injection parameters. Mukhopadhyay [4] observed the MHD viscous and incompressible fluid flow and discussed how transpiration and heat transfer occurred in the boundary layer over the stretching sheet. Belhocine et al. [5] investigated a two-dimensional laminar flow of viscous and incompressible Newtonian fluid at zero pressure gradients in the absence of body forces.

Siddapa and Abel [6] studied the visco-elastic fluid flow in the boundary layer region. This research used a similarity parameter method to obtained the solution of boundary layer equations of motion past a stetching plate. They found that the viscoelastic parameter has a significant impact on the flow velocity. Andersson [7] also investigated the magnetohydrodynamic (MHD) flow of a viscoelastic fluid over a stretching surface. He used the exact analytical solution to solve the non-linear boundary layer equation to show the effect of magnetic field on the fluid flow. Dandapat et al. [8] studied a viscoelastic fluid flow in the presence magnetic field through a stretching surface, by applying the free parameter and separation of variable methods. Mamaloukas et al. [9] found the exact solution of viscoelastic fluid flow of second grade in two dimensions over a stretching surface. Furthermore, Jalili et al. [10] explored the thermal dynamics of non-Newtonian vicoelastic fluid flow between rotating disks under MHD conditions and analyzed the effects of viscous parameter and magnetic field parameter on the velocity and temperature distributions using the Homotopy Perturbation method (HPM) and Akbari-Ganji's method (AGM).

Fang [11] observed the solution of the extented Blasius flow in the boundary layer using the variable transformation method. Batallar [12] studied the Newtonian fluid that had no electric conduction having different conditions; first, when the fluid was at rest over a moving plane and the second, when the fluid was at rest over a flat plane. The momentum equation is solved numerically by using 4th order Runge-Kutta shooting method to observe the static flat-plate (Blasius flow) and moving flate plate (Sakiadis flow). The analysis of the fractional boundary-layer Blasius flow using a finite difference method implemented on a quasi-uniform grid, is analyzed by Jannelli [13].

Motsa et al. [14] studied the effects of MHD and upper-convected Maxwell (UCM) on a fluid flow over a stretching sheet by using successive Taylor series linearization method (STSLM) to solve nonlinear boundary value problems. Motsa and Sibanda [15] also studied the boundary layer region of MHD flow over a non-linearly stretching sheet in the presence of magnetic field. They prefered to use spectral homotopy analysis method (SHAM) and the Matlab in-built numerical solver bvp4c to produce the soution of the flow model. Rosca [16] showed the study

of two-dimensional viscous, incompressible, and electrically conducted MHD fluid flow over a shrinking porous sheets using the function bvp4c. Nadeem et al. [17] examined the MHD fluid flow over a stretching sheet in the boundary region, and to solve nonlinear differential equations this research used the homotopy analysis method (HAM). To investigate the MHD flow and heat transfer over a stretching cylinder in the presence of uniform magnetic field, Mukhopadhyay [18] carried out a numerical analysis by applying the fourth order Runge–Kutta method. Akber et al. [19] studied the two-dimensional boundary layer flow of MHD incompressible Carreau fluid flow over a permeable sheet. The governing model was solved numerically by the shooting method to observe the stretching/shrinking parameter. Khidir [20] attempted to solve the Falker-Skan non-linear boundary layer problem related to MHD fluid by applying the successive linearization method and spectral homotopy perturbation method. Sharada and Shankar [21] studied the boundary layer of MHD fluid flow over a stretching sheet with the effects such as mixed convection, thermal radiation, Dufour, Soret, and chemical reaction. Biswas et al. [22] studied the unstable MHD fluid flow having radiation and reaction-induced vertical place within it. Ahmed et al. [23] recorded their observations regarding the MHD fluid flow over a moving and inclined plate that has variable thermal conductivity and free convection and radiation. Biswas and Ahmed [24] utilized Hall current and chemical reaction effects to study the boundary layer of unsteady MHD fluid. Noor [25] analyzed the two dimensional boundary layer flow of MHD fluid past a stretching sheet which was laminar, time independent and incompressible. The work included the analysis of impact of stretching sheet with Hall current, free convection, and thermophoresis effects by using the numerical solutions obtained through the homotopy analysis method. Raza et al. [26] studied the boundary layer region of MHD nano-Williamson fluid flow over a stretching sheet with an extended magnetic field with numerous slips. Raza et al. [27] also analyzed the boundary layer of MHD non-Newtonian fluid, over a non-linearly sheet. In this article, authors used two different methods; the shooting and 3-stage Lobatto III-A methods to examine the effects of a transverse magnetic field and slip effects on the Casson fluid flow.

Nadeem et al. [28] carried out a study of the Casson fluid on a significantly

shrinking surface. Lare [29] examined the effect of exponential heat generation on a Casson fluid over a stretching sheet along with thermal conductivity. Amlimohamadi et al. [30] studied the Casson fluid flow through a porous medium in two dimensional setting with the effect of Darcy-Forcheimer model. Vellanki et al. [31] examined the effects of radiation and chemical reaction on Casson fluid flow through a porous medium with effects of suction/injection parameters. An investigation of Ali et al. [32] illustrates the flow of the non-Newtonian Casson fluid experiencing pulsation within a channel featuring symmetrical constriction bumps on both upper and lower walls, where the fluid exhibits low electrical conductivity and experiences the influence of a uniform transverse magnetic field, allowing for the exploration of the ensuing Lorentz force effects. Without the influence of the magnetic field and thermal radiation, the impact of transpiration is investigated for a system composed of viscous, in-compressible, electrically conductive fluids along with a combination of Casson fluid, approaching a non-linearly stretched isothermal permeable sheet by Reddy et al. [33]. A comprehensive study has been carried out to examine the heat and mass transfer phenomena of a Casson fluid as it flows past a cylinder within a channel exhibiting wavy features by Majeed et al. [34]. Buzuzi [35] investigated the unsteady MHD Casson fluid flow over an inclined surface, incorporating the effects of a variable magnetic field, heat generation, and an effective Prandtl number.

Rubab and Mustafa [36] studied the Cattaneo-Christov heat flux modal for the magneto-hydrodynamics and UCM fluid in three-dimensional flow over a stretching sheet. Hayat et al. [37] numerically investigated the Cattaneo-Christov double diffusion with three-dimensional flow of Prandtl fluid over a stretching surface. The stagnation point flow behavior of an incompressible fluid over a stretching sheet in a porous medium, incorporating the effects of suction/injection and Cattaneo–Christov model is investigated by Upreti et al. [38].

Kala [39] studied the boundary layer region MHD fluid flow over a nonlinear stretching sheet in a non-Darcy medium and analyzed the effects of Grashof number, modified Grashof number, chemical reaction, suction, slip, and inclination parameters. In-depth evaluation of Kala [40] focused on the effect of magnetic field forcing the transverse direction and fluid with velocity slip flows through a

non-Darcy medium. He used the bvp4c solver to solve the boundary value problem.

1.1 Thesis Contributions

In this thesis, an in-depth evaluation of the flow of a Casson fluid on a strecthing surface has been carried out. The work of Kala et al. [40] has been extended by considering the effects of Cattaneo-Christov double diffusion, Brownian diffusion, thermophoretic effect, and energy activation, which have not been previously examined. The nonlinear partial differential equations (PDEs) have been transformed into a system of dimensionless ordinary differential equations (ODEs) using similarity transformations, and numerical solutions have been obtained through the shooting method. The numerical results have been computed using MATLAB. The effects of key parameters on the velocity distribution $f'(\eta)$, temperature distribution $\theta(\eta)$, concentration distribution $\phi(\eta)$, skin friction coefficient Cf_x, local Nusselt number Nu_x, and local Sherwood number Sh_x have been examined through graphical and tabular analyses.

1.2 Layout of Thesis

The following is the summary of the thesis contents:

Chapter 2 covers essential definitions which would be mandatory and dicussed afterward.
Chapter 3 presents a detailed review of Kala et al. [40].

Chapter 4 extends the proposed framework flow mentioned in Chapter 3 by including the Cattaneo-Christov double diffusion, Energy activaton, Brownian diffusion and thermophoretic effect. The shooting method is used to generate the numerical solutions of the governing flow model.

Chapter 5 summarizes the main findings and conclusions of the thesis.

All references cited in the thesis are listed in the **biblography**.

Chapter 2

Preliminaries

The present chapter outlines crucial definitions and governing laws, that will serve as a foundation in the forthcoming chapters.

2.1 Some Fundamental Terminologies

Definition 2.1.1 (Fluid)

"A fluid is a substance that deforms continuously under the application of a shear (tangential) stress no matter how small the shear stress may be." [41]

Definition 2.1.2 (Fluid Mechanics)

"Fluid mechanics is that branch of science which deals with the behavior of the fluid (liquids or gases) at rest as well as in motion." [42]

Definition 2.1.3 (Fluid Dynamics)

"The area of mathematics and physics that deals with describing and understanding how liquids and gases move." [42]

Definition 2.1.4 (Fluid Statics)

"The study of fluid at rest is called fluid statics." [42]

Definition 2.1.5 (Viscosity)

"Viscosity is defined as the property of a fluid which offers resistance to the movement of one layer of fluid over another adjacent layer of the fluid. Mathematically,

$$\mu = \frac{\tau}{\frac{\partial u}{\partial y}},$$

where μ is viscosity coefficient, τ is shear stress and $\frac{\partial u}{\partial y}$ represents the velocity gradient." [42]

Definition 2.1.6 (Kinematic Viscosity)

"It is defined as the ratio between the dynamic viscosity and density of fluid. It is denoted by symbol ν called **'nu'**. Mathematically,

$$\nu = \frac{\mu}{\rho}." \text{ [42]}$$

Definition 2.1.7 (Thermal Conductivity)

"The Fourier heat conduction law states that the heat flow is proportional to the temperature gradient. The coefficient of proportionality is a material parameter known as the thermal conductivity which may be a function of a number of variables." [43]

Definition 2.1.8 (Thermal Diffusivity)

"The rate at which heat diffuses by conducting through a material depends on the thermal diffusivity. It can be defined as,

$$\alpha = \frac{k}{\rho C_p},$$

where α is the thermal diffusivity, k is the thermal conductivity, ρ is the density and C_p is the specifc heat at constant pressure." [43]

Definition 2.1.9 (Boundary Layer)

"Boundary layer is a flow layer of fluid close to the solid region of the wall in contact where the viscosity effects are significant. The flow in this layer is usually laminar. The boundary layer thickness is the measure of the distance apart from the surface." [43]

2.2 Types of Fluid

Definition 2.2.1 (Ideal Fluid)

"A fluid, which is incompressible and has no viscosity, is known as an ideal fluid. Ideal fluid is only an imaginary fluid as all the fluids, which exist, have some viscosity." [42]

Definition 2.2.2 (Real Fluid)

"A fluid, which possesses viscosity, is known as a real fluid. In actual practice, all the fluids are real fluids." [42]

Definition 2.2.3 (Newtonian Fluid)

"A real fluid, in which the shear stress is directly proportional to the rate of shear strain (or velocity gradient), is known as a Newtonian fluid." Examples are water and alcohol." [42]

Definition 2.2.4 (Non-Newtonian Fluid)

"A real fluid in which the shear stress is not directly proportional to the rate of shear strain (or velocity gradient), is known as a non-Newtonian fluid." Non-Newtonian fluids include substances like toothpaste and honey.

$$\tau_{xy} \propto \left(\frac{du}{dy}\right)^m, \qquad m \neq 1$$

$$\tau_{xy} = \mu\left(\frac{du}{dy}\right)^m." \text{ [42]}$$

Definition 2.2.5 (Magnetohydrodynamics)

"Magnetohydrodynamics (MHD) is concerned with the mutual interaction of fluid flow and magnetic fields. The fluids in question must be electrically conducting and non-magnetic, which limits us to liquid metals, hot ionised gases (plasmas) and strong electrolytes." [44]

2.3 Types of Flow

Definition 2.3.1 (Rotational Flow)

"Rotational flow is that type of flow in which the fluid particles while flowing along stream-lines, also rotate about their own axis." [42]

Definition 2.3.2 (Irrotational Flow)

"Irrotational flow is that type of flow in which the fluid particles while flowing along stream-lines, do not rotate about their own axis then this type of flow is called irrotational flow." [42]

Definition 2.3.3 (Compressible Flow)

"Compressible flow is that type of flow in which the density of the fluid changes from point to point or in other words the density (ρ) is not constant for the fluid. Mathematically,

$$\rho \neq k,$$

where k is constant." [42]

Definition 2.3.4 (Incompressible Flow)

"Incompressible flow is that type of flow in which the density is constant for the fluid. Liquids are generally incompressible while gases are compressible, mathematically,

$$\rho = k,$$

where k is constant." [42]

Definition 2.3.5 (Steady Flow)

"Steady flow is defined as that type of flow in which the fluid characteristics like velocity, pressure, density, etc., at a point do not change with time. Thus for steady flow, mathematically we have

$$\frac{\partial Q}{\partial t} = 0,$$

where Q is any fluid property." [42]

Definition 2.3.6 (Unsteady Flow)

"Unsteady flow is defined as that type of flow in which the fluid characteristics like velocity, pressure, density, etc., at a point do change with time. Thus for Unsteady flow, mathematically, we have

$$\frac{\partial Q}{\partial t} \neq 0,$$

where Q is any fluid property." [42]

Definition 2.3.7 (Internal Flow)

"Flows completely bounded by a solid surfaces are called internal or duct flows." [41]

Definition 2.3.8 (External Flow)

"Flows over bodies immersed in an unbounded fluid are said to be an external flows." [41]

2.4 Modes of Heat Transfer and Mass Transfer

Definition 2.4.1 (Heat Transfer)

"The subject of physics known as *heat transfer* studies how thermal energy moves from one place in one media to another or from one medium to another when there is a temperature difference." [43]

Definition 2.4.2 (Conduction)

"The transfer of heat within a medium due to a diffusion process is called conduction. The Fourier heat conduction law states that the heat flow is proportional to the temperature gradient." During the ironing process, heat is transferred from the iron to the fabric. Chocolate candy in a hand will eventually melt as heat is conducted from a hand to the chocolate. [43]

Definition 2.4.3 (Convection)

"Convection heat transfer is usually defined as energy transport affected by the motion of a fluid. The convection heat transfer between two dissimilar media is governed by Newton's law of cooling. It states that the heat flow is proportional to the difference of the temperatures of the two media. The proportionality coefficient is called the convection heat transfer coefficient." Examples are heating water on the stove and air conditioner [43]

Definition 2.4.4 (Thermal Radiation)

"Thermal Radiation is defined as radiant (electromagnetic) energy emitted by a medium and is due solely to the temperature of the medium." [43]

Definition 2.4.5 (Mass transfer)

"Mass transfer is the flow of molecules from one body to another when these bodies are in contact or within a system consisting of two components when the distribution of materials is not uniform." A common example is drying of clothes or the evaporation of water spilled on the floor when water molecules diffuse into the air surrounding it. Usually mass transfer takes place from a location where the particular component is proportionately high to a location where the component is proportionately low. Mass transfer may also take place due to potentials other than concentration difference.

2.5 Dimensionless Numbers

Definition 2.5.1 (Eckert Number)

"It is the dimensionless number used in continuum mechanics. It describes the relation between flows and the boundary layer enthalpy difference and it is used for characterized heat dissipation. Mathematically,

$$Ec = \frac{u^2}{C_p \nabla T},$$

where C_p denotes the specific heat." [41]

Definition 2.5.2 (Prandtl Number)

"It is the ratio between the momentum diffusivity ν and thermal diffusivity α. Mathematically, it can be defined as

$$Pr = \frac{\nu}{\alpha} = \frac{\frac{\mu}{\rho}}{\frac{k}{C_p \rho}} = \frac{\mu C_p}{k},$$

where μ represents the dynamic viscosity, Cp denotes the specific heat and k stands for thermal conductivity. The relative thickness of thermal and momentum boundary layer is controlled by Prandtl number. For small Pr, heat distributed rapidly corresponds to the momentum." [41]

Definition 2.5.3 (Skin Friction Coefficient)

"The steady flow of an incompressible gas or liquid in a long pipe of internal D (mass diffusivity). The mean velocity is denoted by u_w. The skin friction coefficient can be defined as

$$C_f = \frac{2\tau_0}{\rho u_w^2},$$

where τ_0 denotes the wall shear stress and ρ is the density." [45]

Definition 2.5.4 (Grashof Number)

"It express the buoyancy to viscous forces ratio and its action on fluid. It characterizes the free non-isothermal convection of the fluid due to the density difference caused by the temperature gradient in the fluid. Mathematically,

$$Gr = \frac{H^3 g \beta \Delta T}{\nu^2},$$

where g is acceleration due to Earth's gravity, H is the characteristic length, ΔT is temperature change, ν is the kinematic viscosity, β coefficient of thermal expansion of fluid." [45]

Definition 2.5.5 (Nusselt Number)

"The hot surface is cooled by a cold fluid stream. The heat from the hot surface, which is maintained at a constant temperature, is diffused through a boundary layer and convected away by the cold stream. Mathematically,

$$Nu = \frac{qL}{k},$$

where q stands for the convection heat transfer, L for the characteristic length and k stands for thermal conductivity." [46]

Definition 2.5.6 (Sherwood Number)

"It is the non-dimensional quantity which shows the ratio of the mass transport by convection to the transfer of mass by diffusion. Mathematically,

$$Sh = \frac{kL}{D},$$

Where L is characteristics length, D is the mass diffusivity and k is the mass transfer coeffcient." [47]

Definition 2.5.7 (Reynolds Number)

"It is defined as the ratio of inertia force of a flowing fluid and the viscous force of the fluid. Mathematically,

$$Re = \frac{VL}{\nu},$$

where V denotes the free stream velocity, L is the characteristic length and ν stands for kinematic viscosity." [42]

2.6 Governing Laws

Definition 2.6.1 (Continuity Equation)

"The principle of conservation of mass can be stated as: *the time rate of change of mass is fixed volume is equal to the net rate of flow of mass across the surface*".

Mathematically, it can be written as

$$\frac{\partial \rho}{\partial t} + \nabla.(\rho \mathbf{u}) = 0,$$

where ρ is density, v is the velocity, and ∇ is del operator. [43]

Definition 2.6.2 (Momentum Equation)

"The momentum equation states that *the time rate of change of linear momentum of a given set of particles is equal to the vector sum of all the external forces acting on the particles of the set, provided Newton's Third Law of action and reaction governs the internal forces*". Mathematically, it can be written as:

$$\frac{\partial}{\partial t}(\rho \mathbf{v}) + \nabla.[(\rho \mathbf{v})\mathbf{v}] = \nabla.\sigma + \rho f,$$

where σ is Cauchy stress tensor (N/m^2), ρ is density, v is the velocity, and f is the body force vector. [43]

Definition 2.6.3 (Energy Equation)

"The law of conservation of energy states that the time rate of change of the total energy is equal to the sum of the rate of work done by the applied forces and change of heat content per unit time". Mathematically,

$$\frac{\partial \rho}{\partial t} + \nabla.\rho \mathbf{v} = -\nabla.\mathbf{q} + Q + \phi,$$

where ϕ is the dissipation function, Q is the internat heat generation, and q is the heat flux vector ." [43]

2.7 Shooting Method

It is a numerical approach for resolving the boundary value problems expressed in the form of nonlinear ordinary differential equations. Initially, the higher-order nonlinear ordinary differential equations (ODEs) are converted into a system of first-order ODEs. The missing initial conditions are guessed to have a complete

initial value problem (IVP). To explain the detailed computational procedure, consider the classical Blausius problem in the dimensionless form governed by he following ODEs along with the relavant boundary conditions:

$$\left.\begin{aligned} &af'''(x) + f(x)f''(x) = 0 \\ &f(0) = 0 = f'(0), \quad f' \to 1 \ \ as \ \ x \to \infty. \end{aligned}\right\} \tag{2.1}$$

Introduce the following notations to reduce the order of the above boundary value problem.

$$\left.\begin{aligned} f &= z_1, \\ f' &= z_1' = z_2, \\ f'' &= z_2' = z_3. \end{aligned}\right\} \tag{2.2}$$

As a result, (2.1) is transformed into the following system of first order ODEs:

$$z_1' = z_2, \qquad z_1(0) = 0. \tag{2.3}$$

$$z_2' = z_3, \qquad z_2(0) = 1. \tag{2.4}$$

$$z_3' = -\frac{1}{a}\big[z_1 z_3\big], \qquad z_3(0) = h. \tag{2.5}$$

where h is the missing initial condition which will be guessed to initialize the computational problem.

The RK-4 method will be used for the numerical solution of the provided initial value problem (IVP). The choice of h should be made to meet the condition:

$$z_2(x, h) = 1. \tag{2.6}$$

For convenience, now onward $z_2(x, h)$ will be denoted by $z_2(h)$.

Let us further denote $z_2(h) - 1$ by $\phi(h)$, so that

$$\phi(h) = 0. \tag{2.7}$$

The iterative formula detailed below allows us to implement Newton's method as a solution approach for the previously discussed equation:

$$h_{n+1} = h_n - \frac{\phi(h_n)}{\left(\frac{\partial \phi(h)}{\partial h}\right)_{h=h_n}},$$

or

$$h_{n+1} = h_n - \frac{z_2(h_n) - 1}{\left(\frac{\partial z_2(h)}{\partial t}\right)_{h=h_n}}. \tag{2.8}$$

For $\frac{\partial z_2(h)}{\partial h}$, we introduce the following notations:

$$\frac{\partial z_1}{\partial h} = z_4, \quad \frac{\partial z_2}{\partial h} = z_5, \quad \frac{\partial z_3}{\partial h} = z_6. \tag{2.9}$$

With the use of these notations, representation for iterative scheme of Newton is:

$$h_{n+1} = h_n - \frac{z_2(h_n) - 1}{z_5(h_n)}. \tag{2.10}$$

Differentiating the first-order ODEs (2.3)-(2.4) with respect to h, we derive another system of ODEs as below:

$$z_4' = z_5, \qquad z_4(0) = 0. \tag{2.11}$$
$$z_5' = z_6, \qquad z_5(0) = 0. \tag{2.12}$$
$$z_6' = -\frac{1}{a}\big[z_1 z_6 + z_3 z_4\big], \qquad z_6(0) = 1, \tag{2.13}$$

Writing all the ODEs (2.3)-(2.5) and (2.11)-(2.13) together, we have the following IVP.

$$z_1' = z_2, \qquad z_1(0) = 0.$$
$$z_2' = z_3, \qquad z_2(0) = 1.$$
$$z_3' = -\frac{1}{a}\big[z_1 z_3\big], \qquad z_3(0) = h.$$
$$z_4' = z_5, \qquad z_4(0) = 0.$$
$$z_5' = z_6, \qquad z_5(0) = 0.$$

$$z_6' = -\frac{1}{a}\big[z_1 z_6 + z_3 z_4\big], \qquad z_6(0) = 1.$$

To solve the above IVP, we will apply the fourth-order Runge-Kutta numerical method.

The stopping criteria for the shooting technique is established as:

$$\mid z_2(h) - 1 \mid < \epsilon,$$

where $\epsilon > 0$ is an arbitrarily small positive number.

Chapter 3

A Casson Fluid Flow on a Nonlinear Stretching Surface affected by Magnetic Field and Velocity Slip

3.1 Introduction

The Principal concern of this chapter has been regarding the numerical evaluation of a Casson fluid rotating flow when subjected to the consequence of a magnetic field, viscous dissipation, Joule heating and nonlinear thermal radiation. This model was proposed and numerically computed by Kala et al. [40] by utilizing shooting method.The conversion of the governing nonlinear PDEs into a set of dimensionless ODEs is a requirement for implementing the shooting method. To sum up, the of the result numerical solutions for various parameters are explored for the dimensionless velocity f', temperature distribution θ and concentration distribution ϕ. The acquired numerical results have been presented through tables and graphs.

3.2 Mathematical Modeling

Consider a two-dimensional steady, laminar flow of an incompressible Casson fluid through a non-linearly stretching surface, in a saturated homogeneous Forchheimer porous medium (See Figure 3.1). In this study, the stretching surface has been considering along x-axis inclined at an acute angle α to the vertical. Assume that the velocity of extending sheet is represented by $U_w(x)=cx^n$. Suppose C_w represents the wall concentration and T_w signifies the wall temperature, while $C_\infty < C_w$ and $T_\infty < T_w$ are the ambient concentration and temperature respectively.

During stretching, position of the origin remains unchanged; and stretching velocity at a point of the surface is non-linearly proportional to its distance from origin and B the magnetic field is normal to stretching surface.
The rheological equation for the Casson fluid as follow:

$$\tau_{ij} = \begin{cases} 2e_{ij}\left(\mu_B + \frac{P_y}{\sqrt{2\pi}}\right) & if \quad \pi > \pi_c \\ 2e_{ij}\left(\mu_B + \frac{P_y}{\sqrt{2\pi_c}}\right) & if \quad \pi < \pi_c \end{cases}$$

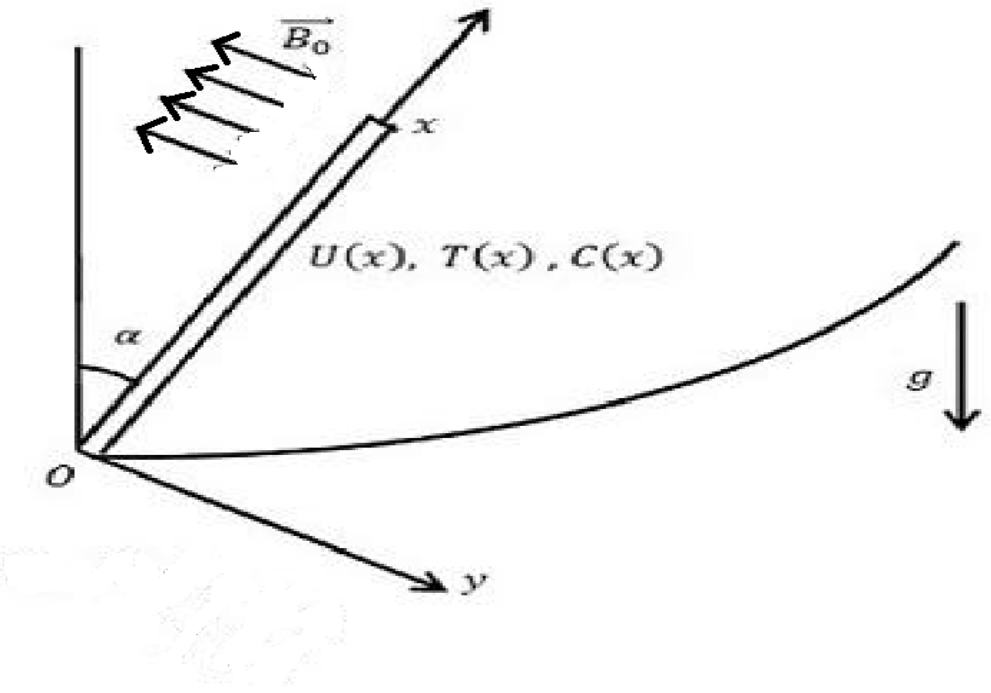

FIGURE 3.1: The boundary layer flow presentation.

The set of equations describing the flow are:

$$\frac{\partial u}{\partial x}+\frac{\partial v}{\partial y}=0, \tag{3.1}$$

$$u\frac{\partial u}{\partial x}+v\frac{\partial u}{\partial y}=v\left(1+\frac{1}{\beta}\right)\frac{\partial^2 u}{\partial y^2}\pm g\left(\beta_T(T-T_\infty)+\beta_C(C-C_\infty)\right)\cos\alpha - \frac{\sigma B^2}{\rho_f}u-\frac{v}{K_d}u-\frac{C_b}{\sqrt{K_d}}u^2, \tag{3.2}$$

$$u\frac{\partial T}{\partial x}+v\frac{\partial T}{\partial y}=\alpha\frac{\partial^2 T}{\partial y^2}, \tag{3.3}$$

$$u\frac{\partial C}{\partial x}+v\frac{\partial C}{\partial y}=D\frac{\partial^2 C}{\partial y^2}-K_C(C-C_\infty). \tag{3.4}$$

The associated BCs have been taken as:

$$\left.\begin{aligned} &y=0: \quad u=U(x)=u_w+u_s=cx^n+N\mu\frac{\partial u}{\partial y},\ v=v_w=-V(x),\\ &y\to\infty: \ u\to 0,\ T\to T_\infty,\ C\to C_\infty,\ C(x)=C_w+C_0\frac{\partial C}{\partial y},\quad .\\ &\qquad\qquad T(x)=T_w+T_0\frac{\partial T}{\partial y}. \end{aligned}\right\} \tag{3.5}$$

With the utilization of the Rosseland approximation for radiation, q_r is presented as the radiative heat flux:

$$q_r=-\frac{4\sigma^*}{3k^*}\frac{\partial T^4}{\partial y},$$

where σ^* presents the Stefan-Boltzmann constant, and k^* symbolizes the absorption coefficient. If the difference of temperature is marginal in significance, then the temperature T^4 can be widened about T_∞ using Taylor series, as follows:

$$T^4=T_\infty^4+4T_\infty^3(T-T_\infty)+6T_\infty^2(T-T_\infty)^2+...$$

Avoiding the terms with higher order, we write:

$$\begin{aligned} T^4&=T_\infty^4+4T_\infty^3(T-T_\infty),\\ &=T_\infty^4+4T_\infty^3T-4T_\infty^4,\\ &=-3T_\infty^4+4T_\infty^3T,\\ &=4T_\infty^3T-3T_\infty^4. \end{aligned}$$

To modify the equations (3.1)-(3.4) to have the form of ODEs, use the following transformations:

$$\left.\begin{aligned}
&\eta = \sqrt{\frac{c(n+1)}{2v}}x^{\frac{n-1}{2}}y, \quad \psi = \sqrt{\frac{2cv}{n+1}}x^{\frac{n+1}{2}}f(\eta), \quad u = \frac{\partial\psi}{\partial y}, \quad v = -\frac{\partial\psi}{\partial x},\\
&u = cx^n f'(\eta), \quad v = -\sqrt{\frac{cv(n+1)}{2}}x^{\frac{n-1}{2}}\left(f(\eta) + \frac{n-1}{n+1}\eta f'(\eta)\right),\\
&\theta(\eta) = \frac{T-T_\infty}{T_w-T_\infty}, \quad \phi(\eta) = \frac{C-C_\infty}{C_w-C_\infty}.
\end{aligned}\right\} \tag{3.6}$$

The detailed method for converting equations (3.1)-(3.4) into the dimensionless form, is discussed below:

$$\begin{aligned}
\eta &= \sqrt{\frac{c(n+1)}{2v}}x^{\frac{n-1}{2}}y.\\
\frac{\partial\eta}{\partial y} &= \sqrt{\frac{c(n+1)}{2v}}x^{\frac{n-1}{2}}.\\
\frac{\partial\eta}{\partial x} &= \frac{\partial}{\partial x}\sqrt{\frac{c(n+1)}{2v}}x^{\frac{n-1}{2}}y,\\
&= \sqrt{\frac{c(n+1)}{2v}}y\frac{\partial}{\partial x}x^{\frac{n-1}{2}},\\
&= \sqrt{\frac{c(n+1)}{2v}}y\frac{n-1}{2}x^{\frac{n-3}{2}}.\\
u &= \frac{\partial\psi}{\partial y},\\
&= \frac{\partial}{\partial y}\left(\sqrt{\frac{2cv}{n+1}}x^{\frac{n+1}{2}}f(\eta)\right),\\
&= \sqrt{\frac{2cv}{n+1}}x^{\frac{n+1}{2}}f'(\eta)\frac{\partial\eta}{\partial y},\\
&= \sqrt{\frac{2cv}{n+1}}x^{\frac{n+1}{2}}f'(\eta)\sqrt{\frac{c(n+1)}{2v}}x^{\frac{n-1}{2}},\\
&= cx^n f'(\eta).\\
\frac{\partial u}{\partial x} &= \frac{\partial}{\partial x}cx^n f'(\eta),\\
&= ncx^{n-1}f'(\eta) + cx^n f''(\eta)\frac{\partial\eta}{\partial x},\\
&= ncx^{n-1}f'(\eta) + cx^n f''(\eta)\sqrt{\frac{c(n+1)}{2v}}y\frac{n-1}{2}x^{\frac{n-3}{2}},
\end{aligned}$$

$$= ncx^{n-1}f'(\eta) + cx^{n-1}f''(\eta)\frac{n-1}{2}\sqrt{\frac{c(n+1)}{2v}}yx^{\frac{n-1}{2}},$$
$$= ncx^{n-1}f'(\eta) + cx^{n-1}f''(\eta)\frac{n-1}{2}\eta. \tag{3.7}$$

$$v = -\frac{\partial\psi}{\partial x},$$
$$= -\frac{\partial}{\partial x}\left[\sqrt{\frac{2cv}{n+1}}x^{\frac{n+1}{2}}f(\eta)\right],$$
$$= -\left[\sqrt{\frac{2cv}{n+1}}\frac{n+1}{2}x^{\frac{n-1}{2}}f(\eta) + \sqrt{\frac{2cv}{n+1}}x^{\frac{n+1}{2}}f'(\eta)\frac{\partial\eta}{\partial x}\right],$$
$$= -\left[\sqrt{\frac{2cv}{n+1}}\frac{n+1}{2}x^{\frac{n-1}{2}}f(\eta) + \sqrt{\frac{2cv}{n+1}}x^{\frac{n+1}{2}}f'(\eta)\sqrt{\frac{c(n+1)}{2v}}y\frac{n-1}{2}x^{\frac{n-3}{2}}\right],$$
$$= -\sqrt{\frac{2cv}{n+1}}x^{\frac{n-1}{2}}\left(\frac{n+1}{2}f(\eta) + f'(\eta)y\sqrt{\frac{c(n+1)}{2v}}\frac{n-1}{2}x^{\frac{n-1}{2}}\right),$$
$$= -\sqrt{\frac{cv(n+1)}{2}}x^{\frac{n-1}{2}}\left[f(\eta) + \frac{n-1}{n+1}\eta f'(\eta)\right].$$

$$\frac{\partial v}{\partial y} = \frac{\partial}{\partial y}\left[-\sqrt{\frac{cv(n+1)}{2}}x^{\frac{n-1}{2}}\left(f(\eta) + \frac{n-1}{n+1}\eta f'(\eta)\right)\right],$$
$$= -\sqrt{\frac{cv(n+1)}{2}}x^{\frac{n-1}{2}}\frac{\partial}{\partial y}\left(f(\eta) + \frac{n-1}{n+1}\eta f'(\eta)\right),$$
$$= -\sqrt{\frac{cv(n+1)}{2}}x^{\frac{n-1}{2}}f'(\eta)\sqrt{\frac{c(n+1)}{2v}}x^{\frac{n-1}{2}} - \sqrt{\frac{cv(n+1)}{2}}x^{\frac{n-1}{2}}\frac{n-1}{n+1}\frac{\partial}{\partial y}(\eta f'(\eta)),$$
$$= -\frac{c(n+1)}{2}x^{\frac{n-1}{2}}x^{\frac{n-1}{2}}f'(\eta) - \sqrt{\frac{cv(n+1)}{2}}x^{\frac{n-1}{2}}\frac{n-1}{n+1}\left[\eta f''(\eta)\sqrt{\frac{c(n+1)}{2v}}x^{\frac{n-1}{2}}\right.$$
$$\left. + f'(\eta)\sqrt{\frac{c(n+1)}{2v}}x^{\frac{n-1}{2}}\right],$$
$$= -\frac{c(n+1)}{2}x^{n-1}f'(\eta) - \sqrt{\frac{cv(n+1)}{2}}x^{\frac{n-1}{2}}\frac{n-1}{n+1}\left[\eta f''(\eta)\sqrt{\frac{c(n+1)}{2v}}x^{\frac{n-1}{2}}\right.$$
$$\left. + f'(\eta)\sqrt{\frac{c(n+1)}{2v}}x^{\frac{n-1}{2}}\right],$$
$$= -\frac{c(n+1)}{2}x^{n-1}f'(\eta) - \eta f''(\eta)\frac{n-1}{n+1}\frac{c(n+1)}{2}x^{n-1} - \frac{n-1}{n+1}\frac{c(n+1)}{2}x^{n-1}f'(\eta),$$
$$= -\frac{c(n+1)}{2}x^{n-1}\left[f'(\eta) + \frac{n-1}{n+1}f'(\eta) + \eta f''(\eta)\frac{n-1}{n+1}\right],$$
$$= -\frac{c(n+1)}{2}x^{n-1}\Big[\frac{n+1+n-1}{n+1}f'(\eta) + \frac{n-1}{n+1}\eta f''(\eta)\Big],$$
$$= -\frac{c(n+1)}{2}x^{n-1}\Big[\frac{2n}{n+1}f'(\eta) + \frac{n-1}{n+1}\eta f''(\eta)\Big],$$
$$= -ncx^{n-1}f'(\eta) - cx^{n-1}\eta f''(\eta)\frac{n-1}{2}. \tag{3.8}$$

The satisfaction of Equation (3.1) by using the results of (3.7) and (3.8), can be seen as follows:

$$\frac{\partial u}{\partial x}+\frac{\partial v}{\partial y}=ncx^{n-1}f'(\eta)+cx^{n-1}\eta f''(\eta)\frac{n-1}{2}-ncx^{n-1}f'(\eta)-cx^{n-1}\eta f''(\eta)\frac{n-1}{2}$$
$$=0.$$

For the left hand side of the equation (3.2), the following derivatives have been determined:

$$\frac{\partial u}{\partial x}=cx^{n-1}\left[nf'(\eta)+\frac{n-1}{2}\eta f''(\eta)\right].$$
$$u\frac{\partial u}{\partial x}=cx^{n}f'(\eta)\left[cx^{n-1}\left(nf'(\eta)+\frac{n-1}{2}\eta f''(\eta)\right)\right],$$
$$=cx^{n}f'(\eta)cx^{n-1}\left(nf'(\eta)+\frac{n-1}{2}\eta f''(\eta)\right).$$
$$\frac{\partial u}{\partial y}=\frac{\partial}{\partial y}cx^{n}f'(\eta),$$
$$=cx^{n}f''(\eta)\frac{\partial}{\partial y}\eta,$$
$$=cx^{n}f''(\eta)\sqrt{\frac{c(n+1)}{2v}}x^{\frac{n-1}{2}}.$$
$$v\frac{\partial u}{\partial y}=-\sqrt{\frac{cv(n+1)}{2}}x^{\frac{n-1}{2}}\left(f(\eta)+\frac{n-1}{n+1}\eta f'(\eta)\right)cx^{n}f''(\eta)\sqrt{\frac{c(n+1)}{2v}}x^{\frac{n-1}{2}}.$$
$$u\frac{\partial u}{\partial x}+v\frac{\partial u}{\partial y}=cx^{n}f'(\eta)cx^{n-1}\left(nf'(\eta)+\frac{n-1}{2}\eta f''(\eta)\right)-\sqrt{\frac{cv(n+1)}{2}}x^{\frac{n-1}{2}}$$
$$\left(f(\eta)+\frac{n-1}{n+1}\eta f'(\eta)\right)cx^{n}f''(\eta)\sqrt{\frac{c(n+1)}{2v}}x^{\frac{n-1}{2}},$$
$$=c^{2}x^{2n-1}f'(\eta)\left(nf'(\eta)+\frac{n-1}{2}\eta f''(\eta)\right)-\frac{c(n+1)}{2}x^{n-1}cx^{n}f''(\eta)$$
$$\left(f(\eta)+\frac{n-1}{n+1}\eta f'(\eta)\right),$$
$$=c^{2}x^{2n-1}\left(nf'^{2}(\eta)+\frac{n-1}{2}\eta f'(\eta)f''(\eta)\right)-c^{2}x^{2n-1}\left(\frac{n+1}{2}f''(\eta)f(\eta)\right.$$
$$\left.+\frac{n+1}{2}\frac{n-1}{n+1}\eta f''(\eta)f'(\eta)\right),$$
$$=c^{2}x^{2n-1}\left(nf'^{2}(\eta)+\frac{n-1}{2}\eta f''(\eta)f'(\eta)-\frac{n+1}{2}f''(\eta)f(\eta)\right.$$
$$\left.-\frac{n-1}{2}\eta f''(\eta)f'(\eta)\right),$$

$$= c^2 x^{2n-1}\left[nf'^2(\eta) - \frac{n+1}{2}f''(\eta)f(\eta)\right]. \tag{3.9}$$

For the right hand side of equation (3.2), the following derivatives have been determined:

$$\begin{aligned}
\frac{\partial^2 u}{\partial y^2} &= \frac{\partial}{\partial y}\left[cx^n\sqrt{\frac{c(n+1)}{2v}}x^{\frac{n-1}{2}}f''(\eta)\right],\\
&= cx^n\sqrt{\frac{c(n+1)}{2v}}x^{\frac{n-1}{2}}f'''(\eta)\frac{\partial \eta}{\partial y},\\
&= cx^n\sqrt{\frac{c(n+1)}{2v}}x^{\frac{n-1}{2}}f'''(\eta)\sqrt{\frac{c(n+1)}{2v}}x^{\frac{n-1}{2}},\\
&= c^2x^{2n-1}\frac{n+1}{2v}f'''(\eta).\\
v\left(1+\frac{1}{\beta}\right)\frac{\partial^2 u}{\partial y^2} &= v\left(1+\frac{1}{\beta}\right)c^2x^{2n-1}\frac{n+1}{2v}f'''(\eta),\\
&= \left(1+\frac{1}{\beta}\right)\left(c^2x^{2n-1}\frac{n+1}{2}f'''(\eta)\right),\\
&= c^2x^{2n-1}\left[\left(1+\frac{1}{\beta}\right)\frac{n+1}{2}f'''(\eta)\right].
\end{aligned} \tag{3.10}$$

$$\begin{aligned}
g(\beta_T(T-T_\infty)+\beta_C(C-C_\infty))\cos\alpha &= g(\beta_T(T_w-T_\infty)\theta(\eta)+\beta_C(C_w-C_\infty)\phi(\eta))\\
&\quad \cos\alpha,\\
&= \left(\frac{G_r v^2}{x^3}\theta(\eta)+\frac{G_c v^2}{x^3}\phi(\eta)\right)cos\alpha,\\
&= \left(\frac{G_r v^2}{x^3 {u_w}^2}{u_w}^2\theta(\eta)+\frac{G_c v^2}{x^3 {u_w}^2}{u_w}^2\phi(\eta)\right)cos\alpha,\\
&= \left(\frac{G_r}{Re^2}{u_w}^2\theta(\eta)+\frac{G_c}{Re^2}{u_w}^2\phi(\eta)\right)\cos\alpha,\\
&= \left(\frac{\gamma^*}{x}(cx)^2\theta(\eta)+\frac{\gamma}{x}(cx)^2\phi(\eta)\right)\cos\alpha,\\
&= \left(\gamma^* c^2x^{2n-1}\theta(\eta)+\gamma c^2x^{2n-1}\theta(\eta)\right)\cos\alpha,\\
&= c^2x^{2n-1}\left(\gamma^*\theta(\eta)+\gamma\phi(\eta)\right)\cos\alpha.
\end{aligned} \tag{3.11}$$

$$\begin{aligned}
\frac{\sigma B_\circ^2}{\rho_f}u &= \frac{\sigma(Bx^{\frac{n-1}{2}})^2}{\rho_f}cx^n f'(\eta),\\
&= \frac{\sigma B_\circ^2}{\rho_f}x^{n-1}cx^n f'(\eta),\\
&= \frac{\sigma B_\circ^2}{c\rho_f}cx^{n-1}cx^n f'(\eta),\\
&= Mc^2x^{2n-1}f'(\eta),\\
&= c^2x^{2n-1}Mf'(\eta).
\end{aligned} \tag{3.12}$$

$$\frac{v}{K_d}u = \frac{cx^{n-1}}{K_p}cx^n f'(\eta),$$
$$= c^2x^{2n-1}\frac{1}{K_p}f'(\eta). \tag{3.13}$$
$$\frac{C_b}{\sqrt{K_d}}u^2 = \frac{F_s}{x}(cx^n f'(\eta))^2,$$
$$= \frac{F_s}{x}c^2x^{2n}f'^2(\eta),$$
$$= c^2x^{2n-1}F_s f'^2(\eta). \tag{3.14}$$

Now, from (3.10) - (3.14) we get:

$$v\left(1+\frac{1}{\beta}\right)\frac{\partial^2 u}{\partial y^2} \pm g\left(\beta_T(T-T_\infty)+\beta_C(C-C_\infty)\right)\cos\alpha - \frac{\sigma B_\circ^2}{\rho_f}u - \frac{v}{K_d}u$$
$$-\frac{C_b}{\sqrt{K_d}}u^2 = c^2x^{2n-1}\left[\left(1+\frac{1}{\beta}\right)\frac{n+1}{2}f'''(\eta)\right] \pm c^2x^{2n-1}\left(\gamma^*\theta(\eta)+\gamma\phi(\eta)\right)cos\alpha$$
$$-c^2x^{2n-1}Mf'(\eta) - c^2x^{2n-1}\frac{1}{K_p}f'(\eta) - c^2x^{2n-1}F_s f'^2(\eta) \tag{3.15}$$

As a result, the dimensionless form of (3.2), becomes:

$$c^2x^{2n-1}\left[nf'^2(\eta) - \frac{n+1}{2}f''(\eta)f(\eta)\right] = c^2x^{2n-1}\left[\left(1+\frac{1}{\beta}\right)\frac{n+1}{2}f'''(\eta)\right]$$
$$\pm c^2x^{2n-1}\left(\gamma^*\theta(\eta)+\gamma\phi(\eta)\right)cos\alpha - c^2x^{2n-1}Mf'(\eta) - c^2x^{2n-1}\frac{1}{K_p}f'(\eta)$$
$$-c^2x^{2n-1}F_s f'^2(\eta),$$
$$\Rightarrow \frac{2n}{n+1}f'^2(\eta) - f''(\eta)f(\eta) = \left(1+\frac{1}{\beta}\right)f'''(\eta) + \frac{2}{n+1}\left(\gamma^*\theta(\eta)+\gamma\phi(\eta)\right)\cos\alpha$$
$$-\frac{2}{n+1}\left[\left(M+1/K_p\right)f'(\eta)+F_s f'^2(\eta)\right],$$
$$\Rightarrow \left(1+\frac{1}{\beta}\right)f'''(\eta) + f''(\eta)f(\eta) - \frac{2n}{n+1}f'^2(\eta) + \frac{2}{n+1}\left(\gamma^*\theta(\eta)+\gamma\phi(\eta)\right)\cos\alpha$$
$$-\frac{2}{n+1}\left[\left(M+\frac{1}{K_p}\right)f'(\eta)+F_s f'^2(\eta)\right] = 0. \tag{3.16}$$

For the energy equation (3.3), the following derivatives have been determined:

$$\theta(\eta) = \frac{T-T_\infty}{T_w-T_\infty},$$
$$T = \theta(\eta)(T_w-T_\infty)+T_\infty.$$
$$\frac{\partial T}{\partial x} = (T_w-T_\infty)\theta'(\eta)\frac{\partial \eta}{\partial x},$$

$$
\begin{aligned}
&= (T_w - T_\infty)\theta'(\eta)\sqrt{\frac{c(n+1)}{2v}}\frac{n-1}{2x}x^{\frac{n-1}{2}}y,\\
&= (T_w - T_\infty)\theta'(\eta)\frac{n-1}{2x}\eta.\\
\frac{\partial T}{\partial y} &= \frac{\partial}{\partial y}\left(T_\infty + (T_w - T_\infty)\theta(\eta)\right),\\
&= (T_w - T_\infty)\theta'(\eta)\frac{\partial \eta}{\partial y},\\
&= (T_w - T_\infty)\theta'(\eta)\sqrt{\frac{c(n+1)}{2v}}x^{\frac{n-1}{2}}.\\
u\frac{\partial T}{\partial x} + v\frac{\partial T}{\partial y} &= cx^n f'(\eta)(T_w - T_\infty)\theta'(\eta)\frac{n-1}{2x}\eta - \sqrt{\frac{cv(n+1)}{2}}x^{\frac{n-1}{2}}\\
&\quad \left(f(\eta) + \frac{n-1}{n+1}\eta f'(\eta)\right)(T_w - T_\infty)\theta'(\eta)\sqrt{\frac{c(n+1)}{2v}}x^{\frac{n-1}{2}},\\
&= cx^n f'(\eta)(T_w - T_\infty)\theta'(\eta)\frac{n-1}{2x}\eta - \frac{c(n+1)}{2}x^{n-1}\\
&\quad \left(f(\eta) + \frac{n-1}{n+1}\eta f'(\eta)\right)(T_w - T_\infty)\theta'(\eta),\\
&= cx^{n-1}(T_w - T_\infty)\theta'(\eta)\Bigg[f'(\eta)\frac{n-1}{2}\eta - \frac{n+1}{2}f(\eta)\\
&\quad - \frac{n+1}{2}\frac{n-1}{n+1}\eta f'(\eta)\Bigg],\\
&= cx^{n-1}(T_w - T_\infty)\theta'(\eta)\left[f'(\eta)\frac{n-1}{2}\eta - \frac{n+1}{2}f(\eta) - \frac{n-1}{2}\eta f'(\eta)\right],\\
&= -cx^{n-1}(T_w - T_\infty)\frac{n+1}{2}\theta'(\eta)f(\eta). \qquad (3.17)
\end{aligned}
$$

Now, for the right hand side of the energy equation (3.3), the following derivatives have been determined:

$$
\begin{aligned}
\alpha\frac{\partial^2 T}{\partial y^2} &= \alpha\frac{\partial}{\partial y}\left((T_w - T_\infty)\theta'(\eta)\sqrt{\frac{c(n+1)}{2v}}x^{\frac{n-1}{2}}\right),\\
&= \alpha(T_w - T_\infty)\sqrt{\frac{c(n+1)}{2v}}x^{\frac{n-1}{2}}\theta''(\eta)\frac{\partial \eta}{\partial y},\\
&= \alpha(T_w - T_\infty)\sqrt{\frac{c(n+1)}{2v}}x^{\frac{n-1}{2}}\theta''(\eta)\sqrt{\frac{c(n+1)}{2v}}x^{\frac{n-1}{2}},\\
&= \alpha(T_w - T_\infty)\frac{c(n+1)}{2v}x^{n-1}\theta''(\eta). \qquad (3.18)
\end{aligned}
$$

As a result, The energy equation (3.3) has been satisfied by using the equations (3.17) and (3.18):

$$
\begin{aligned}
&- cx^{n-1}(T_w - T_\infty)\frac{n+1}{2}\theta'(\eta)f(\eta) = \alpha(T_w - T_\infty)\frac{c(n+1)}{2v}x^{n-1}\theta''(\eta),\\
&\Rightarrow -\theta'(\eta)f(\eta) = \frac{\alpha}{v}\theta''(\eta),\\
&\Rightarrow -\theta'(\eta)f(\eta) = \frac{1}{P_r}\theta''(\eta),\\
&\Rightarrow \frac{1}{P_r}\theta''(\eta) + \theta'(\eta)f(\eta) = 0. \qquad (3.19)
\end{aligned}
$$

For the right hand side of the mass concentration equation (3.4), the following derivatives have been determined:

$$
\begin{aligned}
&C - C_\infty = (C_w - C_\infty)\phi(\eta),\\
&C = C_\infty + (C_w - C_\infty)\phi(\eta).\\
&\frac{\partial C}{\partial x} = \frac{\partial}{\partial x}(C_\infty + (C_w - C_\infty)\phi(\eta)),\\
&\quad = (C_w - C_\infty)\phi'(\eta)\frac{\partial}{\partial x}\eta,\\
&\quad = (C_w - C_\infty)\phi'(\eta)\sqrt{\frac{c(n+1)}{2v}}\frac{n-1}{2}x^{\frac{n-1}{2}}\frac{y}{x},\\
&\quad = (C_w - C_\infty)\phi'(\eta)\sqrt{\frac{c(n+1)}{2v}}\frac{n-1}{2x}x^{\frac{n-1}{2}}y,\\
&\quad = (C_w - C_\infty)\phi'(\eta)\frac{n-1}{2x}\eta.\\
&\frac{\partial C}{\partial y} = \frac{\partial}{\partial y}(C_\infty + (C_w - C_\infty)\phi(\eta)),\\
&\quad = (C_w - C_\infty)\phi'(\eta)\frac{\partial}{\partial y}\eta,\\
&\quad = (C_w - C_\infty)\phi'(\eta)\sqrt{\frac{c(n+1)}{2v}}x^{\frac{n-1}{2}}.\\
&u\frac{\partial C}{\partial x} + v\frac{\partial C}{\partial y} = cx^n f'(\eta)(C_w - C_\infty)\phi'(\eta)\frac{n-1}{2x}\eta - \sqrt{\frac{cv(n+1)}{2}}x^{\frac{n-1}{2}},\\
&\qquad\qquad \left(f(\eta) + \frac{n-1}{n+1}\eta f'(\eta)\right)(C_w - C_\infty)\phi'(\eta)\sqrt{\frac{c(n+1)}{2v}}x^{\frac{n-1}{2}},\\
&\qquad = cx^n f'(\eta)(C_w - C_\infty)\phi'(\eta)\frac{n-1}{2x}\eta - \frac{c(n+1)}{2}x^{n-1}\\
&\qquad\quad \left(f(\eta) + \frac{n-1}{n+1}\eta f'(\eta)\right)(C_w - C_\infty)\phi'(\eta),\\
&\qquad = cx^{n-1}(C_w - C_\infty)\phi'(\eta)\left[f'(\eta)\frac{n-1}{2}\eta - \frac{n+1}{2}f(\eta)\right.\\
&\qquad\quad \left. - \frac{n+1}{2}\frac{n-1}{n+1}\eta f'(\eta)\right],\\
&\qquad = cx^{n-1}(C_w - C_\infty)\phi'(\eta)\left[f'(\eta)\frac{n-1}{2}\eta - \frac{n+1}{2}f(\eta) - \frac{n-1}{2}\eta f'(\eta)\right],
\end{aligned}
$$

$$= -cx^{n-1}(C_w - C_\infty)\frac{n+1}{2}\phi'(\eta)f(\eta). \tag{3.20}$$

Now, for the left hand side conversion of mass concentration equation (3.4), the following derivatives have been carried out:

$$\begin{aligned}
\frac{\partial C}{\partial y} &= (C_w - C_\infty)\phi'(\eta)\sqrt{\frac{c(n+1)}{2v}}x^{\frac{n-1}{2}}.\\
\frac{\partial^2 C}{\partial y^2} &= \frac{\partial}{\partial y}\left((C_w - C_\infty)\phi'(\eta)\sqrt{\frac{c(n+1)}{2v}}x^{\frac{n-1}{2}}\right),\\
&= (C_w - C_\infty)\sqrt{\frac{c(n+1)}{2v}}x^{\frac{n-1}{2}}\frac{\partial}{\partial y}\phi'(\eta),\\
&= (C_w - C_\infty)\sqrt{\frac{c(n+1)}{2v}}x^{\frac{n-1}{2}}\phi''(\eta)\frac{\partial}{\partial y}\eta,\\
&= (C_w - C_\infty)\sqrt{\frac{c(n+1)}{2v}}x^{\frac{n-1}{2}}\phi''(\eta)\sqrt{\frac{c(n+1)}{2v}}x^{\frac{n-1}{2}},\\
&= (C_w - C_\infty)\left(\sqrt{\frac{c(n+1)}{2v}}\right)^2(x^{\frac{n-1}{2}})^2\phi''(\eta),\\
&= (C_w - C_\infty)\frac{c(n+1)}{2v}x^{n-1}\phi''(\eta).\\
D\frac{\partial^2 C}{\partial y^2} - K_C(C - C_\infty) &= D\left((C_w - C_\infty)\frac{c(n+1)}{2v}x^{n-1}\phi''(\eta)\right)\\
&\quad - Kc(C_w - C_\infty)\phi(\eta),\\
&= \frac{D}{v}\left((C_w - C_\infty)\frac{c(n+1)}{2}x^{n-1}\phi''(\eta)\right)\\
&\quad - Kc(C_w - C_\infty)\phi(\eta),\\
&= \frac{1}{Sc}\left((C_w - C_\infty)\frac{c(n+1)}{2}x^{n-1}\phi''(\eta)\right)\\
&\quad - Kc(C_w - C_\infty)\phi(\eta),\\
&= (C_w - C_\infty)cx^{n-1}\frac{n+1}{2}\left(\frac{1}{Sc}\phi''(\eta)\right.\\
&\quad \left. - \frac{K}{x^{n-1}}\frac{2}{n+1}\phi(\eta)\right).
\end{aligned} \tag{3.21}$$

As a result of equations (3.20) and (3.21) the mass concentration becomes:

$$\begin{aligned}
&- cx^{n-1}(C_w - C_\infty)\frac{n+1}{2}\phi'(\eta)f(\eta) = (C_w - C_\infty)cx^{n-1}\frac{n+1}{2}\left[\frac{1}{Sc}\phi''(\eta)\right.\\
&\left. - \frac{K}{x^{n-1}}\frac{2}{n+1}\phi(\eta)\right],
\end{aligned}$$

$$\Rightarrow -\phi'(\eta)f(\eta) = \frac{1}{Sc}\phi''(\eta) - \frac{2}{n+1}Kx^{1-n}\phi(\eta),$$
$$\Rightarrow -\phi'(\eta)f(\eta) = \frac{1}{Sc}\phi''(\eta) - \frac{2}{n+1}K_c\phi(\eta),$$
$$\Rightarrow \frac{1}{Sc}\phi''(\eta) + \phi'(\eta)f(\eta) - \frac{2}{n+1}K_c\phi(\eta) = 0. \tag{3.22}$$

The dimensionless parameters used for the equations (3.2), (3.3) and (3.4) are:

$$Gr=\frac{g\beta_T(T_w-T_\infty)x^3}{v^2},\ Gc=\frac{g\beta_C(C_w-C_\infty)x^3}{v^2},\ \gamma=\frac{Gc}{Re^2},\ Re^2=\frac{u_w}{v},\ M=\frac{\sigma B_\circ^2}{c\rho_f},\ K_p=\frac{cK_dx^{n-1}}{v},$$
$$Fs=\frac{c_bx}{\sqrt{K_d}},\quad \gamma^*=\frac{Gr}{Re^2},\quad Kc=Kx^{1-n},\quad \beta=\mu_bp_y\sqrt{2\pi},\quad \alpha_T=\frac{k}{(\rho C_p)},\ \mu=\left(\mu_B+\frac{p_y}{\sqrt{2\pi}}\right),$$
$$Pr=\frac{\nu}{\alpha_T},\ S=-v_w\sqrt{\frac{2}{vc(n+1)}}x^{1-n/2},\ Vs=N\mu\sqrt{\frac{c(n+1)}{2v}}x^{n-1/2},\ Sc=\frac{v}{D},\ Rd=\frac{16\sigma^*T_\infty^3}{3kk^*}.$$

The final version of the governing model's dimensionless form is:

$$\left(1+\frac{1}{\beta}\right)f'''(\eta) + f''(\eta)f(\eta) - \frac{2n}{n+1}f'^2(\eta) + \frac{2}{n+1}\left(\gamma^*\theta(\eta)+\gamma\phi(\eta)\right)\cos\alpha$$
$$-\frac{2}{n+1}\left[\left(M+\frac{1}{K_p}\right)f'(\eta) + F_sf'^2(\eta)\right] = 0, \tag{3.23}$$
$$\frac{1}{P_r}\theta''(\eta) + \theta'(\eta)f(\eta) = 0, \tag{3.24}$$
$$\frac{1}{Sc}\phi''(\eta) + \phi'(\eta)f(\eta) - \frac{2}{n+1}K_c\phi(\eta) = 0. \tag{3.25}$$

The transformation of corresponding BCs into the non-dimensional form is given below:

$$u = U_w(x) = cx^n, \qquad at \quad y = 0.$$
$$\Rightarrow\ cf'(\eta)x^n = cx^n \qquad at \quad \eta = 0.$$
$$\Rightarrow\ cx^nf'(\eta) = cx^n, \qquad at \quad \eta = 0.$$
$$\Rightarrow\ f'(\eta) = 1, \qquad at \quad \eta = 0.$$
$$\Rightarrow\ f'(0) = 1.$$
$$v = 0, \qquad at \quad y = 0.$$
$$\Rightarrow\ -x^{\frac{n-1}{2}}\sqrt{\frac{(n+1)\nu c}{2}}\left(f(\eta)+\eta f'(\eta)\frac{n-1}{n+1}\right) = 0, \qquad at \quad \eta = 0.$$
$$\Rightarrow\ -x^{\frac{n-1}{2}}\sqrt{\frac{(n+1)\nu c}{2}}f(0) = 0,$$
$$\Rightarrow\ f(0) = 0.$$

$$
\begin{aligned}
& T = T_w, && at \quad y = 0. \\
\Rightarrow\ & \theta(\eta)(T_w - T_\infty) + T_\infty = T_w, && at \quad \eta = 0. \\
\Rightarrow\ & \theta(\eta)(T_w - T_\infty) = T_w - T_\infty, && at \quad \eta = 0. \\
\Rightarrow\ & \theta(\eta) = 1, && at \quad \eta = 0. \\
\Rightarrow\ & \theta(0) = 1. \\
& C = C_w, && at \quad y = 0. \\
\Rightarrow\ & \phi(\eta)(C_w - C_\infty) + C_\infty = C_w, && at \quad \eta = 0. \\
\Rightarrow\ & \phi(\eta)(C_w - C_\infty) = C_w - C_\infty, && at \quad \eta = 0. \\
\Rightarrow\ & \phi(\eta) = 1, && at \quad \eta = 0. \\
\Rightarrow\ & \phi(0) = 1. \\
& u \to 0, && as \quad y \to \infty. \\
\Rightarrow\ & cf'(\eta)x^n \to (0), && as \quad \eta \to \infty. \\
\Rightarrow\ & f'(\eta) \to (0), && as \quad \eta \to \infty. \\
\Rightarrow\ & f'(\infty) \to 0. \\
& T \to T_\infty, && as \quad y \to \infty. \\
\Rightarrow\ & \theta(\eta)(T_w - T_\infty) + T_\infty \to T_\infty, && as \quad \eta \to \infty. \\
\Rightarrow\ & \theta(\eta)(T_w - T_\infty) \to 0, && as \quad \eta \to \infty. \\
\Rightarrow\ & \theta(\eta) \to 0, && as \quad \eta \to \infty. \\
\Rightarrow\ & \theta(\infty) \to 0. \\
& C \to\ C_\infty, && as \quad y \to \infty. \\
\Rightarrow\ & \phi(\eta)(C_w - C_\infty) + C_\infty \to C_\infty, && as \quad \eta \to \infty. \\
\Rightarrow\ & \phi(\eta)(C_w - C_\infty) \to 0, && as \quad \eta \to \infty. \\
\Rightarrow\ & \phi(\eta) \to 0, && as \quad \eta \to \infty. \\
\Rightarrow\ & \phi(\infty) \to 0. \\
& u = u(x) = u_w + u_s, && at \quad y = 0. \\
\Rightarrow\ & cx^n f'(\eta) = cx^n + N\nu \frac{\partial}{\partial y} cx^n f'(\eta), && at \quad \eta = 0. \\
\Rightarrow\ & cx^n f'(\eta) = cx^n \left(1 + N\nu f''(\eta)\sqrt{\frac{c(n+1)}{2\nu}} x^{\frac{n-1}{2}}\right), && at \quad \eta = 0. \\
\Rightarrow\ & f'(\eta) = 1 + V_s f''(\eta), && at \quad \eta = 0. \\
\Rightarrow\ & f'(0) = 1 + V_s f''(0).
\end{aligned}
$$

$$\Rightarrow\ T(x) = T_w + T_0\frac{\partial T}{\partial y}, \qquad as \quad T \to T_\infty.$$

$$\Rightarrow\ T_\infty + \theta(\eta)(T_w - T_\infty) = T_w + T_0\frac{\partial}{\partial y}(T_\infty + \theta(\eta)(T_w - T_\infty)), \qquad as \quad \theta_\eta \to 0.$$

$$\Rightarrow\ \theta(\eta)(T_w - T_\infty) = T_w - T_\infty + T_0\left(\theta'(\eta)(T_w - T_\infty)\frac{\partial}{\partial y}\eta\right), \qquad as \quad \eta \to 0.$$

$$\Rightarrow\ \theta(\eta)(T_w - T_\infty) = T_w - T_\infty + T_0\left(\theta'(\eta)(T_w - T_\infty)\sqrt{\frac{c(n+1)}{2\nu}}x^{\frac{n-1}{2}}\right), \qquad as \quad \eta \to 0.$$

$$\Rightarrow\ \theta(\eta) = 1 + \lambda t\theta'(\eta) \to 0, \qquad as \quad \eta \to 0.$$

$$\Rightarrow\ \theta(0) = 1 + \lambda t\theta'(0) \to 0.$$

$$\Rightarrow\ C(x) = C_w + C_0\frac{\partial C}{\partial y}, \qquad as \quad C \to C_\infty.$$

$$\Rightarrow\ C_\infty + \phi(\eta)(C_w - C_\infty) = C_w + C_0\frac{\partial}{\partial y}(C_\infty + \phi(\eta)(C_w - C_\infty)), \qquad as \quad \eta \to 0.$$

$$\Rightarrow\ \phi(\eta)(C_w - C_0) = C_w - C_\infty + C_0\left(\phi'(\eta)(C_w - C_\infty)\frac{\partial}{\partial y}\eta\right), \qquad as \quad \eta \to 0.$$

$$\Rightarrow\ \phi(\eta)(C_w - C_\infty) = C_w - C_\infty + C_0\left(\phi'(\eta)(C_w - C_\infty)\sqrt{\frac{c(n+1)}{2\nu}}x^{\frac{n-1}{2}}\right), \qquad as \quad \eta \to 0.$$

$$\Rightarrow\ \phi(\eta) = 1 + \lambda t\phi'(\eta) \to 0, \qquad as \quad \eta \to 0.$$

$$\Rightarrow\ \phi(0) = 1 + \lambda t\phi'(0).$$

The dimensionless form of the associated BCs (3.6) is:

$$\left.\begin{aligned} &\eta \to 0 :\ f(0) = S,\ f'(0) = 1 + Vsf''(0),\ \theta(0) = 1 + \lambda_t\theta'(0),\ \phi(0) = 1 + \lambda_c\phi'(0) \\ &\eta \to \infty :\ f' \to 0,\ g \to 0,\ \theta \to 0,\ \phi \to 0. \end{aligned}\right\} \tag{3.26}$$

The skin friction coefficient, is given as follow:

$$C_{fx} = \frac{\tau_w}{\rho U_w^2} \tag{3.27}$$

where, the shearing stress τ_w is defined as:

$$\tau_w = \left(\mu_\beta + \frac{p_y}{\sqrt{2\pi}}\right)\left(\frac{\partial u}{\partial y}\right)_{y=0}. \tag{3.28}$$

Therefore,

$$\begin{aligned}
C_{fx} &= \frac{1}{\rho_f u_w^2}\left(\mu_\beta + \frac{p_y}{\sqrt{2\pi}}\right)\left(\frac{\partial u}{\partial y}\right)_{y=0}, \\
&= \frac{1}{\rho_f (cx^n)^2}\mu_\beta\left(1+\frac{p_y}{\mu_\beta\sqrt{2\pi}}\right) cx^n\sqrt{\frac{c(n+1)}{2\nu}}x^{\frac{n-1}{2}}f''(0), \\
&= \frac{1}{\rho_f\sqrt{\nu}\sqrt{cx^n x}}\mu_\beta\left(1+\frac{p_y}{\mu_\beta\sqrt{2\pi}}\right)\sqrt{\frac{n+1}{2}}f''(0), \\
&= \frac{1}{Re_x^{\frac{1}{2}}}\left(1+\frac{1}{\beta}\right)\sqrt{\frac{n+1}{2}}f''(0). \\
\Rightarrow\ Re_x^{\frac{1}{2}}Cf_x &= \left(1+\frac{1}{\beta}\right)\sqrt{\frac{n+1}{2}}f''(0). \qquad (3.29)
\end{aligned}$$

Similarly, to achive the dimensionless form of Nusselt number Nu_x, the following procedure has been included:

$$\begin{aligned}
Nu_x &= -\frac{x}{T_w - T_\infty}\left(\frac{\partial T}{\partial y}\right)_{y=0}, \qquad (3.30) \\
&= -\frac{x}{(T_w - T_\infty)}(T_w - T_\infty)\sqrt{\frac{c(n+1)}{2\nu}}x^{\frac{n-1}{2}}\theta'(0), \\
&= -\sqrt{\frac{n+1}{2}}\sqrt{\frac{cx^n x}{\nu}}\theta'(0), \\
&= -\sqrt{\frac{n+1}{2}}\sqrt{\frac{u_w x}{\nu}}\theta'(0), \\
&= -Re_x^{\frac{1}{2}}\sqrt{\frac{n+1}{2}}\theta'(0). \\
\Rightarrow\quad Re_x^{\frac{-1}{2}}Nu_x &= -\sqrt{\frac{n+1}{2}}\theta'(0). \qquad (3.31)
\end{aligned}$$

Now, to achive the dimensionless form of the Sherwoood number Sh_x, consider the following procedure:

$$\begin{aligned}
Sh_x &= -\frac{x}{C_w - C_\infty}\left(\frac{\partial C}{\partial y}\right)_{y=0}, \qquad (3.32) \\
&= -\frac{x}{(C_w - C_\infty)}(C_w - C_\infty)\sqrt{\frac{c(n+1)}{2\nu}}x^{\frac{n-1}{2}}\phi'(0), \\
&= -\sqrt{\frac{n+1}{2}}\sqrt{\frac{cx^n x}{\nu}}\phi'(0),
\end{aligned}$$

$$= -\sqrt{\frac{n+1}{2}}\sqrt{\frac{u_w x}{\nu}}\phi'(0),$$
$$= -Re_x^{\frac{1}{2}}\sqrt{\frac{n+1}{2}}\phi'(0).$$
$$\Rightarrow \quad Re_x^{\frac{-1}{2}} Sh_x = -\sqrt{\frac{n+1}{2}}\phi'(0). \tag{3.33}$$

Here $Re_x = \frac{U_w x}{\nu}$ denotes the local Reynolds number.

3.3 Numerical Method for Solution

The system of nonlinear ordinary differential equations (3.23)-(3.25) along with the boundary conditions (3.26) has been tackled numerically using the shooting method based on the Runge–Kutta fourth-order method and Newton's method. The equations will be first transformed into a system of first-order differential equations by using the following notations:

$$f = Z_1, \quad f' = Z_1' = Z_2, \quad f'' = Z_1'' = Z_2' = Z_3,$$
$$\theta = Z_4, \quad \theta' = Z_4' = Z_5, \quad \theta'' = Z_4'' = Z_5',$$
$$\phi = Z_6, \quad \phi' = Z_6' = Z_7, \quad \phi'' = Z_6'' = Z_7'.$$

The equations (3.23)-(3.25) are transformed into the following system of first-order ODEs:

$$Z_1' = Z_2, \qquad Z_1(0) = S.$$
$$Z_2' = Z_3, \qquad Z_2(0) = 1 + V_s p.$$
$$Z_3' = \frac{\beta}{1+\beta}\left[\frac{2n}{n+1}{Z_2}^2 - Z_1 Z_3 - \frac{2}{n+1}(\gamma^* Z_4 + \gamma Z_6)cos\alpha \right.$$
$$\left. + \frac{2}{n+1}\left(M + \frac{1}{K_p}\right) Z_2 + \frac{2}{n+1} F_s {Z_2}^2\right], \qquad Z_3(0) = p.$$
$$Z_4' = Z_5, \qquad Z_4(0) = 1 + \lambda_t q,$$
$$Z_5' = -Pr Z_1 Z_5, \qquad Z_5(0) = q,$$
$$Z_6' = Z_7, \qquad Z_6(0) = 1 + \lambda_c r.$$

$$Z_7' = Sc\left[\frac{2}{n+1}K_c Z_6 + Z_1 Z_7\right], \qquad Z_7(0) = r.$$

RK-4 method has been applied for solving the above IVP. The domain of the problem is considered to be bounded i.e. $[0,\ \eta_\infty]$, where η_∞ represents a +ve real number, for which the variation in the solution is ignorable after $\eta = \eta_\infty$. The missing conditions p, q and r are to be chosen such that:

$$Z_2(\eta_\infty, p, q, r) = 0, \qquad Z_4(\eta_\infty, p, q, r) = 0, \qquad Z_6(\eta_\infty, p, q, r) = 0.$$

Newton's method will be used to find p, q and r. This method has the following iterative scheme:

$$\begin{bmatrix} p \\ q \\ r \end{bmatrix}_{(n+1)} = \begin{bmatrix} p \\ q \\ r \end{bmatrix}_{n} - \begin{bmatrix} \frac{\partial Z_2}{\partial p} & \frac{\partial Z_2}{\partial q} & \frac{\partial Z_2}{\partial r} \\ \frac{\partial Z_4}{\partial p} & \frac{\partial Z_4}{\partial q} & \frac{\partial Z_4}{\partial r} \\ \frac{\partial Z_6}{\partial p} & \frac{\partial Z_6}{\partial q} & \frac{\partial Z_6}{\partial r} \end{bmatrix}^{-1}_{(n)} \begin{bmatrix} Z_2 \\ Z_4 \\ Z_6 \end{bmatrix}_{(n)}.$$

To move further, the following notations have been introduced:

$$\begin{aligned}
&\frac{\partial Z_1}{\partial p} = Z_8, \quad \frac{\partial Z_2}{\partial p} = Z_9, \quad \frac{\partial Z_3}{\partial p} = Z_{10}, \quad \frac{\partial Z_4}{\partial p} = Z_{11}, \quad \frac{\partial Z_5}{\partial p} = Z_{12}, \\
&\frac{\partial Z_6}{\partial p} = Z_{13}, \quad \frac{\partial Z_7}{\partial p} = Z_{14} \quad \frac{\partial Z_1}{\partial q} = Z_{15}, \quad \frac{\partial Z_2}{\partial q} = Z_{16}, \quad \frac{\partial Z_3}{\partial q} = Z_{17}, \\
&\frac{\partial Z_4}{\partial q} = Z_{18}, \quad \frac{\partial Z_5}{\partial q} = Z_{19}, \quad \frac{\partial Z_6}{\partial q} = Z_{20}, \quad \frac{\partial Z_7}{\partial q} = Z_{21}, \quad \frac{\partial Z_1}{\partial r} = Z_{22}, \\
&\frac{\partial Z_2}{\partial r} = Z_{23}, \quad \frac{\partial Z_3}{\partial r} = Z_{24}, \quad \frac{\partial Z_4}{\partial r} = Z_{25}, \quad \frac{\partial Z_5}{\partial r} = Z_{26}, \quad \frac{\partial Z_6}{\partial r} = Z_{27}, \\
&\frac{\partial Z_7}{\partial r} = Z_{28}.
\end{aligned}$$

By using the above notations, the iterative scheme of Newton method is as follows:

$$\begin{bmatrix} p \\ q \\ r \end{bmatrix}_{(n+1)} = \begin{bmatrix} p \\ q \\ r \end{bmatrix}_{(n)} - \begin{bmatrix} Z_9 & Z_{16} & Z_{23} \\ Z_{11} & Z_{18} & Z_{25} \\ Z_{13} & Z_{20} & Z_{27} \end{bmatrix}^{-1}_{(n)} \begin{bmatrix} Z_2 \\ Z_4 \\ Z_6 \end{bmatrix}_{(n)}.$$

Now differentiating the last system of seven first order ODEs first with respect to p, then w.r.t q and finally with respect to r, we get twenty one more ODEs, as

follows:

$$Z_8' = Z_9, \qquad Z_8(0) = 0.$$

$$Z_9' = Z_{10}, \qquad Z_9(0) = V_s.$$

$$Z_{10}' = \frac{\beta}{1+\beta}\Bigg[\frac{4n}{n+1}Z_2Z_9 - Z_1Z_{10} - Z_3Z_8 - \frac{2}{n+1}(\gamma^* Z_{11} + \gamma Z_{13})cos\alpha + \frac{2}{n+1}\left(M + \frac{1}{K_p}\right)Z_9 + \frac{2}{n+1}2F_sZ_2Z_9\Bigg], \qquad Z_{10}(0) = 1.$$

$$Z_{11}' = Z_{12}, \qquad Z_{11}(0) = 0.$$

$$Z_{12}' = -Pr\Big[Z_1Z_{12} + Z_5Z_8\Big], \qquad Z_{12}(0) = 0.$$

$$Z_{13}' = Z_{14}, \qquad Z_{13}(0) = 0.$$

$$Z_{14}' = S_c\Big[\frac{2}{n+1}K_cZ_{13} - Z_1Z_{14} - Z_7Z_8\Big], \qquad Z_{14}(0) = 0.$$

$$Z_{15}' = Z_{16}, \qquad Z_{15}(0) = 0.$$

$$Z_{16}' = Z_{17}, \qquad Z_{16}(0) = 0.$$

$$Z_{17}' = \frac{\beta}{1+\beta}\Bigg[\frac{4n}{n+1}Z_2Z_{16} - Z_1Z_{17} - Z_3Z_{15} - \frac{2}{n+1}(\gamma^* Z_8 + \gamma Z_{20})cos\alpha + \frac{2}{n+1}\left(M + \frac{1}{K_p}\right)Z_{16} + \frac{2}{n+1}2F_sZ_2Z_{16}\Bigg], \qquad Z_{17}(0) = 0.$$

$$Z_{18}' = Z_{19}, \qquad Z_{18}(0) = \lambda_t.$$

$$Z_{19}' = -Pr\Big[Z_5Z_{15} + Z_1Z_{19}\Big], \qquad Z_{19}(0) = 1.$$

$$Z_{20}' = Z_{21}, \qquad Z_{20}(0) = 0.$$

$$Z_{21}' = S_c\Big[\frac{2}{n+1}K_cZ_{20} - Z_7Z_{15} - Z_1Z_{21}\Big], \qquad Z_{21}(0) = 0.$$

$$Z_{22}' = Z_{23}, \qquad Z_{22}(0) = 0.$$

$$Z_{23}' = Z_{24}, \qquad Z_{23}(0) = 0.$$

$$Z_{24}' = \frac{\beta}{1+\beta}\Bigg[\frac{4n}{n+1}Z_2Z_{23} - Z_1Z_{24} - Z_3Z_{22} - \frac{2}{n+1}(\gamma^* Z_{25} + \gamma Z_{27})cos\alpha + \frac{2}{n+1}\left(M + \frac{1}{K_p}\right)Z_{23} + \frac{2}{n+1}2F_sZ_2Z_{23}\Bigg], \qquad Z_{24}(0) = 0.$$

$$Z_{25}' = Z_{26}, \qquad Z_{25}(0) = 0.$$

$$Z_{26}' = -Pr\Big[Z_5Z_{22} + Z_1Z_{26}\Big], \qquad Z_{26}(0) = 0.$$

$$Z_{27}' = Z_{28}, \qquad Z_{27}(0) = \lambda_c.$$

$$Z_{28}' = S_c\Big[\frac{2}{n+1}K_cZ_{27} - Z_7Z_{22} - Z_1Z_{28}\Big], \qquad Z_{28}(0) = 1.$$

For the Newton's technique, the stopping criteria is as follows:

$$max\{\mid Z_2(\eta_\infty, p^n, q^n, r^n) \mid, \mid Z_4(\eta_\infty, p^n, q^n, r^n) \mid\}, \mid Z_6(\eta_\infty, p^n, q^n, r^n) \mid\} < \epsilon,$$

where $\epsilon > 0$ is an arbitrarily small number, which has been considered as 10^{-10}.

3.4 Results and Discussion of Graphs and Tables

In this section, we thoroughly discuss the influence of the dimensionless parameters on the skin friction coefficient $Re_x^{\frac{1}{2}} C_{f_x}$, Nusselt number $Re_x^{-\frac{1}{2}} Nu_x$, Sherwood number $Re_x^{-\frac{1}{2}} Sh_x$, velocity profile, temperature distribution and concentration profile through different graphs and tables.

The growing influence of the skin friction $Re_x^{\frac{1}{2}} C_{f_x}$ is evident in Table 3.1 as the Casson parameter β, the buoyancy parameters γ and γ^*, the velocity slip V_s, and the permiability porosity K_p rise. Increasing the values of the magnetic parameter M, Forchheimer parameter F_s, stretching index n, inclination α, suction parameter S, Prandtl number Pr, Schmidt number S_c, K_c the reaction rate parameter, slip parameters λ_t and λ_c, a decreasing effect on the skin friction $Re_x^{\frac{1}{2}} C_{f_x}$ can be seen.

By raising the permiability porosity K_p, stretching index n, suction parameter S, Prandtl number Pr, and buoyancy parameters γ and γ^*, the Nusselt number $Re_x^{-\frac{1}{2}} Nu_x$ is increased. Upon increasing the magnetic parameter M, Casson parameter β, Forchheimer parameter F_s, velocity slip V_s, inclination α, Schmidt number S_c, K_c, the reaction rate parameter, and slip parameters λ_t and λ_c, it is observed that the Nusselt number $Re_x^{-\frac{1}{2}} Nu_x$ is decreasing.

With raising the values of the response rate parameter K_c, the stretching index n, the suction parameter S, the buoyancy parameters γ and γ^*, the Schmidt number S_c, and the permiability porosity K_p, the Sherwood number $Re_x^{-\frac{1}{2}} Sh_x$ indicates an increasing trend. By increasing the magnetic parameter M, Casson parameter β, Forchheimer parameter F_s, velocity slip V_s, inclination α, Prandtl number Pr, and slip parameters λ_t and λ_c, a decreasing effect is noticed in the Sherwood number

$Re_x^{-\frac{1}{2}} Sh_x$.

Figure 3.2 shows how the velocity profile f' decreases as the magnetic parameter M increases. From a concrete point of view, it shows an inverse relationship between the magnetic parameter and the velocity due to Lorentz force. By rising the magnetic parameter the strength of the magnetic field increases, resulting in a stronger Lorentz force which slows down the fluid flow. Figure 3.3 reflects that the magnetic parameter causes an increases in the temperature. As the magnetic parameter M increases, the strength of the magnetic field increases, resulting in a stronger EMF. The increased EMF generates more heat, which shows an increasing effect in the temperature profile. A force, induced on the particles in the fluid by the magnetic field, is known as magnetophoretic force. A stronger magnetophoretic force is developed when the magnetic field increases by increasing the magnetic parameter M, which further drives the migration of particles towards the region with increased magnetic field strength thus increasing the concentration profile that is reflected in Figure 3.4.

Figure 3.5 illustrates how the velocity profile f' decreases as the Casson parameter β increases. The raising values of Casson parameter β decreases yield stress and suppress the velocity field. The fluid behaves Newtonian fluid as Casson parameter β becomes very large. Figure 3.6 displays the influence of Casson parameter β. A rise in the value of β increases the temperature profile. It is noticed that an increases in the temperature profile along the thermal boundary layer is observed with an enchancement in the Casson parameter as well as the thickness of thermal boundary layer increases. Figure 3.7 describes the impact of Casson parameter β on ϕ. By increasing the values of Casson parameter β, concentration profile also increases. Likewise, the solutal boundary layer thickness increases with increasing values of Casson parameter β.

Figures 3.8-3.10 display the impact of permeability porosity K_p on the velocity, temperature and concentration distributions. It is noticed that permeability porosity K_p increases the velocity, because an increase in the permeability of medium implies less resistance due to the porous matrix present in the medium while it decreases the temperature and concentration.

Figure 3.11 illustrates the effect of the Forchheimer parameter F_s on the velocity profile, demonstrating that as F_s increases, the velocity profile decreases. The

Forchheimer parameter F_s, is the measure of nonlinear drag force on a fluid caused by a porous medium. The drag force is increased with the rise of F_s, opposing the fluid flow and reducing its velocity. Figures 3.12 and 3.13 depict the impact of Forchheimer parameter F_s on temperature and concentration profiles. It is found that the temperature and concentration profiles are increased as Forchheimer parameter F_s values rise.

The stretching index n represents the non-Newtonian behavior of the fluid flow. Figures 3.14-3.16 display the impact of stretching index n on the velocity, temperature and concentration profiles. It has been noted that the velocity and concentration profiles are increased as the stretching index n is enhanced while it decreases the temperature distribution.

Figure 3.17 illustrates the impact of the velocity slip parameter V_s on the velocity field, showing that the thickness of the velocity boundary layer of the velocity decrease as the value of the velocity slip parameter V_s increases. Figures 3.18 and 3.19 show the impact of the velocity slip parameter V_s on temperature and concentration distributions, respectively. As the velocity slip parameter V_s increases, the temperature and concentration profiles also increase.

Figures 3.20-3.22 demonstrate the impact of inclination angle α on the velocity f', temperature θ and concentration ϕ profiles. As the inclination angle α increases, the velocity of the nanofluid flow decreases, due to a decrease in the shear stress. Meanwhile, the temperature and concentration distributions increase with increasing α.

Figure 3.23 shows that an increase in the suction parameter S reduces the fluid's momentum, resulting in a decrease in the velocity. Figures 3.24 and 3.25 illustrate the effects of the suction parameter S on the temperature and concentration profiles. Enhanced suction results in the removal of fluid from the boundary layer, leading to a reduction in temperature and concentration.

Figures 3.26 and 3.29 illustrate the impact of the solutal buoyancy parameters γ and γ^* on velocity profiles. As the solutal buoyancy parameters γ and γ^* increase, the velocity profile f' also increases due to buoyancy force. With rising the solutal buoyancy parameters γ and γ^* the density difference between the fluid and the ambient fluid grows, resulting in a stronger buoyancy force. Figures 3.27 and 3.30 illustrate the impact of γ and γ^* on the temperature profiles. As the parameters

γ and γ^* increase, the buoyancy force intensifies, causing the fluid to rise more rapidly and enhancing convective heat transfer. This leads to a decrease in both temperature profiles. Similarly, Figures 3.28 and 3.31 show that the concentration distribution also decreases with increasing γ and γ^*.

Figures 3.32 and 3.33 show the impact of the Prandtl number Pr on the velocity and temperature profiles, respectively. It is evident that as the value of Pr increases, the velocity and temperature profiles transform into decreasing functions, indicating a significant impact of the Prandtl number on the flow and thermal characteristics of the fluid. Figure 3.34 reveals that the concentration profile ϕ exhibits an increase in response to an increase in the Prandtl number Pr.

Figure 3.35 displays how the Schmidt number S_c affects the velocity profile f'. As Schmit number S_c increases, the fluid velocity decreases due to a decline in mass diffusivity, which in turn reduces the momentum diffusivity. When Schmidt number S_c is enhanced, it can cause the thermal boundary layer to become thicker, leading to a reduction in the convective heat transfer and an increase in the heat retention within the fluid. This leads to a higher temperature profile, as seen in Figure 3.36. Figure 3.37 reflects that as the value of Schmidt number S_c increases, the concentration ϕ changes into a decreasing function due to a rise in the mass transfer rate. This is due to the inverse proportionality between Schmidt number S_c and the diffusion coefficient, which leads to a decrease in diffusion and a subsequent decline in concentration.

Figure 3.38 shows the impact of the reaction rate parameter K_c on f'. As the reaction rate parameter K_c increases, larger consumption of reactants occurs, leading to decrease the momentum, increased resistance to flow, and thicker boundary layer. Consequently, the velocity profile decreases, indicating a slow down the fluid flow. Figure 3.39 shows that increasing the reaction rate parameter K_c leads to a rise in temperature. As illustrated in Figure 3.40, raising the K_c values decreases the concentration distribution ϕ.

Figure 3.41 illustrates the effect of increasing the slip parameter λ_t on the fluid flow. An increase in the slip parameter λ_t leads to a decrease in the velocity due to an increase in the slip velocity of the fluid on the wall. This increase in the slip velocity results in a higher velocity gradient near the wall, causing a greater shear stress that opposes the fluid motion and reduces its velocity. Elevating the slip

parameter λ_t will improve fluid motion on and near the solid boundary, leading to an enhanced heat convection, minimized resistance and therefore, a lowered temperature profile as seen in Figure 3.42. By increasing the value of the slip parameter λ_t, the slip velocity increases, enhancing the fluid flow and leading to a steeper concentration gradient. As a result, the concentration distribution is increased, as shown in Figure 3.43.

Figures 3.44-3.46 depict the impact of the slip parameter λ_c on velocity, temperature and concentration profiles, respectively. An increment in the slip parameter λ_c has dual effects: it reduces both velocity and concentration, while simultaneously increasing the temperature profile.

TABLE 3.1: Numerical Results of Skin Friction, Nusselt Number, and Sherwood Number

M	β	K_p	Fs	n	Vs	α	S	γ	γ^*	Pr	Sc	K_c	Λ_t	Λ_c	$Re_x^{\frac{1}{2}} Cf_x$	$Re_x^{-\frac{1}{2}} Nu_x$	$Re_x^{-\frac{1}{2}} Sh_x$
1	0.5	1	1	1	0.2	0.2	0.2	0.5	0.5	1	1	0.5	1	1	-2.4756	0.4029	0.5049
0.01															-2.1278	0.4159	0.5094
0.2															-2.2004	0.4133	0.5085
	0.2														-3.7775	0.4241	0.5125
	0.3														-3.1050	0.4147	0.5090
		0.9													-2.5105	0.4015	0.5044
		1.5													-2.3663	0.4070	0.5063
			0.8												-2.4396	0.4038	0.5052
			1.2												-2.5106	0.4019	0.5045
				0.8											-2.3952	0.3803	0.4854
				1.5											-2.6627	0.4546	0.5499
					0.6										-1.7486	0.3814	0.4949
					1										-1.3596	0.3670	0.4890
						1									-2.5691	0.3994	0.5037
						1.5									-2.6720	0.3953	0.5023
							0.5								-2.6140	0.4740	0.5483
							1								-2.8352	0.5679	0.6118
								0.2							-2.5265	0.4011	0.5043
								0.8							-2.4251	0.4046	0.5055
									0.3						-2.5244	0.4009	0.5042
									0.9						-2.3805	0.4065	0.5061
										0					-2.3010	0.1111	0.5083
										0.5					-2.4183	0.2921	0.5060
											0.5				-2.4342	0.4052	0.4040
											1.5				-2.4961	0.4019	0.5653
												0.2			-2.4585	0.4037	0.4551
												1			-2.4923	0.4021	0.5581
													0.5		-2.4451	0.5063	0.5053
													1.4		-2.4924	0.3464	0.5047
														0.5	-2.4471	0.4038	0.6760
														1.2	-2.4833	0.4026	0.4585

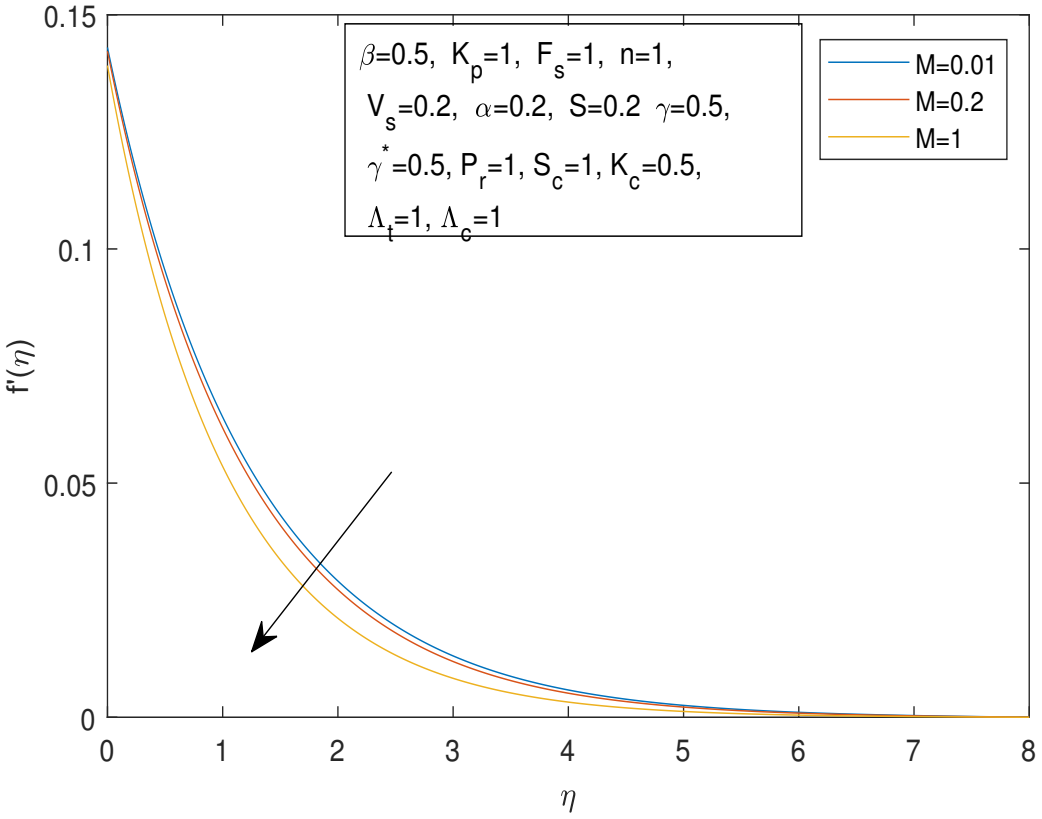

FIGURE 3.2: Velocity Profile $f'(\eta)$ and η against M

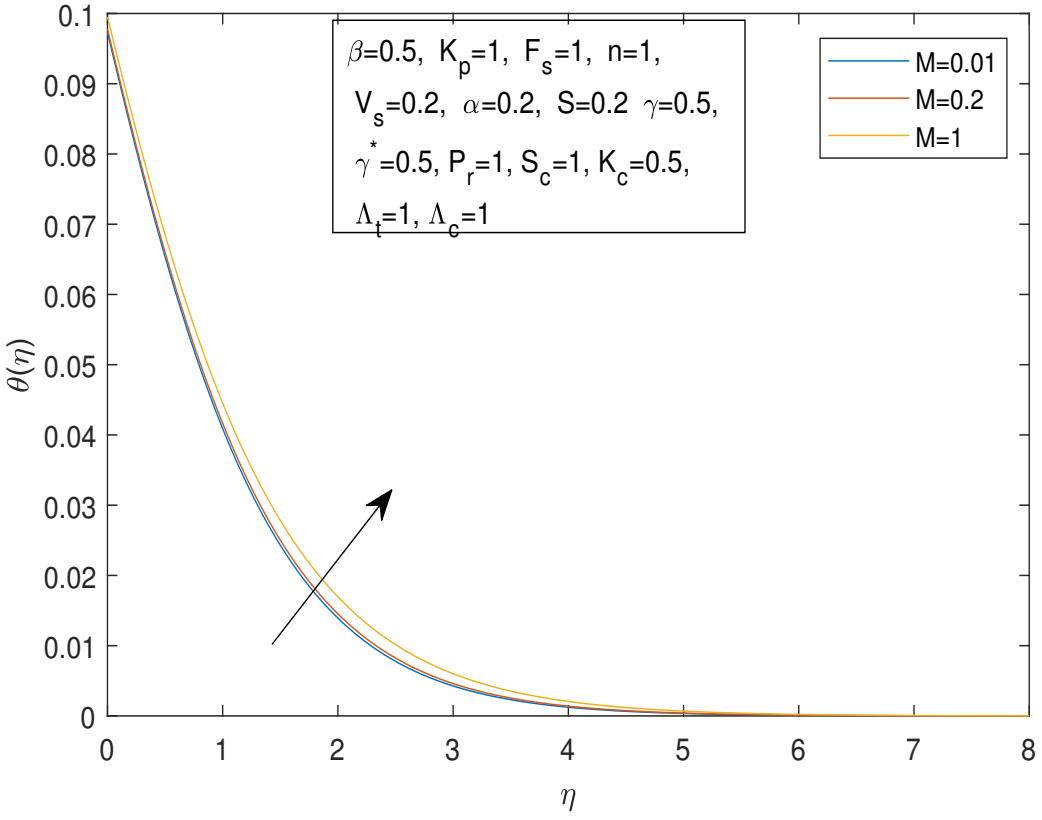

FIGURE 3.3: Temperature Profile $\theta(\eta)$ and η against M

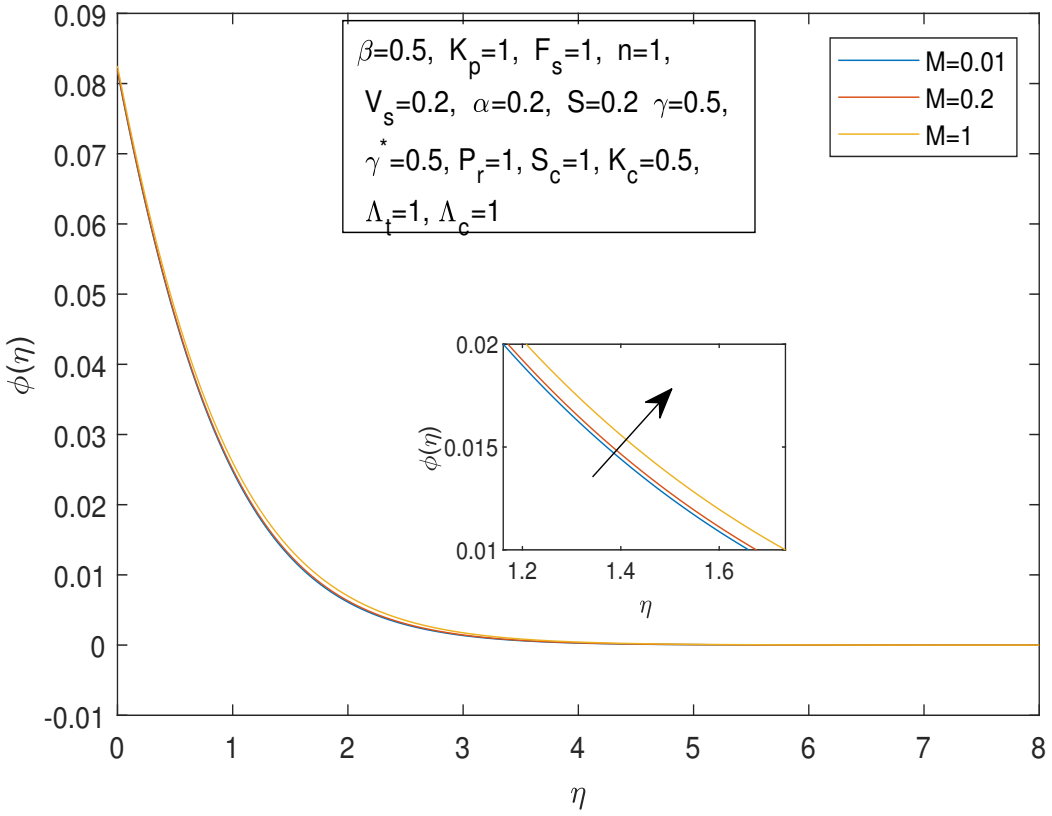

FIGURE 3.4: Concentration Profile $\phi(\eta)$ and η against M

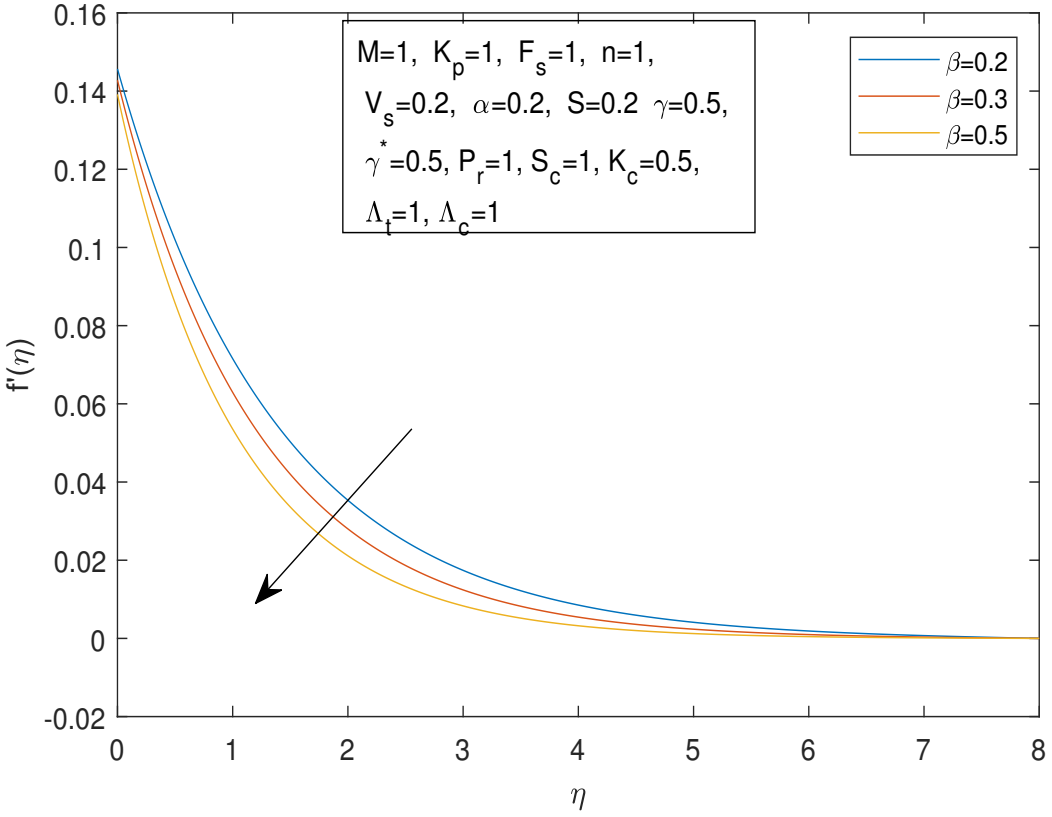

FIGURE 3.5: Velocity Profile $f'(\eta)$ and η against β

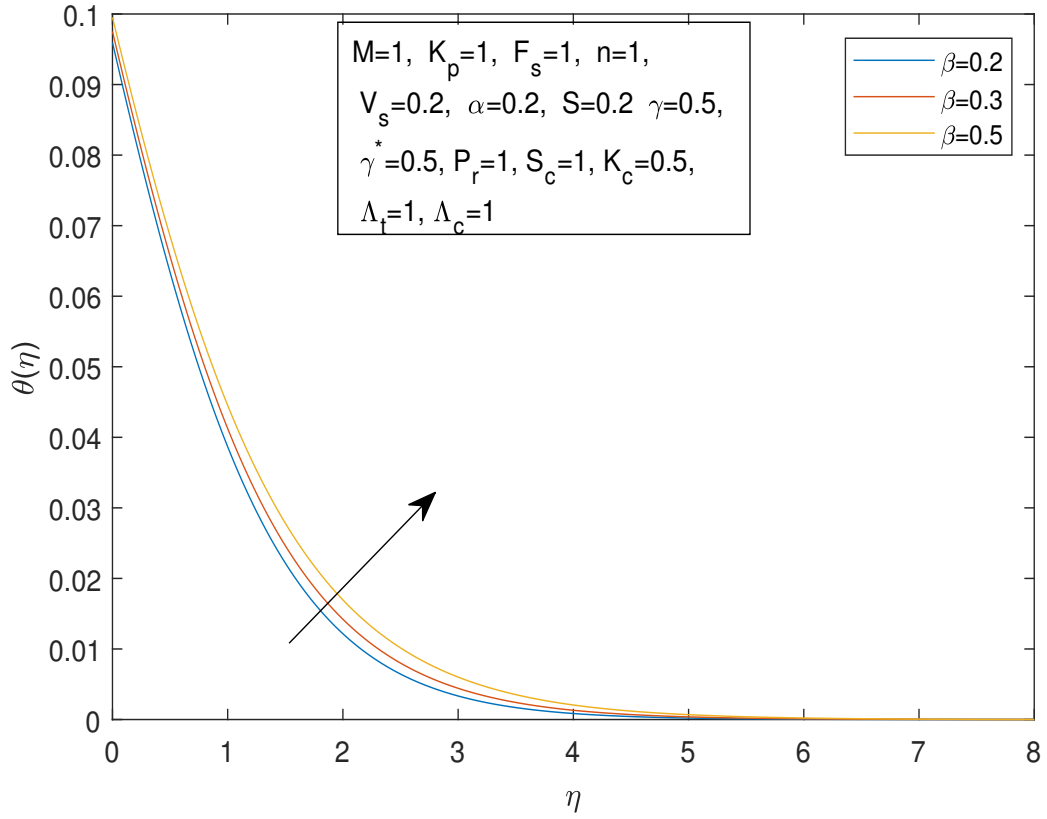

FIGURE 3.6: Temperature Profile $\theta(\eta)$ and η against β

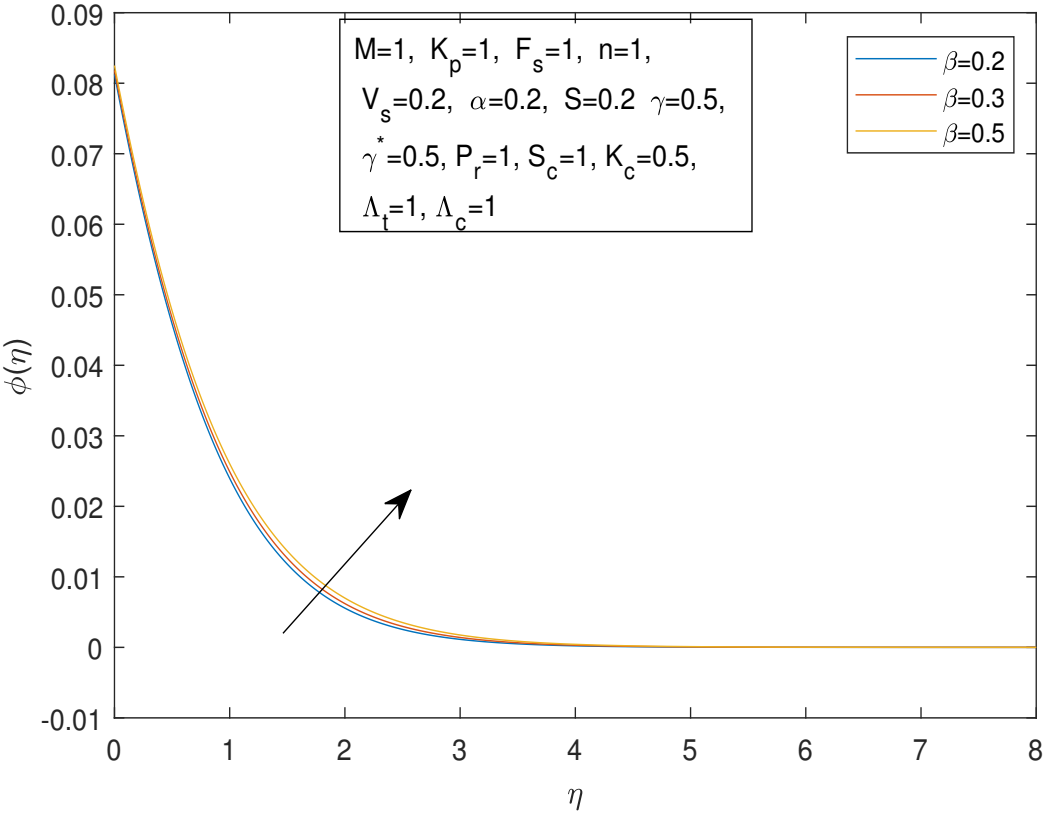

FIGURE 3.7: Concentration Profile $\phi(\eta)$ and η against β

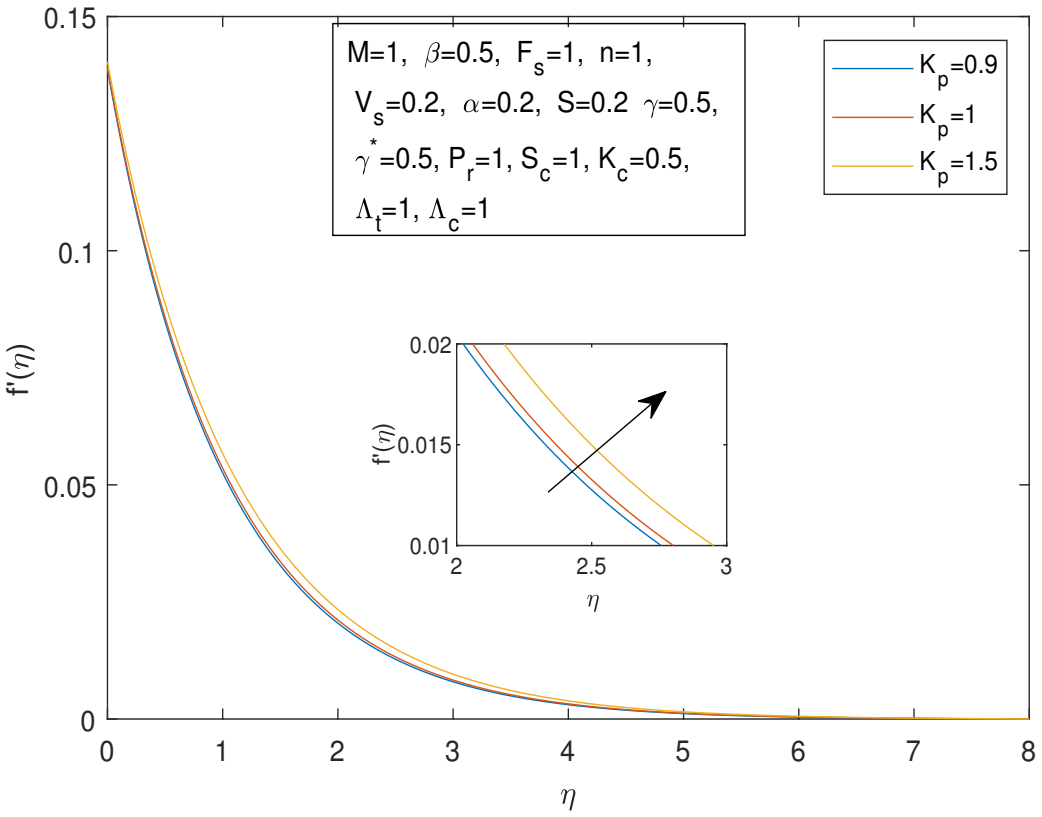

FIGURE 3.8: Velocity Profile $f'(\eta)$ and η against K_p

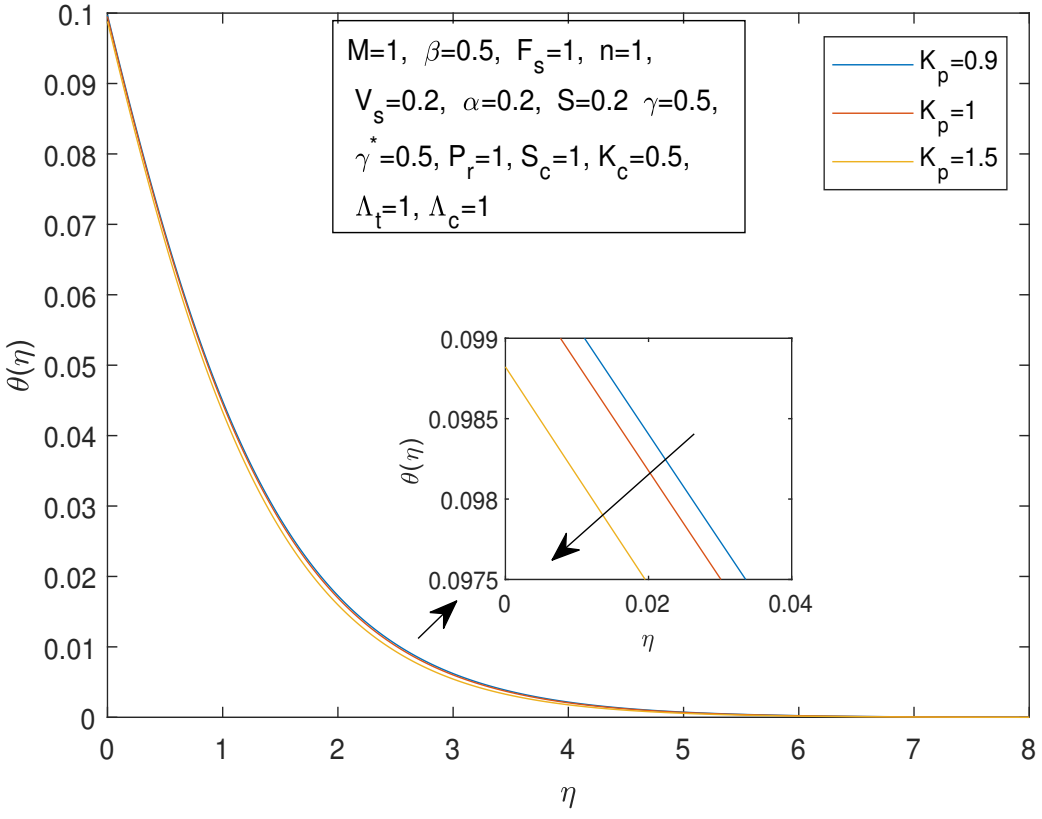

FIGURE 3.9: Temperature Profile $\theta(\eta)$ and η against K_p

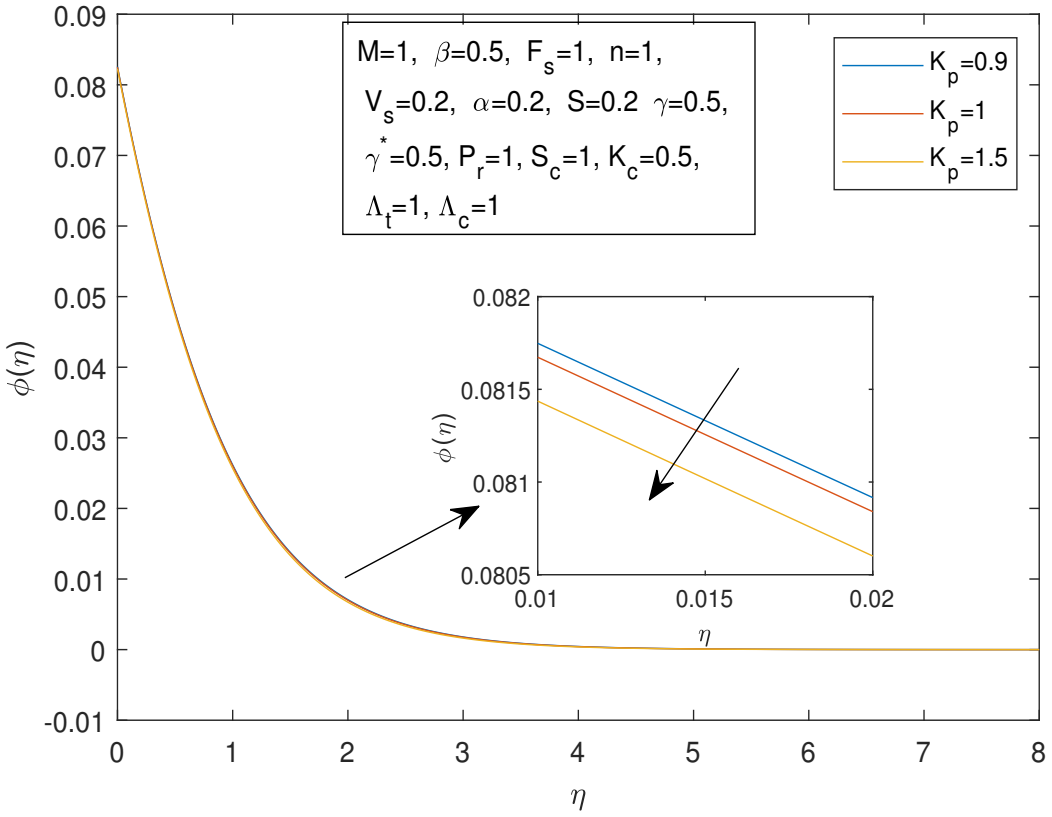

FIGURE 3.10: Concentration Profile $\phi(\eta)$ and η against K_p

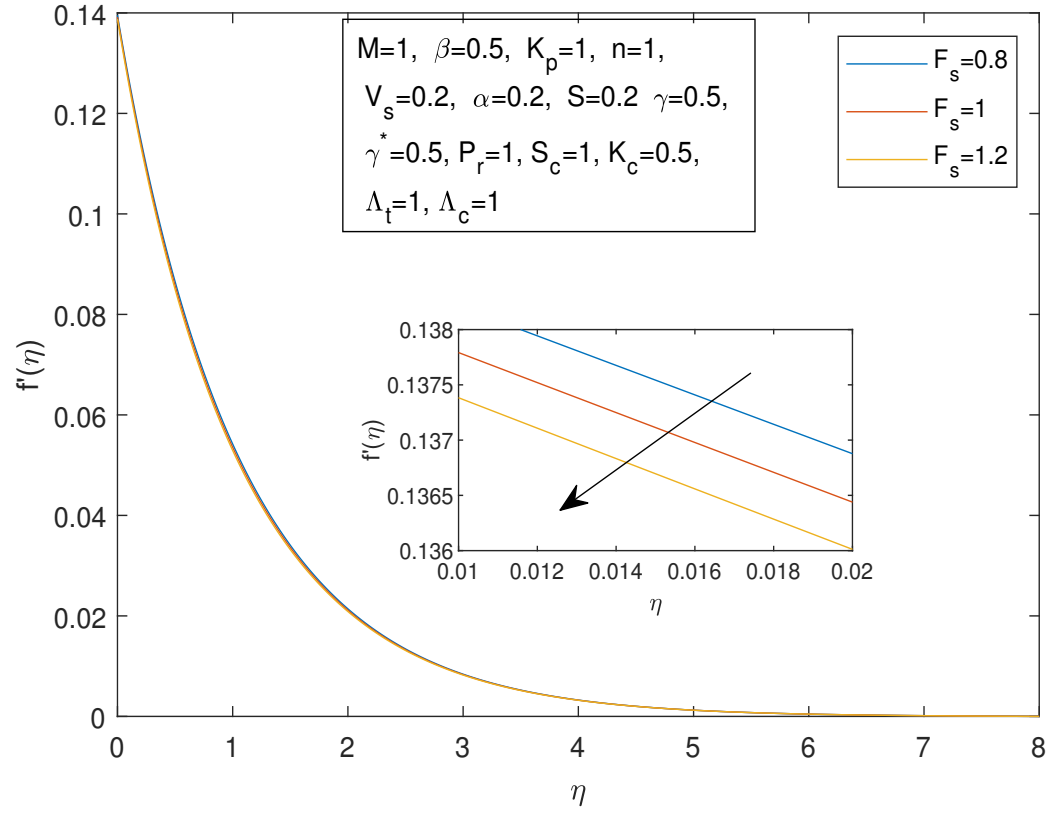

FIGURE 3.11: Velocity Profile $f'(\eta)$ and η against Fs

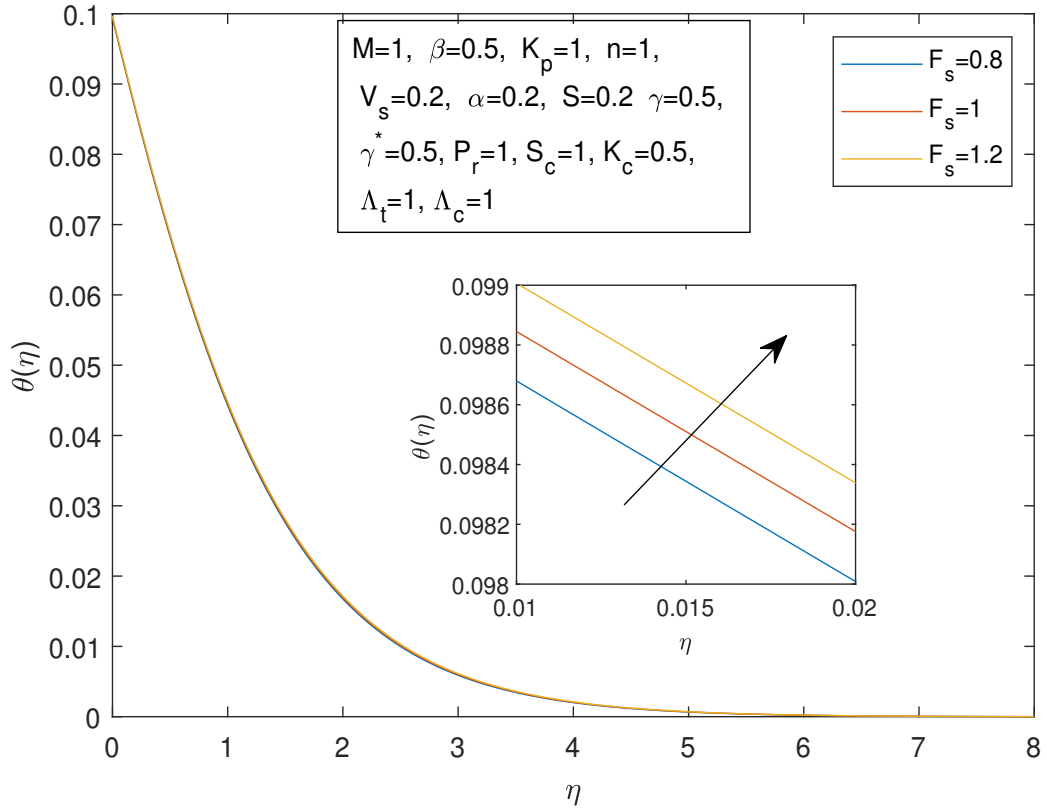

FIGURE 3.12: Temperature Profile $\theta(\eta)$ and η against Fs

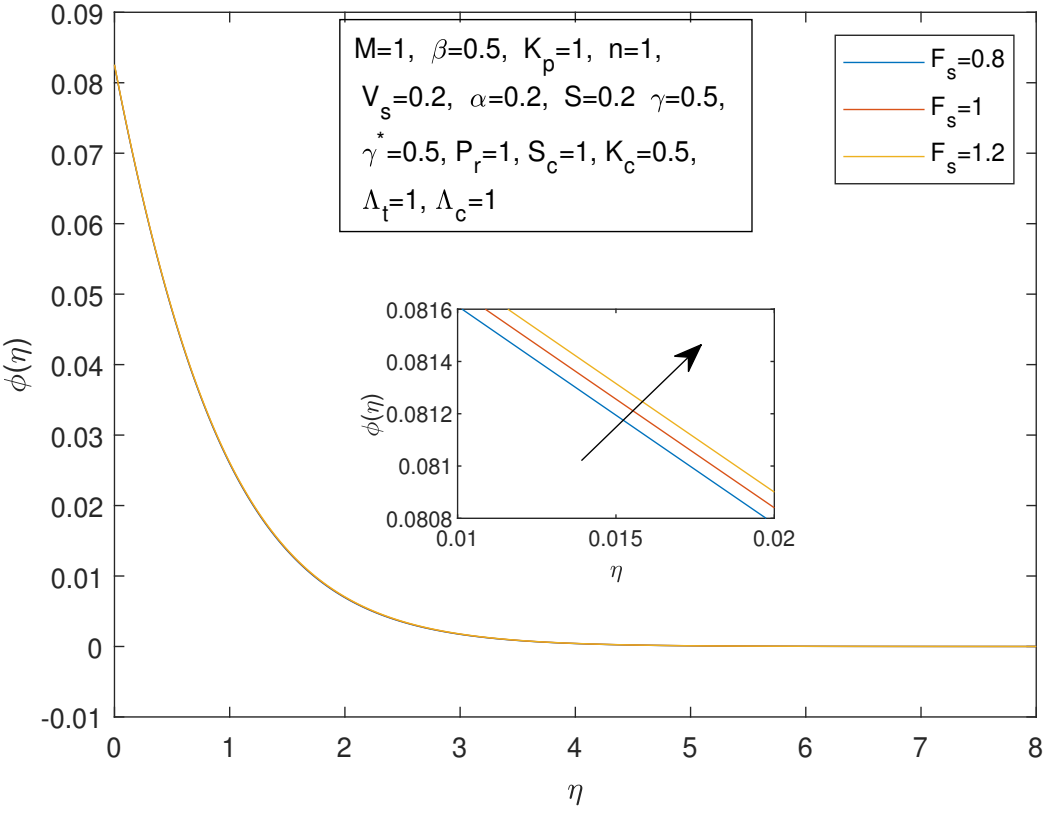

FIGURE 3.13: Concentration Profile $\phi(\eta)$ and η against Fs

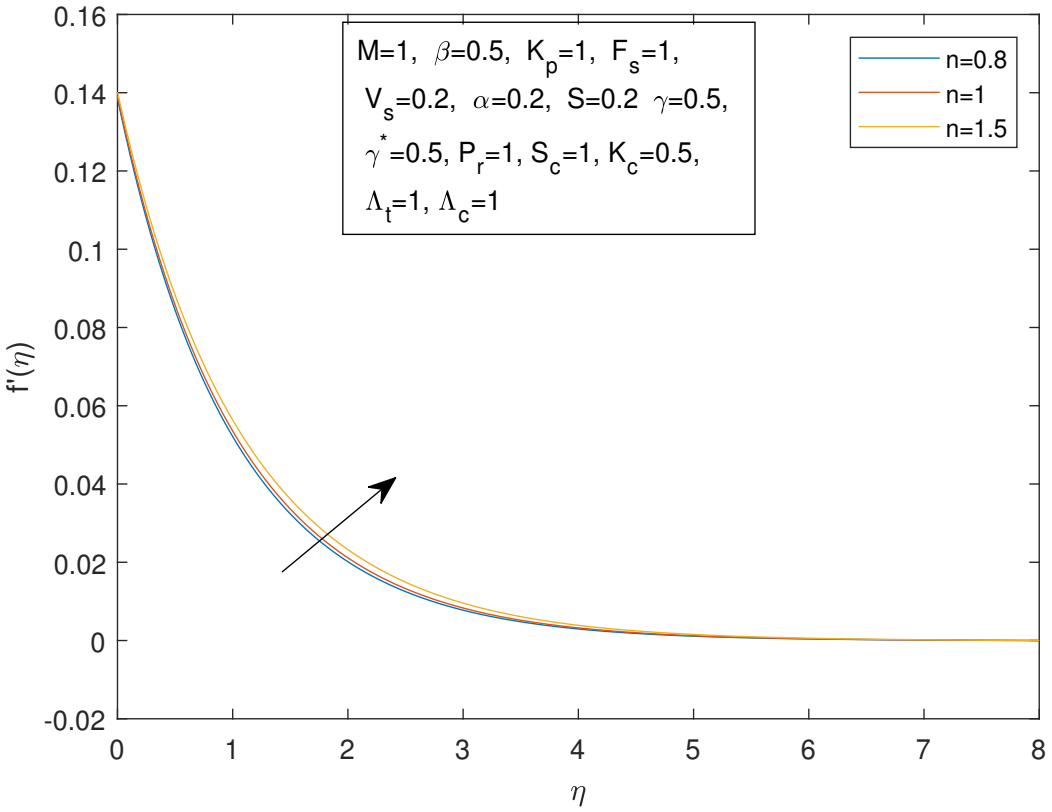

FIGURE 3.14: Velocity Profile $f'(\eta)$ and η against n

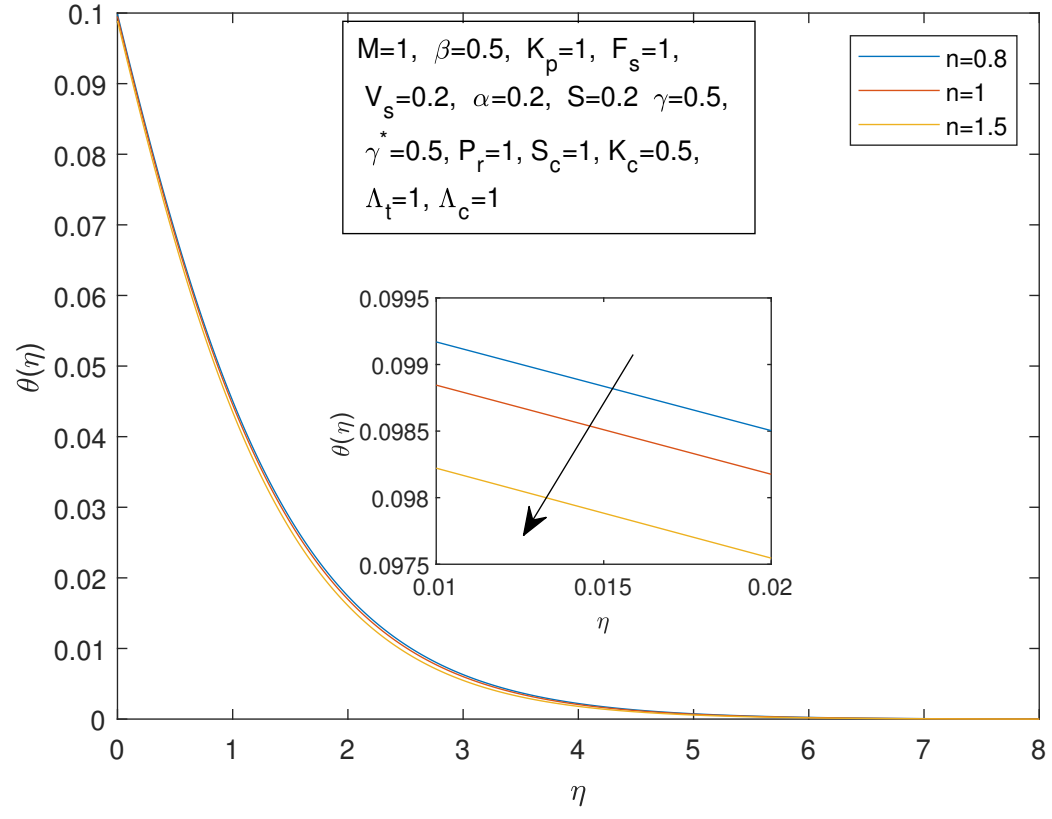

FIGURE 3.15: Temperature Profile $\theta(\eta)$ and η against n

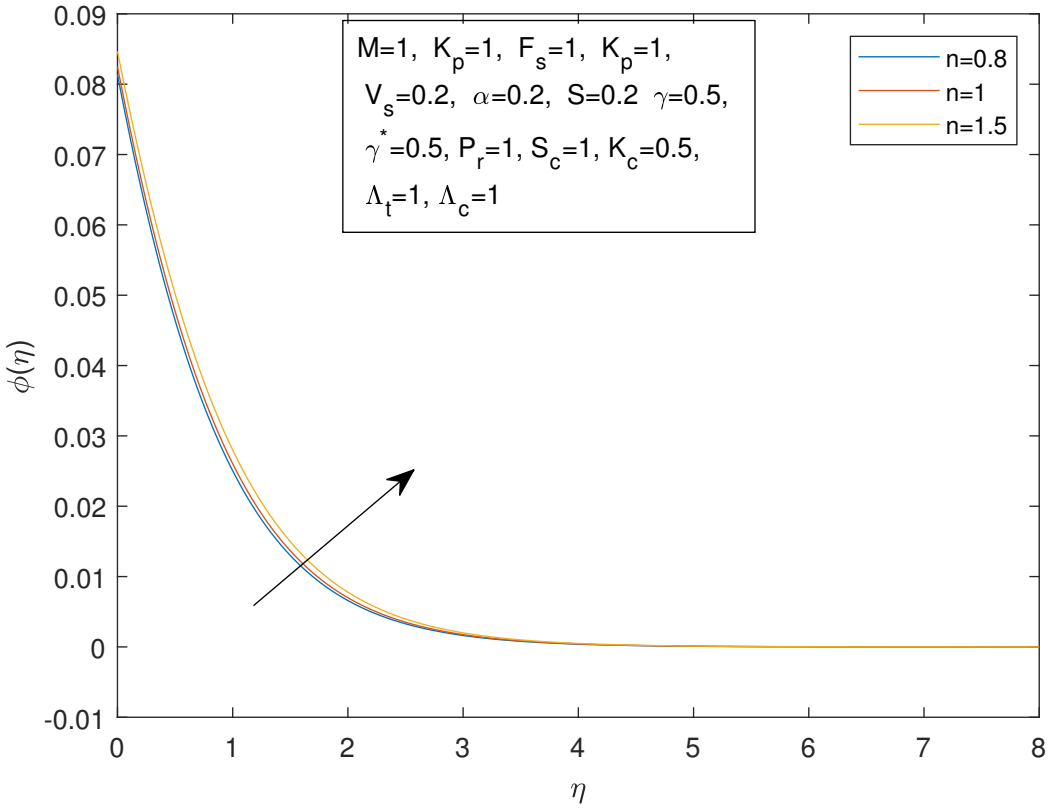

FIGURE 3.16: Concentration Profile $\phi(\eta)$ and η against n

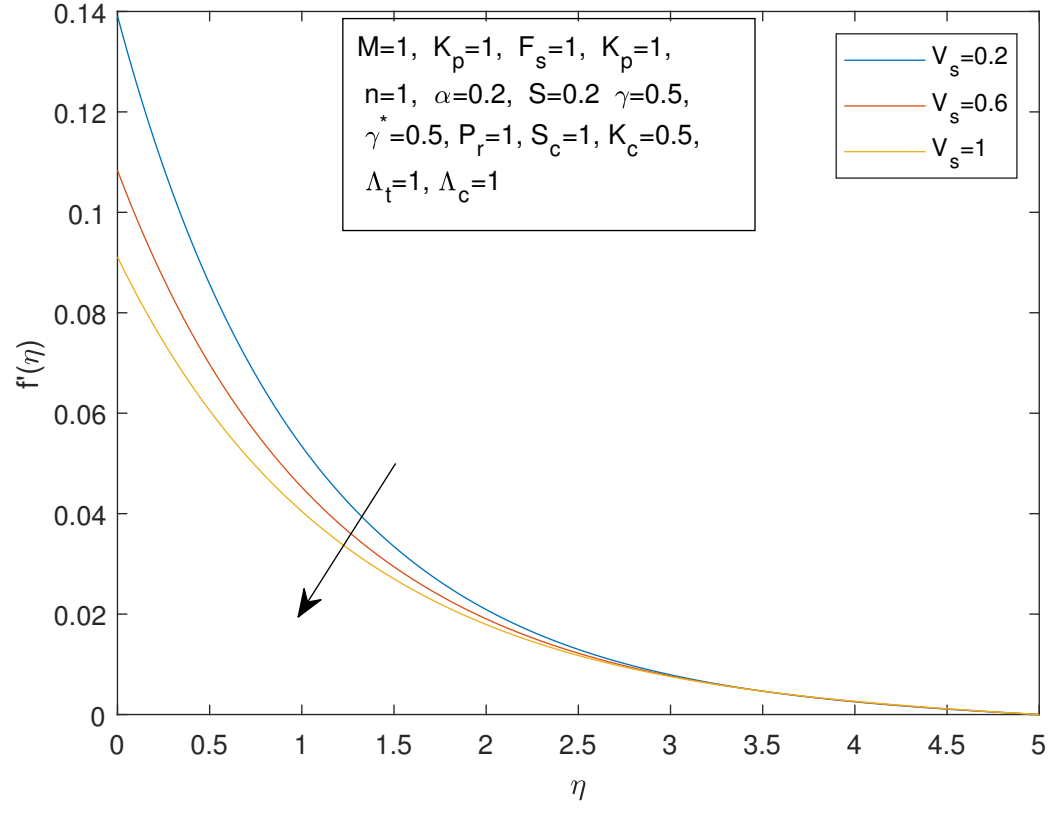

FIGURE 3.17: Velocity Profile $f'(\eta)$ and η against Vs

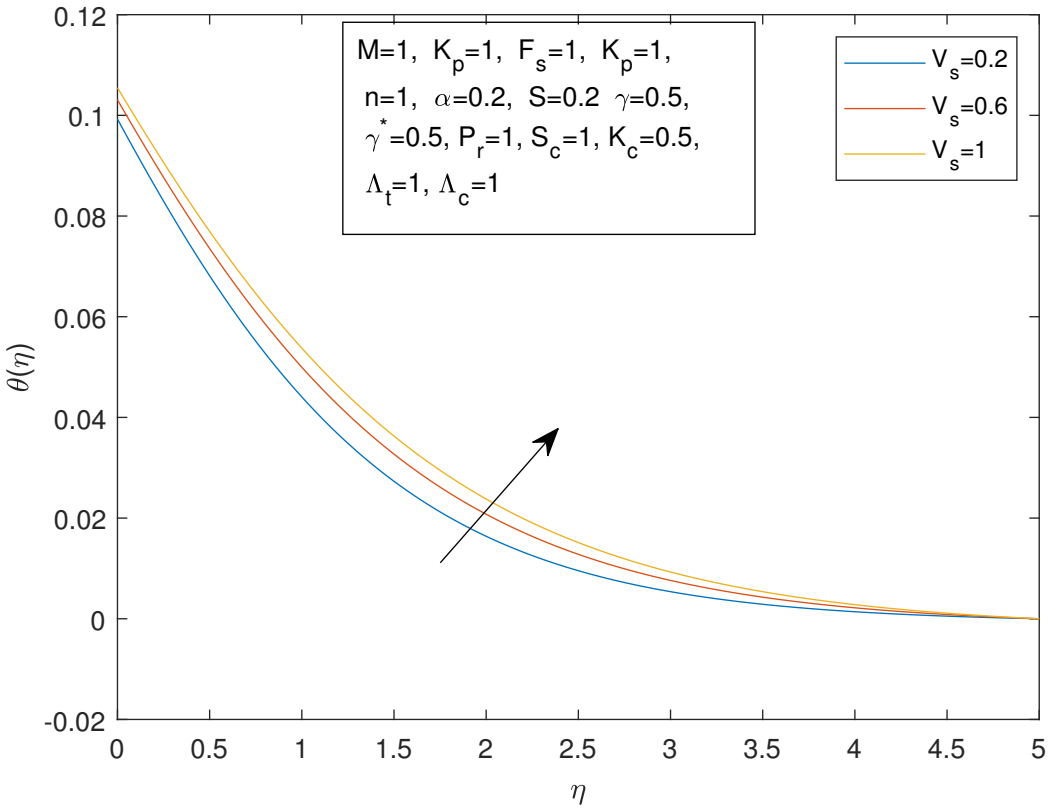

FIGURE 3.18: Temperature Profile $\theta(\eta)$ and η against Vs

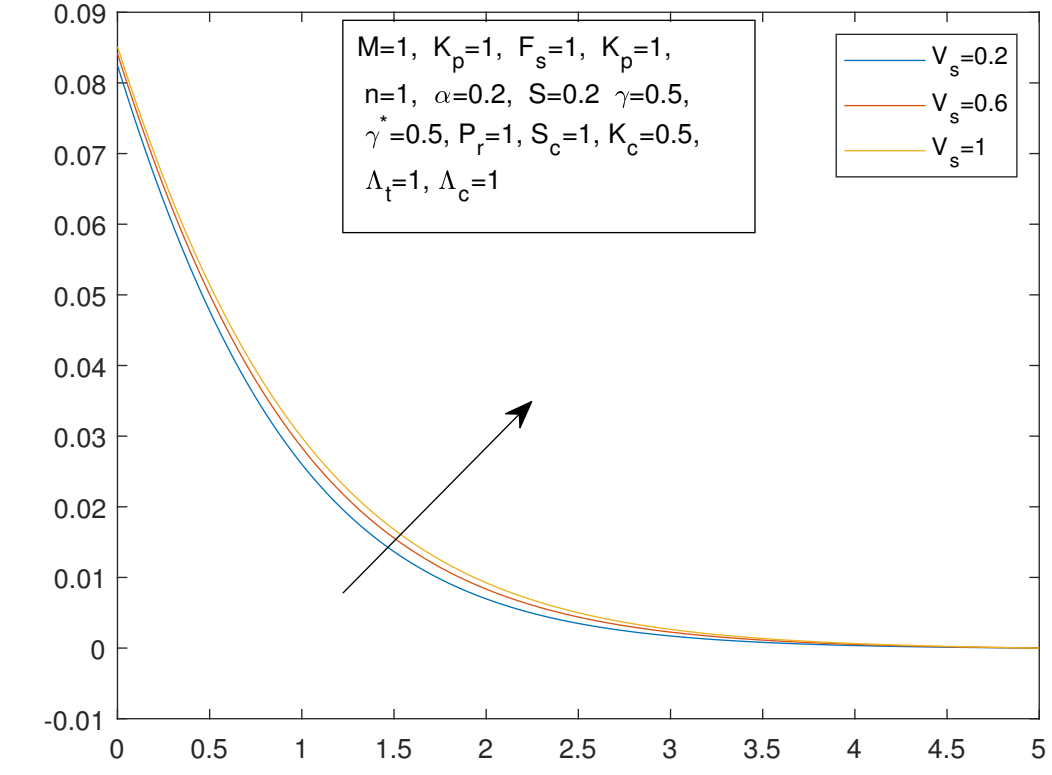

FIGURE 3.19: Concentration Profile $\phi(\eta)$ and η against Vs

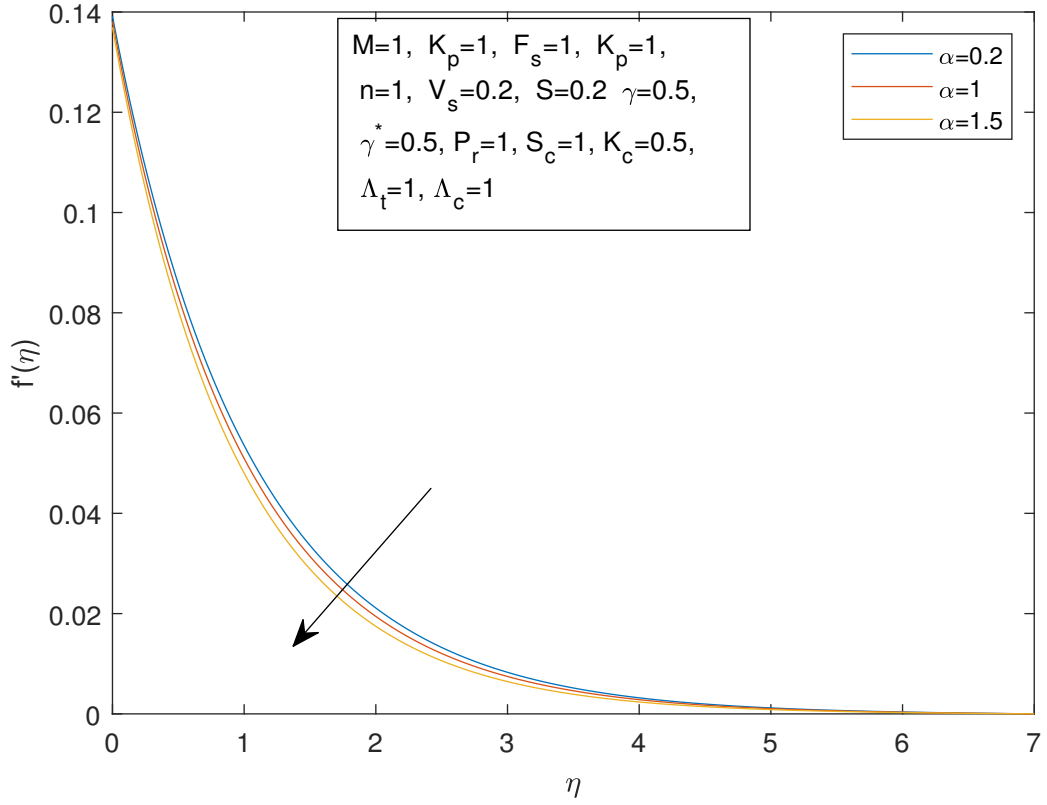

FIGURE 3.20: Velocity Profile $f'(\eta)$ and η against α

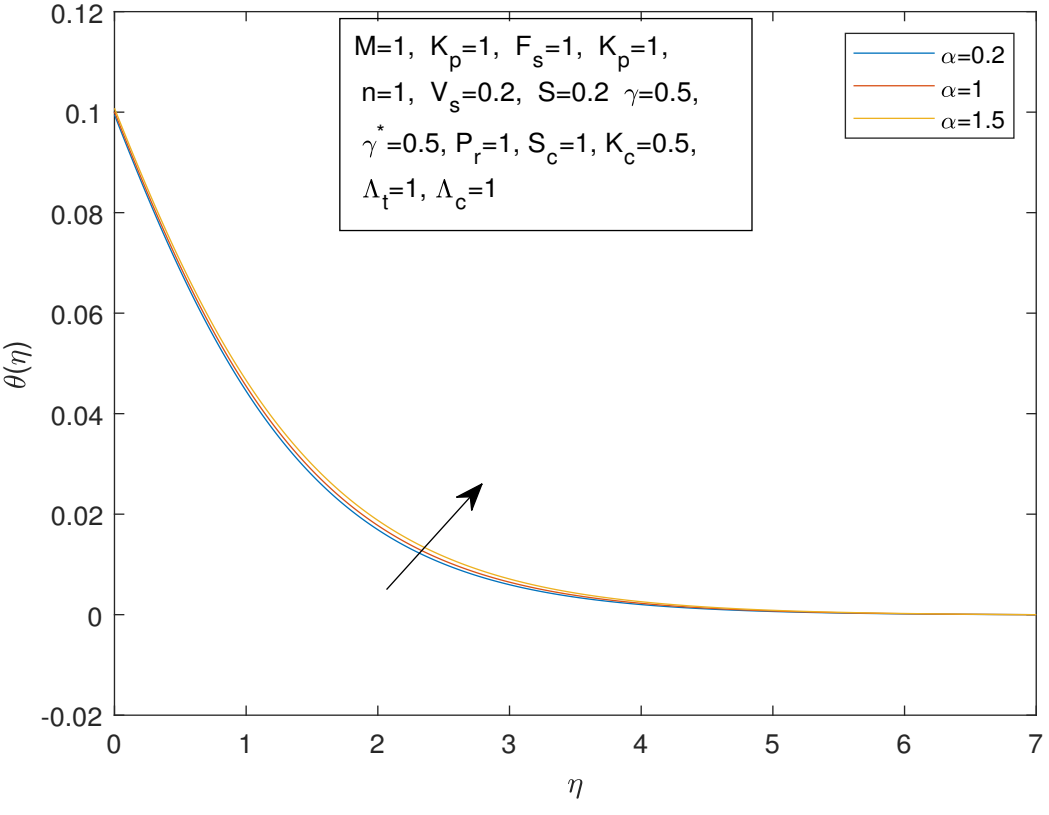

FIGURE 3.21: Temperature Profile $\theta(\eta)$ and η against α

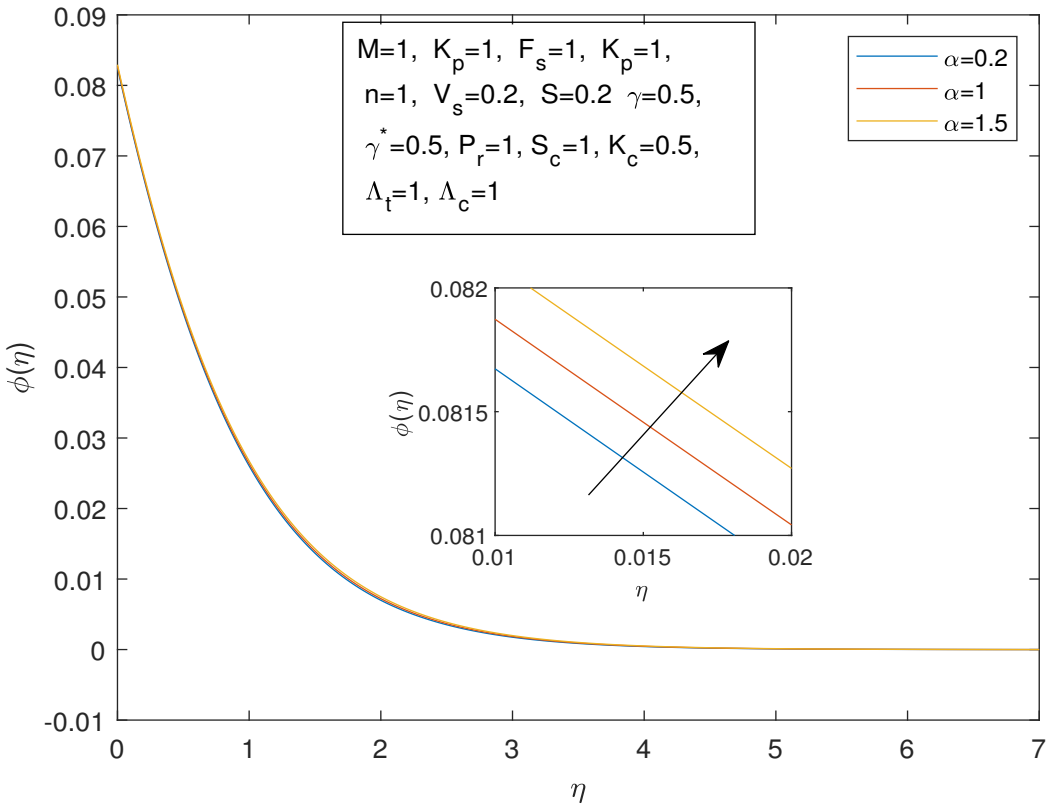

FIGURE 3.22: Concentration Profile $\phi(\eta)$ and η against α

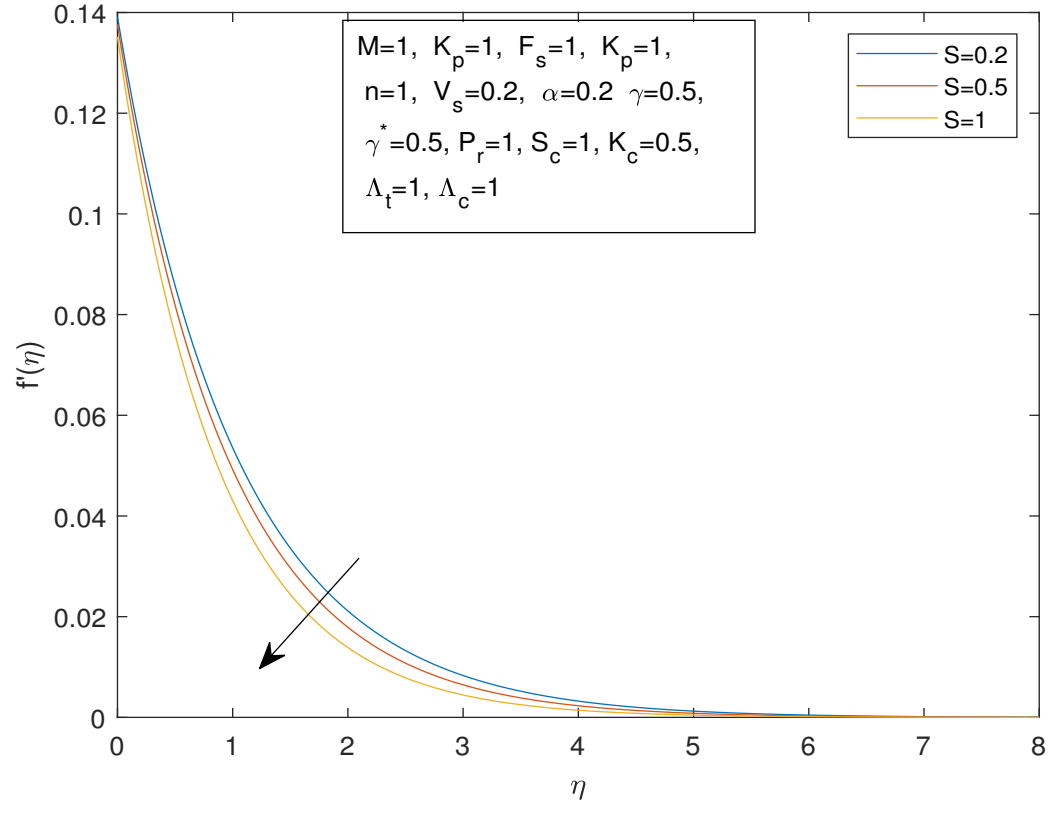

FIGURE 3.23: Velocity Profile $f'(\eta)$ and η against S

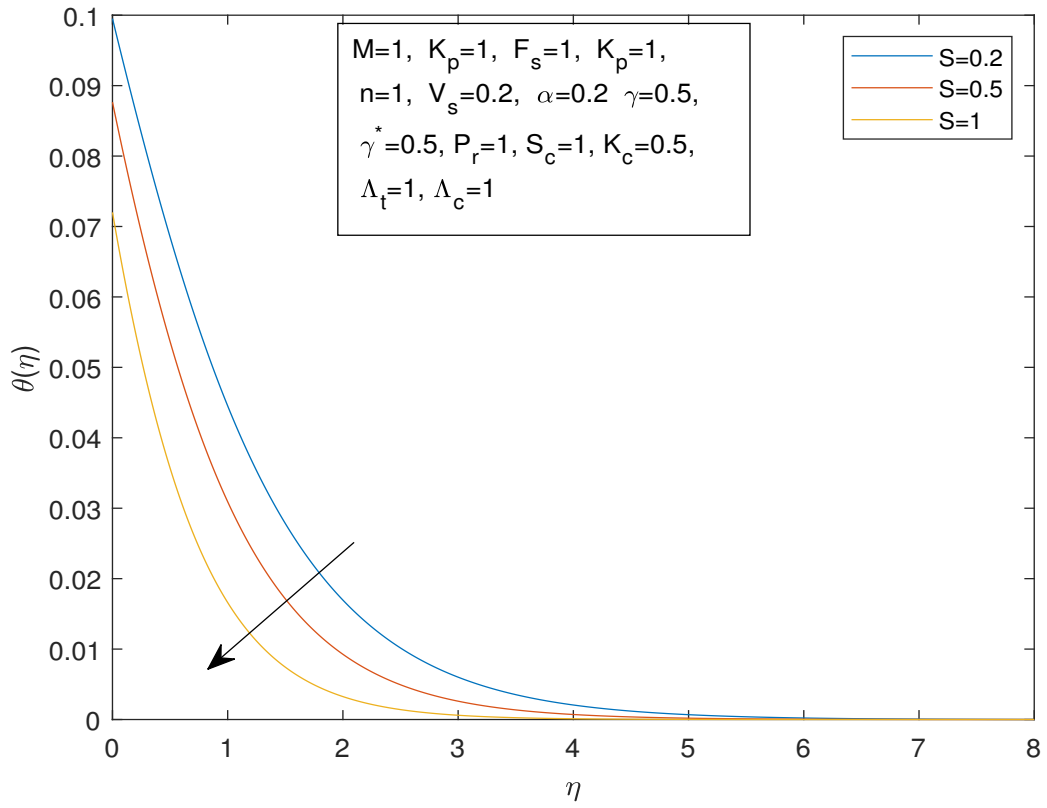

FIGURE 3.24: Temperature Profile $\theta(\eta)$ and η against S

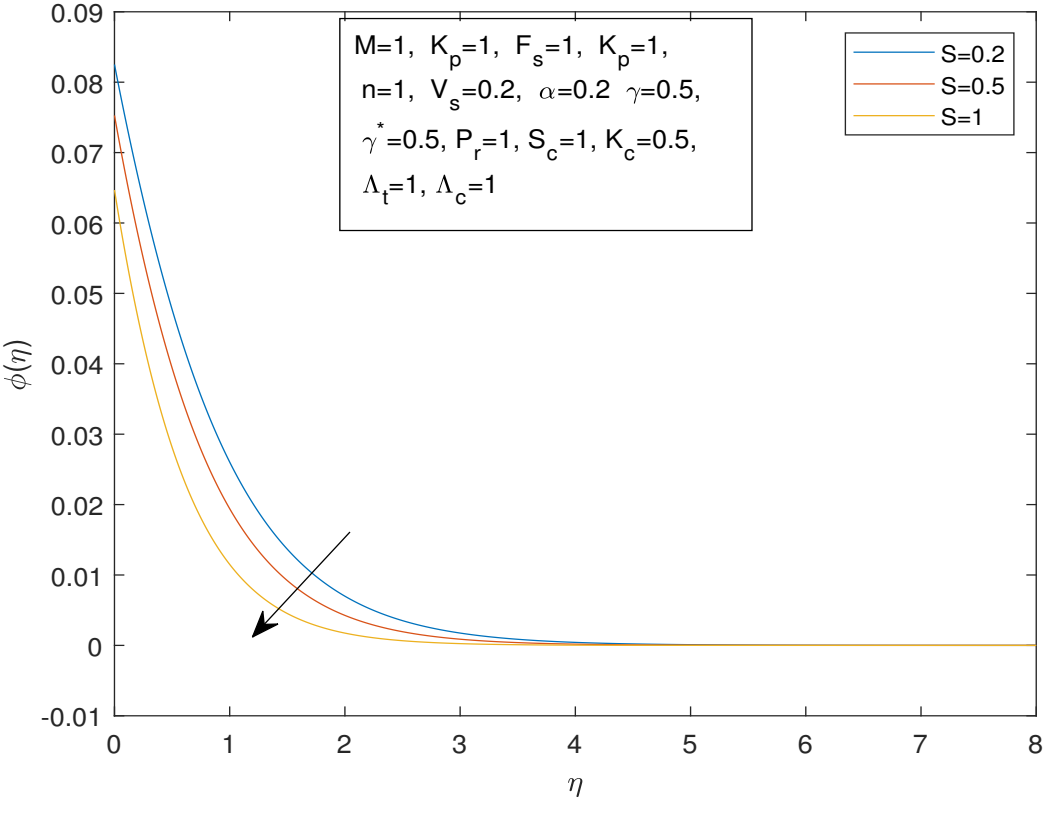

FIGURE 3.25: Concentration Profile $\phi(\eta)$ and η against$S$

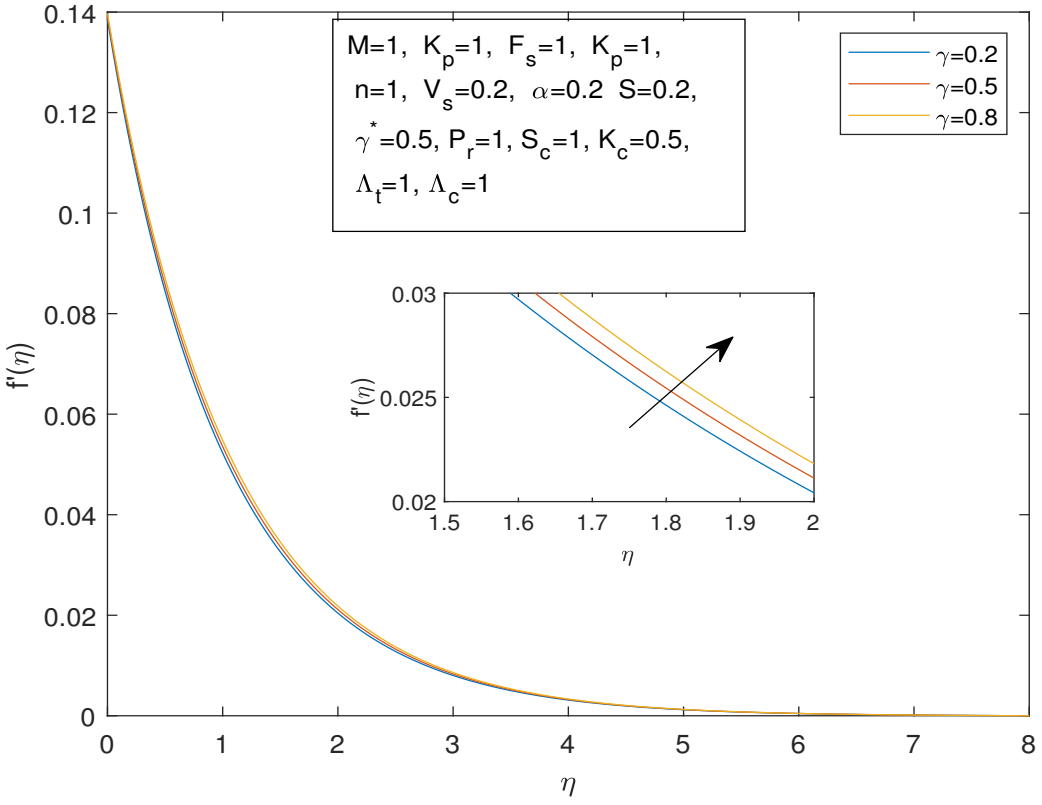

FIGURE 3.26: Velocity Profile $f'(\eta)$ and η against γ

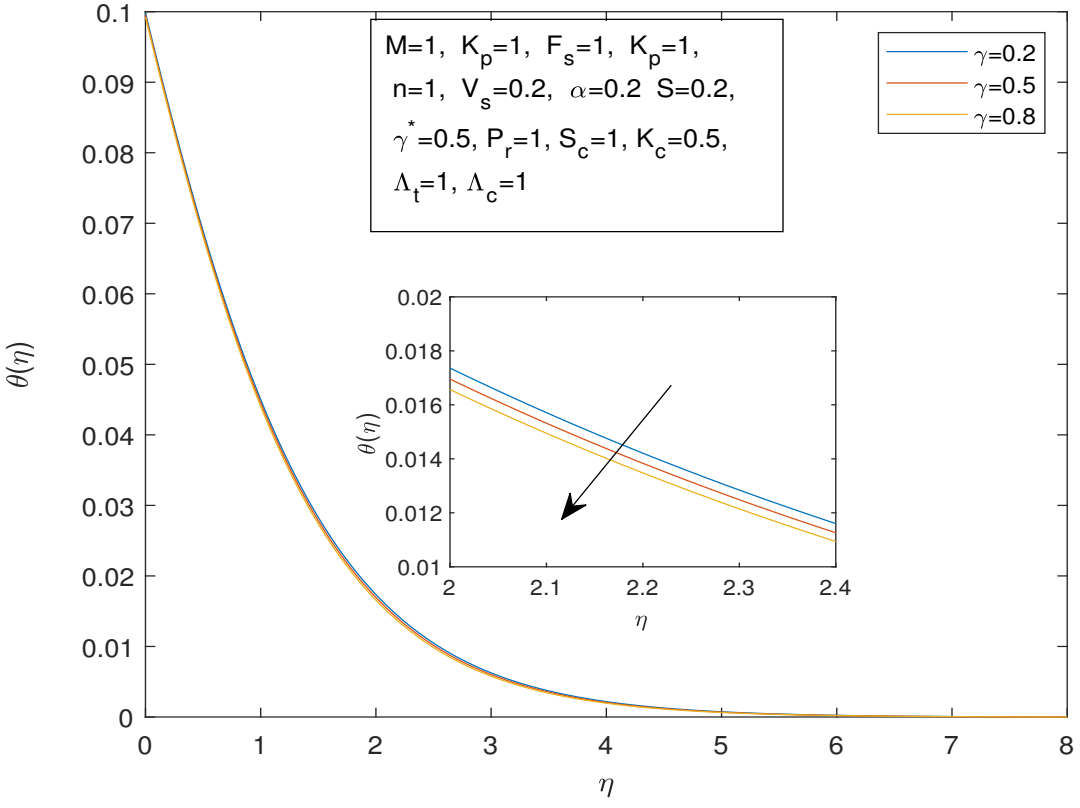

FIGURE 3.27: Temperature Profile $\theta(\eta)$ and η against γ

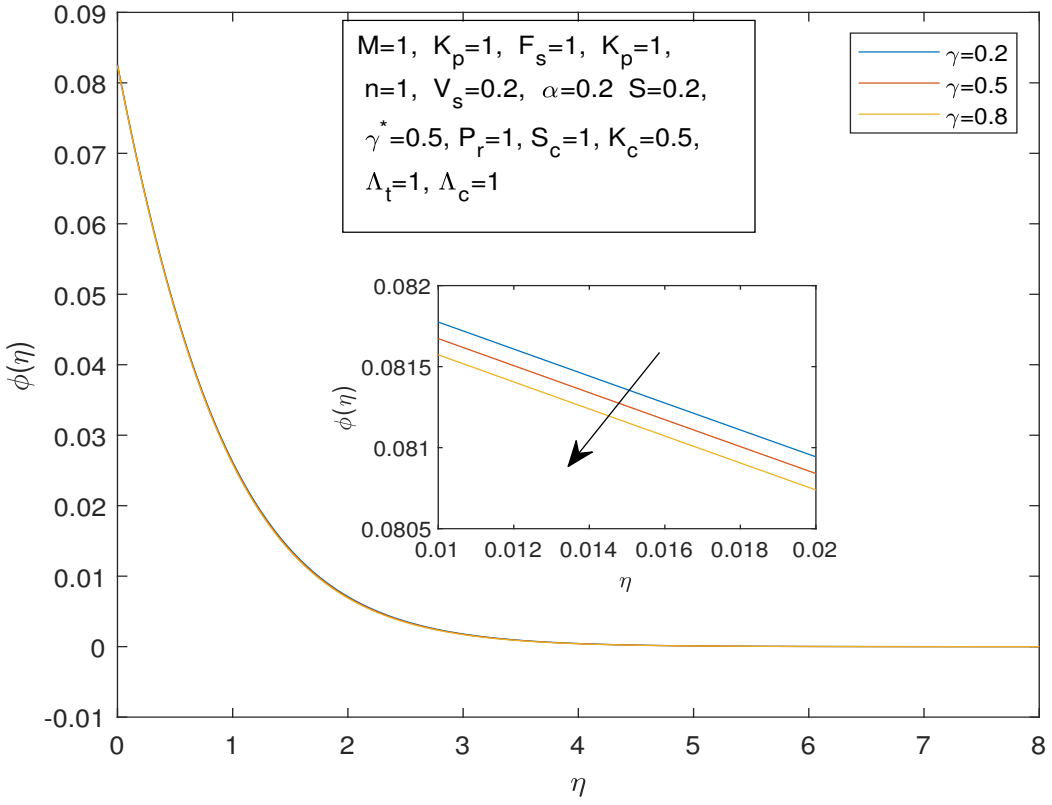

FIGURE 3.28: Concentration Profile $\phi(\eta)$ and η against γ

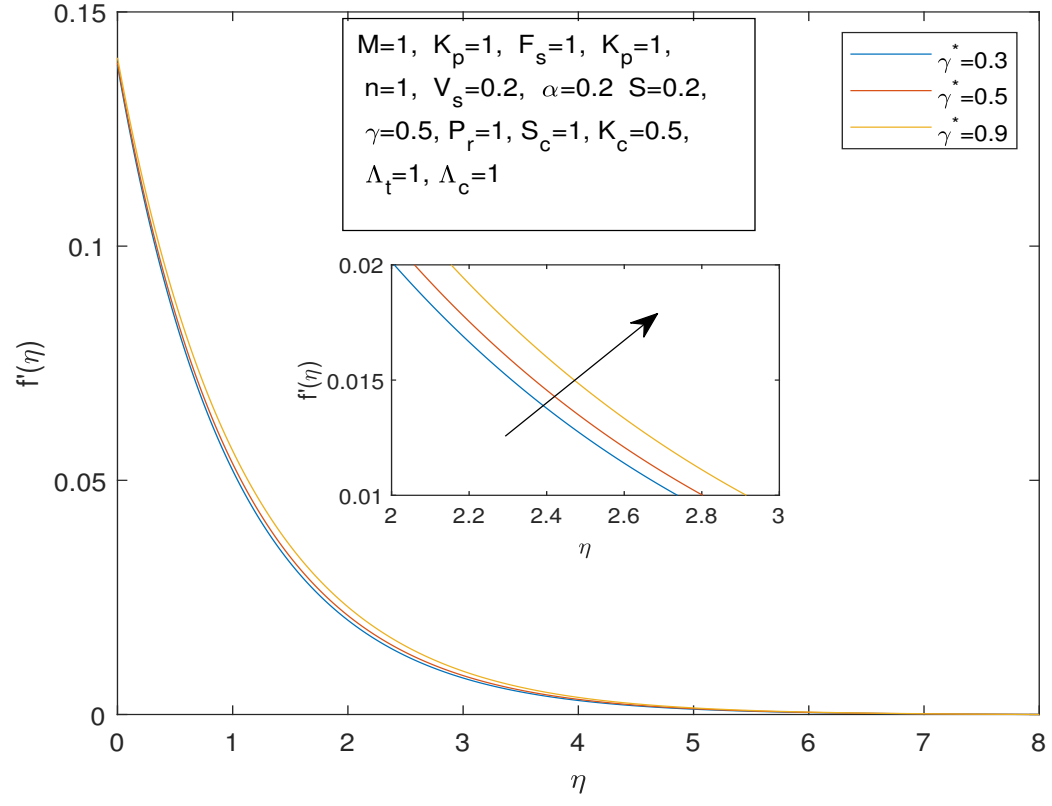

FIGURE 3.29: Velocity Profile $f'(\eta)$ and η against γ^*

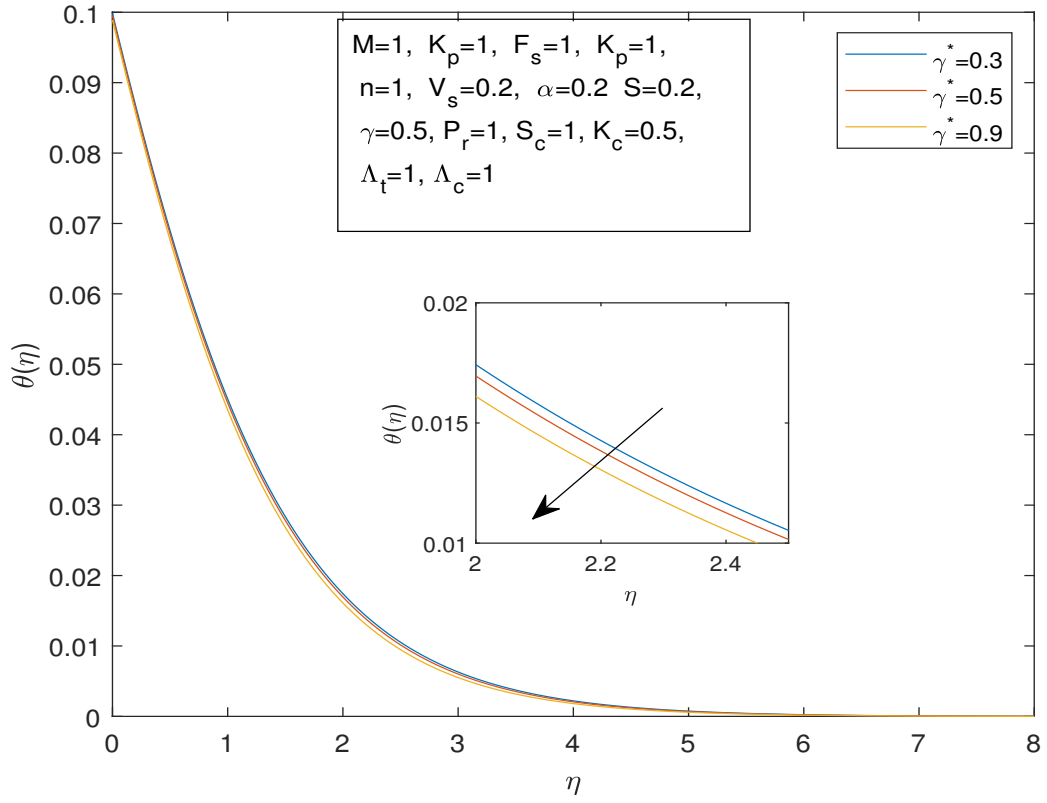

FIGURE 3.30: Temperature Profile $\theta(\eta)$ and η against γ^*

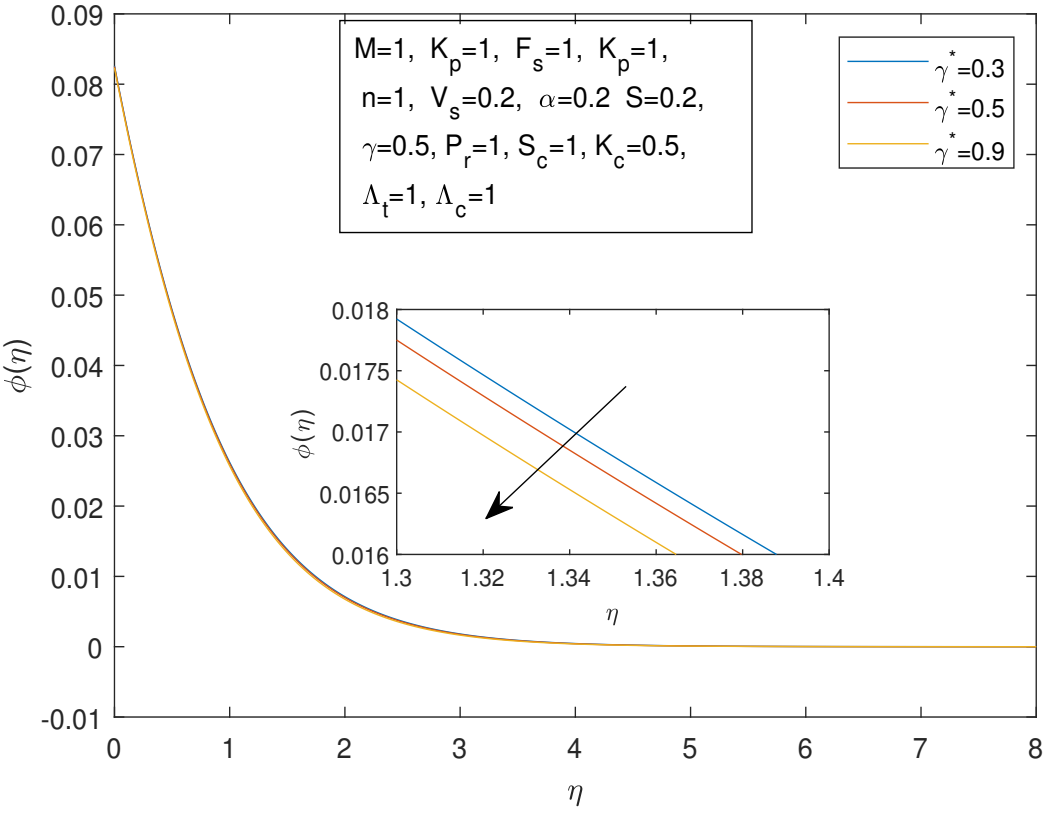

FIGURE 3.31: Concentration Profile $\phi(\eta)$ and η against γ^*

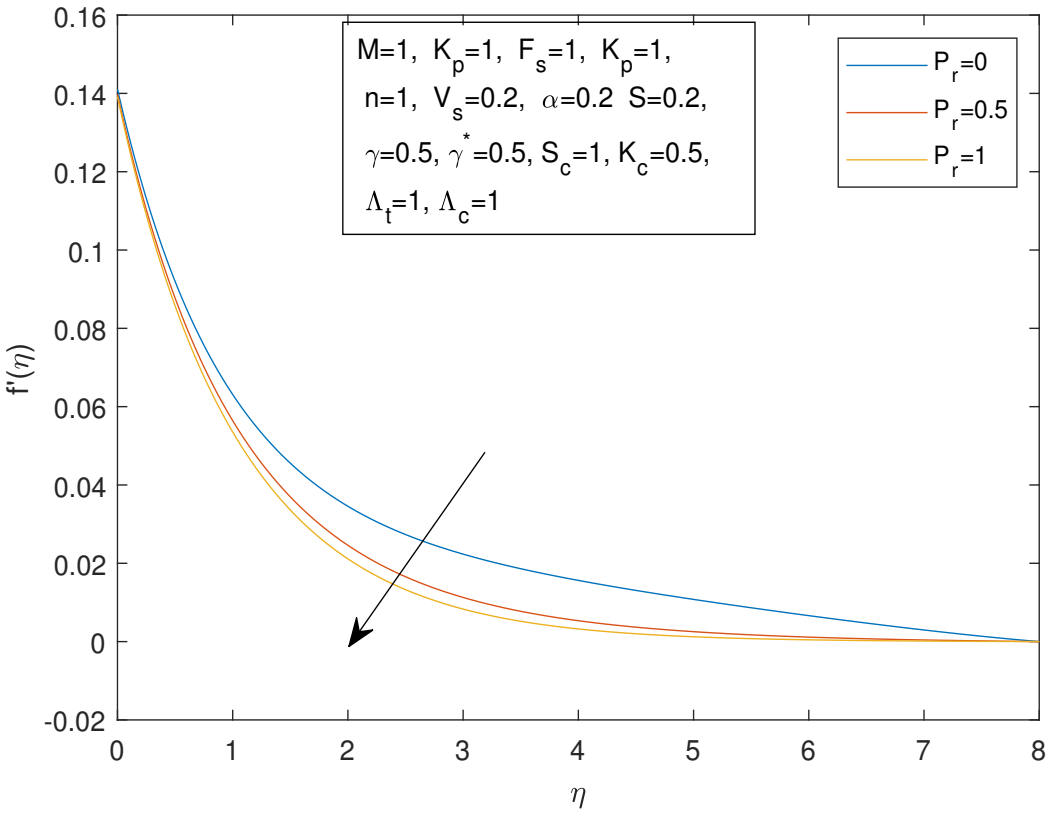

FIGURE 3.32: Velocity Profile $f'(\eta)$ and η against Pr

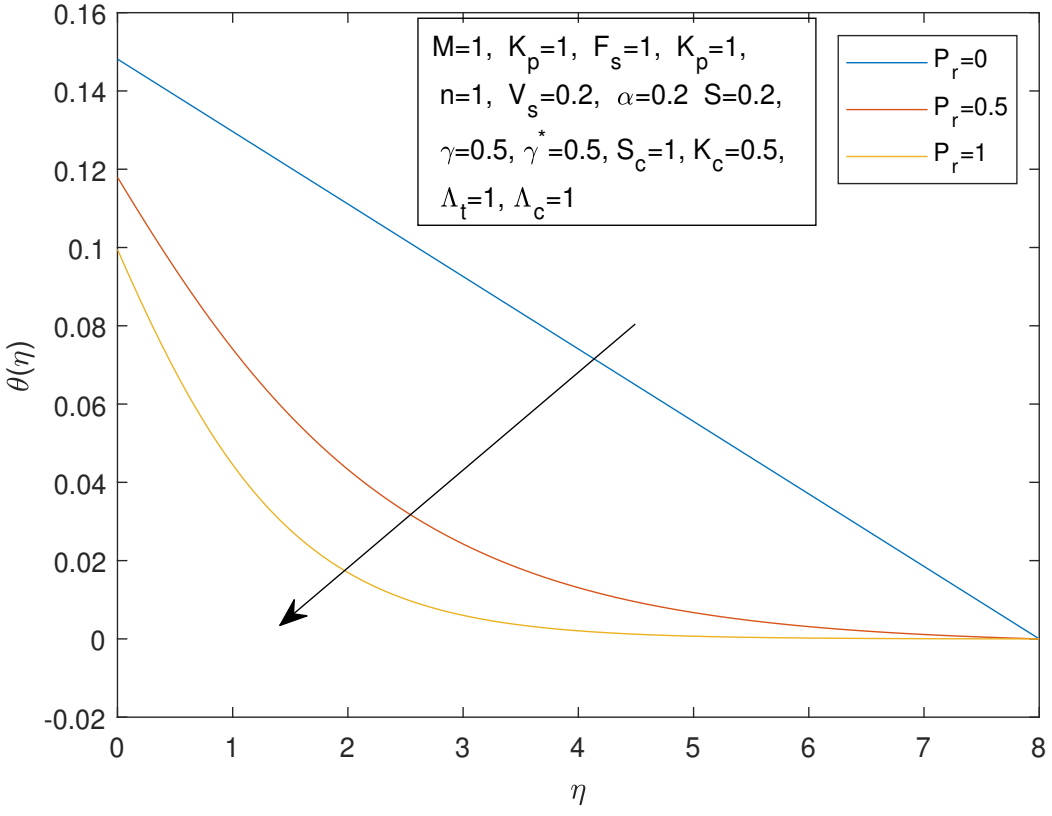

FIGURE 3.33: Temperature Profile $\theta(\eta)$ and η against Pr

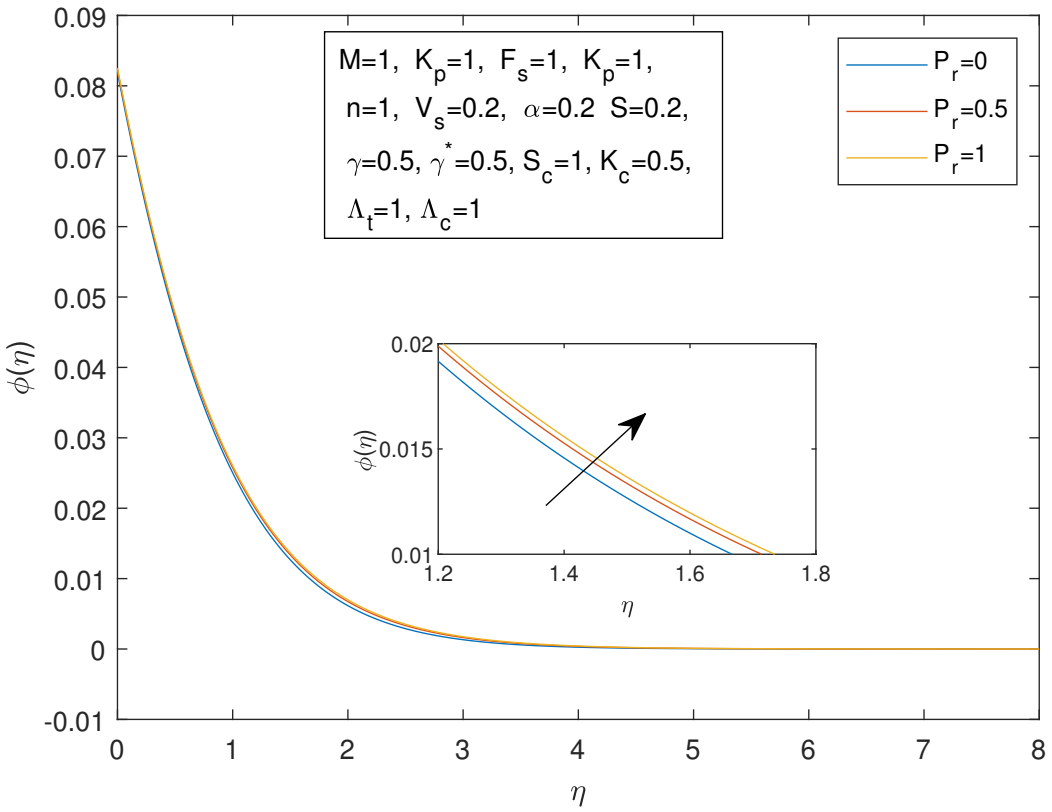

FIGURE 3.34: Concentration Profile $\phi(\eta)$ and η against Pr

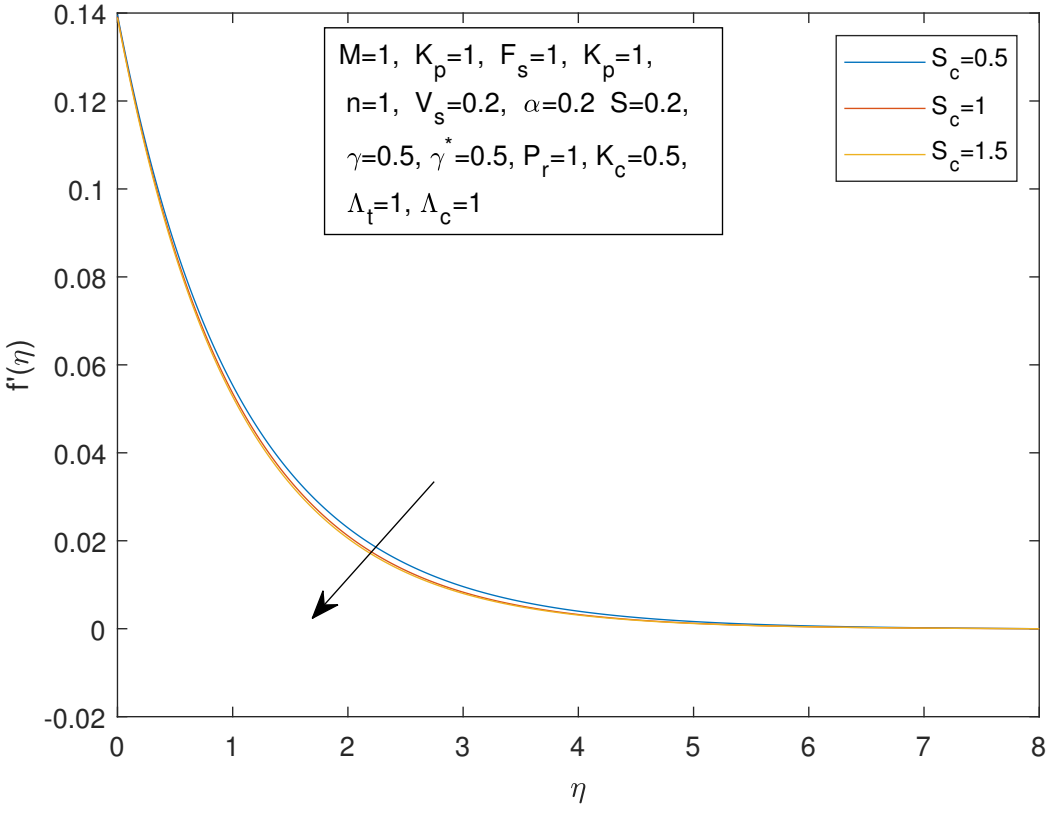

FIGURE 3.35: Velocity Profile $f'(\eta)$ and η against Sc

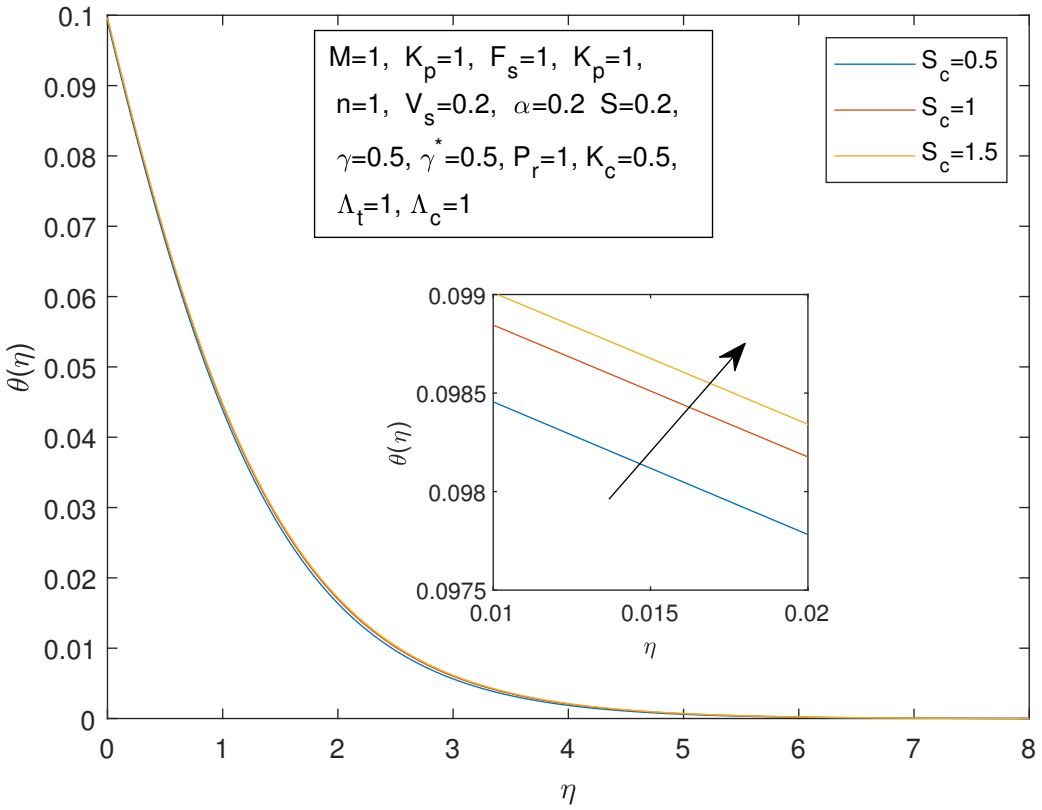

FIGURE 3.36: Temperature Profile $\theta(\eta)$ and η against Sc

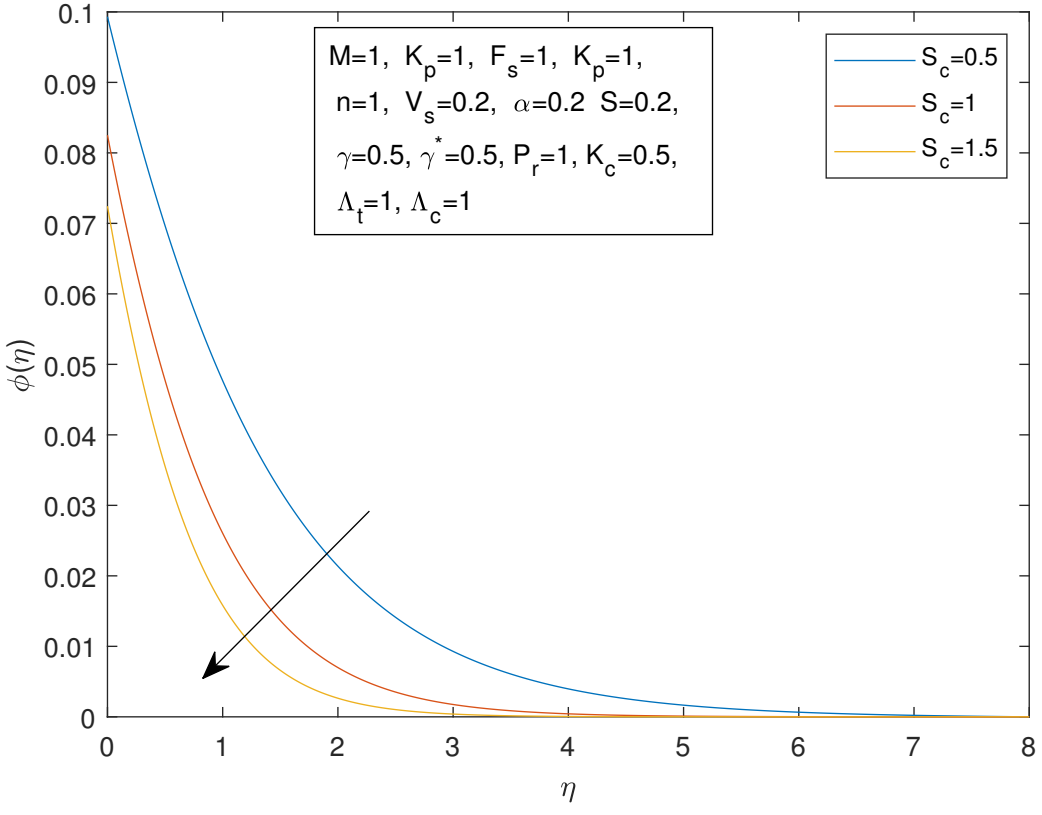

FIGURE 3.37: Concentration Profile $\phi(\eta)$ and η against Sc

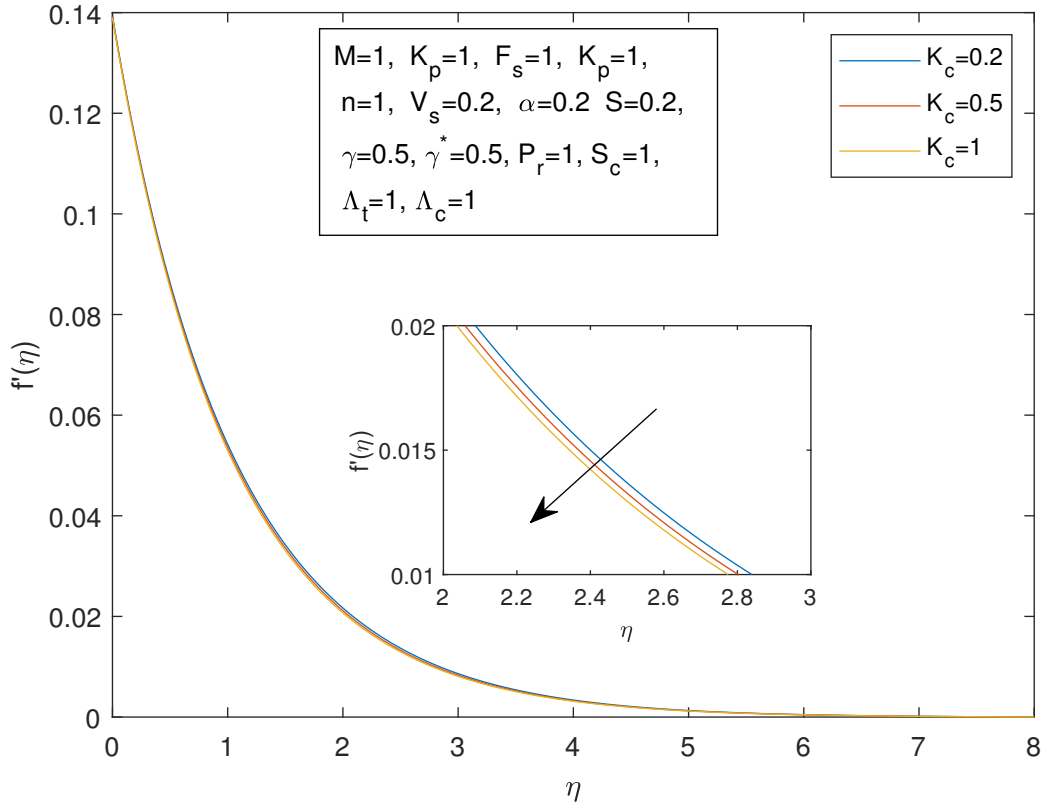

FIGURE 3.38: Velocity Profile $f'(\eta)$ and η against K_c

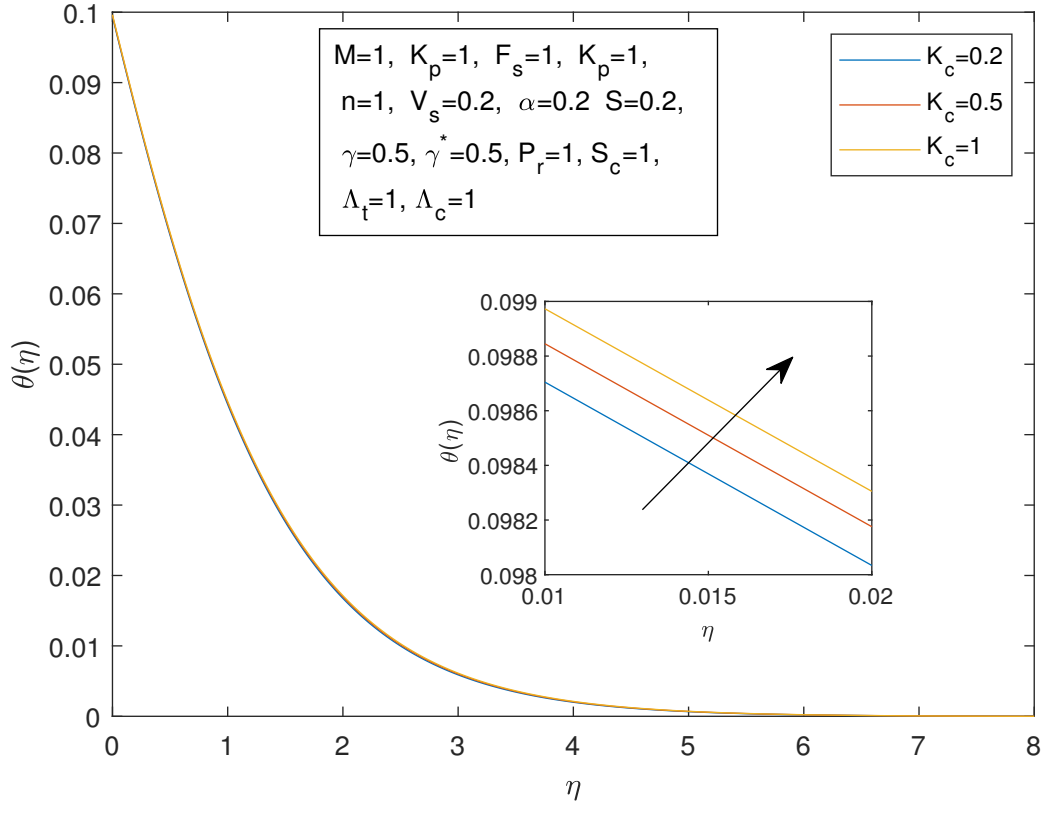

FIGURE 3.39: Temperature Profile $\theta(\eta)$ and η against K_c

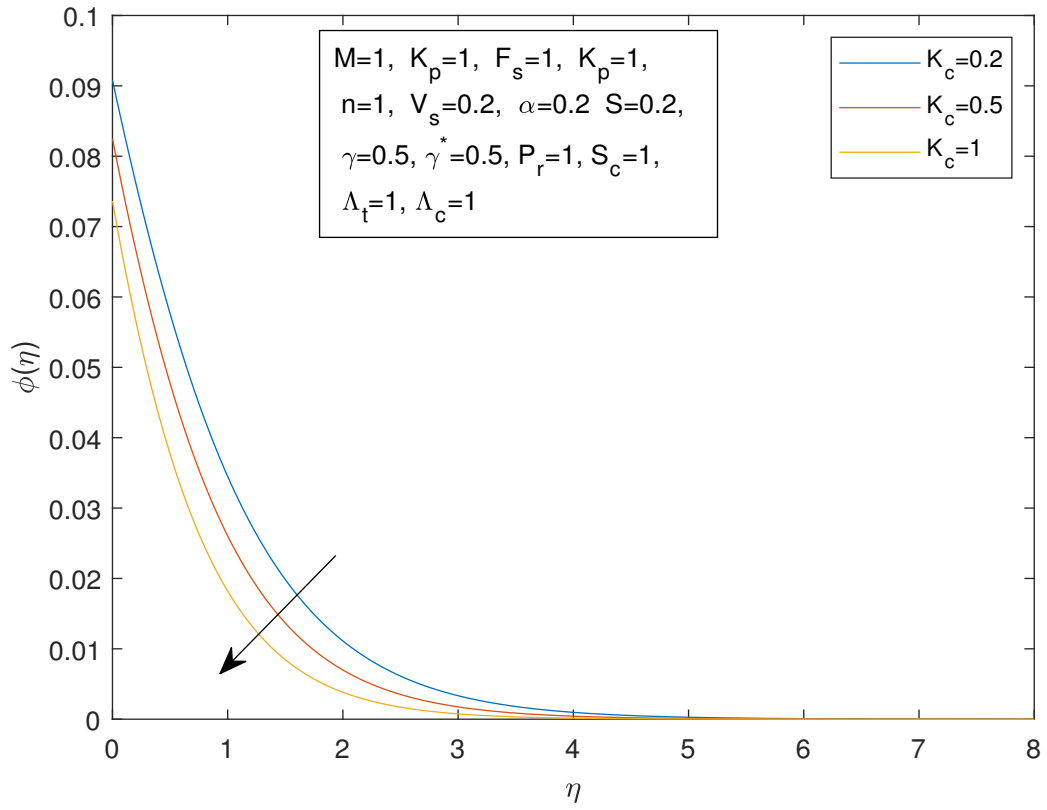

FIGURE 3.40: Concentration Profile $\phi(\eta)$ and η against K_c

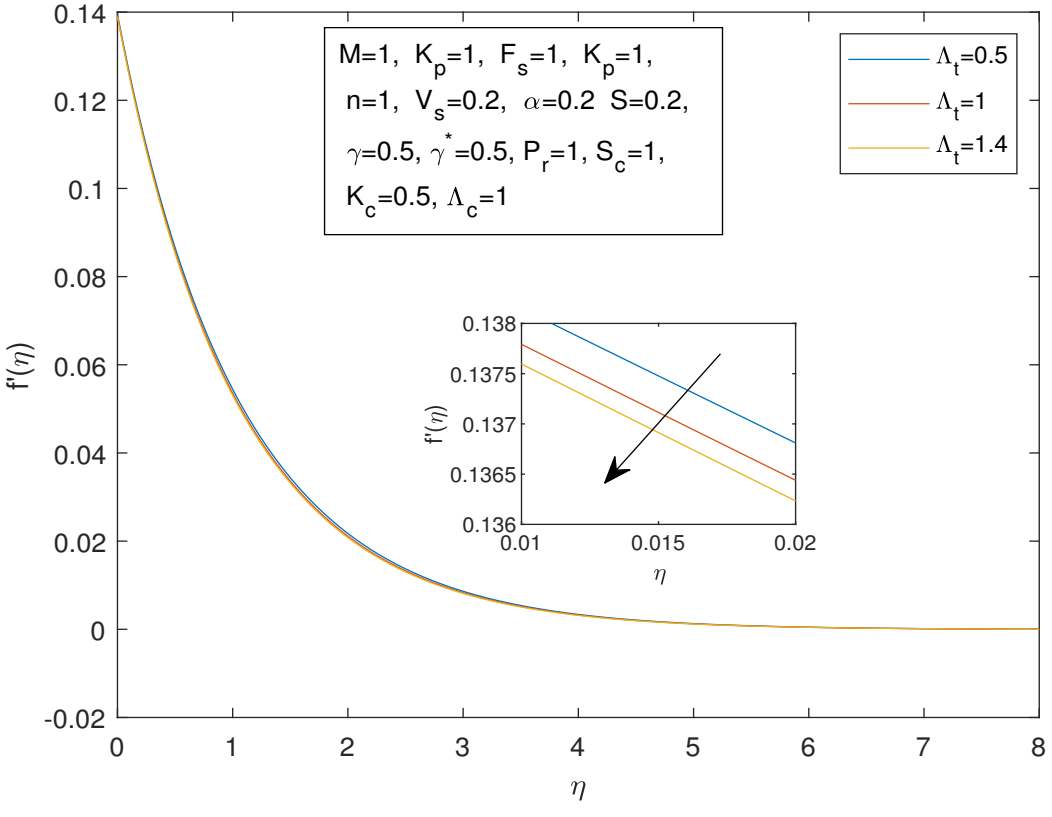

FIGURE 3.41: Velocity Profile $f'(\eta)$ and η against λ_t

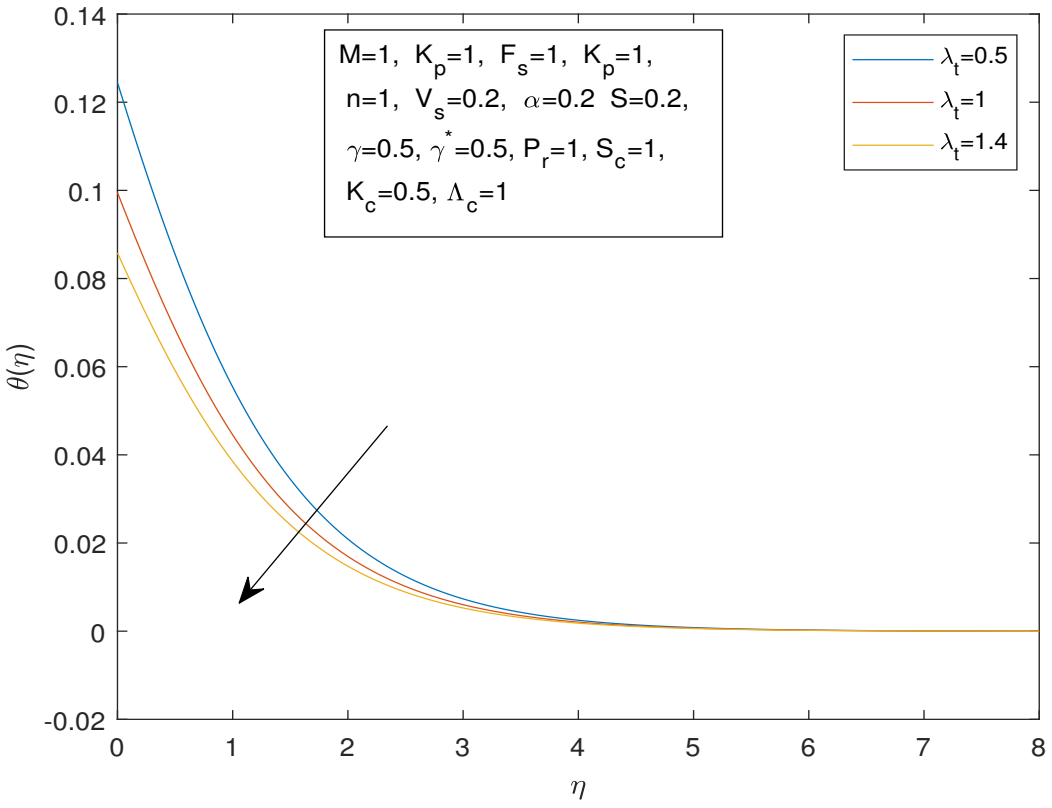

FIGURE 3.42: Temperature Profile $\theta(\eta)$ and η against λ_t

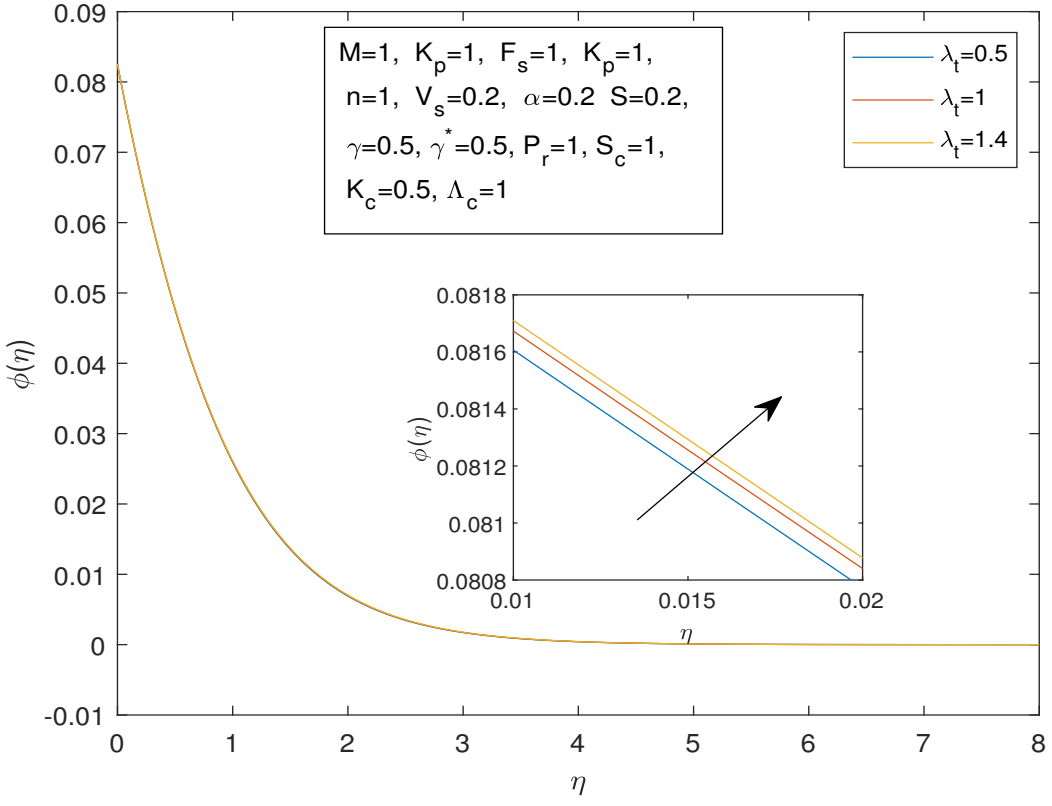

FIGURE 3.43: Concentration Profile $\phi(\eta)$ and η against λ_t

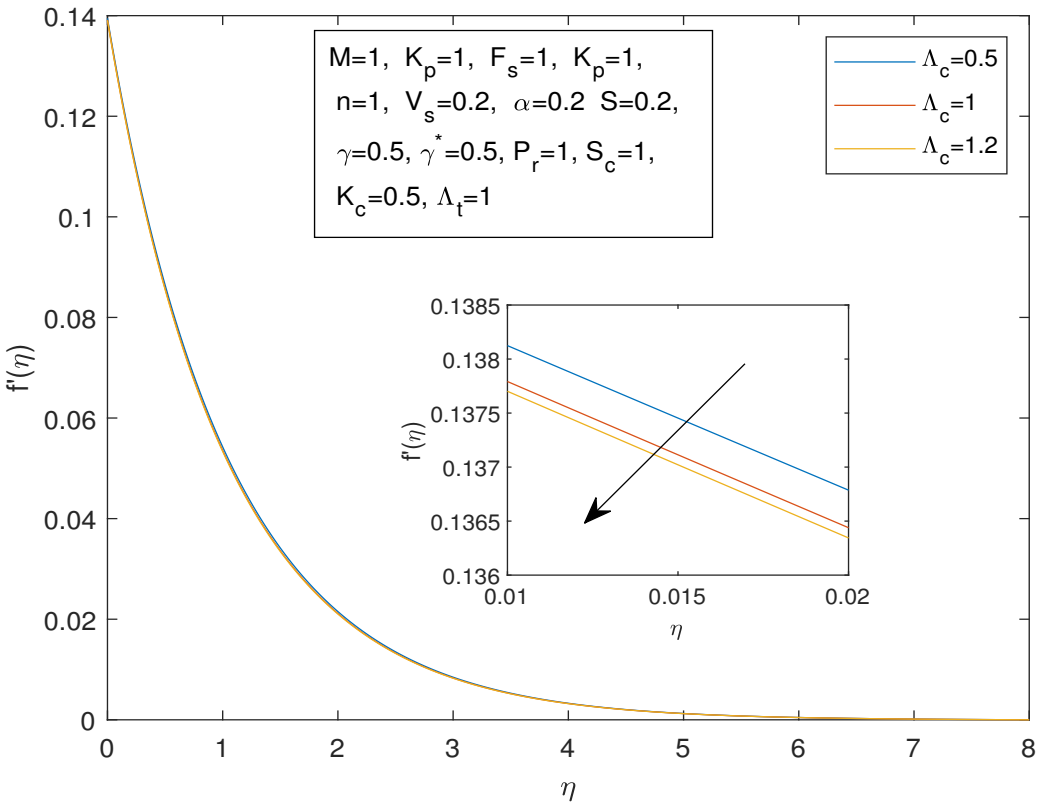

FIGURE 3.44: Velocity Profile $f'(\eta)$ and η against λ_c

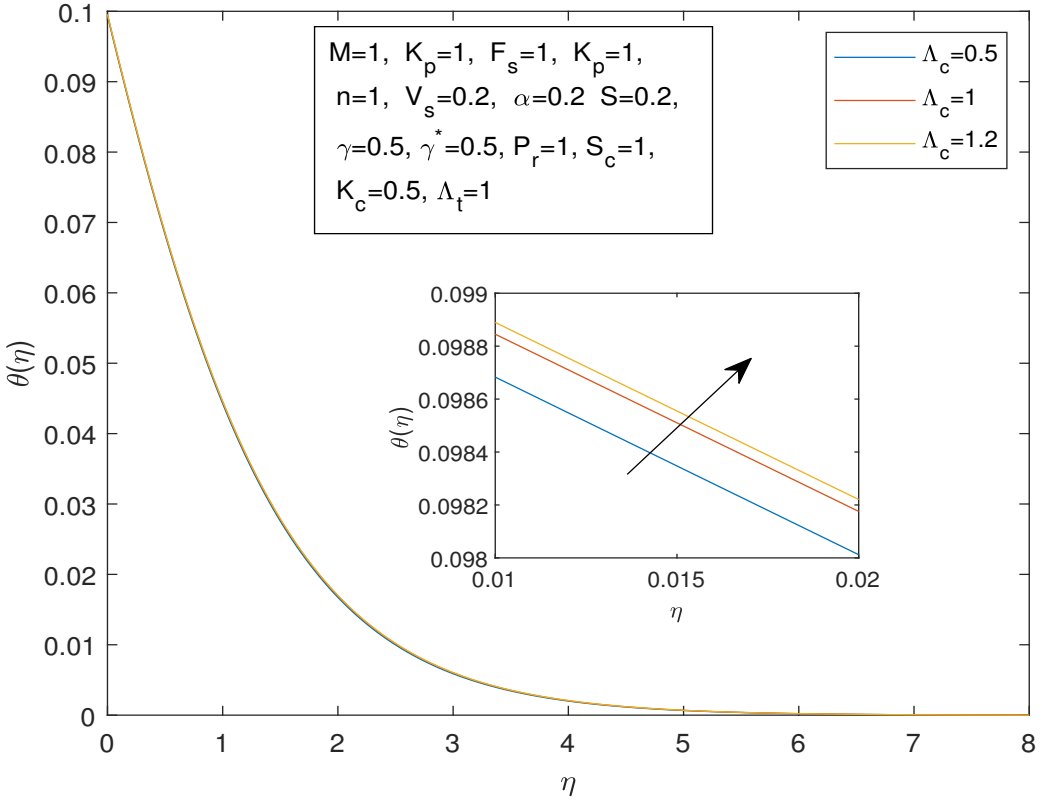

FIGURE 3.45: Temperature Profile $\theta(\eta)$ and η against λ_c

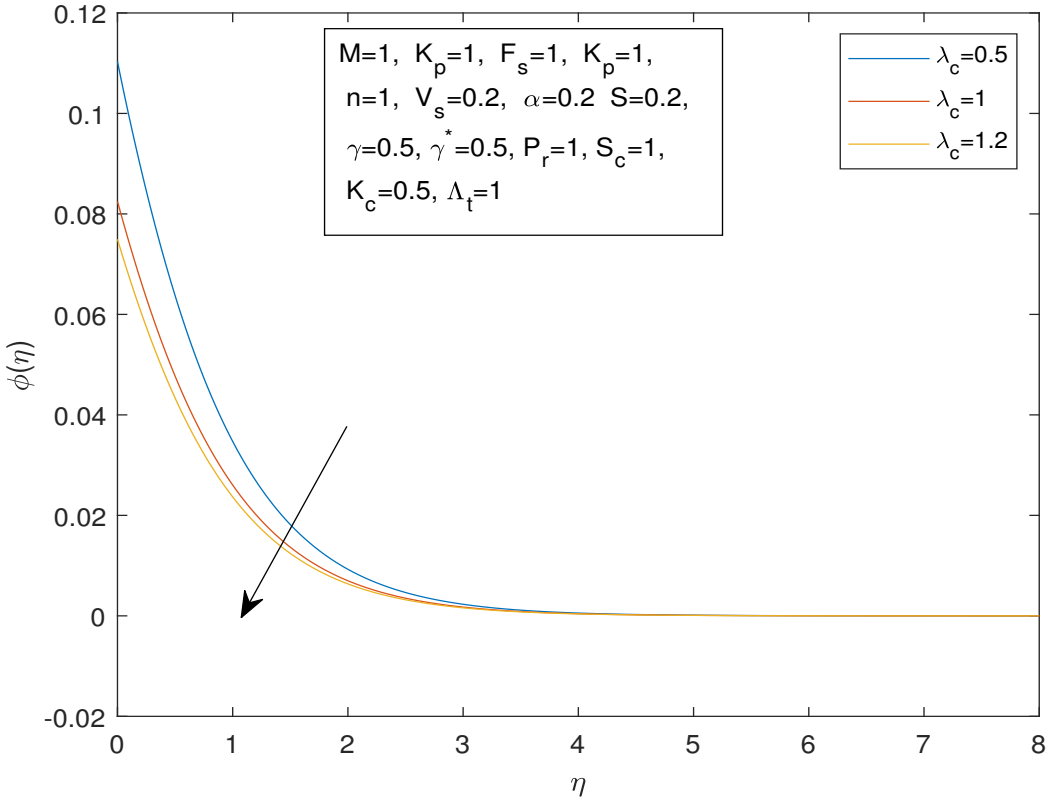

FIGURE 3.46: Concentration Profile $\phi(\eta)$ and η against λ_c

Chapter 4

The Impact of Cattaneo-Christov Double Diffusion, and Energy Activation on a Flow of Casson Fluid over a Stretching Surface

4.1 Introduction

The main objective of the this chapter is to extend the work of Kala et al. [40] discussed in the previous chapter. The model discussed in Chapter 3 has been extended by considering the Cattaneo-Christov Double Diffusion model, Brownian diffusion, thermophoretic effect and energy activation. Using similarity transformations, the governing nonlinear partial differential equations are transformed into a set of dimensionless ordinary differential equations (ODEs). MATLAB is utilized for numerical computations, and the shooting technique is employed as a numerical method to obtain the numerical results. The acquired numerical results have been presented through tables and graphs.

4.2 Mathematical Modeling

Consider a two-dimensional, steady and laminar flow of an incompressible Casson fluid over a nonlinearly stretching surface, embedded in a saturated, homogeneous Forchheimer porous medium (as depicted in Figure 3.1, which shows the fluid flow and stretching surface configuration). In this study, the stretching surface is aligned with the x-axis and inclined at an acute angle α to the vertical, as shown in Figure 3.1. Energy transport analysis is also carried out in the presence of thermal radiation Brownian diffusion, thermophoretic effect and Cattaneo-Christov double diffusion. Moreover, the concentration of flow is discussed with the help of concentration equation under the effect of energy activation and Cattaneo-Christov double diffusion.

The flow is described by the following set of equations:

$$\frac{\partial u}{\partial x}+\frac{\partial v}{\partial y}=0, \tag{4.1}$$

$$u\frac{\partial u}{\partial x}+v\frac{\partial u}{\partial y}=v\left(1+\frac{1}{\beta}\right)\frac{\partial^2 u}{\partial y^2}\pm g\left(\beta_T(T-T_\infty)+\beta_C(C-C_\infty)\right)\cos\alpha - \frac{\sigma B^2}{\rho_f}u-\frac{v}{K_d}u-\frac{C_b}{\sqrt{K_d}}u^2, \tag{4.2}$$

$$u\frac{\partial T}{\partial x}+v\frac{\partial T}{\partial y}+\Gamma_e\left[u\frac{\partial u}{\partial x}\frac{\partial T}{\partial x}+v\frac{\partial u}{\partial y}\frac{\partial T}{\partial x}+u\frac{\partial v}{\partial x}\frac{\partial T}{\partial y}+v\frac{\partial v}{\partial y}\frac{\partial T}{\partial y}+u^2\frac{\partial^2 T}{\partial x^2} + v^2\frac{\partial^2 T}{\partial y^2}+2uv\frac{\partial^2 T}{\partial x\partial y}\right]=\alpha\frac{\partial^2 T}{\partial y^2}+\tau\left[D_B\frac{\partial C}{\partial y}\frac{\partial T}{\partial y}+\frac{D_T}{T_\infty}\left(\frac{\partial T}{\partial y}\right)^2\right], \tag{4.3}$$

$$u\frac{\partial C}{\partial x}+v\frac{\partial C}{\partial y}+\Gamma_c\left[u\frac{\partial u}{\partial x}\frac{\partial C}{\partial x}+v\frac{\partial u}{\partial y}\frac{\partial C}{\partial x}+u\frac{\partial v}{\partial x}\frac{\partial C}{\partial y}+v\frac{\partial v}{\partial y}\frac{\partial C}{\partial y}+u^2\frac{\partial^2 C}{\partial x^2} + v^2\frac{\partial^2 C}{\partial y^2}+2uv\frac{\partial^2 C}{\partial x\partial y}\right]=D\frac{\partial^2 C}{\partial y^2}-K_C(C-C_\infty) - K_r^2(C-C_\infty)\left[\frac{T}{T_\infty}\right]^m\exp\left(\frac{-E_a}{kT}\right). \tag{4.4}$$

The BCs associated with this problem are:

$$\left.\begin{aligned} &y=0:\quad u=U(x)=u_w+u_s=cx^n+N\mu\frac{\partial u}{\partial y},\ v=v_w=-V(x),\\ &y\to\infty:\ u\to 0,\ T\to T_\infty,\ C\to C_\infty,\ C(x)=C_w+C_0\frac{\partial C}{\partial y},\quad .\\ &\qquad\qquad T(x)=T_w+T_0\frac{\partial T}{\partial y}. \end{aligned}\right\} \tag{4.5}$$

4.3 Conversion of PDEs into ODEs

To modify the equations (4.1)-(4.4) to have the form of ODEs, use the following transformations:

$$\left.\begin{aligned}
&\eta = \sqrt{\frac{c(n+1)}{2v}}x^{\frac{n-1}{2}}y, \quad \psi = \sqrt{\frac{2cv}{n+1}}x^{\frac{n+1}{2}}f(\eta), \quad u = \frac{\partial\psi}{\partial y}, \quad v = -\frac{\partial\psi}{\partial x},\\
&u = cx^n f'(\eta), \quad v = -\sqrt{\frac{cv(n+1)}{2}}x^{\frac{n-1}{2}}\left(f(\eta) + \frac{n-1}{n+1}\eta f'(\eta)\right),\\
&\theta(\eta) = \frac{T-T_\infty}{T_w-T_\infty}, \quad \phi(\eta) = \frac{C-C_\infty}{C_w-C_\infty}.
\end{aligned}\right\} \tag{4.6}$$

The identical satisfaction of equation 4.1 is already established in Chapter 3 because it is equation 3.1 of that chapter. The conversion of equation 4.2 into the dimensionless form is already included in Chapter 3 because it is the same as equation 3.2.

To convert equations 4.3 and 4.4 into dimensionless, most of the derivatives are already available in Chapter 3. The new derivatives have been determined for equation 4.3 shown below:

$$\begin{aligned}
\frac{\partial v}{\partial x} &= \frac{\partial}{\partial x}\left(-\sqrt{\frac{cv(n+1)}{2}}x^{\frac{n-1}{2}}\left(f(\eta) + \frac{n-1}{n+1}\eta f'(\eta)\right)\right)\\
&= -\sqrt{\frac{cv(n+1)}{2}}\left[x^{\frac{n-1}{2}}\frac{\partial}{\partial x}\left(f(\eta) + \frac{n-1}{n+1}\eta f'(\eta)\right)\right.\\
&\quad \left. + \left(f(\eta) + \frac{n-1}{n+1}\eta f'(\eta)\right)\frac{\partial}{\partial x}x^{\frac{n-1}{2}}\right]\\
&= -\sqrt{\frac{cv(n+1)}{2}}\left[x^{\frac{n-1}{2}}\left(f'(\eta)\frac{n-1}{2x}\eta + \frac{n-1}{n+1}\frac{n-1}{2x}\eta f'(\eta)\right.\right.\\
&\quad \left.\left. + \frac{n-1}{n+1}\frac{n-1}{2x}\eta f''(\eta)\eta\right) + \left(f(\eta) + \frac{n-1}{n+1}\eta f'(\eta)\right)\frac{n-1}{2x}x^{\frac{n-1}{2}}\right]\\
&= -\sqrt{\frac{cv(n+1)}{2}}\frac{x^{\frac{n-1}{2}}}{x}\left[\frac{n-1}{2}\eta f'(\eta) + \frac{(n-1)^2}{2(n+1)}\eta f'(\eta) + \frac{(n-1)^2}{2(n+1)}\eta^2 f''(\eta)\right.\\
&\quad \left. + \frac{n-1}{2}f(\eta) + \frac{(n-1)^2}{2(n+1)}\eta f'(\eta)\right].\\
\frac{\partial \eta}{\partial x} &= \frac{\partial}{\partial x}\left(\sqrt{\frac{c(n+1)}{2v}}x^{\frac{n-1}{2}}y\right)\\
&= \sqrt{\frac{c(n+1)}{2v}}\frac{n-1}{2x}x^{\frac{n-1}{2}}y
\end{aligned}$$

$$= \frac{n-1}{2x}\eta.$$

$$\frac{\partial^2 T}{\partial x^2} = \frac{\partial}{\partial x}\left((T_w - T_\infty)\theta'(\eta)\frac{n-1}{2x}\eta\right)$$

$$= (T_w - T_\infty)\frac{\partial}{\partial x}\left(\theta'(\eta)\frac{n-1}{2}\frac{\eta}{x}\right)$$

$$= (T_w - T_\infty)\left(\theta''(\eta)\frac{n-1}{2}\frac{\eta}{x}\frac{\partial}{\partial x}\eta + \theta'(\eta)\frac{n-1}{2}\eta\frac{\partial}{\partial x}x^{-1} + \theta'(\eta)\frac{n-1}{2x}\frac{\partial}{\partial x}\eta\right)$$

$$= (T_w - T_\infty)\left(\theta''(\eta)\left(\frac{n-1}{2}\right)^2\frac{\eta^2}{x^2} - \theta'(\eta)\frac{n-1}{2}\frac{\eta}{x^2} + \theta'(\eta)\left(\frac{n-1}{2}\right)^2\frac{\eta}{x^2}\right)$$

$$= (T_w - T_\infty)\frac{1}{x^2}\left[\left(\frac{n-1}{2}\right)^2\eta^2\theta''(\eta) - \frac{n-1}{2}\eta\theta'(\eta) + \left(\frac{n-1}{2}\right)^2\eta\theta'(\eta)\right].$$

$$\frac{\partial^2 T}{\partial x \partial y} = \frac{\partial}{\partial x}\left((T_w - T_\infty)\theta'(\eta)\sqrt{\frac{c(n+1)}{2v}}x^{\frac{n-1}{2}}\right)$$

$$= (T_w - T_\infty)\theta'(\eta)\sqrt{\frac{c(n+1)}{2v}}\frac{\partial}{\partial x}\left(\theta'(\eta)x^{\frac{n-1}{2}}\right)$$

$$= (T_w - T_\infty)\theta'(\eta)\sqrt{\frac{c(n+1)}{2v}}\left[x^{\frac{n-1}{2}}\frac{\partial}{\partial x}\theta'(\eta) + \theta'(\eta)\frac{\partial}{\partial x}x^{\frac{n-1}{2}}\right]$$

$$= (T_w - T_\infty)\theta'(\eta)\sqrt{\frac{c(n+1)}{2v}}\left[x^{\frac{n-1}{2}}\theta\text{”}(\eta)\frac{\partial}{\partial x}\eta + \theta'(\eta)\frac{n-1}{2x}x^{\frac{n-1}{2}}\right]$$

$$= (T_w - T_\infty)\theta'(\eta)\sqrt{\frac{c(n+1)}{2v}}\frac{x^{\frac{n-1}{2}}}{x}\left[\frac{n-1}{2}\eta\theta\text{”}(\eta) + \frac{n-1}{2}\theta'(\eta)\right].$$

$$u\frac{\partial u}{\partial x}\frac{\partial T}{\partial x} = cx^n f'(\eta)\left(ncx^{n-1}f'(\eta) + cx^{n-1}f''(\eta)\frac{n-1}{2}\eta\right)\left((T_w - T_\infty)\theta'(\eta)\frac{n-1}{2x}\eta\right)$$

$$= (cx^{n-1})^2 f'(\eta)\theta'(\eta)(T_w - T_\infty)\frac{n-1}{2}\eta\left[nf'(\eta) + \eta\frac{n-1}{2}f''(\eta)\right]$$

$$= (cx^{n-1})^2(T_w - T_\infty)\left[nf'(\eta)^2\theta'(\eta)\frac{n-1}{2}\eta + \eta^2\left(\frac{n-1}{2}\right)^2 f'(\eta)\theta'(\eta)f''(\eta)\right]$$

$$= (cx^{n-1})^2(T_w - T_\infty)\frac{n+1}{2}\left[\frac{n(n-1)}{n+1}f'(\eta)^2\theta'(\eta)\eta\right.$$

$$\left. + \frac{(n-1)^2}{2(n+1)}\eta^2 f'(\eta)\theta'(\eta)f''(\eta)\right]. \tag{4.7}$$

$$v\frac{\partial u}{\partial y}\frac{\partial T}{\partial x} = -\sqrt{\frac{cv(n+1)}{2}}x^{\frac{n-1}{2}}\left[f(\eta) + \frac{n-1}{n+1}\eta f'(\eta)\right]\left(cx^n f''(\eta)\sqrt{\frac{c(n+1)}{2v}}x^{\frac{n-1}{2}}\right)$$

$$\left((T_w - T_\infty)\theta'(\eta)\frac{n-1}{2x}\eta\right)$$

$$= -(cx^{n-1})^2(T_w - T_\infty)\frac{n+1}{2}\frac{n-1}{2}\eta f''(\eta)\theta'(\eta)\left[f(\eta) + \frac{n-1}{n+1}\eta f'(\eta)\right]$$

$$= -(cx^{n-1})^2(T_w - T_\infty)\frac{n+1}{2}\left[\frac{n-1}{2}\eta f''(\eta)\theta'(\eta)f(\eta)\right.$$

$$\left. + \frac{(n-1)^2}{2(n+1)}\eta^2 f'(\eta)f''(\eta)\theta'(\eta)\right]$$

$$= (cx^{n-1})^2(T_w - T_\infty)\frac{n+1}{2}\bigg[- \frac{n-1}{2}\eta f''(\eta)\theta'(\eta)f(\eta)$$
$$- \frac{(n-1)^2}{2(n+1)}\eta^2 f'(\eta)f''(\eta)\theta'(\eta)\bigg]. \tag{4.8}$$

$$u\frac{\partial v}{\partial x}\frac{\partial T}{\partial y} = cx^n f'(\eta)\left(-\sqrt{\frac{cv(n+1)}{2}}\frac{x^{\frac{n-1}{2}}}{x}\right)\bigg[\frac{n-1}{2}\eta f'(\eta) + \frac{(n-1)^2}{2(n+1)}\eta f'(\eta)$$
$$+ \frac{(n-1)^2}{2(n+1)}\eta^2 f''(\eta) + \frac{n-1}{2}f(\eta)$$
$$+ \frac{(n-1)^2}{2(n+1)}\eta f'(\eta)\bigg]\left((T_w - T_\infty)\theta'(\eta)\sqrt{\frac{c(n+1)}{2v}}x^{\frac{n-1}{2}}\right)$$
$$= cx^n f'(\eta)\left(-\sqrt{\frac{cv(n+1)}{2}}\frac{x^{\frac{n-1}{2}}}{x}\right)\bigg[\frac{n-1}{2}\eta f'(\eta) + \frac{(n-1)^2}{n+1}\eta f'(\eta)$$
$$+ \frac{(n-1)^2}{2(n+1)}\eta^2 f''(\eta) + \frac{n-1}{2}f(\eta)\bigg]\left((T_w - T_\infty)\theta'(\eta)\sqrt{\frac{c(n+1)}{2v}}x^{\frac{n-1}{2}}\right)$$
$$= -(cx^{n-1})^2(T_w - T_\infty)\frac{n+1}{2}\eta f'(\eta)\theta'(\eta)\bigg[\frac{n-1}{2}\eta f'(\eta) + \frac{(n-1)^2}{n+1}\eta f'(\eta)$$
$$+ \frac{(n-1)^2}{2(n+1)}\eta^2 f''(\eta) + \frac{n-1}{2}f(\eta)\bigg]$$
$$= (cx^{n-1})^2(T_w - T_\infty)\frac{n+1}{2}\bigg[- \frac{(3n-1)(n-1)}{2(n+1)}\eta f'^2(\eta)\theta'(\eta)$$
$$- \frac{(n-1)^2}{2(n+1)}\eta^2 f'(\eta)\theta'(\eta)f''(\eta) - \frac{n-1}{2}f(\eta)f'(\eta)\theta'(\eta)\bigg]. \tag{4.9}$$

$$v\frac{\partial v}{\partial y}\frac{\partial T}{\partial y} = \bigg(- \sqrt{\frac{cv(n+1)}{2}}x^{\frac{n-1}{2}}\left[f(\eta) + \frac{n-1}{n+1}\eta f'(\eta)\right]\bigg)\bigg(- cx^{n-1}\bigg[nf'(\eta)$$
$$+ \frac{n-1}{2}\eta f''(\eta)\bigg]\bigg)\left((T_w - T_\infty)\theta'(\eta)\sqrt{\frac{c(n+1)}{2v}}x^{\frac{n-1}{2}}\right)$$
$$= (cx^{n-1})^2(T_w - T_\infty)\frac{n+1}{2}\left(f(\eta)\theta'(\eta) + \frac{n-1}{n+1}\eta f'(\eta)\theta'(\eta)\right)\left(nf'(\eta)\right.$$
$$\left. + \frac{n-1}{2}\eta f''(\eta)\right)$$
$$= (cx^{n-1})^2(T_w - T_\infty)\frac{n+1}{2}\bigg[nf(\eta)f'(\eta)\theta'(\eta) + \frac{n-1}{2}\eta f(\eta)f''(\eta)\theta'(\eta)$$
$$+ \frac{n(n-1)}{n+1}\eta f'^2(\eta)\theta'(\eta) + \frac{(n-1)^2}{2(n+1)}\eta^2 f'(\eta)\theta'(\eta)f''(\eta)\bigg]. \tag{4.10}$$

$$u^2\frac{\partial^2 T}{\partial x^2} = (cx^n f'(\eta))^2(T_w - T_\infty)\frac{1}{x^2}\bigg[\left(\frac{n-1}{2}\right)^2\eta^2\theta''(\eta) - \frac{n-1}{2}\eta\theta'(\eta)$$
$$+ \left(\frac{n-1}{2}\right)^2\eta\theta'(\eta)\bigg]$$
$$= (cx^n f'(\eta))^2(T_w - T_\infty)\frac{1}{x^2}\bigg[\left(\frac{n-1}{2}\right)^2\eta^2\theta''(\eta)$$
$$+ \frac{(n-1)^2 - 2(n-1)}{4}\theta'(\eta)\eta\bigg]$$

$$= (cx^n f'(\eta))^2 (T_w - T_\infty) \frac{1}{x^2} \left[\left(\frac{n-1}{2} \right)^2 \eta^2 \theta''(\eta) + \frac{(n-1)(n-3)}{4} \theta'(\eta) \eta \right]$$

$$= (cx^{n-1})^2 (T_w - T_\infty) \frac{n+1}{2} \left[\frac{2}{n+1} \left(\frac{n-1}{2} \right)^2 \eta^2 \theta''(\eta) f'^2(\eta) \right.$$

$$\left. + \frac{2}{n+1} \frac{(n-1)(n-3)}{4} \theta'(\eta) \eta f'^2(\eta) \right]$$

$$= (cx^{n-1})^2 (T_w - T_\infty) \frac{n+1}{2} \left[\frac{(n-1)^2}{2(n+1)} \eta^2 \theta''(\eta) f'^2(\eta) \right.$$

$$\left. + \frac{(n-1)(n-3)}{2(n+1)} \theta'(\eta) \eta f'^2(\eta) \right]. \tag{4.11}$$

$$2uv \frac{\partial^2 T}{\partial x \partial y} = 2cx^n f'(\eta) \left(-\sqrt{\frac{cv(n+1)}{2}} x^{\frac{n-1}{2}} \left[f(\eta) + \frac{n-1}{n+1} \eta f'(\eta) \right] \right) \left(T_w - T_\infty \right.$$

$$\left. \sqrt{\frac{c(n+1)}{2v}} \frac{x^{\frac{n-1}{2}}}{x} \left[\frac{n-1}{2} \eta \theta''(\eta) + \frac{n-1}{2} \theta'(\eta) \right] \right)$$

$$= -2(cx^{n-1})^2 (T_w - T_\infty) \frac{n+1}{2} \left[\frac{n-1}{2} \eta f(\eta) f'(\eta) \theta''(\eta) \right.$$

$$+ \frac{n-1}{2} f(\eta) f'(\eta) \theta'(\eta) + \frac{(n-1)^2}{2(n+1)} \eta^2 f'^2(\eta) \theta''(\eta)$$

$$\left. + \frac{(n-1)^2}{2(n+1)} \eta f'^2(\eta) \theta'(\eta) \right]$$

$$= (cx^{n-1})^2 (T_w - T_\infty) \frac{n+1}{2} \left[-(n-1) \eta f(\eta) f'(\eta) \theta''(\eta) \right.$$

$$- (n-1) f(\eta) f'(\eta) \theta'(\eta) - \frac{(n-1)^2}{n+1} \eta^2 f'^2(\eta) \theta''(\eta)$$

$$\left. - \frac{(n-1)^2}{n+1} \eta f'^2(\eta) \theta'(\eta) \right]. \tag{4.12}$$

$$v^2 \frac{\partial^2 T}{\partial y^2} = \left(-\sqrt{\frac{cv(n+1)}{2}} x^{\frac{n-1}{2}} \left(f(\eta) + \frac{n-1}{n+1} \eta f'(\eta) \right) \right)^2$$

$$\left((T_w - T_\infty) \theta''(\eta) \frac{c(n+1)}{2v} x^{n-1} \right)$$

$$= (cx^{n-1})^2 (T_w - T_\infty) \left(\frac{n+1}{2} \right)^2 \left[f^2(\eta) \theta''(\eta) + \left(\frac{n-1}{n+1} \right)^2 \eta^2 f'^2(\eta) \theta''(\eta) \right.$$

$$\left. + \frac{2(n-1)}{n+1} \eta f(\eta) f'(\eta) \theta''(\eta) \right]$$

$$= (cx^{n-1})^2 (T_w - T_\infty) \frac{n+1}{2} \left[\frac{n+1}{2} f^2(\eta) \theta''(\eta) + \frac{(n-1)^2}{2(n+1)} \eta^2 f'^2(\eta) \theta''(\eta) \right.$$

$$\left. + (n-1) \eta f(\eta) f'(\eta) \theta''(\eta) \right]. \tag{4.13}$$

$$u \frac{\partial u}{\partial x} \frac{\partial T}{\partial x} + v \frac{\partial v}{\partial y} \frac{\partial T}{\partial y} + u \frac{\partial v}{\partial x} \frac{\partial T}{\partial y} + v \frac{\partial u}{\partial y} \frac{\partial T}{\partial x} + 2uv \frac{\partial^2 T}{\partial x \partial y} + u^2 \frac{\partial^2 T}{\partial x^2} + v^2 \frac{\partial^2 T}{\partial y^2}$$

$$= (cx^{n-1})^2 (T_w - T_\infty) \frac{n+1}{2} \left[\frac{n(n-1)}{n+1} f'(\eta)^2 \theta'(\eta) \eta + \frac{(n-1)^2}{2(n+1)} \eta^2 f'(\eta) \theta'(\eta) f''(\eta) \right.$$

$$
\begin{aligned}
&+ nf(\eta)f'(\eta)\theta'(\eta) + \frac{n-1}{2}\eta f(\eta)f''(\eta)\theta'(\eta) + \frac{n(n-1)}{n+1}\eta f'^2(\eta)\theta'(\eta) \\
&+ \frac{(n-1)^2}{2(n+1)}\eta^2 f'(\eta)\theta'(\eta)f''(\eta) - \frac{(3n-1)(n-1)}{2(n+1)}\eta f'^2(\eta)\theta'(\eta) \\
&- \frac{(n-1)^2}{2(n+1)}\eta^2 f'(\eta)\theta'(\eta)f''(\eta) - \frac{n-1}{2}f(\eta)f'(\eta)\theta'(\eta) - \frac{n-1}{2}\eta f''(\eta)\theta'(\eta)f(\eta) \\
&- \frac{(n-1)^2}{2(n+1)}\eta^2 f'(\eta)f''(\eta)\theta'(\eta) - (n-1)\eta f(\eta)f'(\eta)\theta''(\eta) - (n-1)f(\eta)f'(\eta)\theta'(\eta) \\
&- \frac{(n-1)^2}{n+1}\eta^2 f'^2(\eta)\theta''(\eta) - \frac{(n-1)^2}{n+1}\eta f'^2(\eta)\theta'(\eta) + \frac{(n-1)^2}{2(n+1)}\eta^2\theta''(\eta)f'^2(\eta) \\
&+ \frac{(n-1)(n-3)}{2(n+1)}\theta'(\eta)\eta f'^2(\eta) + \frac{n+1}{2}f^2(\eta)\theta''(\eta) + \frac{(n-1)^2}{2(n+1)}\eta^2 f'^2(\eta)\theta''(\eta) \\
&+ (n-1)\eta f(\eta)f'(\eta)\theta''(\eta)\Bigg] \\
&= (cx^{n-1})^2(T_w - T_\infty)\frac{n+1}{2}\Bigg[\frac{n(n-1)}{n+1}f'(\eta)^2\theta'(\eta)\eta + \frac{(n-1)^2}{2(n+1)}\eta^2 f'(\eta)\theta'(\eta)f''(\eta) \\
&+ nf(\eta)f'(\eta)\theta'(\eta) + \frac{n-1}{2}\eta f(\eta)f''(\eta)\theta'(\eta) + \frac{n(n-1)}{n+1}\eta f'^2(\eta)\theta'(\eta) \\
&+ \frac{(n-1)^2}{2(n+1)}\eta^2 f'(\eta)\theta'(\eta)f''(\eta) - \frac{(3n-1)(n-1)}{2(n+1)}\eta f'^2(\eta)\theta'(\eta) \\
&- \frac{(n-1)^2}{2(n+1)}\eta^2 f'(\eta)\theta'(\eta)f''(\eta) - \frac{n-1}{2}f(\eta)f'(\eta)\theta'(\eta) - \frac{n-1}{2}\eta f''(\eta)\theta'(\eta)f(\eta) \\
&- \frac{(n-1)^2}{2(n+1)}\eta^2 f'(\eta)f''(\eta)\theta'(\eta) - (n-1)\eta f(\eta)f'(\eta)\theta''(\eta) - (n-1)f(\eta)f'(\eta)\theta'(\eta) \\
&- \frac{(n-1)^2}{n+1}\eta^2 f'^2(\eta)\theta''(\eta) - \frac{(n-1)^2}{n+1}\eta f'^2(\eta)\theta'(\eta) + \frac{(n-1)^2}{2(n+1)}\eta^2\theta''(\eta)f'^2(\eta) \\
&+ \frac{(n-1)(n-3)}{2(n+1)}\theta'(\eta)\eta f'^2(\eta) + \frac{n+1}{2}f^2(\eta)\theta''(\eta) + \frac{(n-1)^2}{2(n+1)}\eta^2 f'^2(\eta)\theta''(\eta) \\
&+ (n-1)\eta f(\eta)f'(\eta)\theta''(\eta)\Bigg] \\
&= (cx^{n-1})^2(T_w - T_\infty)\frac{n+1}{2}\Bigg[\left(\frac{n(n-1)}{n+1} - \frac{(3n-1)(n-1)}{2(n+1)} + \frac{n(n-1)}{n+1}\right. \\
&\quad \left. + \frac{(n-1)(n-3)}{2(n+1)} - \frac{(n-1)^2}{n+1}\right)\eta f'^2(\eta)\theta'(\eta) \\
&\quad + \left(n - \frac{n-1}{2} - (n-1)\right)f(\eta)f'(\eta)\theta'(\eta) + \left(\frac{n+1}{2}\right)f^2(\eta)\theta''(\eta)\Bigg] \\
&= (cx^{n-1})^2(T_w - T_\infty)\frac{n+1}{2} \\
&\quad \Bigg[\frac{n-1}{n+1}\left(\frac{2n-3n+1+2n+n-3-2n+2}{2}\right)\eta f'^2(\eta)\theta'(\eta) \\
&\quad + \left(\frac{2n-n+1-2n+2}{2}\right)f(\eta)f'(\eta)\theta'(\eta) + \frac{n+1}{2}f^2(\eta)\theta''(\eta)\Bigg] \\
&= (cx^{n-1})^2\,(T_w - T_\infty)\left[\frac{n+1}{2}f^2(\eta)\theta''(\eta) - \frac{n-3}{2}f(\eta)f'(\eta)\theta'(\eta)\right]
\end{aligned}
$$

$$= cx^{n-1}\left(T_w - T_\infty\right)\left[cx^{n-1}\frac{n+1}{2}f^2(\eta)\theta''(\eta) - cx^{n-1}\frac{n-3}{2}f(\eta)f'(\eta)\theta'(\eta)\right]. \quad (4.14)$$

$$\Rightarrow u\frac{\partial T}{\partial x} + v\frac{\partial T}{\partial y} + \lambda_T\left[u\frac{\partial u}{\partial x}\frac{\partial T}{\partial x} + v\frac{\partial u}{\partial y}\frac{\partial T}{\partial x} + u\frac{\partial v}{\partial x}\frac{\partial T}{\partial y} + v\frac{\partial v}{\partial y}\frac{\partial T}{\partial y} + u^2\frac{\partial^2 T}{\partial x^2}\right.$$
$$\left. + v^2\frac{\partial^2 T}{\partial y^2} + 2uv\frac{\partial^2 T}{\partial x \partial y}\right] = -(T_w - T_\infty)cx^{n-1}\frac{n+1}{2}f(\eta)\theta'(\eta)$$
$$+ \lambda_T\left((cx^{n-1})^2(T_w - T_\infty)\frac{n+1}{2}\right)\left[\frac{n+1}{2}f^2(\eta)\theta''(\eta) - \frac{n-3}{2}f(\eta)f'(\eta)\theta'(\eta)\right]$$
$$= (T_w - T_\infty)cx^{n-1}\frac{n+1}{2}\left[-f(\eta)\theta'(\eta) + \lambda_T cx^{n-1}\frac{n+1}{2}f^2(\eta)\theta''(\eta)\right.$$
$$\left. - \lambda_T cx^{n-1}\frac{n-3}{2}f(\eta)f'(\eta)\theta'(\eta)\right].$$
$$= (T_w - T_\infty)cx^{n-1}\frac{n+1}{2}\left[-f(\eta)\theta'(\eta) + L_T\frac{n+1}{2}f^2(\eta)\theta''(\eta)\right.$$
$$\left. - L_T\frac{n-3}{2}f(\eta)f'(\eta)\theta'(\eta)\right]. \quad (4.15)$$

$$\tau\left(D_B\left(\frac{\partial T}{\partial y}\frac{\partial C}{\partial y}\right) + \frac{D_T}{T_\infty}\left(\frac{\partial T}{\partial y}\right)^2\right)$$
$$= \tau\left[D_B(T_w - T_\infty)\theta'(\eta)\sqrt{\frac{c(n+1)}{2v}}x^{\frac{n-1}{2}}(C_w - C_\infty)\phi'(\eta)\sqrt{\frac{c(n+1)}{2v}}x^{\frac{n-1}{2}}\right.$$
$$\left. + \frac{D_T}{T_\infty}\left((T_w - T_\infty)\theta'(\eta)\sqrt{\frac{c(n+1)}{2v}}x^{\frac{n-1}{2}}\right)^2\right]$$
$$= \tau\left[D_B(T_w - T_\infty)\theta'(\eta)(C_w - C_\infty)\phi'(\eta)cx^{n-1}\frac{n+1}{2v}\right.$$
$$\left. + \frac{D_T}{T_\infty}((T_w - T_\infty)^2\theta'(\eta))^2 cx^{n-1}\frac{n+1}{2v}\right]$$
$$= (T_w - T_\infty)cx^{n-1}\frac{n+1}{2}\left[\frac{\tau D_B(C_w - C_\infty)}{v}\theta'(\eta)\phi'(\eta) + \frac{\tau D_T(T_w - T_\infty)}{T_\infty v}\theta'^2(\eta)\right]$$
$$= (T_w - T_\infty)cx^{n-1}\frac{n+1}{2}\left(N_b\theta'(\eta)\phi'(\eta) + N_t\theta'^2(\eta)\right). \quad (4.16)$$

$$\Rightarrow \alpha\frac{\partial^2 T}{\partial y^2} + \tau\left[D_B\frac{\partial C}{\partial y}\frac{\partial T}{\partial y} + \frac{D_T}{T_\infty}\left(\frac{\partial T}{\partial y}\right)^2\right] = (T_w - T_\infty)cx^{n-1}\frac{n+1}{2}\frac{1}{P_r}\theta''(\eta)$$
$$+ (T_w - T_\infty)cx^{n-1}\frac{n+1}{2}\left(N_b\theta'(\eta)\phi'(\eta) + N_t\theta'^2(\eta)\right)$$
$$= (T_w - T_\infty)cx^{n-1}\frac{n+1}{2}\left[\frac{1}{P_r}\theta''(\eta) + (N_b\theta'(\eta)\phi'(\eta) + N_t\theta'^2(\eta)\right]. \quad (4.17)$$

As a result of (4.15) and (4.17), the dimensionless form of (4.3), becomes;

$$(T_w - T_\infty)cx^{n-1}\frac{n+1}{2}\left[-f(\eta)\theta'(\eta) + L_T\frac{n+1}{2}f^2(\eta)\theta''(\eta)\right.$$
$$\left. - L_T\frac{n-3}{2}f(\eta)f'(\eta)\theta'(\eta)\right] = (T_w - T_\infty)cx^{n-1}\frac{n+1}{2}\left[\frac{1}{P_r}\theta''(\eta) + (N_b\theta'(\eta)\phi'(\eta)\right.$$

$$+ N_t\theta'^2(\eta)\Big]$$

$$\Rightarrow \Big[- f(\eta)\theta'(\eta) + L_T\frac{n+1}{2}f^2(\eta)\theta''(\eta) - L_T\frac{n-3}{2}f(\eta)f'(\eta)\theta'(\eta)\Big] = \Big[\frac{1}{P_r}\theta''(\eta) + N_b\theta'(\eta)\phi'(\eta) + N_t\theta'^2(\eta)\Big]$$

$$\Rightarrow \theta''(\eta)\Big[\frac{1}{Pr} - L_T\frac{n+1}{2}f^2(\eta)\Big] + f(\eta)\theta'(\eta) + L_T\frac{n-3}{2}f(\eta)f'(\eta)\theta'(\eta) + N_b\theta'(\eta)\phi'(\eta) + N_t\theta'^2(\eta) = 0. \tag{4.18}$$

Most of the derivatives for the concentration equation (4.4) already discussed in Chapter 3, the remaining derivatives have been determined shown below:

$$\begin{aligned}
\frac{\partial^2 C}{\partial x^2} &= \frac{\partial}{\partial x}\left((C_w - C_\infty)\phi'(\eta)\frac{n-1}{2x}\eta\right)\\
&= (C_w - C_\infty)\frac{\partial}{\partial x}\left(\phi'(\eta)\frac{n-1}{2}\frac{\eta}{x}\right)\\
&= (C_w - C_\infty)\left(\phi"(\eta)\frac{n-1}{2}\frac{\eta}{x}\frac{\partial}{\partial x}\eta + \phi'(\eta)\frac{n-1}{2}\eta\frac{\partial}{\partial x}x^{-1} + \phi'(\eta)\frac{n-1}{2x}\frac{\partial}{\partial x}\eta\right)\\
&= (C_w - C_\infty)\left(\phi''(\eta)\left(\frac{n-1}{2}\right)^2\frac{\eta^2}{x^2} - \phi'(\eta)\frac{n-1}{2}\frac{\eta}{x^2} + \phi'(\eta)\left(\frac{n-1}{2}\right)^2\frac{\eta}{x^2}\right)\\
&= (C_w - C_\infty)\frac{1}{x^2}\left[\left(\frac{n-1}{2}\right)^2\eta^2\phi''(\eta) - \frac{n-1}{2}\eta\phi'(\eta) + \left(\frac{n-1}{2}\right)^2\eta\phi'(\eta)\right].\\
\frac{\partial^2 C}{\partial x\partial y} &= \frac{\partial}{\partial x}\left((C_w - C_\infty)\phi'(\eta)\sqrt{\frac{c(n+1)}{2v}}x^{\frac{n-1}{2}}\right)\\
&= (C_w - C_\infty)\phi'(\eta)\sqrt{\frac{c(n+1)}{2v}}\frac{\partial}{\partial x}\left(\phi'(\eta)x^{\frac{n-1}{2}}\right)\\
&= (C_w - C_\infty)\phi'(\eta)\sqrt{\frac{c(n+1)}{2v}}\left[x^{\frac{n-1}{2}}\frac{\partial}{\partial x}\phi'(\eta) + \phi'(\eta)\frac{\partial}{\partial x}x^{\frac{n-1}{2}}\right]\\
&= (C_w - C_\infty)\phi'(\eta)\sqrt{\frac{c(n+1)}{2v}}\left[x^{\frac{n-1}{2}}\phi"(\eta)\frac{\partial}{\partial x}\eta + \phi'(\eta)\frac{n-1}{2x}x^{\frac{n-1}{2}}\right]\\
&= (C_w - C_\infty)\phi'(\eta)\sqrt{\frac{c(n+1)}{2v}}\frac{x^{\frac{n-1}{2}}}{x}\left[\frac{n-1}{2}\eta\phi"(\eta) + \frac{n-1}{2}\theta'(\eta)\right].
\end{aligned} \tag{4.19}$$

$$\begin{aligned}
u\frac{\partial u}{\partial x}\frac{\partial C}{\partial x} &= cx^n f'(\eta)\left(ncx^{n-1}f'(\eta) + cx^{n-1}f''(\eta)\frac{n-1}{2}\eta\right)\left((T_w - T_\infty)\phi'(\eta)\frac{n-1}{2x}\eta\right)\\
&= (cx^{n-1})^2 f'(\eta)\phi'(\eta)(C_w - C_\infty)\frac{n-1}{2}\eta\left[nf'(\eta) + \eta\frac{n-1}{2}f''(\eta)\right]\\
&= (cx^{n-1})^2(C_w - C_\infty)\left[nf'(\eta)^2\phi'(\eta)\frac{n-1}{2}\eta + \eta^2\left(\frac{n-1}{2}\right)^2 f'(\eta)\phi'(\eta)f''(\eta)\right]\\
&= (cx^{n-1})^2(C_w - C_\infty)\frac{n+1}{2}\left[\frac{n(n-1)}{n+1}f'(\eta)^2\phi'(\eta)\eta\right.
\end{aligned}$$

$$+\frac{(n-1)^2}{2(n+1)}\eta^2 f'(\eta)\phi'(\eta)f''(\eta)\Big]. \tag{4.20}$$

$$v\frac{\partial u}{\partial y}\frac{\partial C}{\partial x} = -\sqrt{\frac{cv(n+1)}{2}}x^{\frac{n-1}{2}}\left[f(\eta)+\frac{n-1}{n+1}\eta f'(\eta)\right]\left(cx^n f''(\eta)\sqrt{\frac{c(n+1)}{2v}}x^{\frac{n-1}{2}}\right)$$
$$\left((C_w-C_\infty)\phi'(\eta)\frac{n-1}{2x}\eta\right)$$
$$= -(cx^{n-1})^2(C_w-C_\infty)\frac{n+1}{2}\frac{n-1}{2}\eta f''(\eta)\phi'(\eta)\left[f(\eta)+\frac{n-1}{n+1}\eta f'(\eta)\right]$$
$$= -(cx^{n-1})^2(C_w-C_\infty)\frac{n+1}{2}\left[\frac{n-1}{2}\eta f''(\eta)\phi'(\eta)f(\eta)\right.$$
$$\left.+\frac{(n-1)^2}{2(n+1)}\eta^2 f'(\eta)f''(\eta)\phi'(\eta)\right]$$
$$= (cx^{n-1})^2(C_w-C_\infty)\frac{n+1}{2}\Big[-\frac{n-1}{2}\eta f''(\eta)\phi'(\eta)f(\eta)$$
$$-\frac{(n-1)^2}{2(n+1)}\eta^2 f'(\eta)f''(\eta)\phi'(\eta)\Big]. \tag{4.21}$$

$$u\frac{\partial v}{\partial x}\frac{\partial C}{\partial y} = cx^n f'(\eta)\left(-\sqrt{\frac{cv(n+1)}{2}}\frac{x^{\frac{n-1}{2}}}{x}\right)\left[\frac{n-1}{2}\eta f'(\eta)+\frac{(n-1)^2}{2(n+1)}\eta f'(\eta)\right.$$
$$\left.+\frac{(n-1)^2}{2(n+1)}\eta^2 f''(\eta)+\frac{n-1}{2}f(\eta)+\frac{(n-1)^2}{2(n+1)}\eta f'(\eta)\right]$$
$$\left((C_w-C_\infty)\phi'(\eta)\sqrt{\frac{c(n+1)}{2v}}x^{\frac{n-1}{2}}\right)$$
$$= cx^n f'(\eta)\left(-\sqrt{\frac{cv(n+1)}{2}}\frac{x^{\frac{n-1}{2}}}{x}\right)\left[\frac{n-1}{2}\eta f'(\eta)+\frac{(n-1)^2}{n+1}\eta f'(\eta)\right.$$
$$\left.+\frac{(n-1)^2}{2(n+1)}\eta^2 f''(\eta)+\frac{n-1}{2}f(\eta)\right]\left((C_w-C_\infty)\phi'(\eta)\sqrt{\frac{c(n+1)}{2v}}x^{\frac{n-1}{2}}\right)$$
$$= -(cx^{n-1})^2(C_w-C_\infty)\frac{n+1}{2}\eta f'(\eta)\phi'(\eta)\left[\frac{n-1}{2}\eta f'(\eta)+\frac{(n-1)^2}{n+1}\eta f'(\eta)\right.$$
$$\left.+\frac{(n-1)^2}{2(n+1)}\eta^2 f''(\eta)+\frac{n-1}{2}f(\eta)\right]$$
$$= (cx^{n-1})^2(C_w-C_\infty)\frac{n+1}{2}\Big[-\frac{(3n-1)(n-1)}{2(n+1)}\eta f'^2(\eta)\phi'(\eta)$$
$$-\frac{(n-1)^2}{2(n+1)}\eta^2 f'(\eta)\phi'(\eta)f''(\eta)-\frac{n-1}{2}f(\eta)f'(\eta)\phi'(\eta)\Big]. \tag{4.22}$$

$$v\frac{\partial v}{\partial y}\frac{\partial C}{\partial y} = \left(-\sqrt{\frac{cv(n+1)}{2}}x^{\frac{n-1}{2}}\left[f(\eta)+\frac{n-1}{n+1}\eta f'(\eta)\right]\right)\left(-cx^{n-1}\left[nf'(\eta)\right.\right.$$
$$\left.\left.+\frac{n-1}{2}\eta f''(\eta)\right]\right)\left((C_w-C_\infty)\phi'(\eta)\sqrt{\frac{c(n+1)}{2v}}x^{\frac{n-1}{2}}\right)$$
$$= (cx^{n-1})^2(C_w-C_\infty)\frac{n+1}{2}\left(f(\eta)\phi'(\eta)+\frac{n-1}{n+1}\eta f'(\eta)\phi'(\eta)\right)\left(nf'(\eta)\right.$$
$$\left.+\frac{n-1}{2}\eta f''(\eta)\right)$$

$$= (cx^{n-1})^2(C_w - C_\infty)\frac{n+1}{2}\bigg[nf(\eta)f'(\eta)\phi'(\eta) + \frac{n-1}{2}\eta f(\eta)f''(\eta)\phi'(\eta)$$
$$+ \frac{n(n-1)}{n+1}\eta f'^2(\eta)\phi'(\eta) + \frac{(n-1)^2}{2(n+1)}\eta^2 f'(\eta)\phi'(\eta)f''(\eta)\bigg]. \tag{4.23}$$

$$u^2\frac{\partial^2 C}{\partial x^2} = (cx^n f'(\eta))^2(C_w - C_\infty)\frac{1}{x^2}\bigg[\left(\frac{n-1}{2}\right)^2\eta^2\phi''(\eta) - \frac{n-1}{2}\eta\phi'(\eta)$$
$$+ \left(\frac{n-1}{2}\right)^2\eta\phi'(\eta)\bigg]$$
$$= (cx^n f'(\eta))^2(C_w - C_\infty)\frac{1}{x^2}\bigg[\left(\frac{n-1}{2}\right)^2\eta^2\phi''(\eta)$$
$$+ \frac{(n-1)^2 - 2(n-1)}{4}\phi'(\eta)\eta\bigg]$$
$$= (cx^n f'(\eta))^2(C_w - C_\infty)\frac{1}{x^2}\bigg[\left(\frac{n-1}{2}\right)^2\eta^2\phi''(\eta) + \frac{(n-1)(n-3)}{4}\phi'(\eta)\eta\bigg]$$
$$= (cx^{n-1})^2(C_w - C_\infty)\frac{n+1}{2}\bigg[\frac{2}{n+1}\left(\frac{n-1}{2}\right)^2\eta^2\phi''(\eta)f'^2(\eta)$$
$$+ \frac{2}{n+1}\frac{(n-1)(n-3)}{4}\phi'(\eta)\eta f'^2(\eta)\bigg]$$
$$= (cx^{n-1})^2(C_w - C_\infty)\frac{n+1}{2}\bigg[\frac{(n-1)^2}{2(n+1)}\eta^2\phi''(\eta)f'^2(\eta)$$
$$+ \frac{(n-1)(n-3)}{2(n+1)}\phi'(\eta)\eta f'^2(\eta)\bigg]. \tag{4.24}$$

$$2uv\frac{\partial^2 C}{\partial x\partial y} = 2cx^n f'(\eta)\left(-\sqrt{\frac{cv(n+1)}{2}}x^{\frac{n-1}{2}}\left[f(\eta) + \frac{n-1}{n+1}\eta f'(\eta)\right]\right)$$
$$\left(C_w - C_\infty\sqrt{\frac{c(n+1)}{2v}}\frac{x^{\frac{n-1}{2}}}{x}\left[\frac{n-1}{2}\eta\phi''(\eta) + \frac{n-1}{2}\phi'(\eta)\right]\right)$$
$$= -2(cx^{n-1})^2(C_w - C_\infty)\frac{n+1}{2}\bigg[\frac{n-1}{2}\eta f(\eta)f'(\eta)\phi''(\eta)$$
$$+ \frac{n-1}{2}f(\eta)f'(\eta)\phi'(\eta) + \frac{(n-1)^2}{2(n+1)}\eta^2 f'^2(\eta)\phi''(\eta)$$
$$+ \frac{(n-1)^2}{2(n+1)}\eta f'^2(\eta)\phi'(\eta)\bigg]$$
$$= (cx^{n-1})^2(C_w - C_\infty)\frac{n+1}{2}\bigg[-(n-1)\eta f(\eta)f'(\eta)\phi''(\eta)$$
$$- (n-1)f(\eta)f'(\eta)\phi'(\eta) - \frac{(n-1)^2}{n+1}\eta^2 f'^2(\eta)\phi''(\eta)$$
$$- \frac{(n-1)^2}{n+1}\eta f'^2(\eta)\phi'(\eta)\bigg]. \tag{4.25}$$

$$v^2\frac{\partial^2 C}{\partial y^2} = \left(-\sqrt{\frac{cv(n+1)}{2}}x^{\frac{n-1}{2}}\left(f(\eta) + \frac{n-1}{n+1}\eta f'(\eta)\right)\right)^2\left((C_w - C_\infty)\phi''(\eta)\right.$$
$$\left.\frac{c(n+1)}{2v}x^{n-1}\right)$$

$$= (cx^{n-1})^2(C_w - C_\infty)\left(\frac{n+1}{2}\right)^2\left[f^2(\eta)\phi''(\eta) + \left(\frac{n-1}{n+1}\right)^2\eta^2 f'^2(\eta)\phi''(\eta) + \frac{2(n-1)}{n+1}\eta f(\eta)f'(\eta)\phi''(\eta)\right]$$

$$= (cx^{n-1})^2(C_w - C_\infty)\frac{n+1}{2}\left[\frac{n+1}{2}f^2(\eta)\phi''(\eta) + \frac{(n-1)^2}{2(n+1)}\eta^2 f'^2(\eta)\phi''(\eta) + (n-1)\eta f(\eta)f'(\eta)\phi''(\eta)\right]. \tag{4.26}$$

$$u\frac{\partial u}{\partial x}\frac{\partial C}{\partial x} + v\frac{\partial v}{\partial y}\frac{\partial C}{\partial y} + u\frac{\partial v}{\partial x}\frac{\partial C}{\partial y} + v\frac{\partial u}{\partial y}\frac{\partial C}{\partial x} + 2uv\frac{\partial^2 C}{\partial x\partial y} + u^2\frac{\partial^2 C}{\partial x^2} + v^2\frac{\partial^2 C}{\partial y^2}$$

$$= (cx^{n-1})^2(C_w - C_\infty)\frac{n+1}{2}\left[\frac{n(n-1)}{n+1}f'(\eta)^2\phi'(\eta)\eta + \frac{(n-1)^2}{2(n+1)}\eta^2 f'(\eta)\phi'(\eta)f''(\eta)\right.$$
$$+ nf(\eta)f'(\eta)\phi'(\eta) + \frac{n-1}{2}\eta f(\eta)f''(\eta)\phi'(\eta) + \frac{n(n-1)}{n+1}\eta f'^2(\eta)\phi'(\eta)$$
$$+ \frac{(n-1)^2}{2(n+1)}\eta^2 f'(\eta)\phi'(\eta)f''(\eta) - \frac{(3n-1)(n-1)}{2(n+1)}\eta f'^2(\eta)\phi'(\eta)$$
$$- \frac{(n-1)^2}{2(n+1)}\eta^2 f'(\eta)\phi'(\eta)f''(\eta) - \frac{n-1}{2}f(\eta)f'(\eta)\phi'(\eta) - \frac{n-1}{2}\eta f''(\eta)\phi'(\eta)f(\eta)$$
$$- \frac{(n-1)^2}{2(n+1)}\eta^2 f'(\eta)f''(\eta)\phi'(\eta) - (n-1)\eta f(\eta)f'(\eta)\phi''(\eta) - (n-1)f(\eta)f'(\eta)\phi'(\eta)$$
$$- \frac{(n-1)^2}{n+1}\eta^2 f'^2(\eta)\phi''(\eta) - \frac{(n-1)^2}{n+1}\eta f'^2(\eta)\phi'(\eta) + \frac{(n-1)^2}{2(n+1)}\eta^2\phi''(\eta)f'^2(\eta)$$
$$+ \frac{(n-1)(n-3)}{2(n+1)}\phi'(\eta)\eta f'^2(\eta) + \frac{n+1}{2}f^2(\eta)\phi''(\eta) + \frac{(n-1)^2}{2(n+1)}\eta^2 f'^2(\eta)\phi''(\eta)$$
$$\left.+ (n-1)\eta f(\eta)f'(\eta)\phi''(\eta)\right]$$

$$= (cx^{n-1})^2(C_w - C_\infty)\frac{n+1}{2}\left[\frac{n(n-1)}{n+1}f'(\eta)^2\phi'(\eta)\eta + \frac{(n-1)^2}{2(n+1)}\eta^2 f'(\eta)\phi'(\eta)f''(\eta)\right.$$
$$+ nf(\eta)f'(\eta)\phi'(\eta) + \frac{n-1}{2}\eta f(\eta)f''(\eta)\phi'(\eta) + \frac{n(n-1)}{n+1}\eta f'^2(\eta)\phi'(\eta)$$
$$+ \frac{(n-1)^2}{2(n+1)}\eta^2 f'(\eta)\phi'(\eta)f''(\eta) - \frac{(3n-1)(n-1)}{2(n+1)}\eta f'^2(\eta)\phi'(\eta)$$
$$- \frac{(n-1)^2}{2(n+1)}\eta^2 f'(\eta)\phi'(\eta)f''(\eta) - \frac{n-1}{2}f(\eta)f'(\eta)\phi'(\eta) - \frac{n-1}{2}\eta f''(\eta)\phi'(\eta)f(\eta)$$
$$- \frac{(n-1)^2}{2(n+1)}\eta^2 f'(\eta)f''(\eta)\phi'(\eta) - (n-1)\eta f(\eta)f'(\eta)\phi''(\eta) - (n-1)f(\eta)f'(\eta)\phi'(\eta)$$
$$- \frac{(n-1)^2}{n+1}\eta^2 f'^2(\eta)\phi''(\eta) - \frac{(n-1)^2}{n+1}\eta f'^2(\eta)\phi'(\eta) + \frac{(n-1)^2}{2(n+1)}\eta^2\phi''(\eta)f'^2(\eta)$$
$$+ \frac{(n-1)(n-3)}{2(n+1)}\phi'(\eta)\eta f'^2(\eta) + \frac{n+1}{2}f^2(\eta)\phi''(\eta) + \frac{(n-1)^2}{2(n+1)}\eta^2 f'^2(\eta)\phi''(\eta)$$
$$\left.+ (n-1)\eta f(\eta)f'(\eta)\phi''(\eta)\right]$$

$$= (cx^{n-1})^2(C_w - C_\infty)\frac{n+1}{2}\left[\left(\frac{n(n-1)}{n+1} - \frac{(3n-1)(n-1)}{2(n+1)} + \frac{n(n-1)}{n+1}\right.\right.$$

$$
\begin{aligned}
&+\frac{(n-1)(n-3)}{2(n+1)}-\frac{(n-1)^2}{n+1}\Big)\eta f'^2(\eta)\phi'(\eta)\\
&+\left(n-\frac{n-1}{2}-(n-1)\right)f(\eta)f'(\eta)\phi'(\eta)+\left(\frac{n+1}{2}\right)f^2(\eta)\phi''(\eta)\Big]\\
&=(cx^{n-1})^2(C_w-C_\infty)\frac{n+1}{2}\\
&\Big[\frac{n-1}{n+1}\left(\frac{2n-3n+1+2n+n-3-2n+2}{2}\right)\eta f'^2(\eta)\phi'(\eta)\\
&+\left(\frac{2n-n+1-2n+2}{2}\right)f(\eta)f'(\eta)\phi'(\eta)+\frac{n+1}{2}f^2(\eta)\phi''(\eta)\Big]\\
&=(cx^{n-1})^2\,(C_w-C_\infty)\,\frac{n+1}{2}\left[\frac{n+1}{2}f^2(\eta)\phi''(\eta)-\frac{n-3}{2}f(\eta)f'(\eta)\phi'(\eta)\right]\\
&=cx^{n-1}\,(C_w-C_\infty)\,\frac{n+1}{2}\left[cx^{n-1}\frac{n+1}{2}f^2(\eta)\phi''(\eta)-cx^{n-1}\frac{n-3}{2}f(\eta)f'(\eta)\phi'(\eta)\right].
\end{aligned}
\tag{4.27}
$$

For the L.H.S of the equation (4.4), the following derivatives have been determined:

$$
\begin{aligned}
&u\frac{\partial C}{\partial x}+v\frac{\partial C}{\partial y}+\lambda_C\Big[u\frac{\partial u}{\partial x}\frac{\partial C}{\partial x}+v\frac{\partial u}{\partial y}\frac{\partial C}{\partial x}+u\frac{\partial v}{\partial x}\frac{\partial C}{\partial y}+v\frac{\partial v}{\partial y}\frac{\partial C}{\partial y}+u^2\frac{\partial^2 C}{\partial x^2}+v^2\frac{\partial^2 C}{\partial y^2}\\
&+2uv\frac{\partial^2 C}{\partial x\partial y}\Big]=-cx^{n-1}(C_w-C_\infty)\frac{n+1}{2}\phi'(\eta)f(\eta)+\lambda_C(cx^{n-1})^2(C_w-C_\infty)\frac{n+1}{2}\\
&\qquad\Big[\frac{n+1}{2}f^2(\eta)\phi''(\eta)-\frac{n-3}{2}f(\eta)f'(\eta)\phi'(\eta)\Big]\\
&\qquad=cx^{n-1}(C_w-C_\infty)\frac{n+1}{2}\Big[-\phi'(\eta)f(\eta)\\
&\qquad\quad+\lambda_C cx^{n-1}\frac{n+1}{2}f^2(\eta)\phi''(\eta)-\lambda_C cx^{n-1}\frac{n-3}{2}f(\eta)f'(\eta)\phi'(\eta)\Big]\\
&\qquad=cx^{n-1}(C_w-C_\infty)\frac{n+1}{2}\Big[-\phi'(\eta)f(\eta)+L_C\frac{n+1}{2}f^2(\eta)\phi''(\eta)\\
&\qquad\quad-L_C\frac{n-3}{2}f(\eta)f'(\eta)\phi'(\eta)\Big].
\end{aligned}
\tag{4.28}
$$

Some dimensionless form of equation 4.4 were previously determined in Chapter 3 for equation 3.4.

Now, For the remaining dimensionless form for the R.H.S of the equation (4.4), the following derivatives have been determined below:

$$
\begin{aligned}
&K_r^2(C-C_\infty)\left[\frac{T}{T_\infty}\right]^m\exp\left(\frac{-E_a}{kT}\right)\\
&=K_r^2(C-C_\infty)\left[\frac{T_\infty(1+(\theta_w-1)\theta(\eta))}{T_\infty}\right]^m\exp\left(\frac{-E_a}{KT_\infty(1+(\theta_w-1)\theta(\eta))}\right)
\end{aligned}
$$

$$= K_r^2\phi(\eta)(C_w - C_\infty)\left[1 + (T_w - 1)\theta_\eta\right]^m \exp\left(\frac{-E_a}{KT_\infty(1 + (\theta_w - 1)\theta(\eta))}\right)$$

$$= (C_w - C_\infty)cx^{n-1}\frac{n+1}{2}\frac{2}{n+1}\frac{1}{cx^{n-1}(C_w - C_\infty)}K_r^2\phi(\eta)(C_w - C_\infty)\left[1 + (\theta_w - 1)\theta_\eta\right]^m$$
$$\exp\left(\frac{-E_a}{KT_\infty(1 + (\theta_w - 1)\theta(\eta))}\right)$$

$$= (C_w - C_\infty)cx^{n-1}\frac{n+1}{2}\left[\frac{2}{n+1}\phi(\eta)\frac{K_r^2}{cx^{n-1}}\left[1 + (\theta_w - 1)\theta_\eta\right]^m\right.$$
$$\left.\exp\left(\frac{-E_a}{KT_\infty(1 + (\theta_w - 1)\theta(\eta))}\right)\right]$$

$$= (C_w - C_\infty)cx^{n-1}\frac{n+1}{2}\left[\frac{2}{n+1}\phi(\eta)\gamma_1\left[1 + (\theta_w - 1)\theta_\eta\right]^m \exp\left(\frac{-E}{(1 + (\theta_w - 1)\theta(\eta))}\right)\right].$$

$$D\frac{\partial^2 C}{\partial y^2} - K_C(C - C_\infty) - K_r^2(C - C_\infty)\left[\frac{T}{T_\infty}\right]^m \exp\left(\frac{-E_a}{kT_\infty}\right) = (C_w - C_\infty)cx^{n-1}$$

$$\frac{n+1}{2}\left[\frac{1}{Sc}\phi''(\eta) - \frac{2}{n+1}K_c\phi(\eta) + \frac{2}{n+1}\gamma_1\phi(\eta)(1 + (\theta_w - 1)\theta(\eta))^m\right.$$
$$\left.\exp\left[\frac{-E}{1 + (\theta_w - 1)\theta(\eta)}\right]\right. \tag{4.29}$$

As a result, The concentration equation (4.4) has been satisfied by using the equations (4.28) and (4.29):

$$\Rightarrow \quad -\frac{n+1}{2}\phi'(\eta)f(\eta) + L_C\frac{n+1}{2}f^2(\eta)\phi''(\eta) - L_C\frac{n-3}{2}f(\eta)f'(\eta)\phi'(\eta) = \frac{1}{Sc}\phi''(\eta)$$
$$-\frac{2}{n+1}K_c\phi(\eta) - \frac{2}{n+1}\gamma_1\phi(\eta)(1 + (\theta_w - 1)\theta(\eta))^m \exp\left(\frac{-E}{1 + (\theta_w - 1)\theta(\eta)}\right)$$

$$\Rightarrow \quad \frac{1}{Sc}\phi''(\eta) - L_C\frac{n+1}{2}f^2(\eta)\phi''(\eta) + \phi'(\eta)f(\eta) - \frac{2}{n+1}K_c\phi(\eta) + L_C\frac{n-3}{2}$$
$$f(\eta)f'(\eta)\phi'(\eta) + \frac{2}{n+1}\gamma_1\phi(\eta)(1 + (\theta_w - 1)\theta(\eta))^m \exp\left(\frac{-E}{1 + (\theta_w - 1)\theta(\eta)}\right)$$
$$= 0 \tag{4.30}$$

The following dimensionless parameters are used in equations (4.3) and (4.4):

$$M{=}\tfrac{\sigma B_0^2}{\rho a},\ Rd{=}\tfrac{16\sigma^* T_\infty^3}{3kk^*},\ Pr{=}\tfrac{\nu}{\alpha},\ L_T = \lambda_t cx^{n-1},\ \lambda_C{=}\mathrm{c}\Gamma_c,\ K_c = \tfrac{K_c^*}{a},\ Sc{=}\tfrac{\nu}{D_B}$$
$$L_C = \lambda_c cx^{n-1},\quad Nb{=}\tfrac{\tau D_B(C_w - C_\infty)}{\nu},\quad Nt{=}\tfrac{\tau D_T(T_w - T_\infty)}{\nu T_\infty},\quad Ec{=}\tfrac{U_w^2}{(c_p)_f(T_w - T_\infty)}.$$

The final version of the governing model's dimensionless form is:

$$\Rightarrow \quad \left(1 + \frac{1}{\beta}\right)f'''(\eta) + f''(\eta)f(\eta) - \frac{2n}{n+1}f'^2(\eta) + \frac{2}{n+1}\left(\gamma^*\theta(\eta) + \gamma\phi(\eta)\right)\cos\alpha$$
$$-\frac{2}{n+1}\left[\left(M + 1/K_p\right)f'(\eta) + F_s f'^2(\eta)\right] = 0, \tag{4.31}$$

$$\Rightarrow \theta''(\eta)\left[\frac{1}{Pr} - L_T\frac{n+1}{2}f^2(\eta)\right] + f(\eta)\theta'(\eta) + L_T\frac{n-3}{2}f(\eta)f'(\eta)\theta'(\eta) + N_b\theta'(\eta)\phi'(\eta) + N_t\theta'^2(\eta) = 0, \tag{4.32}$$

$$\Rightarrow \frac{1}{Sc}\phi''(\eta) - L_C\frac{n+1}{2}f^2(\eta)\phi''(\eta) + \phi'(\eta)f(\eta) - \frac{2}{n+1}K_c\phi(\eta) + L_C\frac{n-3}{2}f(\eta)f'(\eta)\phi'(\eta) + \frac{2}{n+1}\gamma_1\phi(\eta)(1+(\theta_w-1)\theta(\eta))^m \exp\left(\frac{-E}{1+(\theta_w-1)\theta(\eta)}\right) = 0. \tag{4.33}$$

The dimensionless form of the associated BCs (4.5) is:

$$\left.\begin{aligned} &\eta \to 0: \ f(0) = S, \ f'(0) = 1 + V_s f''(\eta), \ \theta(0) = 1 + \lambda_t\theta'(0), \ \phi(0) = 1 + \lambda_c\phi'(0) \\ &\eta \to \infty: \ f' \to 0, \ g \to 0, \ \theta \to 0, \ \phi \to 0. \end{aligned}\right\} \tag{4.34}$$

The skin friction coefficient, Nusselt number and sherwood number are already discussed in chap 3 (3.29), (3.31) and (3.33) respectively.

$$Re_x^{\frac{1}{2}}Cf_x = \left(1+\frac{1}{\beta}\right)\sqrt{\frac{n+1}{2}}f''(0). \tag{4.35}$$

$$Re_x^{\frac{-1}{2}}Nu_x = -\sqrt{\frac{n+1}{2}}\theta'(0). \tag{4.36}$$

$$Re_x^{\frac{-1}{2}}Sh_x = -\sqrt{\frac{n+1}{2}}\phi'(0). \tag{4.37}$$

4.4 Numerical Method for Solution

The ordinary differential equations (4.34) to (4.36) have been resolved using the shooting method.

$$f''' = \frac{1}{\left(1+\frac{1}{\beta}\right)}\left[\frac{2n}{n+1}f'^2 - ff'' - \frac{2}{n+1}(\gamma^*\theta + \gamma\phi)cos\alpha + \frac{2}{n+1}\left(M + \frac{1}{K_p}\right)f' + \frac{2}{n+1}Fsf'^2\right].$$

$$\theta'' = \left(\frac{1}{Pr} - L_T\frac{n+1}{2}f^2\right)^{-1}\left[-\theta' f - L_T\frac{n-3}{2}ff'\theta' - Nb\theta'\phi' - Nt\theta'^2\right].$$

$$\phi'' = \left(\frac{1}{Sc} - L_C\frac{n+1}{2}f^2\right)^{-1}\left[\frac{2}{n+1}Kc\phi - \phi' f - L_C\frac{n-3}{2}ff'\phi'\right.$$

$$+\frac{2}{n+1}\gamma_1\phi\left(1+(\theta_w-1)\theta\right)^m\exp\left(\frac{-E}{1+(\theta_w-1)\theta}\right)\Bigg].$$

For this purpose, the following notations have been taken:

$$\begin{aligned}
&f=Z_1, \quad f'=Z_1'=Z_2, \quad f''=Z_1''=Z_2'=Z_3,\\
&\theta=Z_4, \quad \theta'=Z_4'=Z_5, \quad \theta''=Z_4''=Z_5',\\
&\phi=Z_6, \quad \phi'=Z_6'=Z_7, \quad \phi''=Z_6''=Z_7'.
\end{aligned}$$

The equations (4.34)-(4.36) are transformed into the following system of first-order ODEs:

$$Z_1'=Z_2, \qquad Z_1(0)=S.$$

$$Z_2'=Z_3, \qquad Z_2(0)=1+V_sp.$$

$$\begin{aligned}
Z_3'=&\frac{\beta}{1+\beta}\Bigg[\frac{2n}{n+1}{Z_2}^2-Z_1Z_3-\frac{2}{n+1}(\gamma^*Z_4+\gamma Z_6)cos\alpha\\
&+\frac{2}{n+1}\left(M+\frac{1}{K_p}\right)Z_2+\frac{2}{n+1}Fs{Z_2}^2\Bigg], \qquad Z_3(0)=p.
\end{aligned}$$

$$Z_4'=Z_5, \qquad Z_4(0)=1+\lambda_tq.$$

$$\begin{aligned}
Z_5'=&\left(\frac{1}{Pr}-L_T\frac{n+1}{2}{Z_1}^2\right)^{-1}\Bigg[-Z_1Z_5-L_T\frac{n-3}{2}Z_1Z_2Z_5-NbZ_5Z_7-Nt{Z_5}^2\Bigg]\\
&Z_5(0)=q.
\end{aligned}$$

$$Z_6'=Z_7, \qquad Z_6(0)=1+\lambda_cr.$$

$$\begin{aligned}
Z_7'=&\left(\frac{1}{Sc}-L_C\frac{n+1}{2}{Z_1}^2\right)^{-1}\Bigg[\frac{2}{n+1}KcZ_6-Z_1Z_7-L_C\frac{n-3}{2}Z_1Z_2Z_7\\
&+\frac{2}{n+1}\gamma_1Z_6\left(1+(\theta_w-1)Z_4\right)^m\exp\left(\frac{-E}{1+(\theta_w-1)Z_4}\right)\Bigg], \qquad Z_7(0)=r.
\end{aligned}$$

RK-4 method has been applied to compute the above IVP. The domain of the problem is considered to be bounded i.e. $[0,\ \eta_\infty]$, where η_∞ represents a +ve real number, for which the variation in the solution is ignorable after $\eta=\eta_\infty$. The missing conditions p, q and r are to be chosen such that:

$$Z_2(\eta_\infty,p,q,r)=0, \qquad Z_4(\eta_\infty,p,q,r)=0, \qquad Z_6(\eta_\infty,p,q,r)=0.$$

Newton's method will be used to find p, q and r. This method has the following iterative scheme:

$$\begin{bmatrix} p \\ q \\ r \end{bmatrix}_{(n+1)} = \begin{bmatrix} p \\ q \\ r \end{bmatrix}_{n} - \begin{bmatrix} \frac{\partial Z_2}{\partial p} & \frac{\partial Z_2}{\partial q} & \frac{\partial Z_2}{\partial r} \\ \frac{\partial Z_4}{\partial p} & \frac{\partial Z_4}{\partial q} & \frac{\partial Z_4}{\partial r} \\ \frac{\partial Z_6}{\partial p} & \frac{\partial Z_6}{\partial q} & \frac{\partial Z_6}{\partial r} \end{bmatrix}^{-1}_{(n)} \begin{bmatrix} Z_2 \\ Z_4 \\ Z_6 \end{bmatrix}_{(n)}. \tag{4.38}$$

To move further, the following notations have been introduced:

$$\begin{aligned}
&\frac{\partial Z_1}{\partial p} = Z_8, \quad \frac{\partial Z_2}{\partial p} = Z_9, \quad \frac{\partial Z_3}{\partial p} = Z_{10}, \quad \frac{\partial Z_4}{\partial p} = Z_{11}, \quad \frac{\partial Z_5}{\partial p} = Z_{12}, \\
&\frac{\partial Z_6}{\partial p} = Z_{13}, \quad \frac{\partial Z_7}{\partial p} = Z_{14} \quad \frac{\partial Z_1}{\partial q} = Z_{15}, \quad \frac{\partial Z_2}{\partial q} = Z_{16}, \quad \frac{\partial Z_3}{\partial q} = Z_{17}, \\
&\frac{\partial Z_4}{\partial q} = Z_{18}, \quad \frac{\partial Z_5}{\partial q} = Z_{19}, \quad \frac{\partial Z_6}{\partial q} = Z_{20}, \quad \frac{\partial Z_7}{\partial q} = Z_{21}, \quad \frac{\partial Z_1}{\partial r} = Z_{22}, \\
&\frac{\partial Z_2}{\partial r} = Z_{23}, \quad \frac{\partial Z_3}{\partial r} = Z_{24}, \quad \frac{\partial Z_4}{\partial r} = Z_{25}, \quad \frac{\partial Z_5}{\partial r} = Z_{26}, \quad \frac{\partial Z_6}{\partial r} = Z_{27}, \\
&\frac{\partial Z_7}{\partial r} = Z_{28}.
\end{aligned}$$

By using the above notations, the iterative scheme of Newton method is as follows:

$$\begin{bmatrix} p \\ q \\ r \end{bmatrix}_{(n+1)} = \begin{bmatrix} p \\ q \\ r \end{bmatrix}_{(n)} - \begin{bmatrix} Z_9 & Z_{16} & Z_{23} \\ Z_{11} & Z_{18} & Z_{25} \\ Z_{13} & Z_{20} & Z_{27} \end{bmatrix}^{-1}_{(n)} \begin{bmatrix} Z_2 \\ Z_4 \\ Z_6 \end{bmatrix}_{(n)}. \tag{4.39}$$

Now differentiating the last system of seven first order ODEs first with respect to p, then w.r.t q and finally with respect to r, we get twenty one more ODEs, as follows:

$$Z_8' = Z_9, \qquad Z_8(0) = 0.$$

$$Z_9' = Z_{10}, \qquad Z_9(0) = V_s.$$

$$\begin{aligned}
Z_{10}' = \left(\frac{\beta}{1+\beta}\right) \Bigg[&\frac{4n}{n+1} Z_2 Z_9 - Z_1 Z_{10} - Z_3 Z_8 - \frac{2}{n+1}(\gamma^* Z_{11} + \gamma Z_{13}) cos\alpha \\
&+ \frac{2}{n+1}\left(M + \frac{1}{K_p}\right) Z_9 + \frac{2}{n+1} 2Fs Z_2 Z_9 \Bigg], \qquad Z_{10}(0) = 1.
\end{aligned}$$

$$Z_{11}' = Z_{12}, \qquad Z_{11}(0) = 0.$$

$$Z'_{12} = \left(\frac{1}{Pr} - L_T\frac{n+1}{2}{Z_1}^2\right)^{-1}\Bigg[- Z_1Z_{12} - Z_5Z_8 - L_T\frac{n-3}{2}Z_2Z_5Z_8 - L_T\frac{n-3}{2}Z_1Z_5Z_9 - L_T\frac{n-3}{2}Z_1Z_2Z_{12} - NbZ_7Z_{12} - NbZ_5Z_{14} - 2NtZ_5Z_{12}\Bigg] + \left(\frac{1}{Pr} - L_T\frac{n+1}{2}{Z_1}^2\right)^{-2}(L_T(n+1)Z_1Z_8)\Bigg[- Z_1Z_5 - L_T\frac{n-3}{2}Z_1Z_2Z_5 - NbZ_5Z_7 - Nt{Z_5}^2\Bigg], \qquad Z_{12}(0) = 0.$$

$$Z'_{13} = Z_{14}, \qquad Z_{13}(0) = 0.$$

$$Z'_{14} = \left(\frac{1}{Sc} - L_C\frac{n+1}{2}{Z_1}^2\right)^{-1}\Bigg[\frac{2}{n+1}KcZ_{13} - Z_7Z_8 - Z_1Z_{14} - L_C\frac{n-3}{2}Z_2Z_7Z_8 - L_C\frac{n-3}{2}Z_1Z_7Z_9 - L_C\frac{n-3}{2}Z_1Z_2Z_{14} + \frac{2}{n+1}\gamma_1Z_{13}\left(1+(\theta_w-1)Z_4\right)^m\exp\left(\frac{-E}{1+(\theta_w-1)Z_4}\right) + \frac{2}{n+1}m\gamma_1Z_6Z_{11}(T_w-1)\left(1+(\theta_w-1)Z_4\right)^{m-1}\exp\left(\frac{-E}{1+(\theta_w-1)Z_4}\right) + \frac{2}{n+1}\gamma_1Z_6\left(1+(\theta_w-1)Z_4\right)^m\exp\left(\frac{-E}{1+(\theta_w-1)Z_4}\right)\frac{E(\theta_w-1)Z_{11}}{(1+(\theta_w-1)Z_4)^2}\Bigg] + \left(\frac{1}{Sc} - L_C\frac{n+1}{2}{Z_1}^2\right)^{-2}(L_C(n+1)Z_1Z_8)\Bigg[\frac{2}{n+1}KcZ_6 - Z_1Z_7 - L_C\frac{n-3}{2}Z_1Z_2Z_7 + \frac{2}{n+1}\gamma_1Z_6\left(1+(\theta_w-1)Z_4\right)^m\exp\left(\frac{-E}{1+(\theta_w-1)Z_4}\right)\Bigg], \qquad Z_{14}(0) = 0.$$

$$Z'_{15} = Z_{16}, \qquad Z_{15}(0) = 0.$$

$$Z'_{16} = Z_{17}, \qquad Z_{16}(0) = 0.$$

$$Z'_{17} = \left(\frac{\beta}{1+\beta}\right)\Bigg[\frac{4n}{n+1}Z_2Z_{16} - Z_1Z_{17} - Z_3Z_{15} - \frac{2}{n+1}(\gamma^*Z_8 + \gamma Z_{20})cos\alpha + \frac{2}{n+1}\left(M + \frac{1}{K_p}\right)Z_{16} + \frac{2}{n+1}2FsZ_2Z_{16}\Bigg], \qquad Z_{17}(0) = 0.$$

$$Z'_{18} = Z_{19}, \qquad Z_{18}(0) = \lambda_t.$$

$$Z'_{19} = \left(\frac{1}{Pr} - L_T\frac{n+1}{2}{Z_1}^2\right)^{-1}\Bigg[- Z_5Z_{15} - Z_1Z_{19} - L_T\frac{n-3}{2}Z_2Z_5Z_{12} - L_T\frac{n-3}{2}Z_1Z_5Z_{16} - L_T\frac{n-3}{2}Z_1Z_2Z_{19} - NbZ_7Z_{19} - NbZ_5Z_{21} - 2NtZ_5Z_{19}\Bigg] + \left(\frac{1}{Pr} - L_T\frac{n+1}{2}{Z_1}^2\right)^{-2}(L_T(n+1)Z_1Z_{15})\Bigg[- Z_1Z_5 - L_T\frac{n-3}{2}Z_1Z_2Z_5 - NbZ_5Z_7 - Nt{Z_5}^2\Bigg], \qquad Z_{19}(0) = 1.$$

$$Z'_{20} = Z_{21}, \qquad Z_{20}(0) = 0.$$

$$Z_{21}' = \left(\frac{1}{Sc} - L_C\frac{n+1}{2}{Z_1}^2\right)^{-1}\left[\frac{2}{n+1}KcZ_{20} - Z_7Z_{15} - Z_1Z_{21} - L_C\frac{n-3}{2}Z_2Z_7Z_{15}\right.$$
$$- L_C\frac{n-3}{2}Z_1Z_7Z_{16} - L_C\frac{n-3}{2}Z_1Z_2Z_{21}$$
$$+ \frac{2}{n+1}\gamma_1 Z_{20}\left(1+(\theta_w-1)Z_4\right)^m \exp\left(\frac{-E}{1+(\theta_w-1)Z_4}\right)$$
$$+ \frac{2}{n+1}m\gamma_1 Z_6Z_{18}(T_w-1)\left(1+(\theta_w-1)Z_4\right)^{m-1}\exp\left(\frac{-E}{1+(\theta_w-1)Z_4}\right)$$
$$\left.+ \frac{2}{n+1}\gamma_1 Z_6\left(1+(\theta_w-1)Z_4\right)^m \exp\left(\frac{-E}{1+(\theta_w-1)Z_4}\right)\frac{E(\theta_w-1)Z_{18}}{(1+(\theta_w-1)Z_4)^2}\right]$$
$$+ \left(\frac{1}{Sc} - L_C\frac{n+1}{2}{Z_1}^2\right)^{-2}(L_C(n+1)Z_1Z_{15})\left[\frac{2}{n+1}KcZ_6 - Z_1Z_7\right.$$
$$\left.- L_C\frac{n-3}{2}Z_1Z_2Z_7 + \frac{2}{n+1}\gamma_1 Z_6\left(1+(\theta_w-1)Z_4\right)^m\exp\left(\frac{-E}{1+(\theta_w-1)Z_4}\right)\right], \qquad Z_{21}(0)=0.$$

$$Z_{22}' = Z_{23}, \qquad Z_{22}(0)=0.$$

$$Z_{23}' = Z_{24}, \qquad Z_{23}(0)=0.$$

$$Z_{24}' = \left(\frac{\beta}{1+\beta}\right)\left[\frac{4n}{n+1}Z_2Z_{23} - Z_1Z_{24} - Z_3Z_{22} - \frac{2}{n+1}(\gamma^*Z_{25}+\gamma Z_{27})cos\alpha\right.$$
$$\left.+ \frac{2}{n+1}\left(M+\frac{1}{K_p}\right)Z_{23} + \frac{2}{n+1}2FsZ_2Z_{23}\right], \qquad Z_{24}(0)=0.$$

$$Z_{25}' = Z_{26}, \qquad Z_{25}(0)=0.$$

$$Z_{26}' = \left(\frac{1}{Pr} - L_T\frac{n+1}{2}{Z_1}^2\right)^{-1}\left[-Z_5Z_{22} - Z_1Z_{26} - L_T\frac{n-3}{2}Z_2Z_5Z_{22}\right.$$
$$- L_T\frac{n-3}{2}Z_1Z_5Z_{23} - L_T\frac{n-3}{2}Z_1Z_2Z_{26} - NbZ_7Z_{26} - NbZ_5Z_{28}$$
$$\left.- 2NtZ_5Z_{26}\right] + \left(\frac{1}{Pr} - L_T\frac{n+1}{2}{Z_1}^2\right)^{-2}(L_T(n+1)Z_1Z_{22})\left[-Z_1Z_5\right.$$
$$\left.- L_T\frac{n-3}{2}Z_1Z_2Z_5 - NbZ_5Z_7 - Nt{Z_5}^2\right], \qquad Z_{26}(0)=0.$$

$$Z_{27}' = Z_{28}, \qquad Z_{27}(0)=\lambda_c.$$

$$Z_{28}' = \left(\frac{1}{Sc} - L_C\frac{n+1}{2}{Z_1}^2\right)^{-1}\left[\frac{2}{n+1}KcZ_{27} - Z_7Z_{22} - Z_1Z_{28} - L_C\frac{n-3}{2}Z_2Z_7Z_{22}\right.$$
$$- L_C\frac{n-3}{2}Z_1Z_7Z_{23} - L_C\frac{n-3}{2}Z_1Z_2Z_{28}$$
$$+ \frac{2}{n+1}\gamma_1 Z_{27}\left(1+(\theta_w-1)Z_4\right)^m\exp\left(\frac{-E}{1+(\theta_w-1)Z_4}\right)$$
$$+ \frac{2}{n+1}m\gamma_1 Z_6Z_{25}(\theta_w-1)\left(1+(\theta_w-1)Z_4\right)^{m-1}\exp\left(\frac{-E}{1+(\theta_w-1)Z_4}\right)$$
$$\left.+ \frac{2}{n+1}\gamma_1 Z_6\left(1+(\theta_w-1)Z_4\right)^m\exp\left(\frac{-E}{1+(\theta_w-1)Z_4}\right)\frac{E(\theta_w-1)Z_{25}}{(1+(\theta_w-1)Z_4)^2}\right]$$

$$+\left(\frac{1}{Sc}-L_C\frac{n+1}{2}{Z_1}^2\right)^{-2}(L_C(n+1)Z_1Z_{22})\left[\frac{2}{n+1}KcZ_6-Z_1Z_7\right.$$
$$\left.-L_C\frac{n-3}{2}Z_1Z_2Z_7+\frac{2}{n+1}\gamma_1Z_6\left(1+(\theta_w-1)Z_4\right)^m\exp\left(\frac{-E}{1+(\theta_w-1)Z_4}\right)\right],$$
$$Z_{28}(0)=1.$$

For the Newton's technique, the stopping criteria is as follows::

$$max\{|\ Z_2(\eta_\infty,p^n,q^n,r^n)\ |,|\ Z_4(\eta_\infty,p^n,q^n,r^n)\ |,|\ Z_6(\eta_\infty,p^n,q^n,r^n)\ |\}<\epsilon,$$

where $\epsilon>0$ is a sufficiently small number, which has been considered as 10^{-10}.

4.5 Representation of Graphs and Tables

In this section, we thoroughly discuss the influence of the dimensionless parameters on the skin friction coefficient $Re_x^{\frac{1}{2}}C_{f_x}$, Nusselt number $Re_x^{-\frac{1}{2}}Nu_x$, Sherwood number $Re_x^{-\frac{1}{2}}Sh_x$, velocity profile, temperature distribution and concentration profile through different graphs and tables.

The impacts of different parameters are displayed in Table 4.1. An increase in the Casson parameter β, permeability porosity K_p, velocity slip V_s, buoyancy parameters γ and γ^*, activation energy parameter E, Brownian parameter N_b, and thermophoresis parameter N_t all have a positive impact on the skin friction, leading to an increase in its value. In contrast, an increase in the magnetic parameter M, Forchheimer parameter F_s, stretching index n, inclination α, suction parameter S, Prandtl number Pr, Schmidt number S_c, reaction rate parameter K_c, slip parameters λ_t and λ_c, thermal relaxation parameter L_T, dimensionless mass relaxation L_C, chemical reaction rate parameter γ_1, and temperature ratio parameter θ_w, a decreasing effect on the skin friction $Re_x^{\frac{1}{2}}C_{f_x}$ can be seen.

The Nusselt number $Re_x^{-\frac{1}{2}}Nu_x$ is increased by increasing the permeability porosity K_p, stretching index n, suction parameter S, Prandtl number Pr, and buoyancy parameters γ and γ^*, slip parameter λ_c, thermal relaxation parameter L_T, activation energy parameter E, and temperature ratio parameter θ_w. On the other hand, the Nusselt number $Re_x^{-\frac{1}{2}}Nu_x$ is decreased by raising the magnetic parameter M,

Casson parameter β, Forchheimer parameter F_s, velocity slip V_s, inclination α, Schmidt number S_c, reaction rate parameter K_c, slip parameter λ_t, dimensionless mass relaxation L_C, Brownian parameter N_b, thermophoresis parameter N_t, and chemical reaction rate parameter γ_1.

With increasing the values of the permeability porosity K_p, stretching index n, suction parameter S, buoyancy parameters γ and γ^*, Schmidt number S_c, reaction rate parameter K_c, dimensionless mass relaxation L_C, chemical reaction rate parameter γ_1, Brownian parameter N_b, thermophoresis parameter N_t, and temperature ratio parameter θ_w, the Sherwood number $Re_x^{-\frac{1}{2}} Sh_x$ indicates an increasing trend. By raising the magnetic parameter M, Casson parameter β, Forchheimer parameter F_s, velocity slip V_s, inclination α, Prandtl number Pr, slip parameters λ_t and λ_c, thermal relaxation parameter L_T, and activation energy parameter E, a decreasing effect is observed in the Sherwood number $Re_x^{-\frac{1}{2}} Sh_x$.

Figure 4.1 illustrates the effect of the velocity profile f' decreases as the magnetic parameter M rises. From a practical perspective, it shows an inverse relationship between the magnetic parameter and the velocity due to Lorentz force. By increasing the magnetic parameter the strength of the magnetic field increases, resulting in a stronger Lorentz force which slows down the fluid flow. Figure 4.2 shows how the magnetic parameter causes an increases in the temperature. As the magnetic parameter M increases, the strength of the magnetic field increases, resulting in a stronger EMF. The increased EMF generates more heat, which shows an increasing effect in the temperature profile. A force, induced on the particles in the fluid by the magnetic field, is known as magnetophoretic force. A stronger magnetophoretic force is developed when the magnetic field increases by raising the magnetic parameter M, which further drives the migration of particles towards the region with increased magnetic field strength thus increasing the concentration profile that is reflected in Figure 4.3.

Figure 4.1 shows that f' decreases with increasing Casson parameter β. The raising values of Casson parameter β decreases yield stress and lower the velocity field. The fluid behaves Newtonian fluid as Casson parameter β becomes very large. Figure 4.5 displays the influence of Casson parameter β. A rise in the value of β increases the temperature profile. It is noticed that an increases in

the temperature profile along the thermal boundary layer is observed with an enchancement in the Casson parameter as well as the thickness of thermal boundary layer increases. Figure 4.6 describes the impact of Casson parameter β on ϕ. By increasing the values of Casson parameter β, concentration profile also increases. Likewise, the solutal boundary layer thickness increases with increasing values of Casson parameter β.

Figures 4.7-4.9 display the impact of permeability porosity K_p on the velocity, temperature and concentration distributions. It is noticed that permeability porosity K_p increases the velocity, because a raise in the permeability K_p of medium implies less resistance due to the porous matrix present in the medium while it reduces the temperature and concentration.

Figure 4.10 shows the impact of the Forchheimer parameter F_s on the velocity profile, this figure demonstrates that as the Forchheimer parameter F_s increases, the velocity profile decreases. The Forchheimer parameter F_s, is the measure of nonlinear drag force on a fluid caused by a porous medium. The drag force is increased with the rise of F_s, opposing the fluid flow and reducing its velocity. Figures 4.11 and 4.12 depict the impact of Forchheimer parameter F_s on temperature and concentration profiles. It is found that the temperature and concentration profiles are increased as Forchheimer parameter F_s values rise.

The stretching index n represents the non-Newtonian behavior of the fluid. Figures 4.13-4.15 illustrate the impact of stretching index n on the velocity, temperature and concentration profiles. It has been noted that as the stretching index n increases, the velocity and concentration profiles exhibit an enhancement, whereas the temperature distribution undergoes a reduction.

Figure 4.16 displays the effect of the velocity slip parameter V_s on the velocity profile, showing that the thickness of the velocity boundary layer of the velocity decrease as the value of the velocity slip parameter V_s increases. Figures 4.17 and 4.18 illustrate the effect of the velocity slip parameter V_s on temperature and concentration distributions, respectively. As the velocity slip parameter V_s increases, the temperature and concentration profiles also increase.

Figures 4.19-4.21 display the influence of inclination angle α on the velocity f', temperature θ and concentration ϕ distributions. As the inclination angle α increases, the velocity of the nanofluid flow decreases, due to a decrease in the shear

stress. Meanwhile, the temperature and concentration distributions raise with raising α.

Figure 4.22 illustrates that an increase in the suction parameter S leads to a reduction in fluid momentum, consequently causing a decrease in velocity. Figures 4.23 and 4.24 illustrate the effects of the suction parameter S on the temperature and concentration profiles. Enhanced suction results in the removal of fluid from the boundary layer, leading to a reduction in temperature and concentration.

Figures 4.25 and 4.28 demonstrate the effect of the solutal buoyancy parameters γ and γ^* on velocity profiles. As the solutal buoyancy parameters γ and γ^* increase, the velocity profile f' also increases due to buoyancy force. With rising the solutal buoyancy parameters γ and γ^* the density difference between the fluid and the ambient fluid grows, resulting in a stronger buoyancy force. Figures 4.26 and 4.29 display the influence of γ and γ^* on the temperature profiles. As the parameters γ and γ^* increase, the buoyancy force intensifies, causing the fluid to rise more rapidly and enhancing convective heat transfer. This leads to a decrease in both temperature profiles. Similarly, Figures 4.27 and 4.30 show that the concentration distribution also decreases with increasing γ and γ^*.

Figures 4.31 and 4.32 show the impact of the Prandtl number Pr on the velocity and temperature profiles, respectively. It is evident that as the value of Pr increases, the velocity and temperature profiles are decreased. Figure 4.33 reveals that the concentration profile ϕ exhibits an increase in response to an increase in the Prandtl number Pr.

Figure 4.34 illustrates the influence of the Schmidt number S_c on the velocity profile f'. As Schmit number S_c increases, the fluid velocity decreases due to a decline in mass diffusivity, which in turn reduces the momentum diffusivity. When Schmidt number S_c is enhanced, it can cause the thermal boundary layer to become thicker, leading to a reduction in the convective heat transfer and an increase in the heat retention within the fluid. This leads to a higher temperature profile, as seen in Figure 4.35. Figure 4.36 reflects that as the value of Schmidt number S_c increases, the concentration ϕ is decreased.

Figure 4.37 illustrates the effect of the reaction rate parameter K_c on the velocity f'. As the reaction rate parameter K_c increases, larger consumption of reactants occurs, leading to decrease the momentum, increased resistance to flow,

and thicker boundary layer. Consequently, the velocity profile decreases, indicating a slow down the fluid flow. As shown in Figure 4.38, when K_c increases, the temperature profile decreases due to the enhanced chemical reaction rate, which consumes reactants more quickly and releases heat faster. As illustrated in Figure 4.39, increasing the K_c values reduces the concentration distribution ϕ.

Figure 4.40 illustrates the effect of increasing the slip parameter λ_t on the fluid flow. An increase in the slip parameter λ_t leads to a decrease in the velocity. Elevating the slip parameter λ_t will improve fluid motion on and near the solid boundary, leading to an enhanced heat convection, minimized resistance and therefore, a lowered temperature profile as seen in Figure 4.41. By increasing the value of the slip parameter λ_t, the slip velocity increases, enhancing the fluid flow and leading to a steeper concentration gradient. As a result, the concentration distribution is increased, as shown in Figure 4.42.

Figures 4.43-4.45 demonstrate the influence of the slip parameter λ_c on velocity, temperature, and concentration profiles. As λ_c increases, all three profiles exhibit a decline, indicating a reduction in fluid flow, heat transfer, and mass transport due to the enhanced slip effect.

Figure 4.46 shows how the velocity profile f' decreases as the thermal relaxation parameter L_T increases. Figure 4.47 illustrates the impact of the thermal relaxation parameter L_T on the temperature θ. It has been noted that less heat is transferred from the sheet to the fluid when L_T is increased. The increase in L_T increases the concentration ϕ in the Figure 4.48. An increase in L_T enhances thermal-driven diffusion and reaction rates, leading to an increase in the concentration profile.

Figure 4.49 shows the impact of the mass relaxation parameter L_C on f'. An increase the mass relaxation parameter L_C leads to decrease in the velocity profile. Figure 4.50 shows that, an increase in L_C increases the temperature distribution ϕ. Figure 4.51 displays how the mass relaxation parameter L_C affects the concentration distribution. As mass relaxation parameter L_C increases, the concentration profile is decreased. The reason for this decrease is that the fluid takes more time to diffuse. Higher values of the mass relaxation parameter L_C correspond to a situation where the material begins to behave more like a solid, resulting in a reduction of the concentration profile.

Figures 4.52 and 4.54 illustrate the impact of the activation energy parameter E on velocity and concentration profiles. An increase in E indicates a reduction in this energy barrier, leading to enhanced chemical reactions, increased molecular motion, and reduced viscosity, ultimately resulting in increased velocity and concentration profiles. Figure 4.53 reflects that as the value of E increases,the temperature θ is decreased.

Figures 4.55 and 4.57 depict the impact of the chemical reaction rate parameter γ_1 on velocity and concentration profiles. The chemical reaction rate parameter γ_1 represents the rate at which chemical reactions occur. An increase in γ_1 indicates a faster reaction rate, leading to enhanced consumption of reactants, increased sink terms, and reduced the fluid motion, ultimately resulting in decreased velocity and concentration profiles. Figure 4.57 shows that raising γ_1 leads to a rise in temperature distribution.

Figures 4.58-4.60 display the impact of the relative temperature ratio parameter θ_w on the velocity, temperature and concentration profiles. The relative temperature ratio parameter θ_w represents the ratio of the wall temperature to the fluid temperature. An increase in θ_w indicates a greater temperature difference, leading to enhanced heat transfer, increased thermal boundary layer thickness, reduced species transport, and a cooling effect, ultimately resulting in decreased velocity, temperature, and concentration profiles.

Figures 4.61 and 4.62 reflect that, Increasing Brownian parameter N_b increase both velocity and temperature profiles. The Brownian parameter N_b measures how much Brownian motion affects the movement of fluids. When N_b increases, Brownian motion plays a bigger role in transporting energy and momentum leading to more mixing and collisions between particles. This means that as N_b goes up, the fluid's motion and energy transfer become more intense, leading to higher velocity and temperature throughout the fluid. As N_b increases, causing a lower concentration profile in a Figure 4.63.

Figures 4.64 and 4.65 clearly illustrate, when thermophoresis parameter N_t increase, the velocity f' and temperature θ are increased. When the thermophoretic N_t is enhanced, particle migration, thermal convection, and thermal diffusion are all enhanced, while viscous dissipation is reduced. As a result, particle kinetic energy increases, leading to increased velocity and temperature profiles. The effect

of thermophoresis parameter N_t on the concentration θ is shown in Figure 4.66. raising the values of the thermophoresis parameter N_t reduces the concentration distribution.

TABLE 4.1: Numerical Results of Skin Friction, Nusselt Number, and Sherwood Number

M	β	K_p	F_s	n	V_s	α	S	γ	γ^*	P_r	S_c	K_c	Λ_t	Λ_c	L_T	L_C	E	γ_1	θ_w	N_b	N_t	$Re_x^{\frac{1}{2}} Cf_x$	$Re_x^{-\frac{1}{2}} Nu_x$	$Re_x^{-\frac{1}{2}} Sh_x$
1	0.5	1	1	1	0.2	0.2	0.2	0.5	0.5	1	1	0.5	1	1	0.2	0.2	3	0.3	0.5	0.3	0.3	-2.4697	0.3672	0.5096
0.9																						-2.4387	0.3689	0.5100
1.1																						-2.5019	0.3664	0.5091
	0.3																					-3.1029	0.3801	0.5141
	0.4																					-2.7199	0.3730	0.5115
		0.9																				-2.5053	0.3663	0.5091
		1.5																				-2.3620	0.3720	0.5115
			0.8																			-2.4338	0.3683	0.5100
			0.9																			-2.4519	0.3677	0.5098
				1.1																		-2.5100	0.3787	0.5202
				1.2																		-2.5496	0.3901	0.5307
					0.3																	-2.2365	0.3619	0.5062
					0.4																	-2.0429	0.3556	0.5034
						0.01																-2.4654	0.3674	0.5096
						0.05																-2.4657	0.3673	0.5096
							0															-2.3697	0.3099	0.4765
							0.1															-2.4196	0.3386	0.4928
								0.6														-2.4535	0.3678	0.5098
								0.7														-2.4374	0.3683	0.5100
									0.6													-2.4441	0.3683	0.5099
									0.7													-2.4186	0.3694	0.5103
										1.5												-2.4974	0.4225	0.5092
										2												-2.5143	0.4601	0.5090
											1.2											-2.4796	0.3669	0.5393
											1.3											-2.4837	0.3668	0.5492
												0.6										-2.4736	0.3672	0.5219
												0.7										-2.4772	0.3672	0.5330
													0.7									-2.4526	0.4099	0.5097
													0.8									-2.4587	0.3947	0.5097
														0.9								-2.4658	0.3666	0.5370
														1.1								-2.4749	0.3686	0.4848
															0.05							-2.4650	0.3618	0.5097
															0.1							-2.4666	0.3636	0.5096
																0.05						-2.4677	0.3676	0.5067
																0.1						-2.4683	0.3675	0.5077
																	4					-2.4695	0.3672	0.5090
																	5					-2.4694	0.3672	0.5089
																		1				-2.4704	0.3672	0.5114
																		1.5				-2.4708	0.3671	0.5126
																			1			-2.4700	0.3672	0.5107
																			2			-2.4710	0.3672	0.5142
																				0.01		-2.4770	0.3886	0.5095
																				0.1		-2.4748	0.3820	0.5095
																					0.01	-2.4779	0.3896	0.5095
																					0.1	-2.4754	0.3827	0.5095

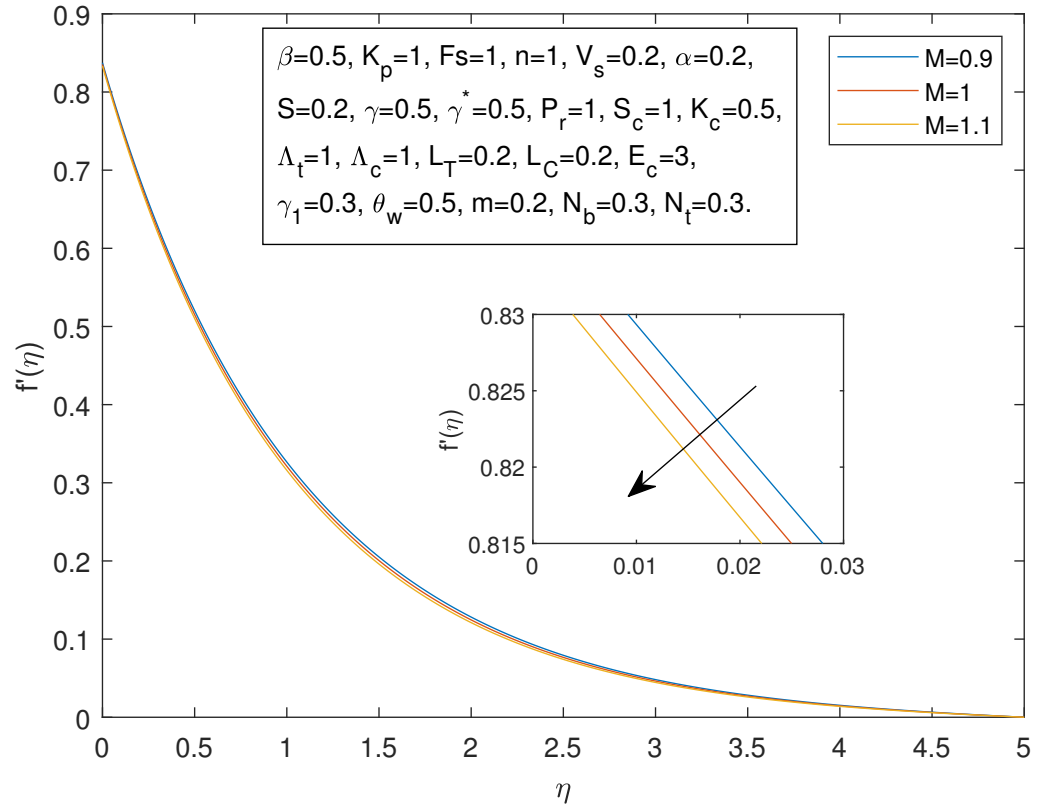

FIGURE 4.1: Velocity Profile $f'(\eta)$ and η against M

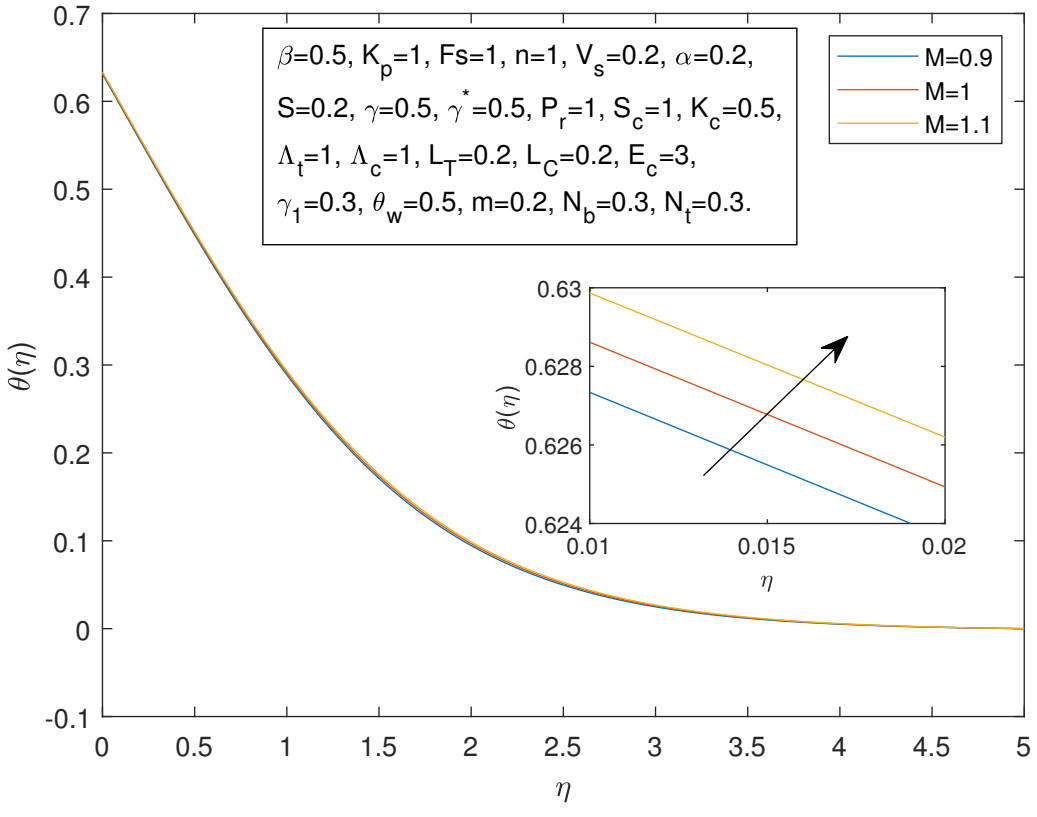

FIGURE 4.2: Temperature Profile $\theta(\eta)$ and η against M

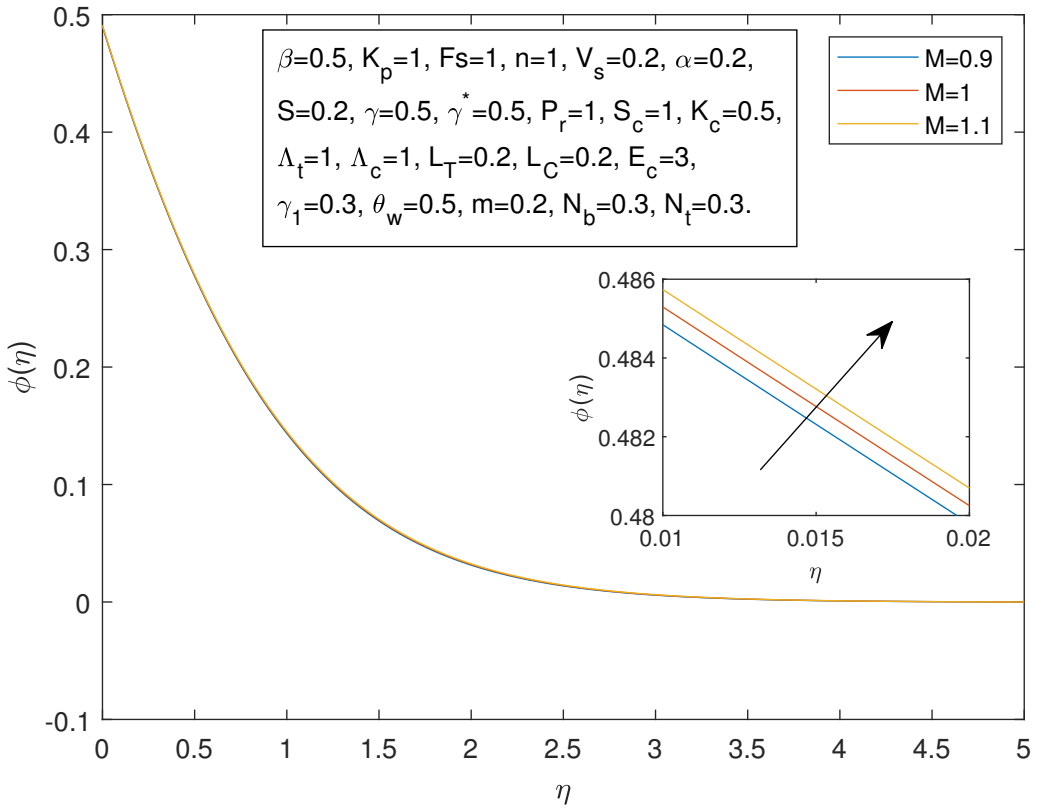

FIGURE 4.3: Concentration Profile $\phi(\eta)$ and η against M

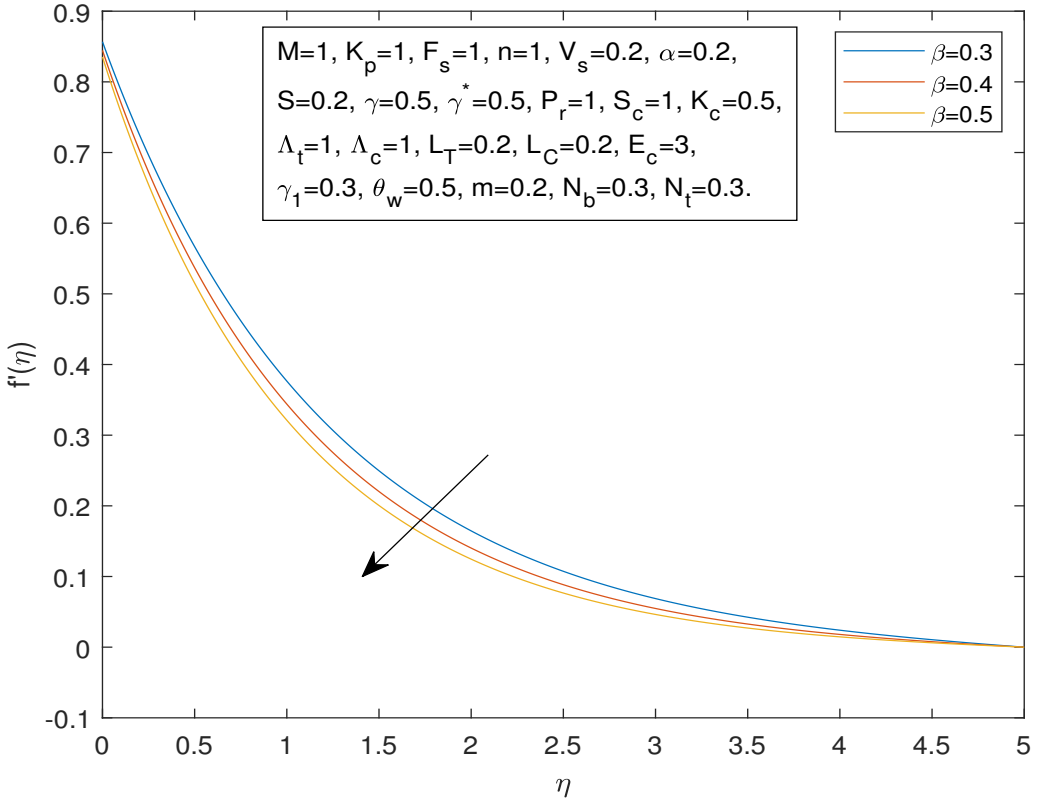

FIGURE 4.4: Velocity Profile $f'(\eta)$ and η against β

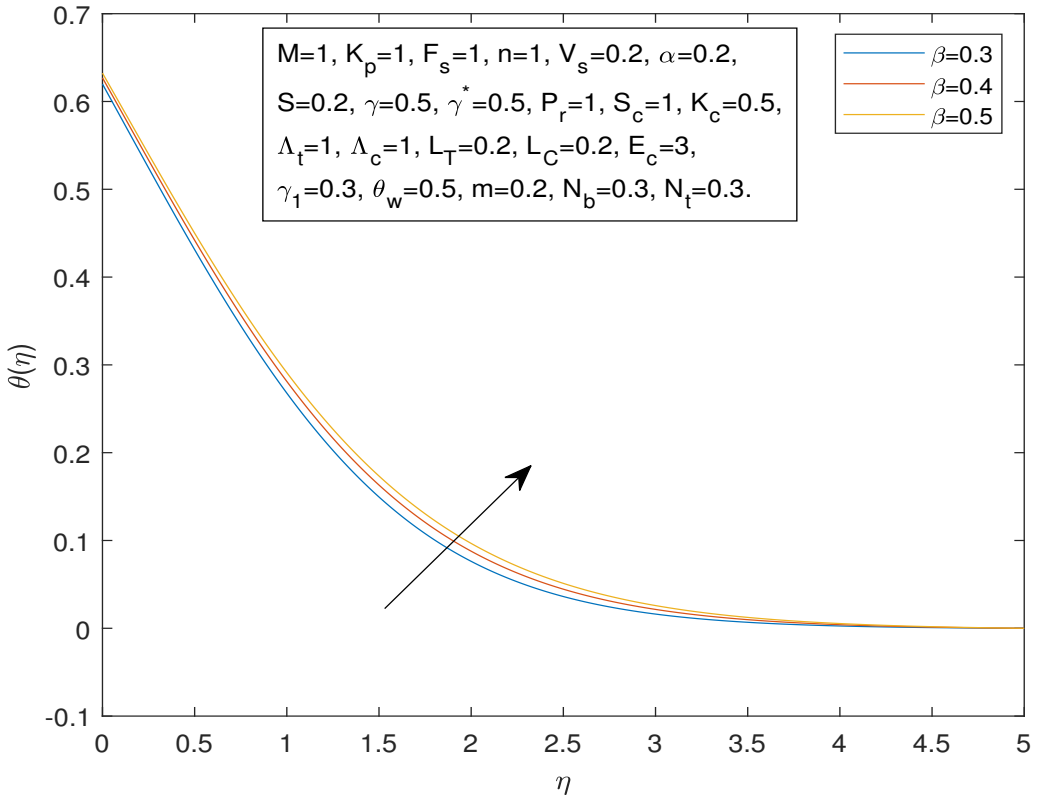

FIGURE 4.5: Temperature Profile $\theta(\eta)$ and η against β

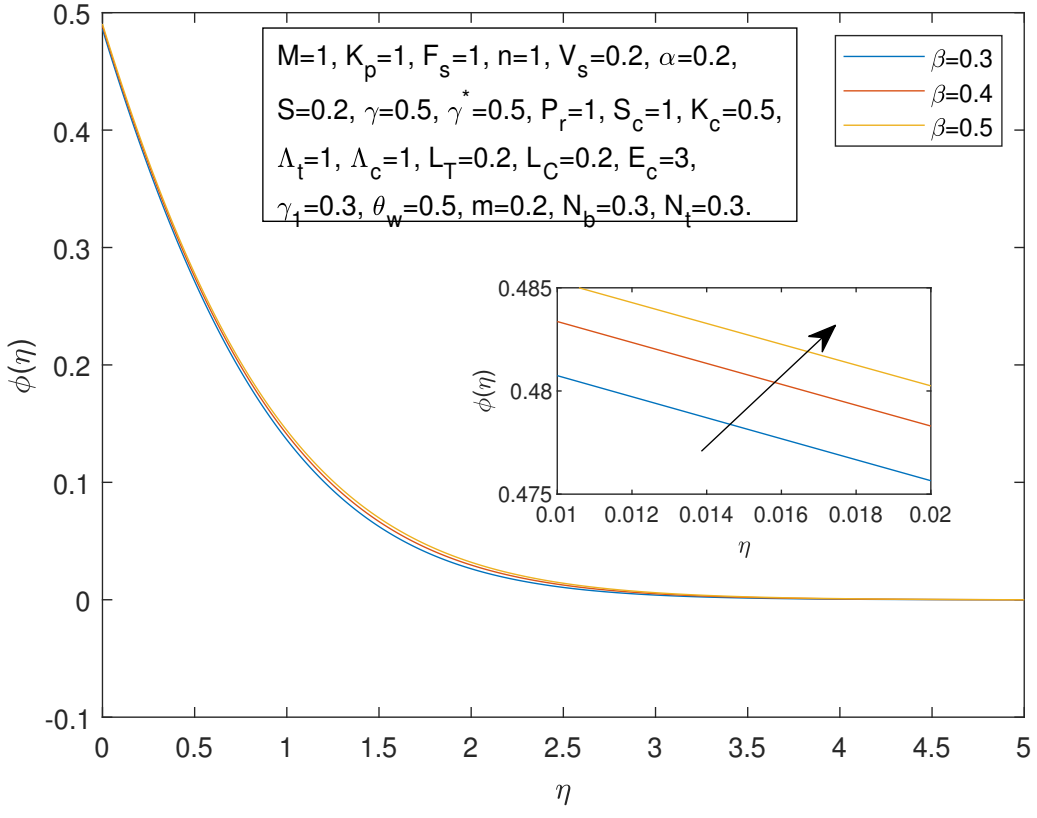

FIGURE 4.6: Concentration Profile $\phi(\eta)$ and η against β

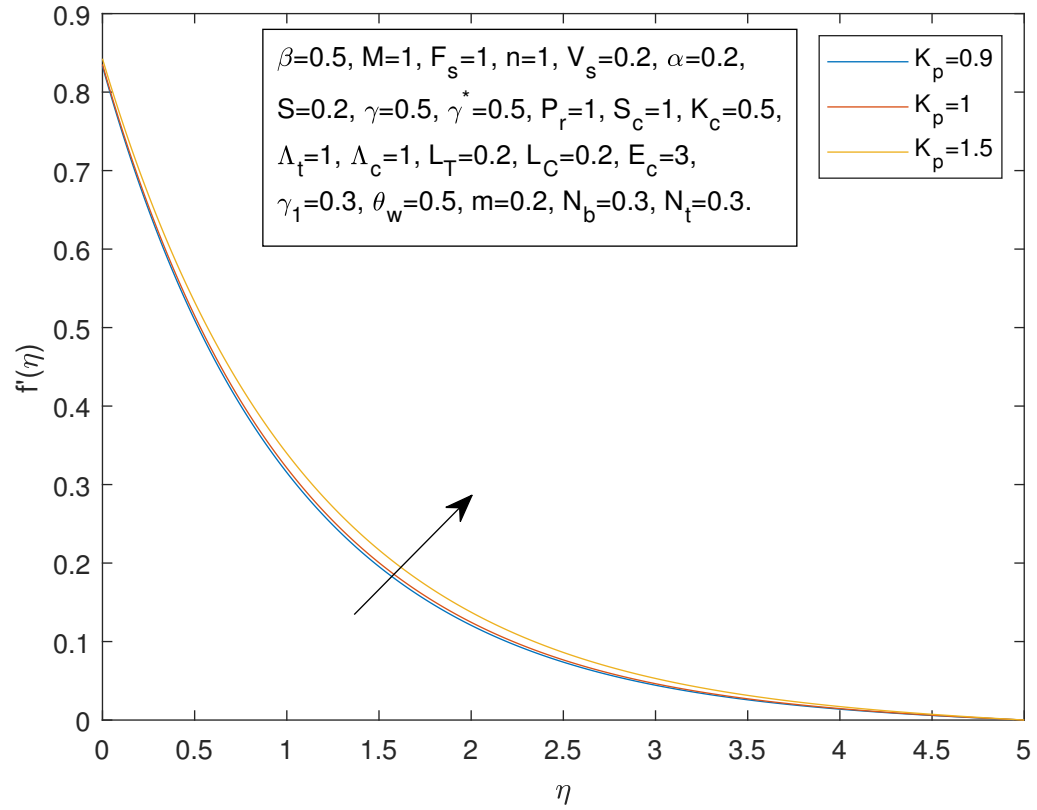

FIGURE 4.7: Velocity Profile $f'(\eta)$ and η against K_p

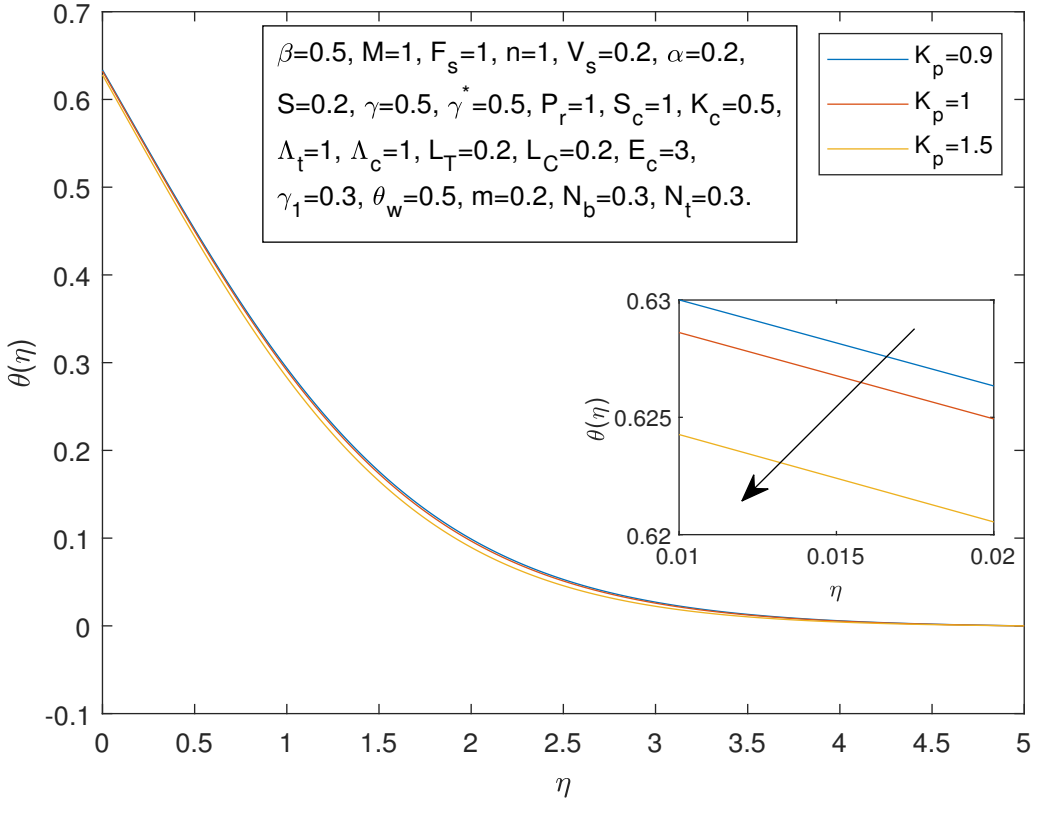

FIGURE 4.8: Temperature Profile $\theta(\eta)$ and η against K_p

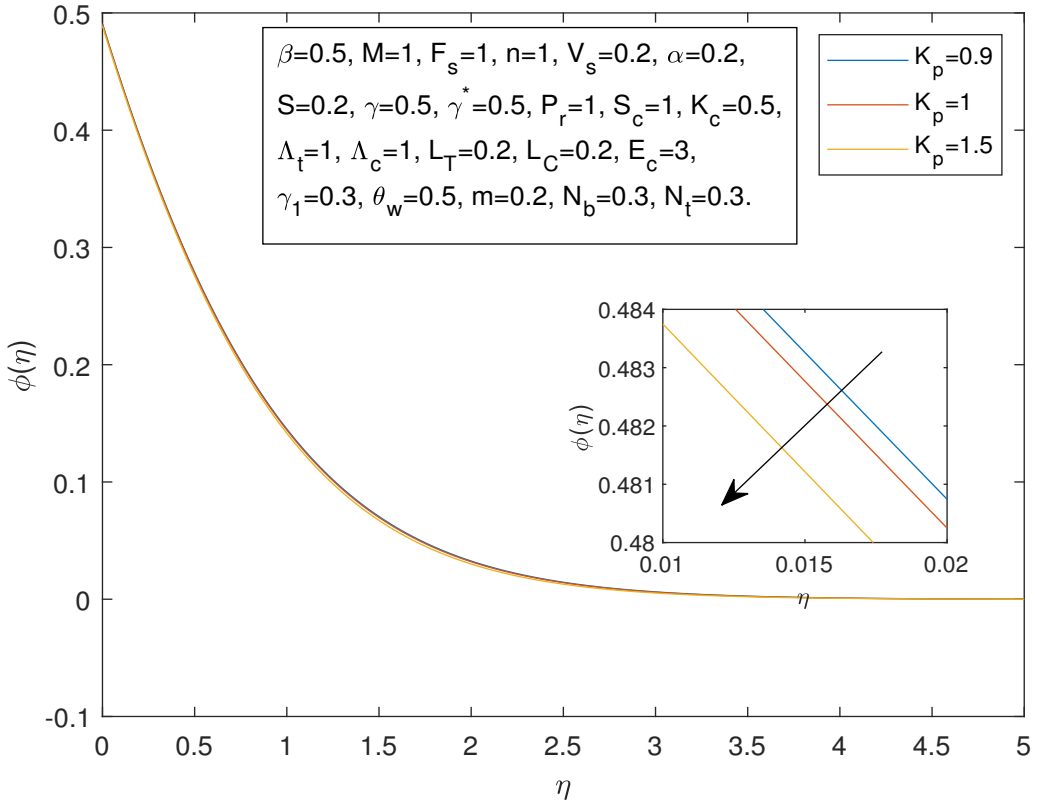

FIGURE 4.9: Concentration Profile $\phi(\eta)$ and η against K_p

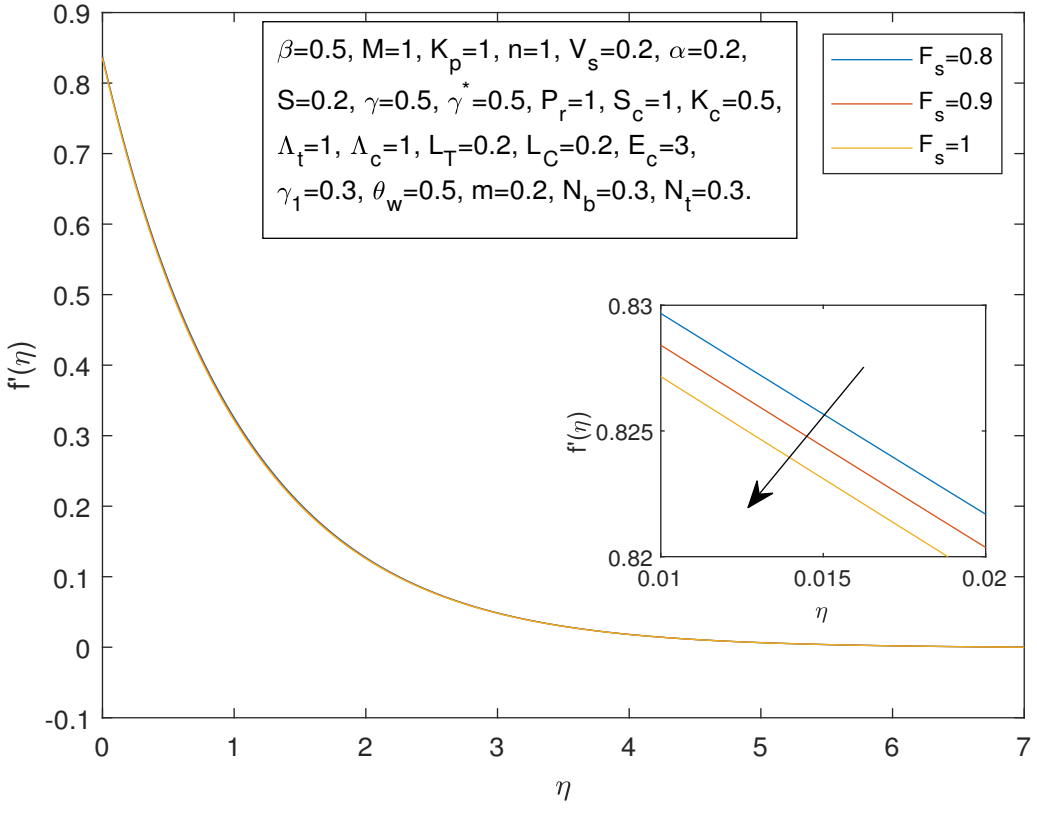

FIGURE 4.10: Velocity Profile $f'(\eta)$ and η against Fs

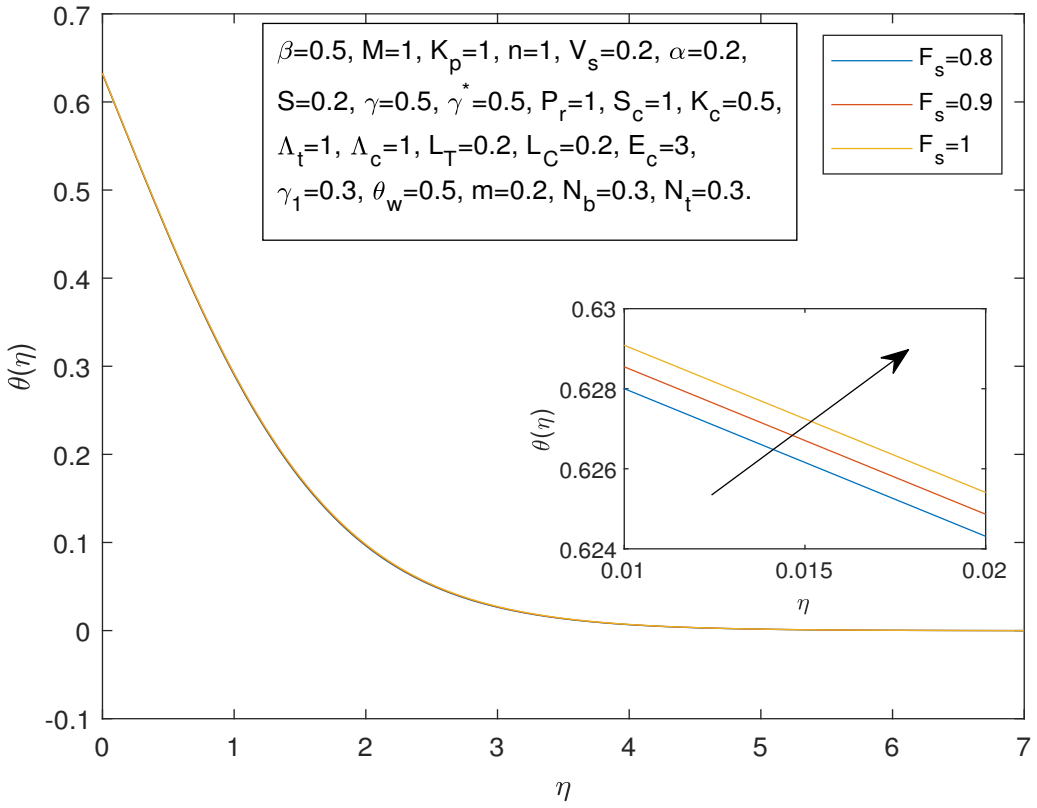

FIGURE 4.11: Temperature Profile $\theta(\eta)$ and η against Fs

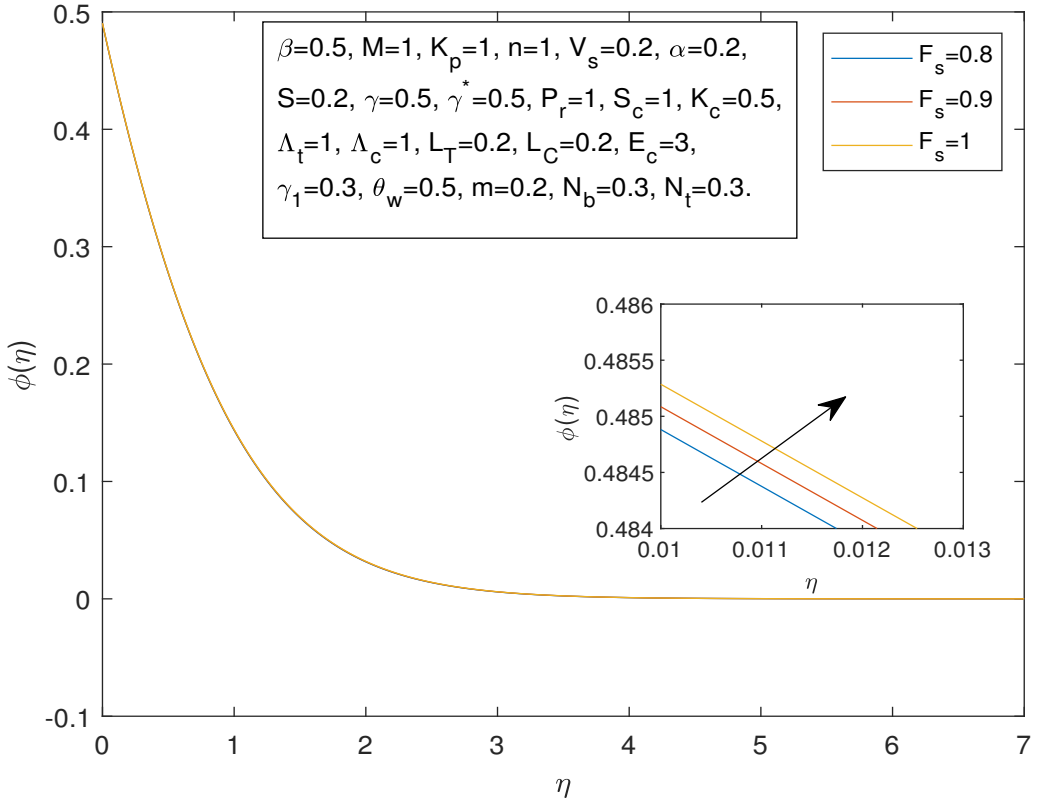

FIGURE 4.12: Concentration Profile $\phi(\eta)$ and η against Fs

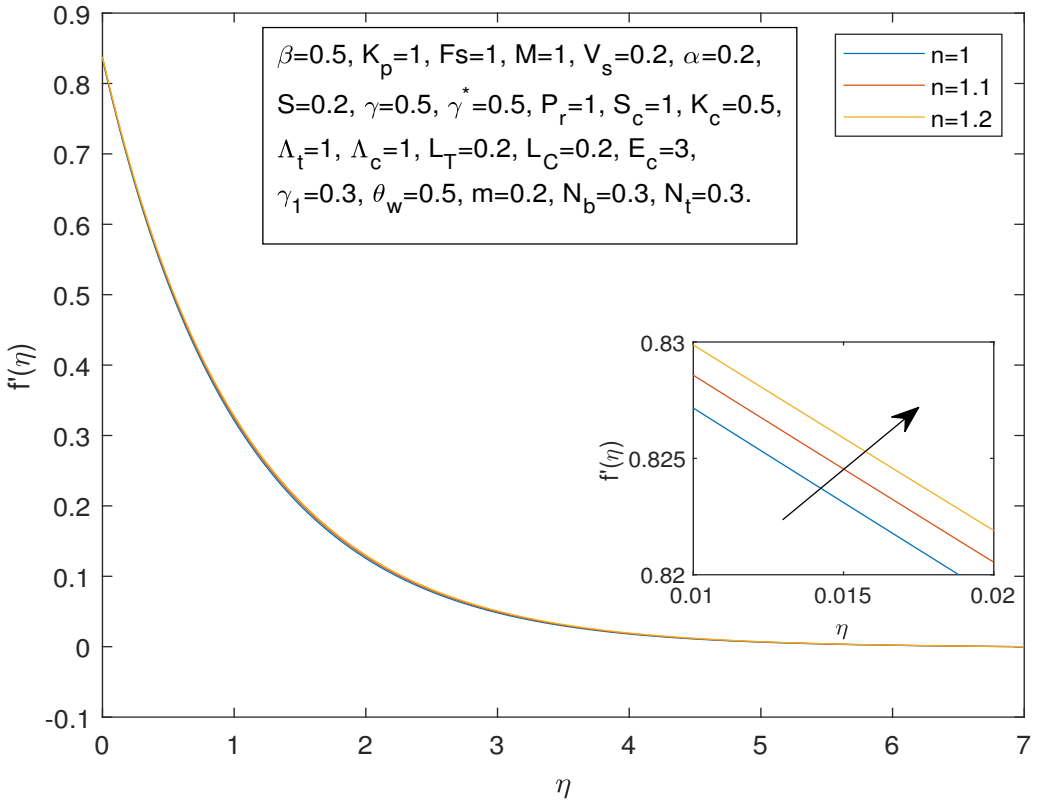

FIGURE 4.13: Velocity Profile $f'(\eta)$ and η against n

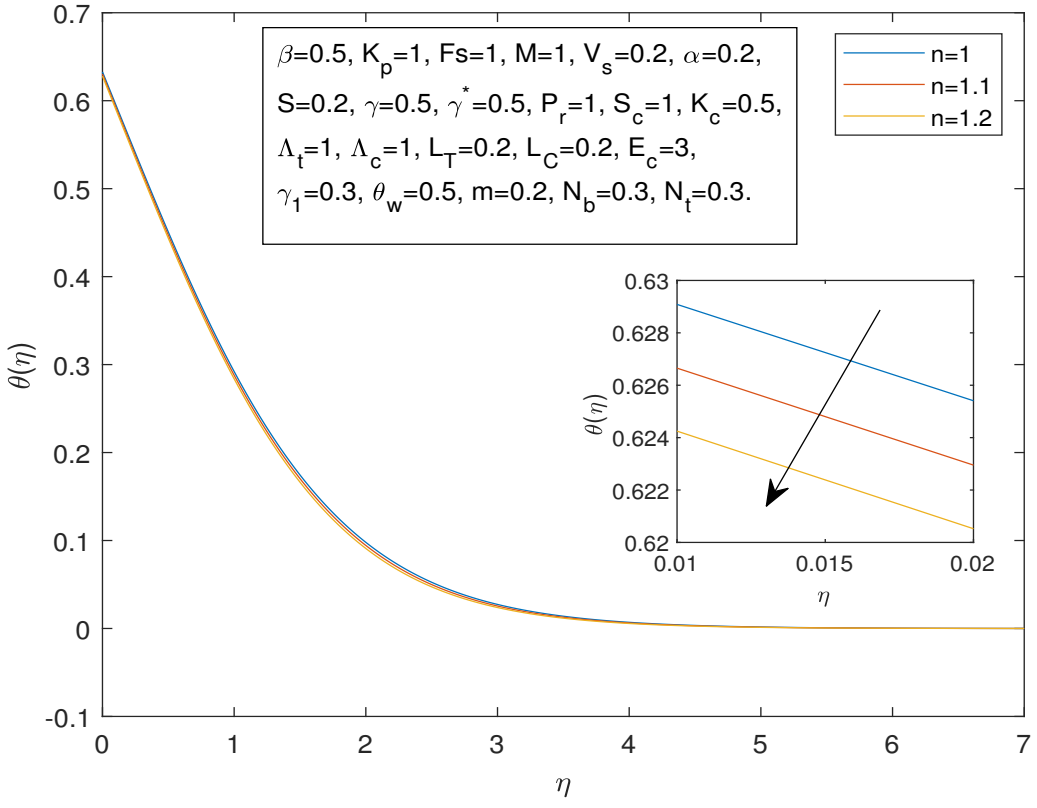

FIGURE 4.14: Temperature Profile $\theta(\eta)$ and η against n

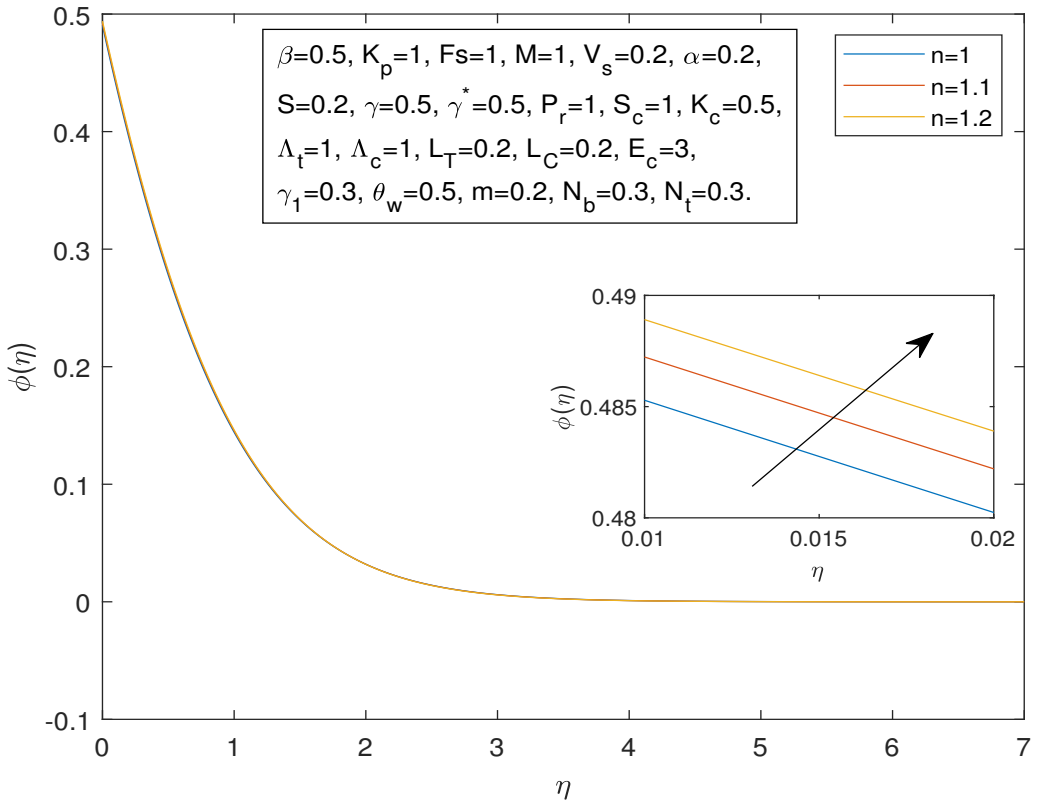

FIGURE 4.15: Concentration Profile $\phi(\eta)$ and η against n

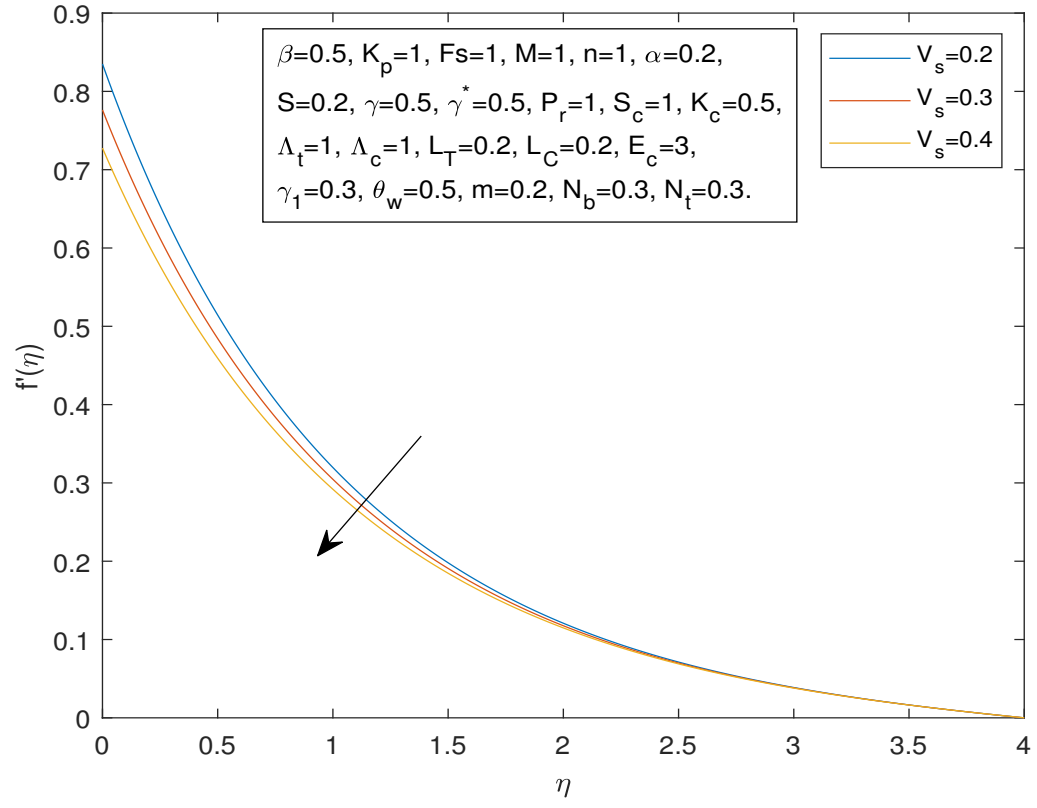

FIGURE 4.16: Velocity Profile $f'(\eta)$ and η against Vs

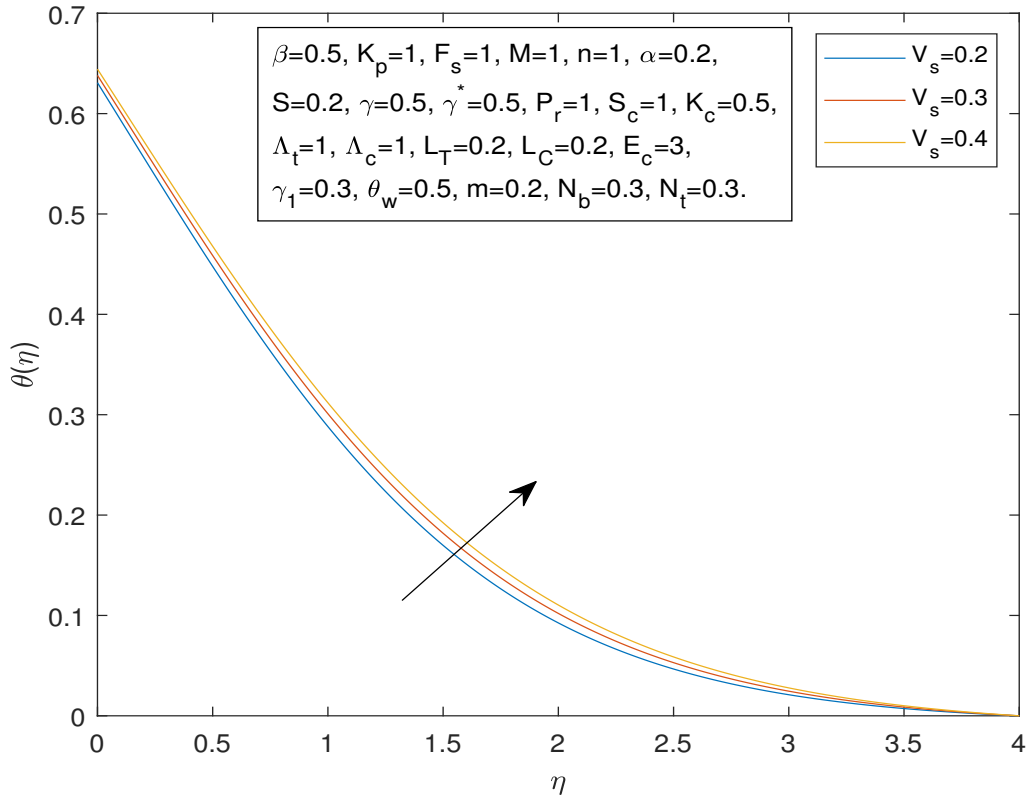

FIGURE 4.17: Temperature Profile $\theta(\eta)$ and η against Vs

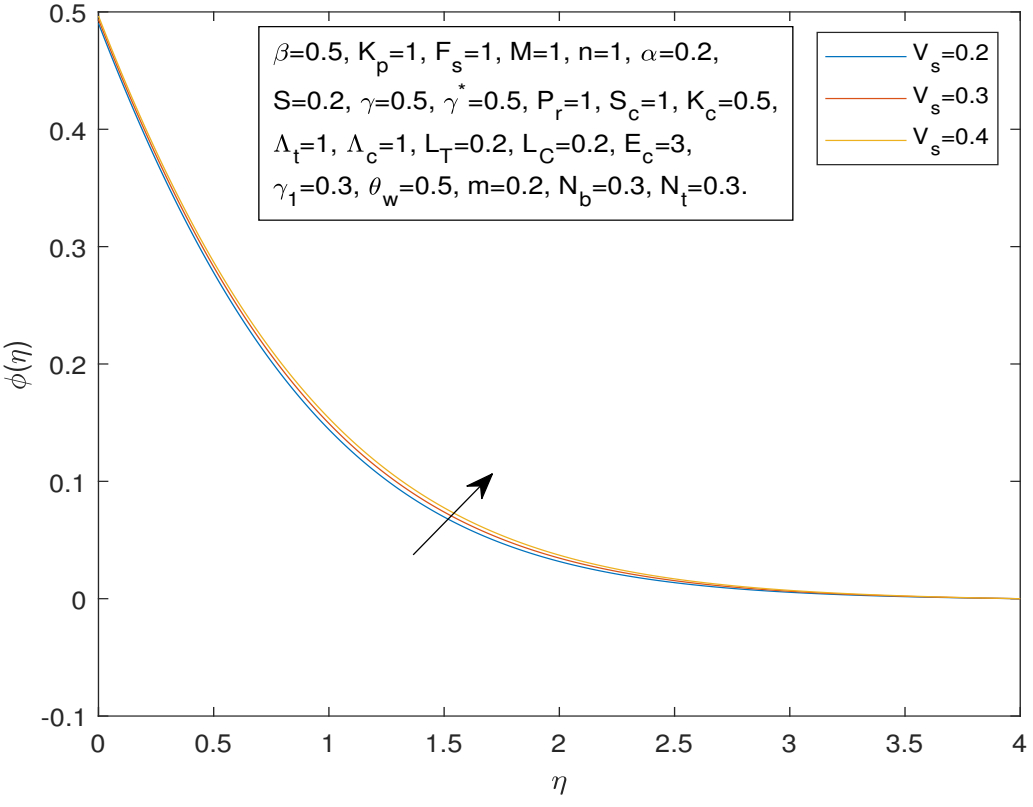

FIGURE 4.18: Concentration Profile $\phi(\eta)$ and η against Vs

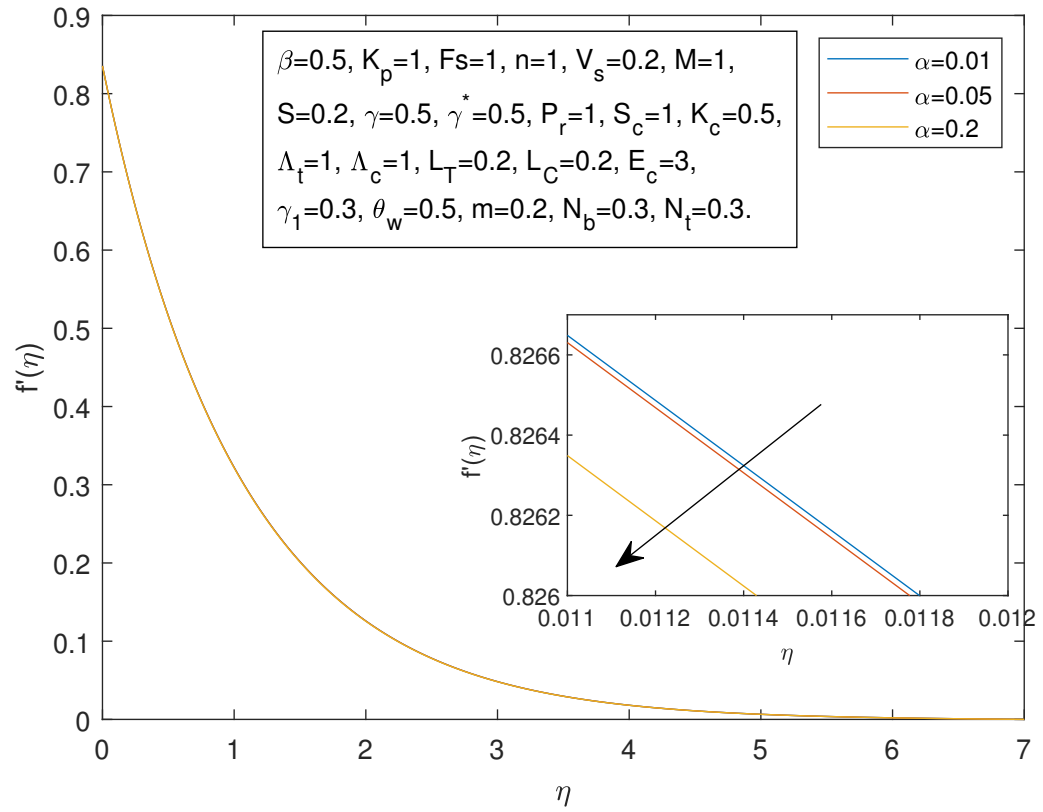

FIGURE 4.19: Velocity Profile $f'(\eta)$ and η against α

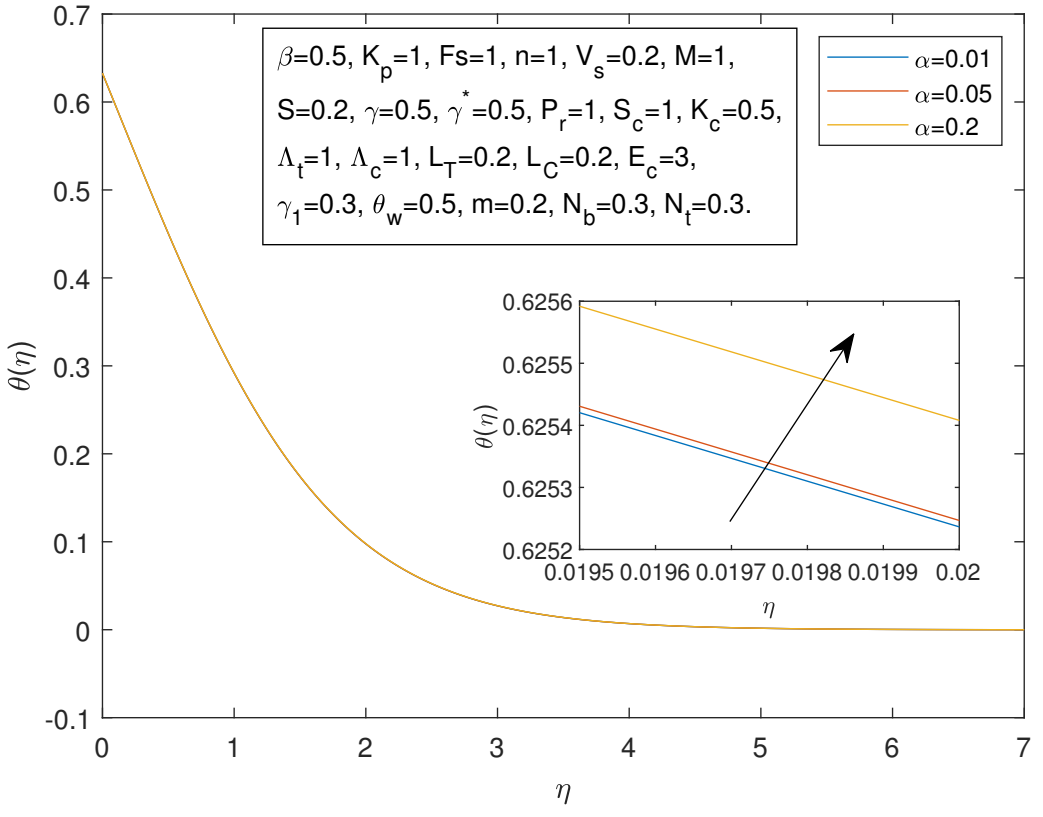

FIGURE 4.20: Temperature Profile $\theta(\eta)$ and η against α

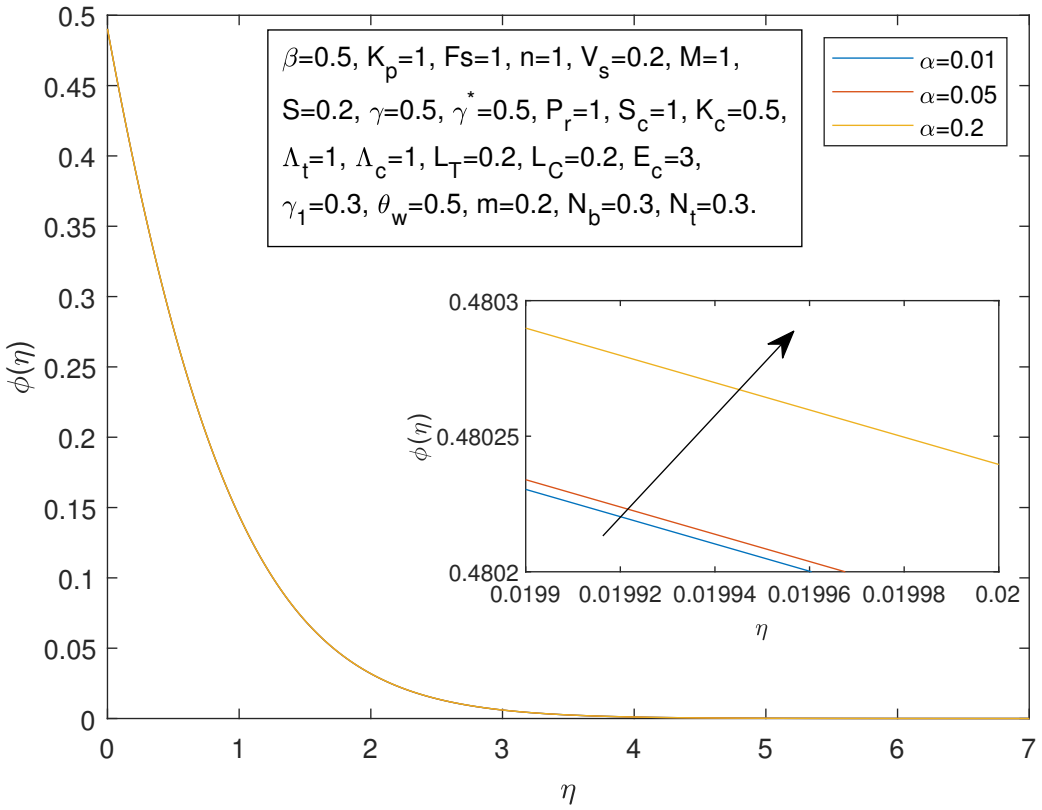

FIGURE 4.21: Concentration Profile $\phi(\eta)$ and η against α

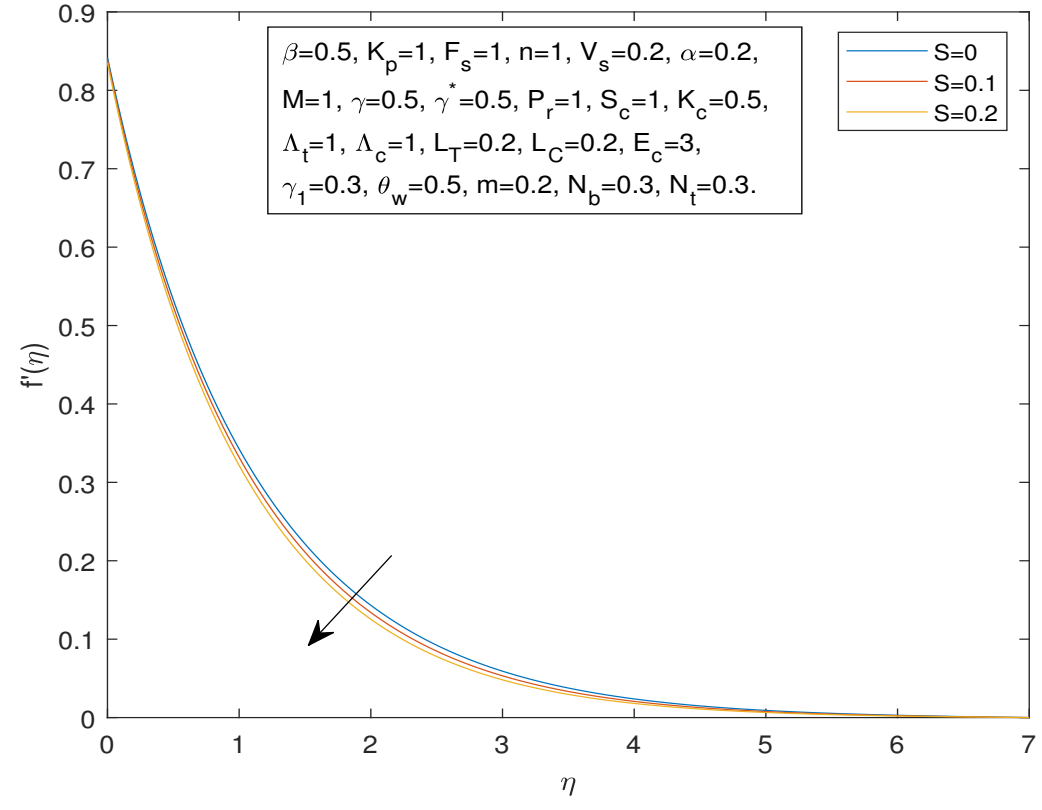

FIGURE 4.22: Velocity Profile $f'(\eta)$ and η against S

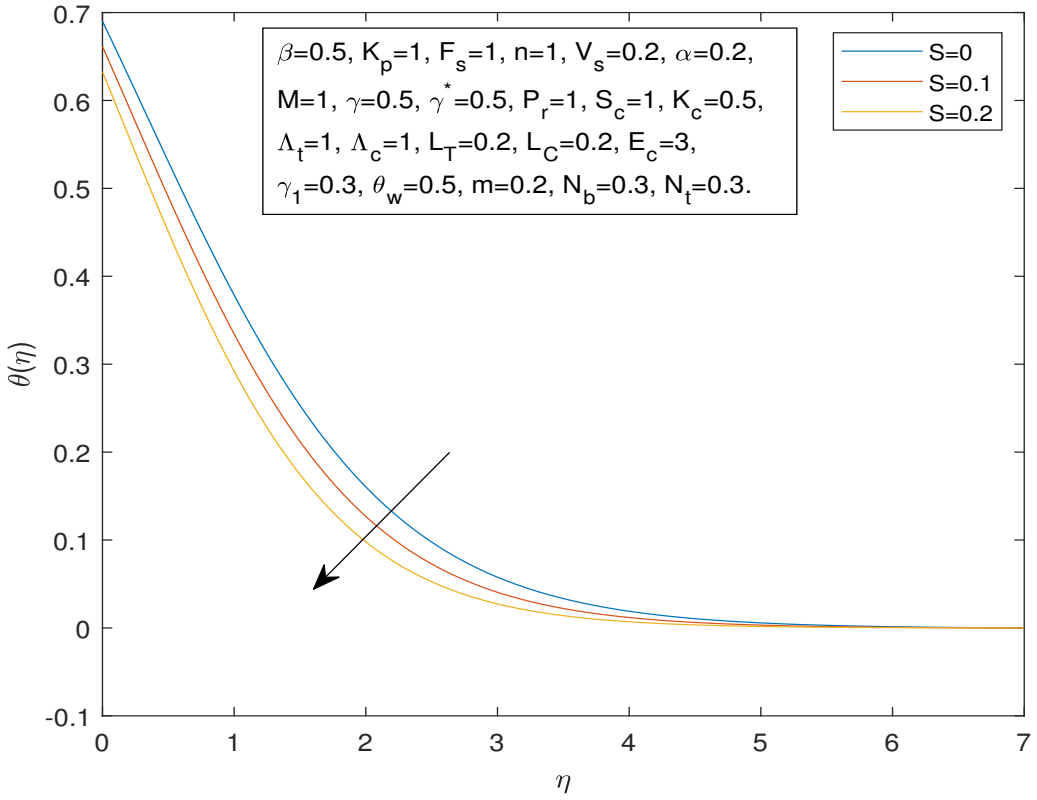

FIGURE 4.23: Temperature Profile $\theta(\eta)$ and η against S

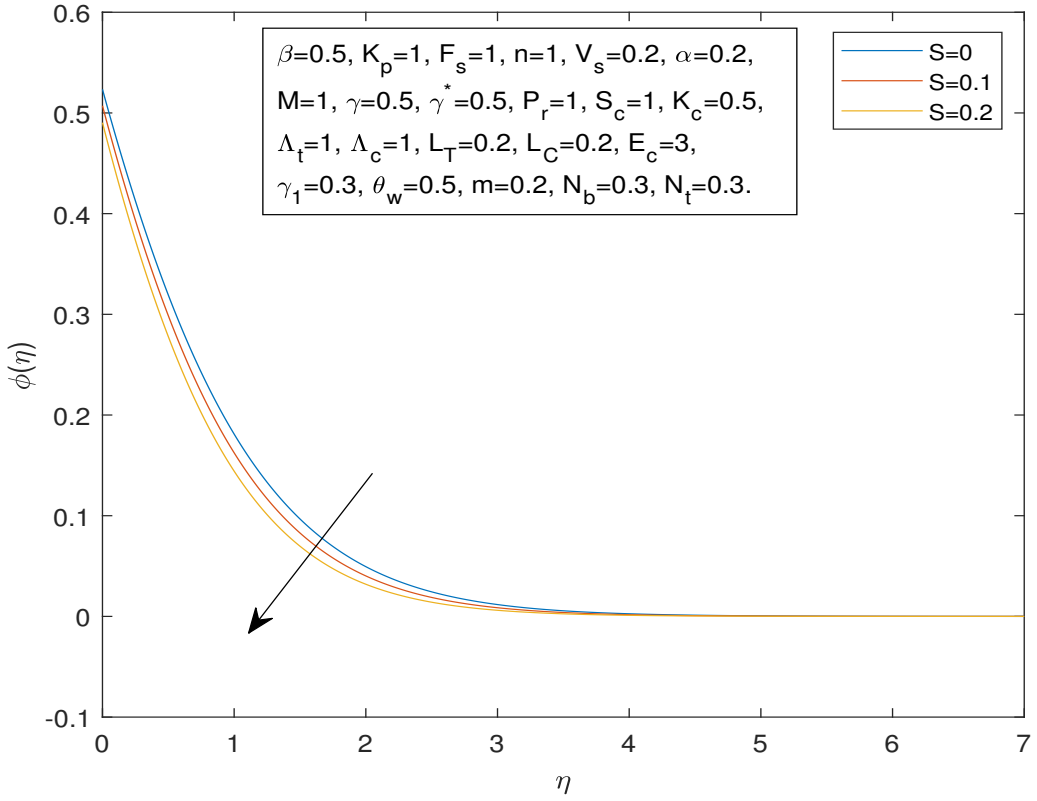

FIGURE 4.24: Concentration Profile $\phi(\eta)$ and η against S

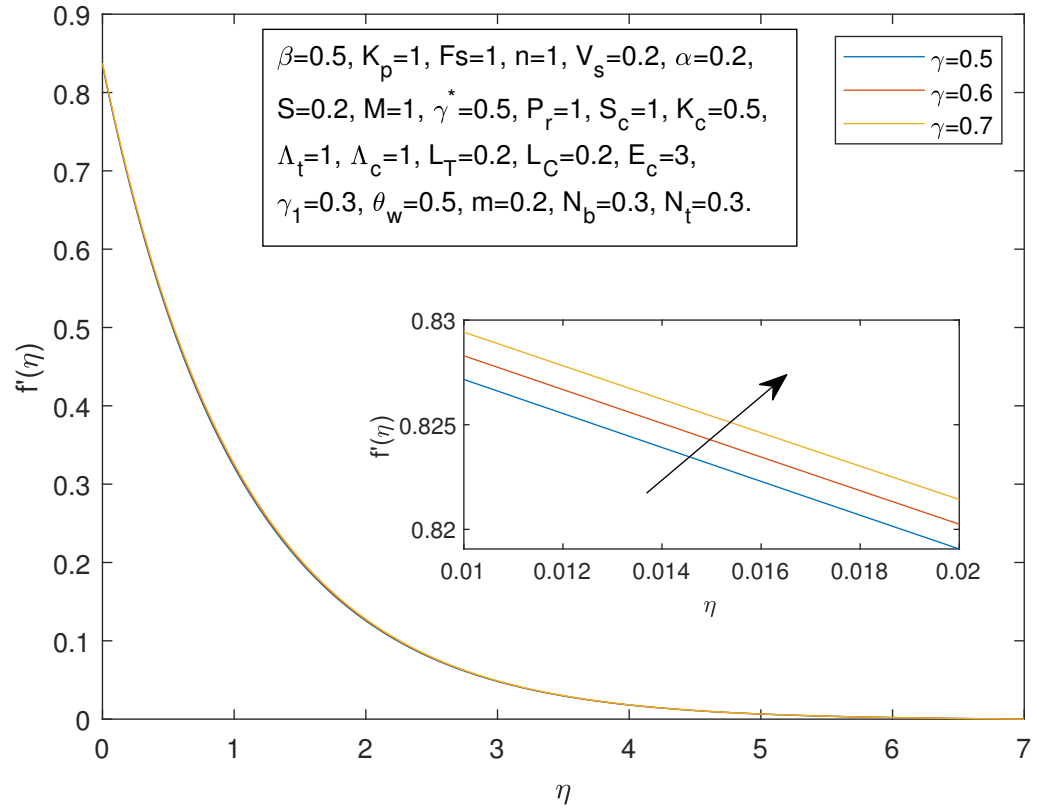

FIGURE 4.25: Velocity Profile $f'(\eta)$ and η against γ

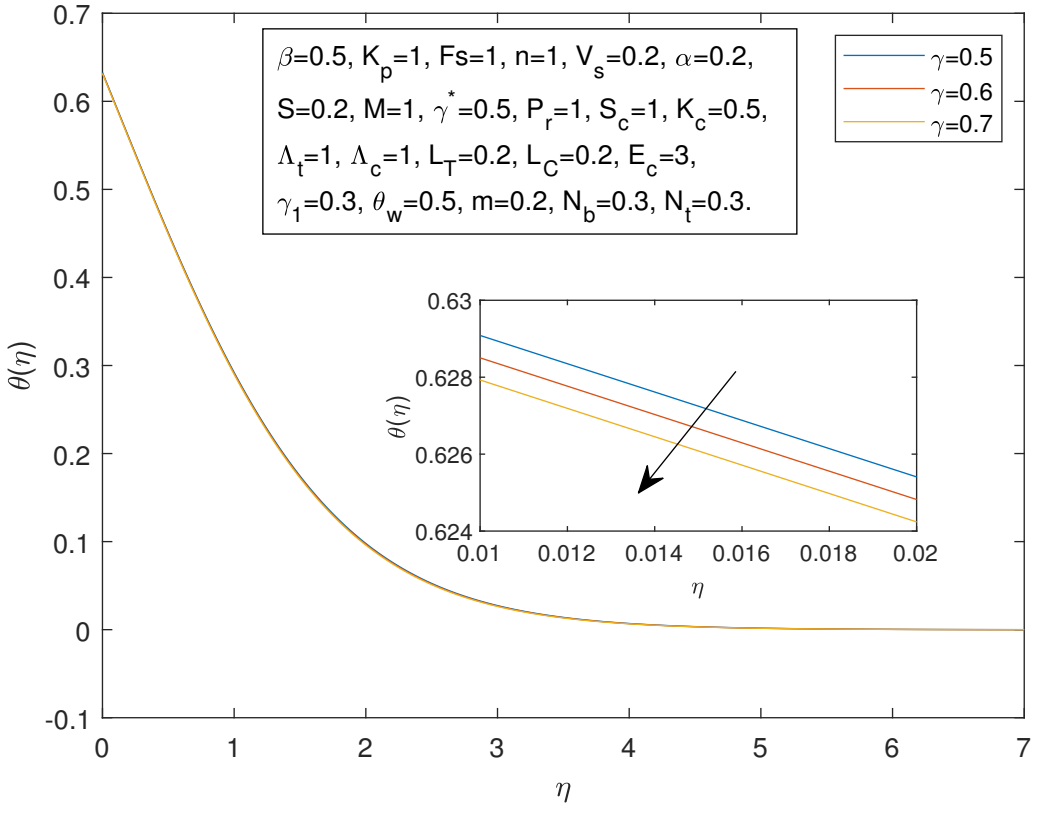

FIGURE 4.26: Temperature Profile $\theta(\eta)$ and η against γ

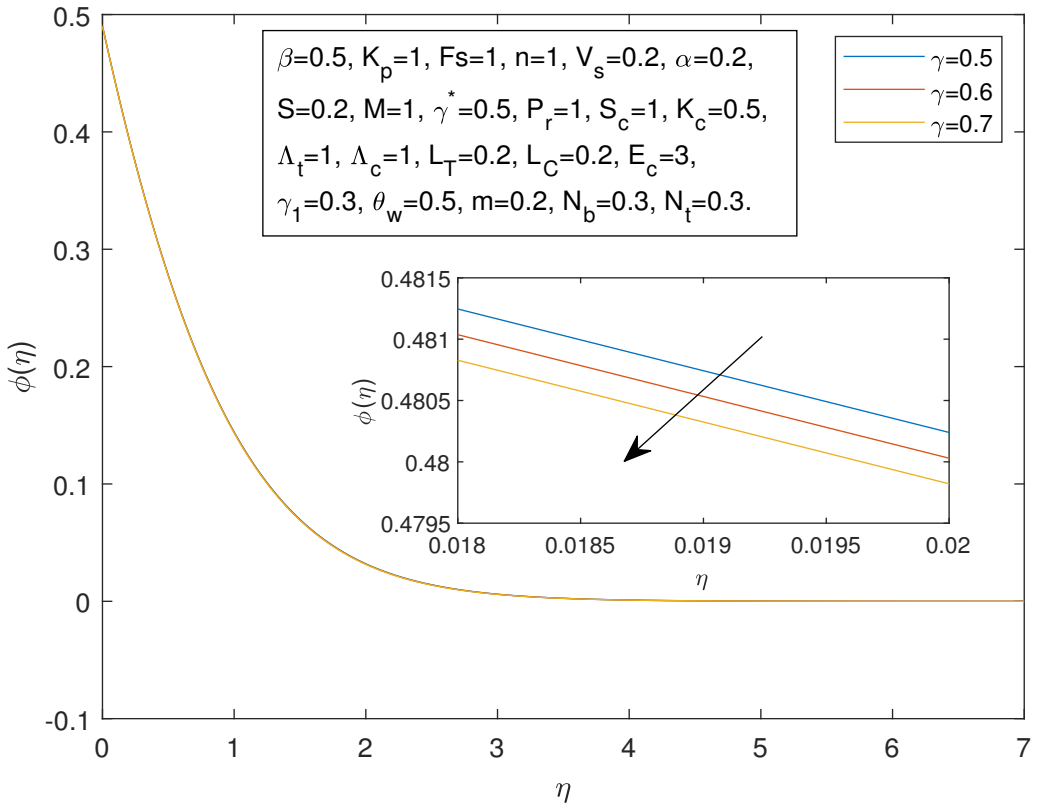

FIGURE 4.27: Concentration Profile $\phi(\eta)$ and η against γ

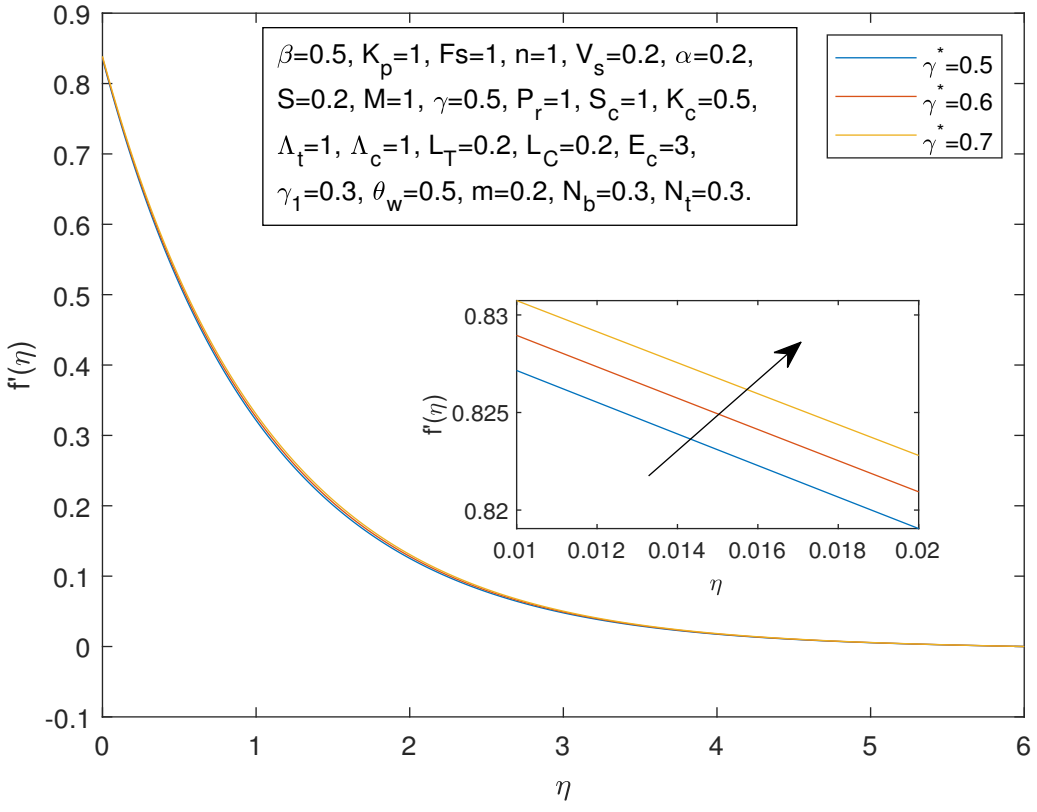

FIGURE 4.28: Velocity Profile $f'(\eta)$ and η against γ^*

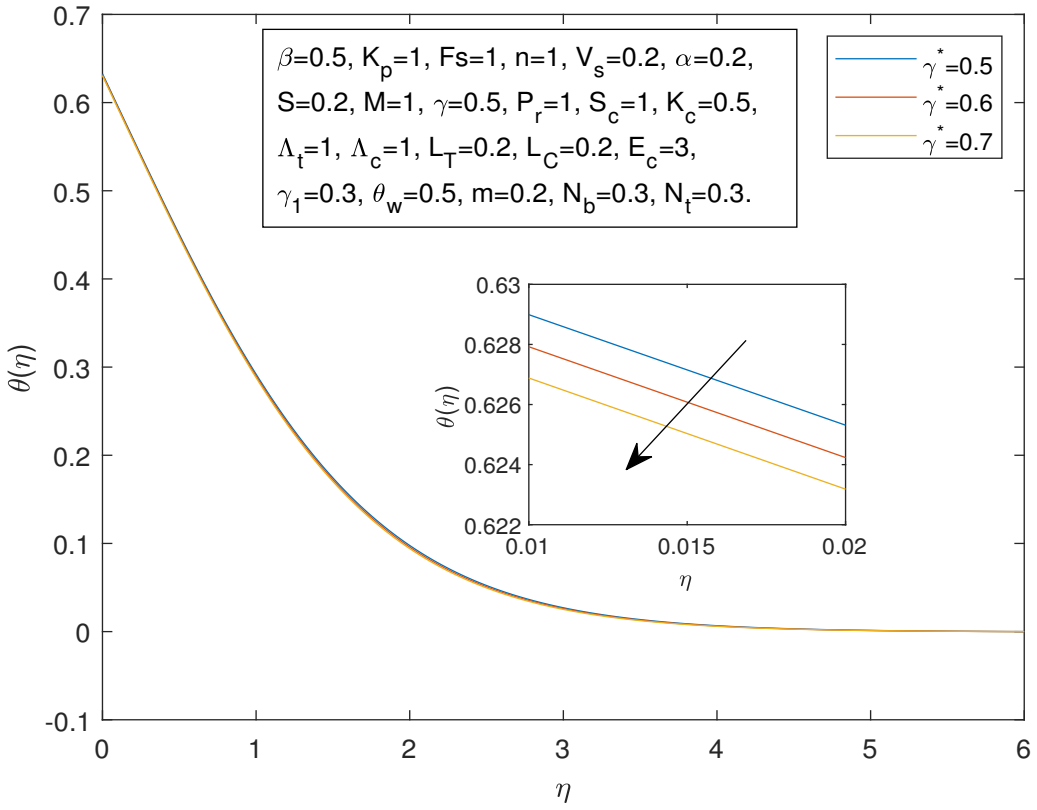

FIGURE 4.29: Temperature Profile $\theta(\eta)$ and η against γ^*

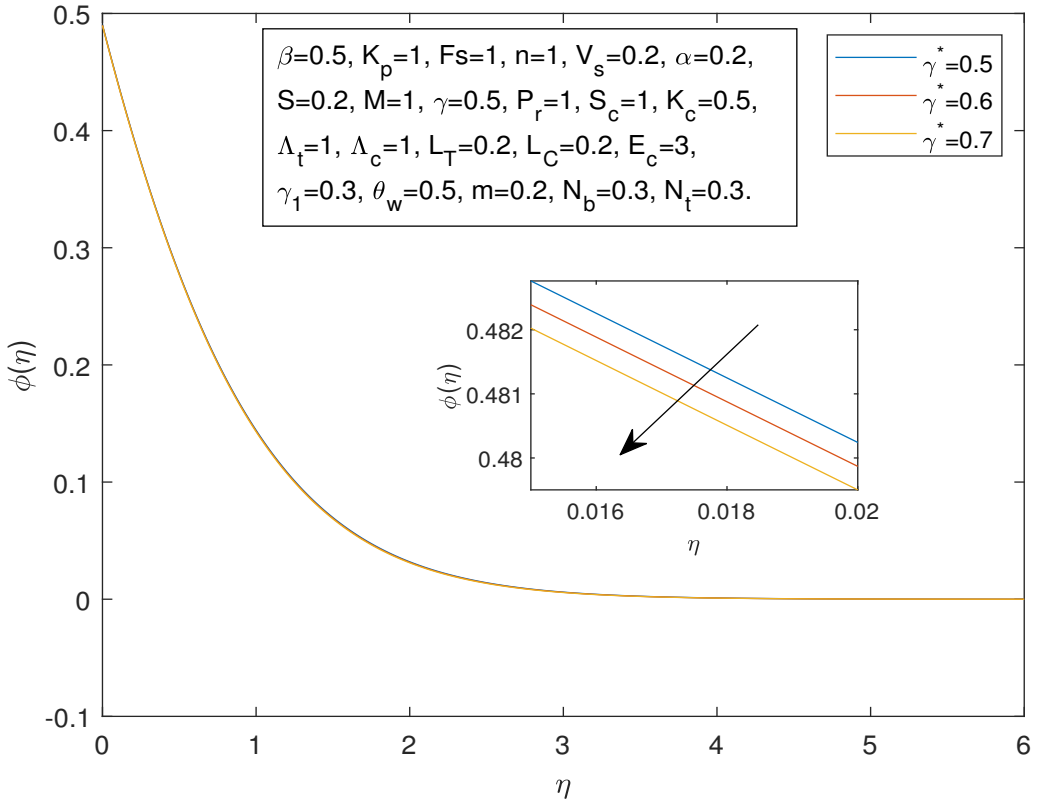

FIGURE 4.30: Concentration Profile $\phi(\eta)$ and η against γ^*

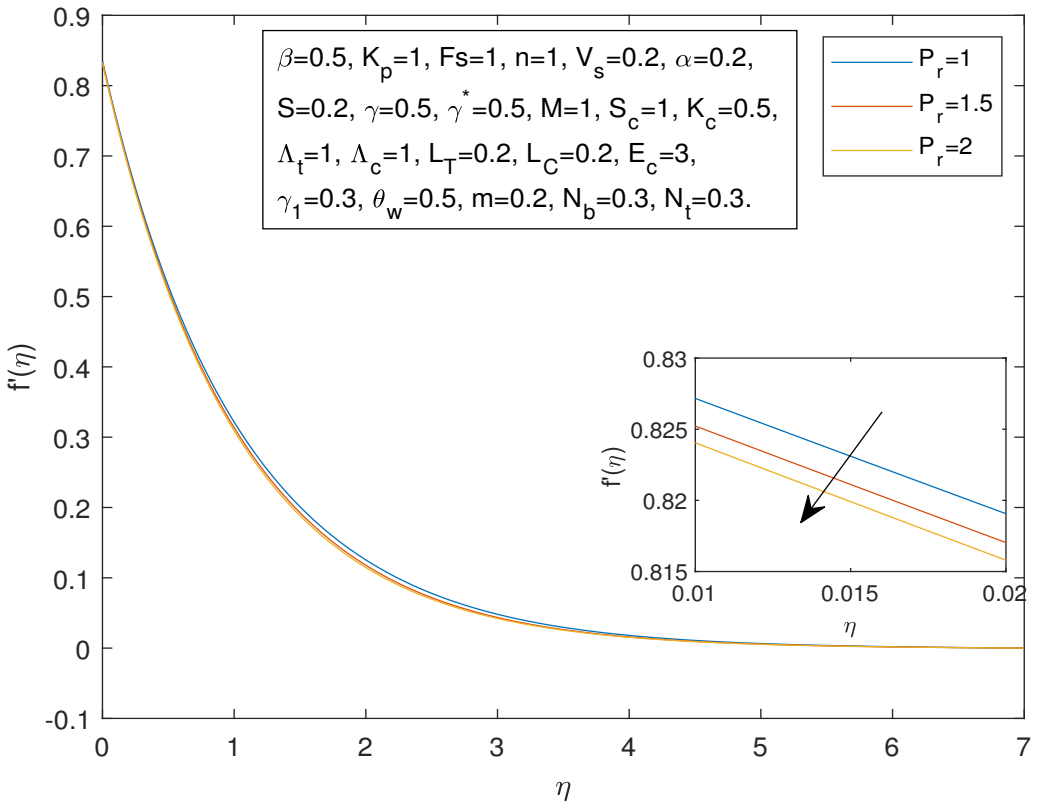

FIGURE 4.31: Velocity Profile $f'(\eta)$ and η against Pr

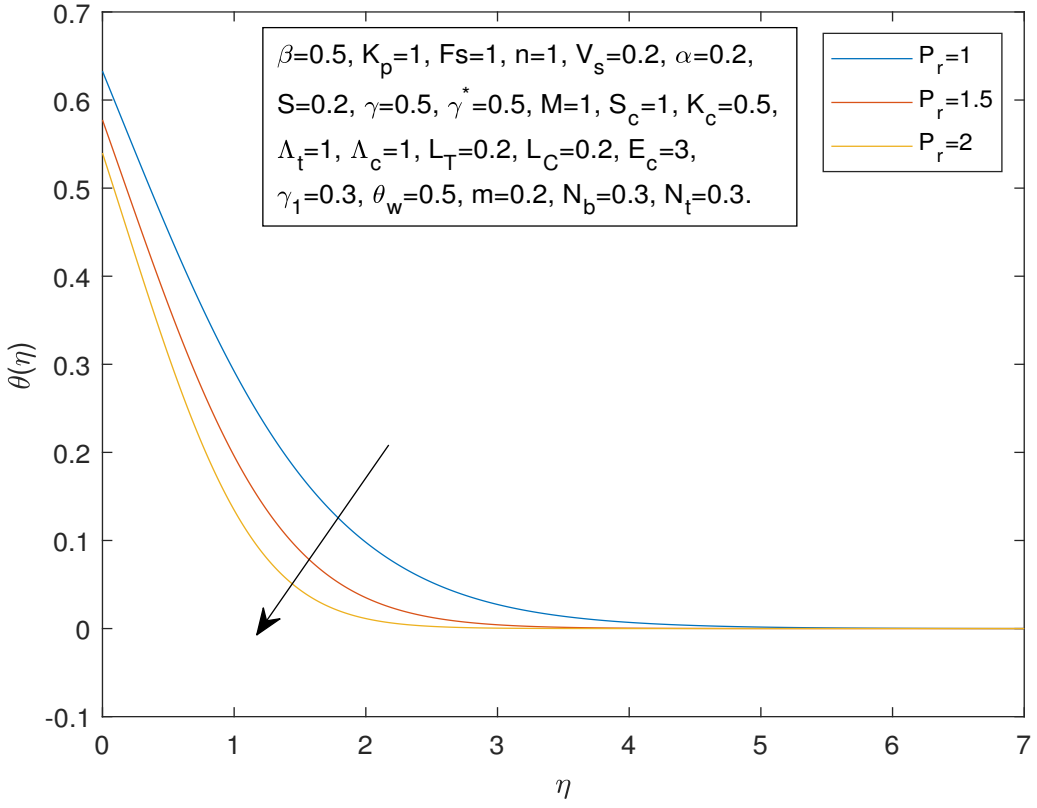

FIGURE 4.32: Temperature Profile $\theta(\eta)$ and η against Pr

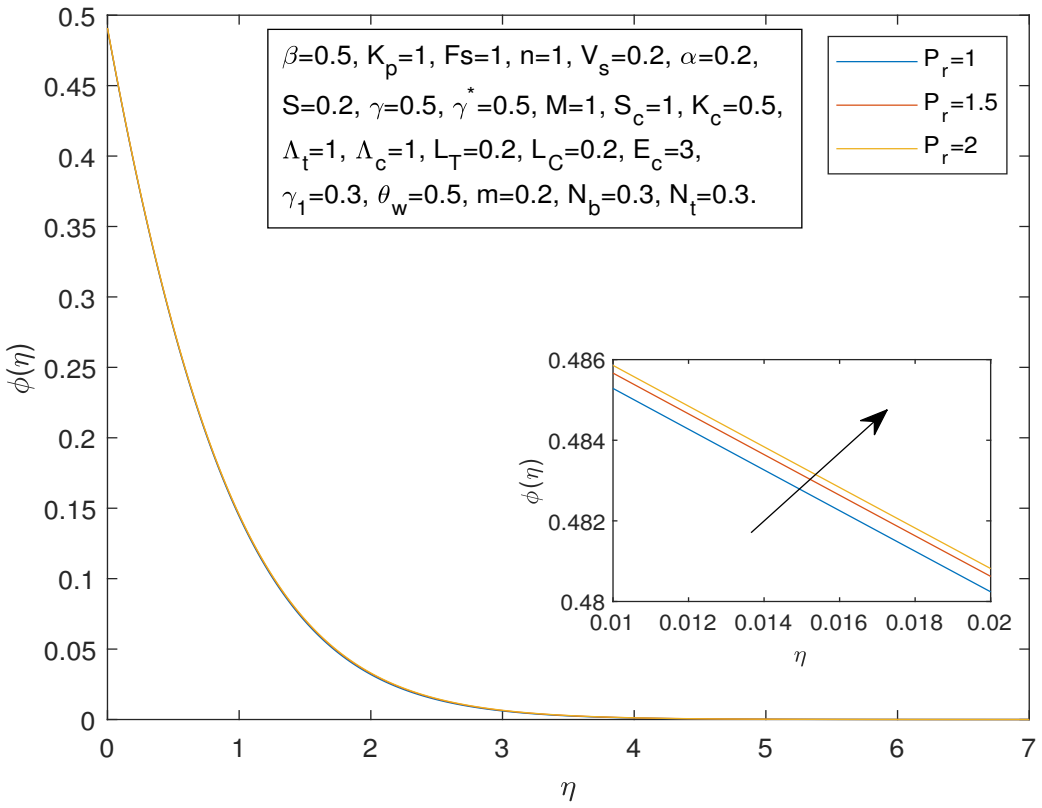

FIGURE 4.33: Concentration Profile $\phi(\eta)$ and η against Pr

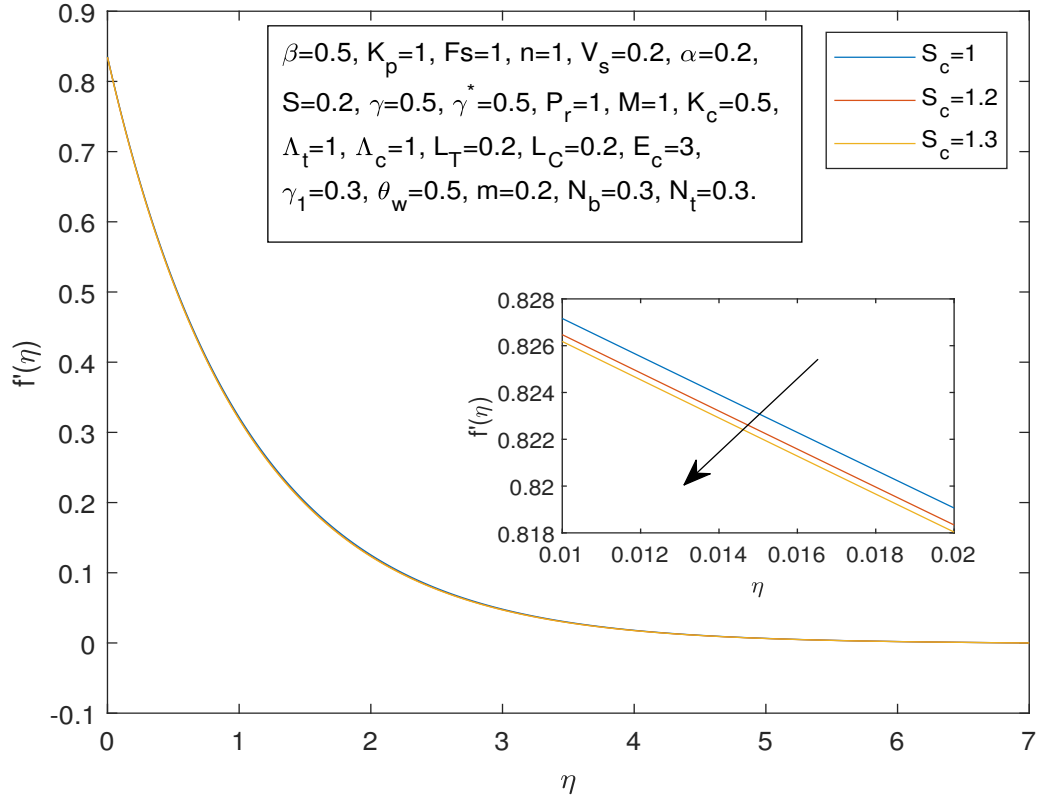

FIGURE 4.34: Velocity Profile $f'(\eta)$ and η against Sc

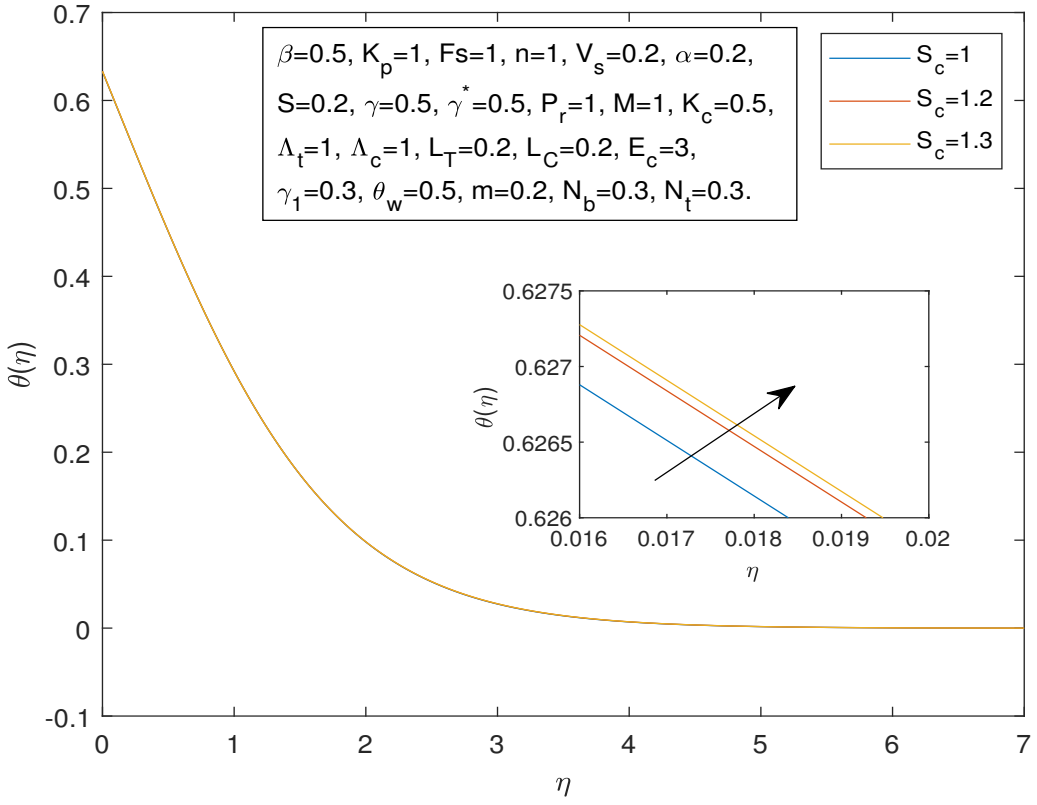

FIGURE 4.35: Temperature Profile $\theta(\eta)$ and η against Sc

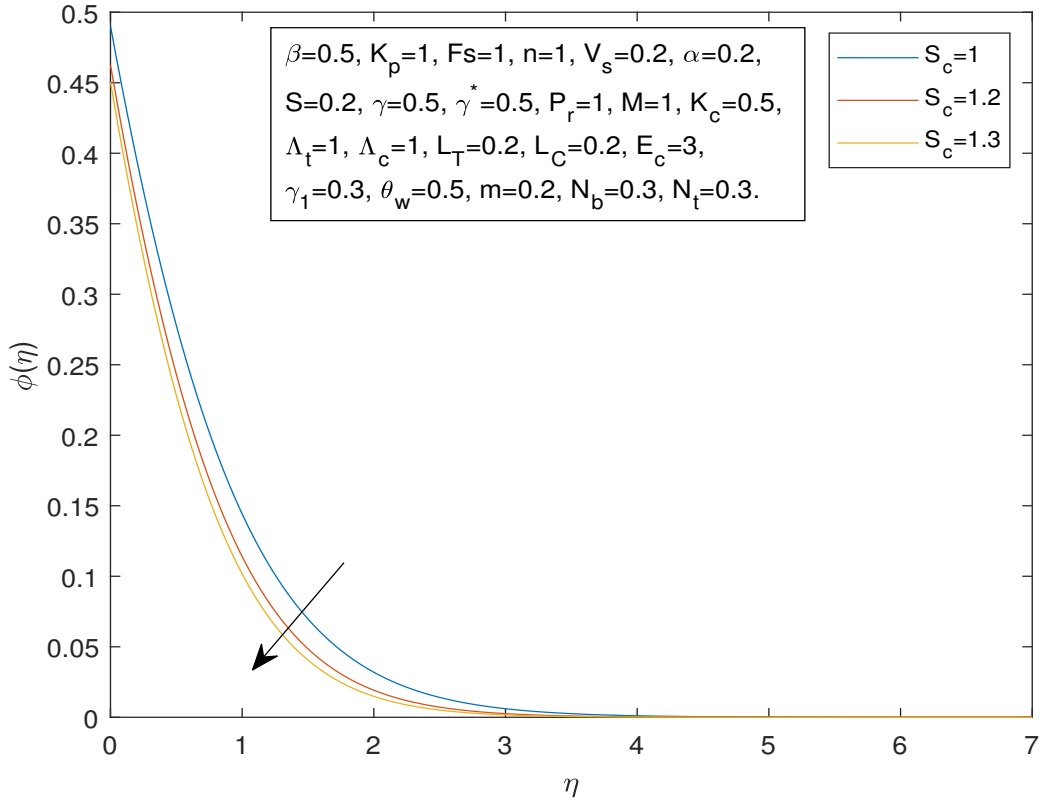

FIGURE 4.36: Concentration Profile $\phi(\eta)$ and η against Sc

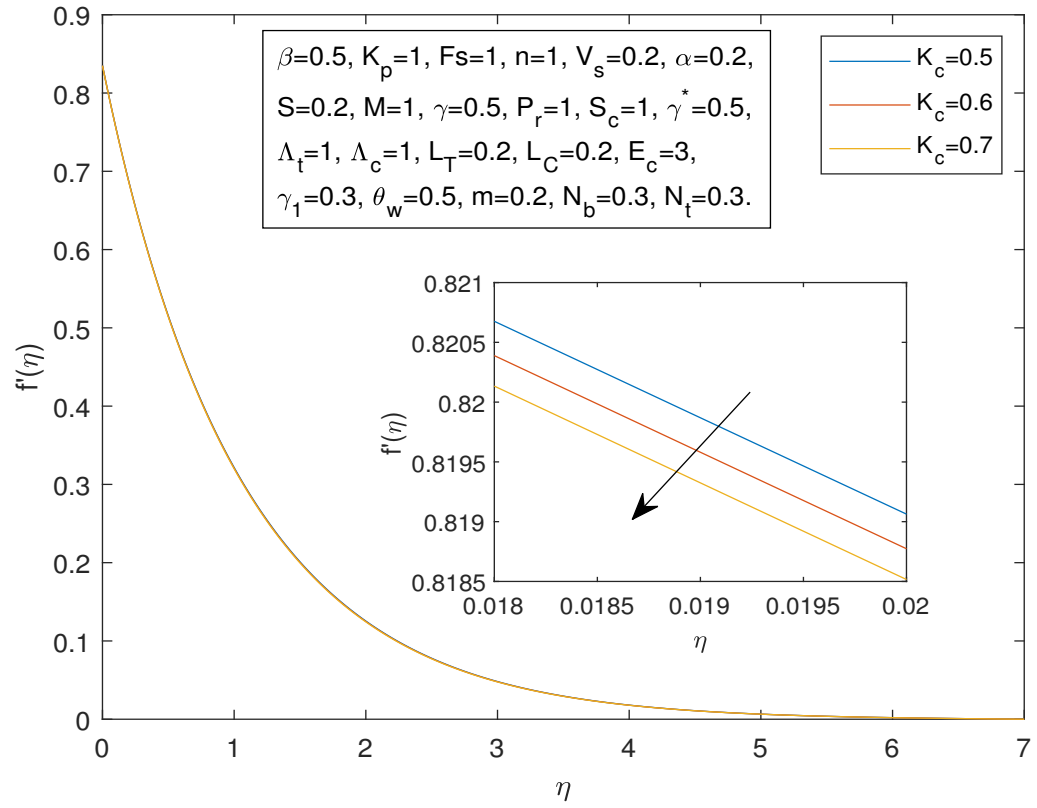

FIGURE 4.37: Velocity Profile $f'(\eta)$ and η against K_c

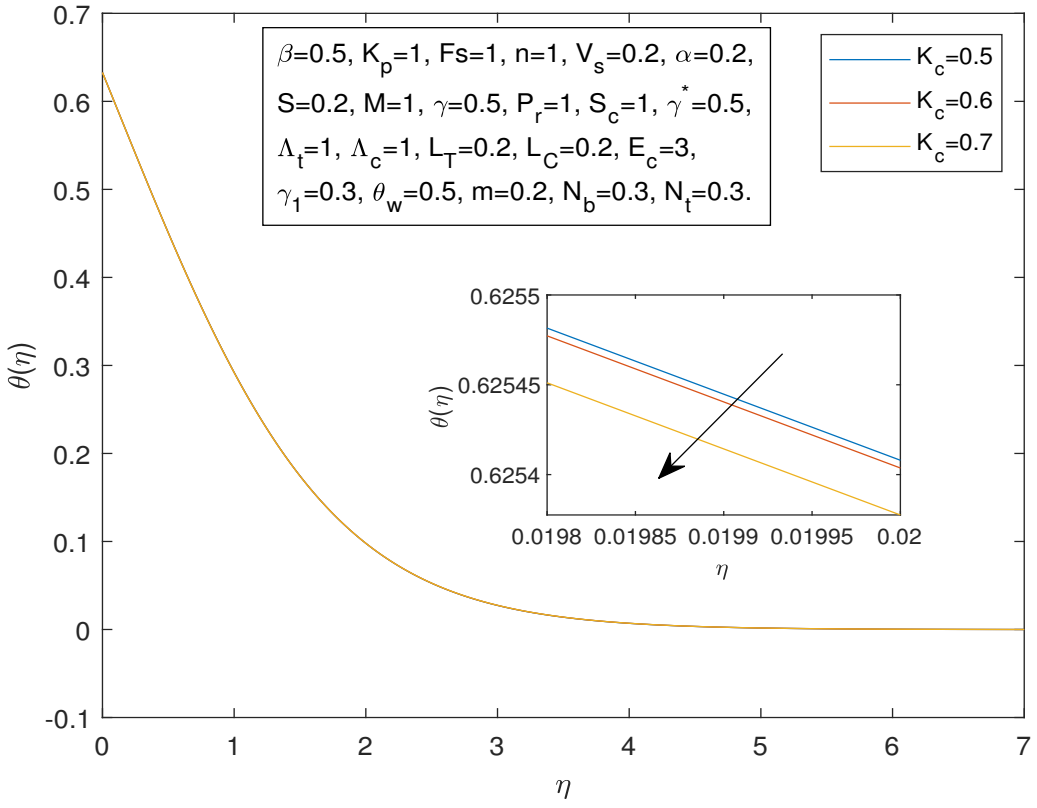

FIGURE 4.38: Temperature Profile $\theta(\eta)$ and η against K_c

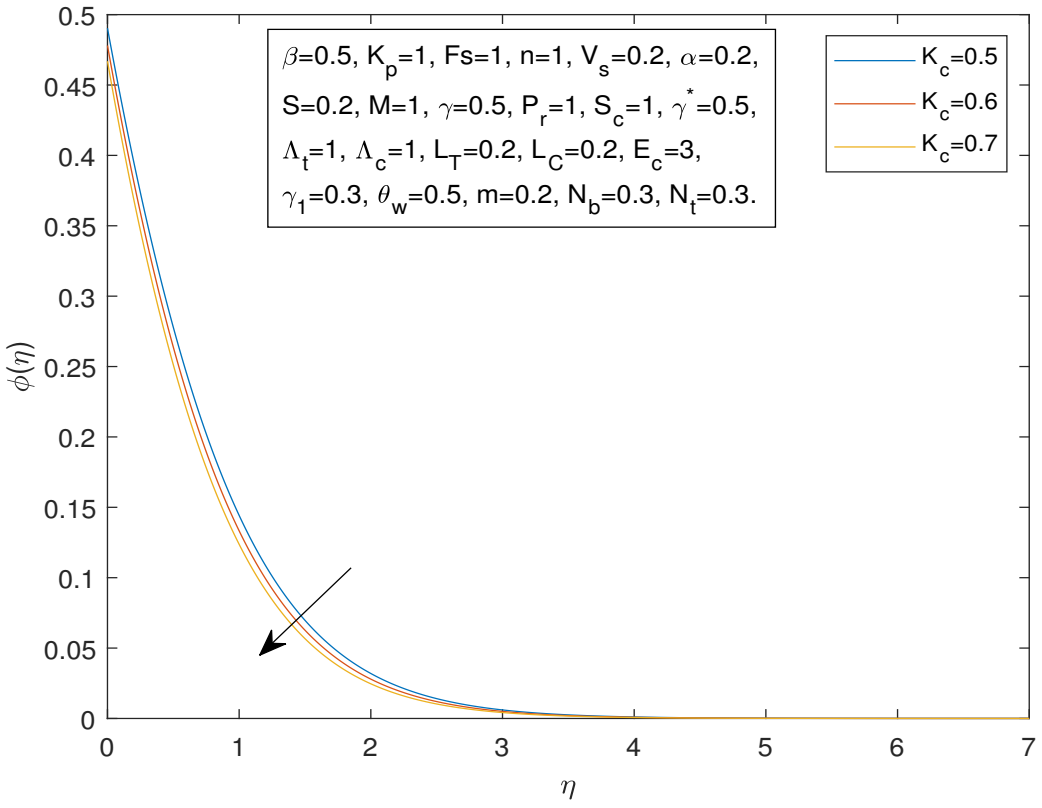

FIGURE 4.39: Concentration Profile $\phi(\eta)$ and η against K_c

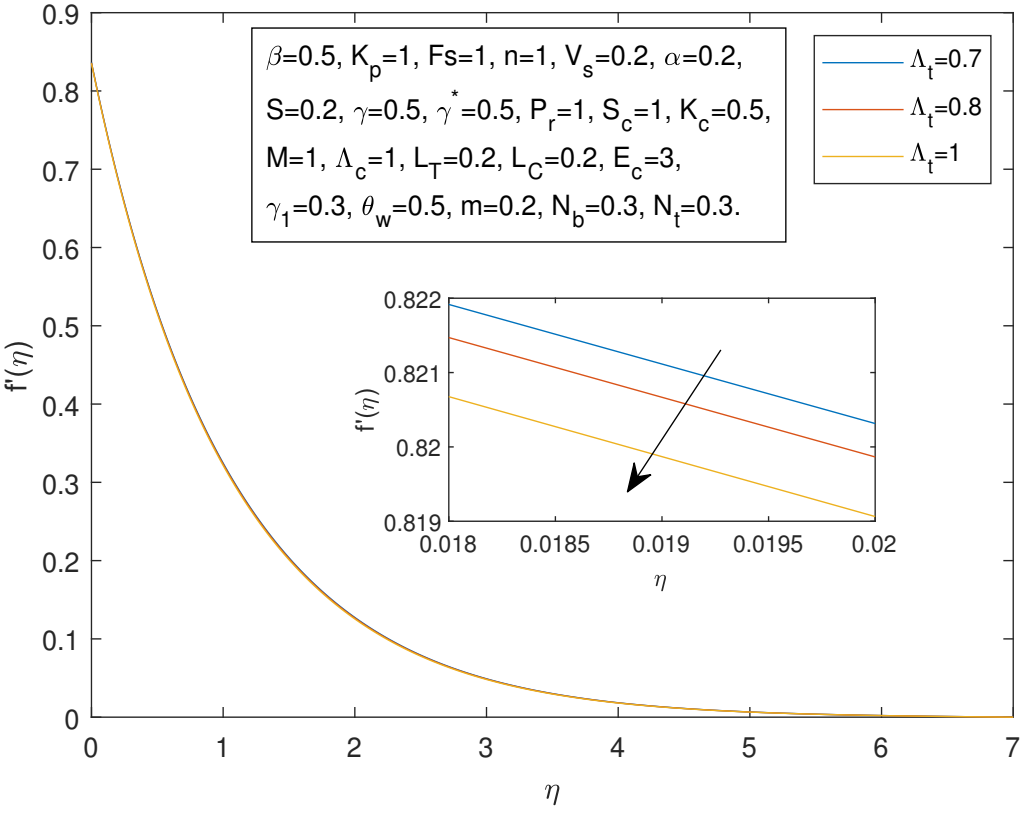

FIGURE 4.40: Velocity Profile $f'(\eta)$ and η against λ_t

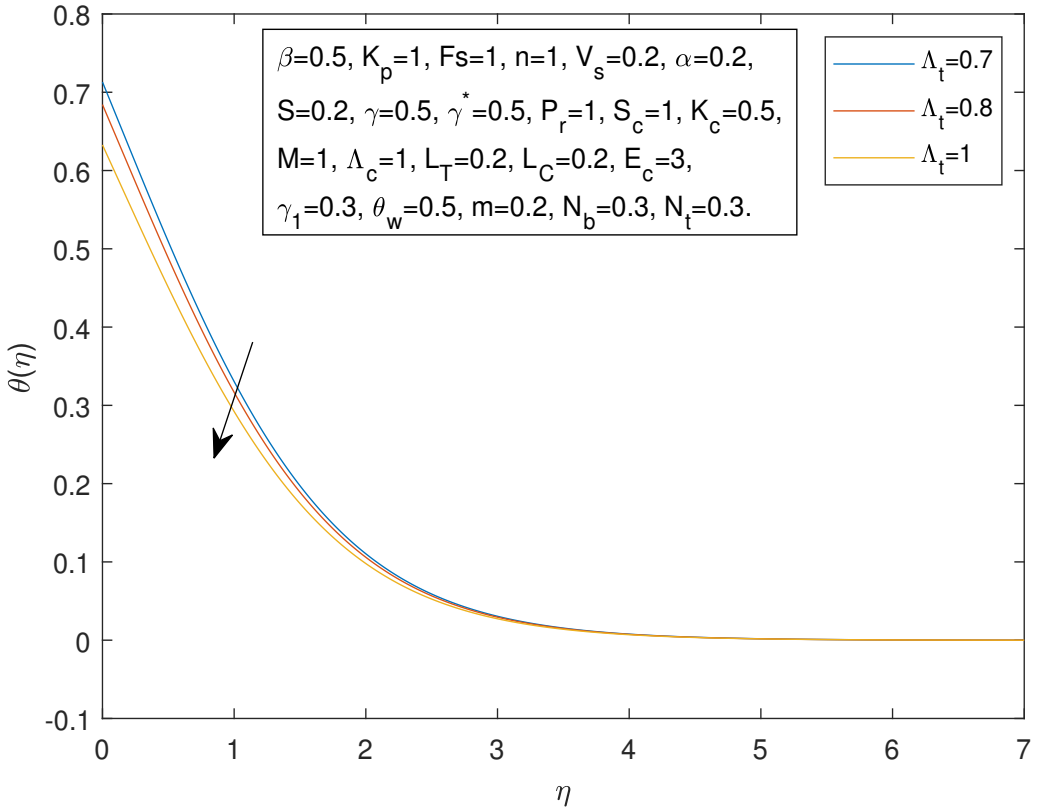

FIGURE 4.41: Temperature Profile $\theta(\eta)$ and η against λ_t

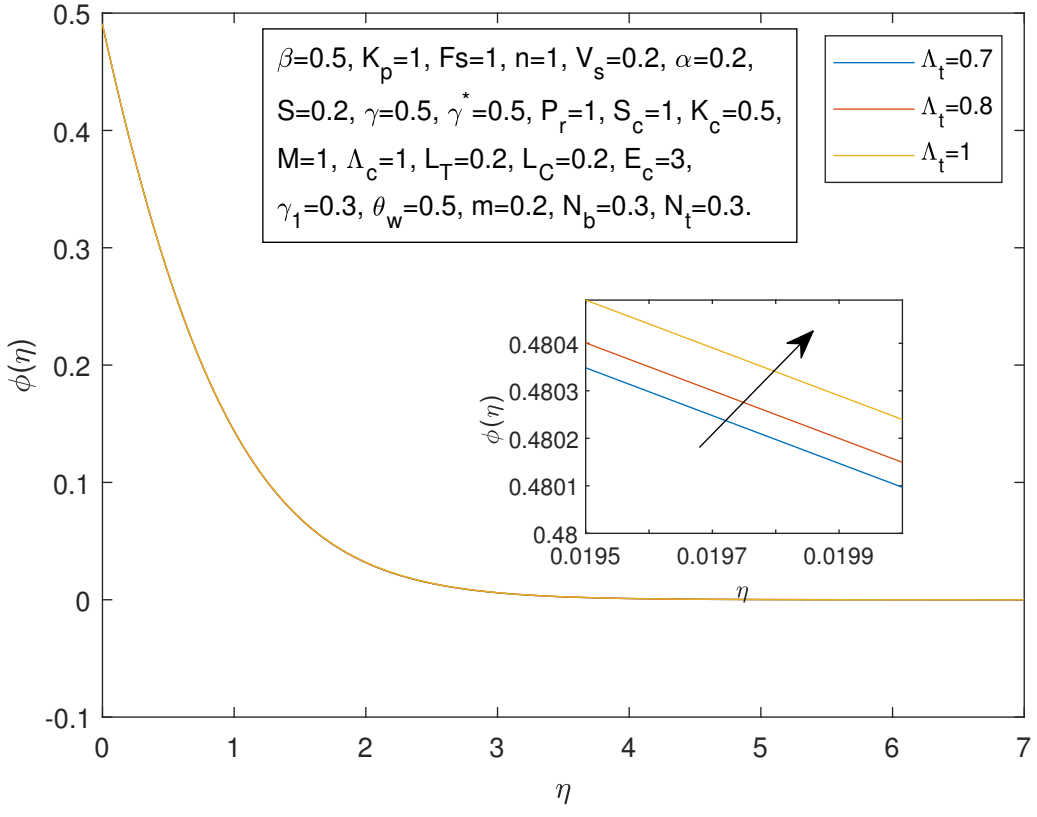

FIGURE 4.42: Concentration Profile $\phi(\eta)$ and η against λ_t

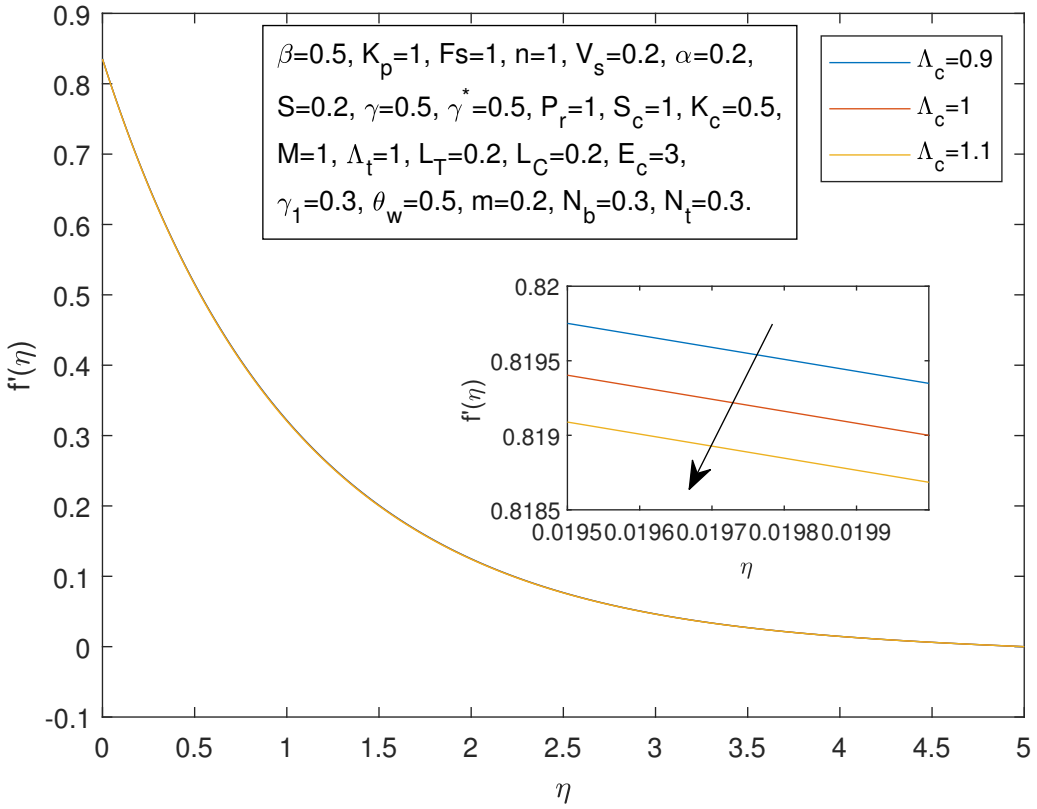

FIGURE 4.43: Velocity Profile $f'(\eta)$ and η against λ_c

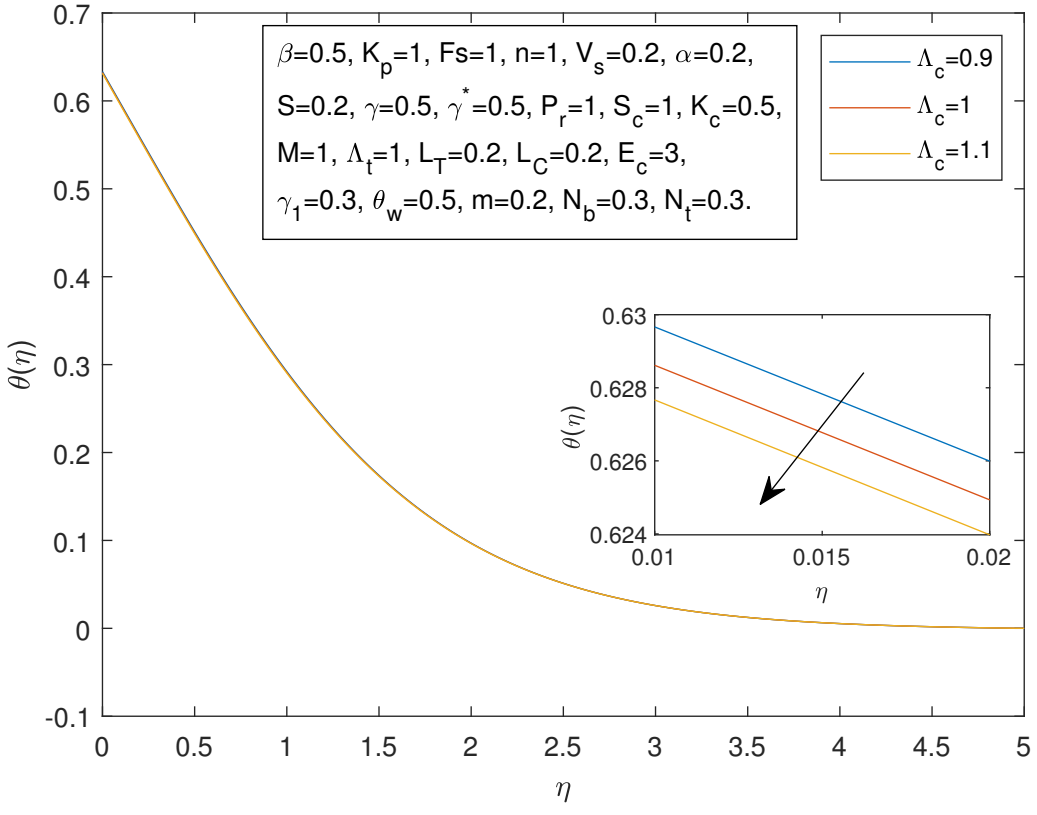

FIGURE 4.44: Temperature Profile $\theta(\eta)$ and η against λ_c

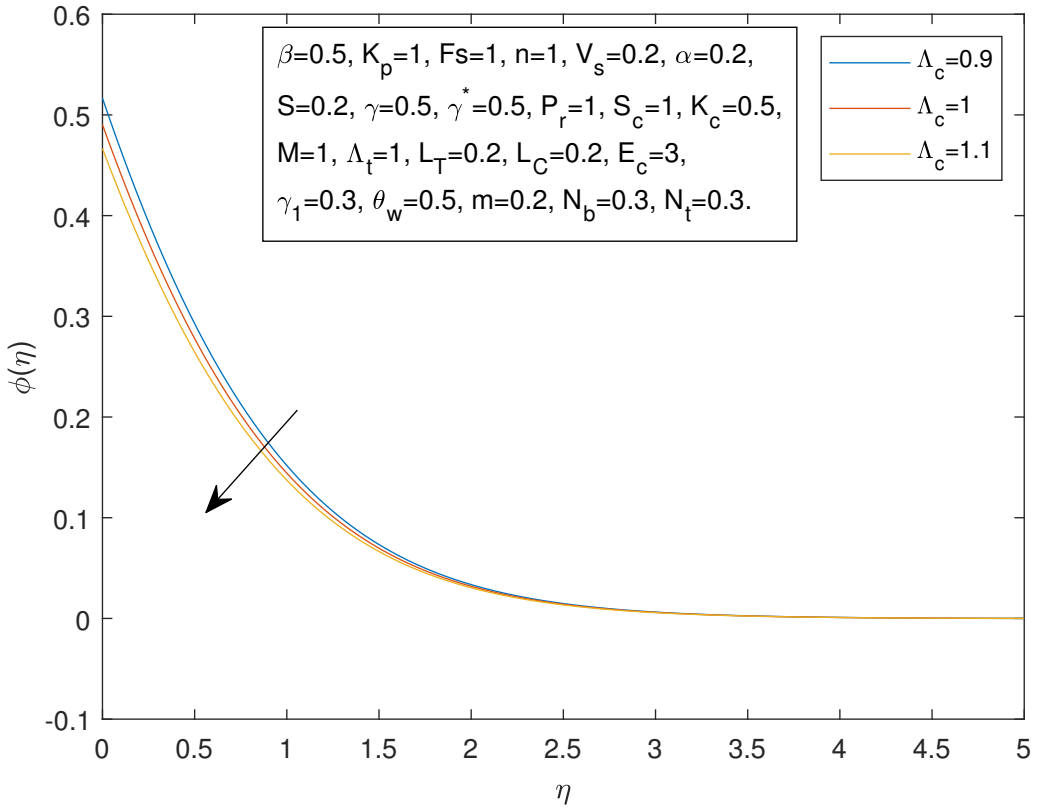

FIGURE 4.45: Concentration Profile $\phi(\eta)$ and η against λ_c

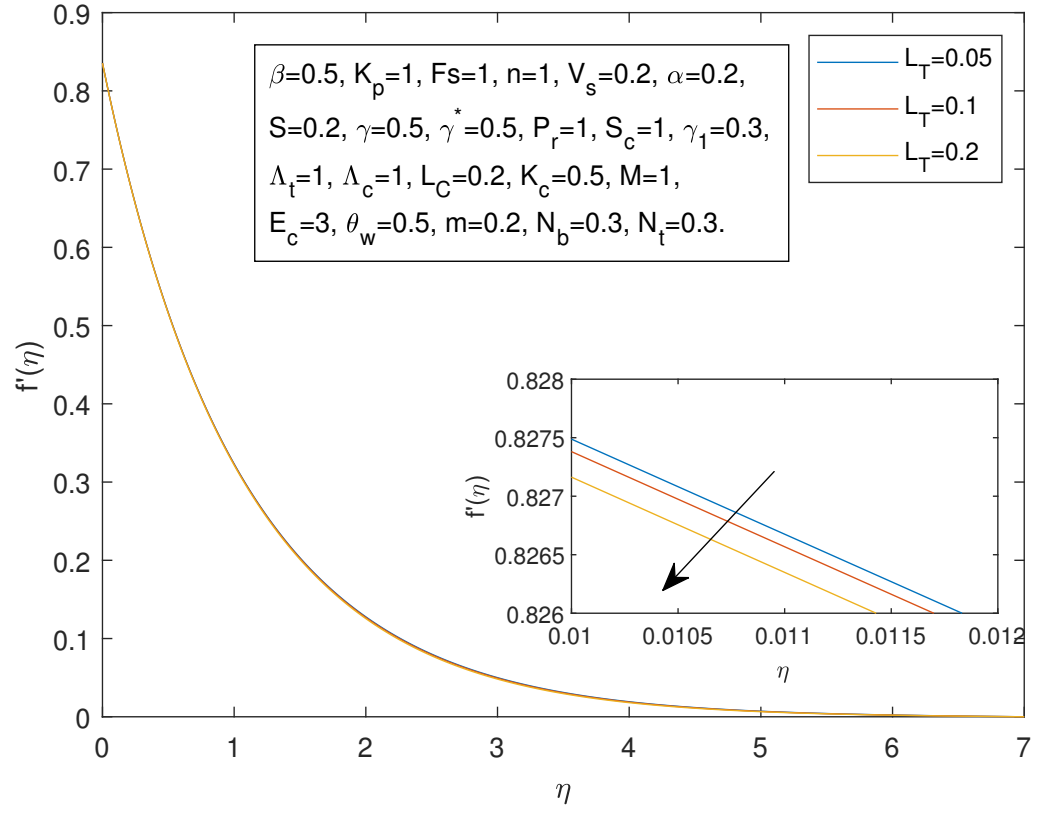

FIGURE 4.46: Velocity Profile $f'(\eta)$ and η against L_T

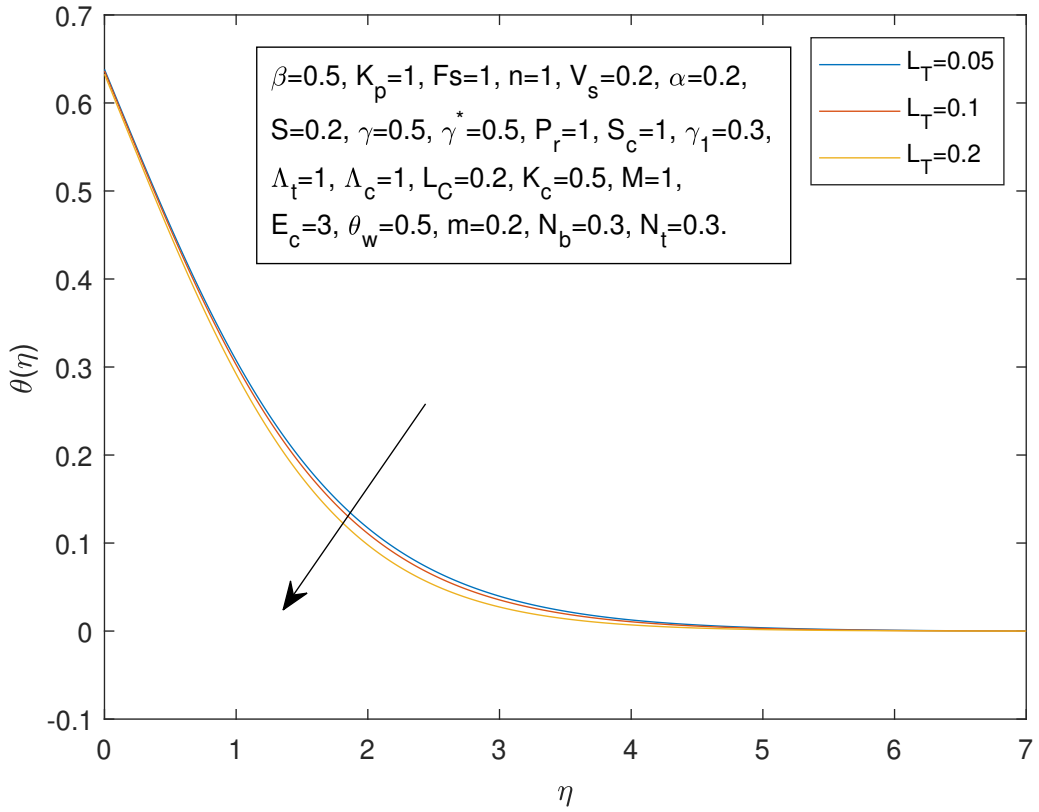

FIGURE 4.47: Temperature Profile $\theta(\eta)$ and η against L_T

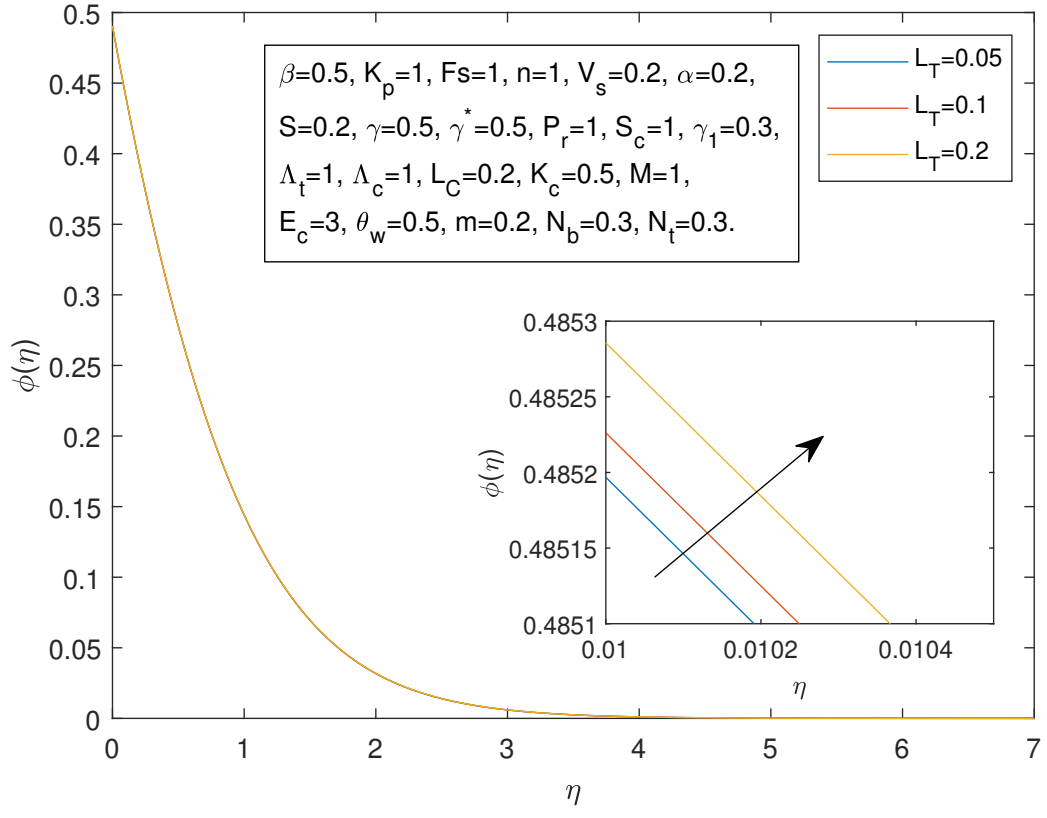

FIGURE 4.48: Concentration Profile $\phi(\eta)$ and η against L_T

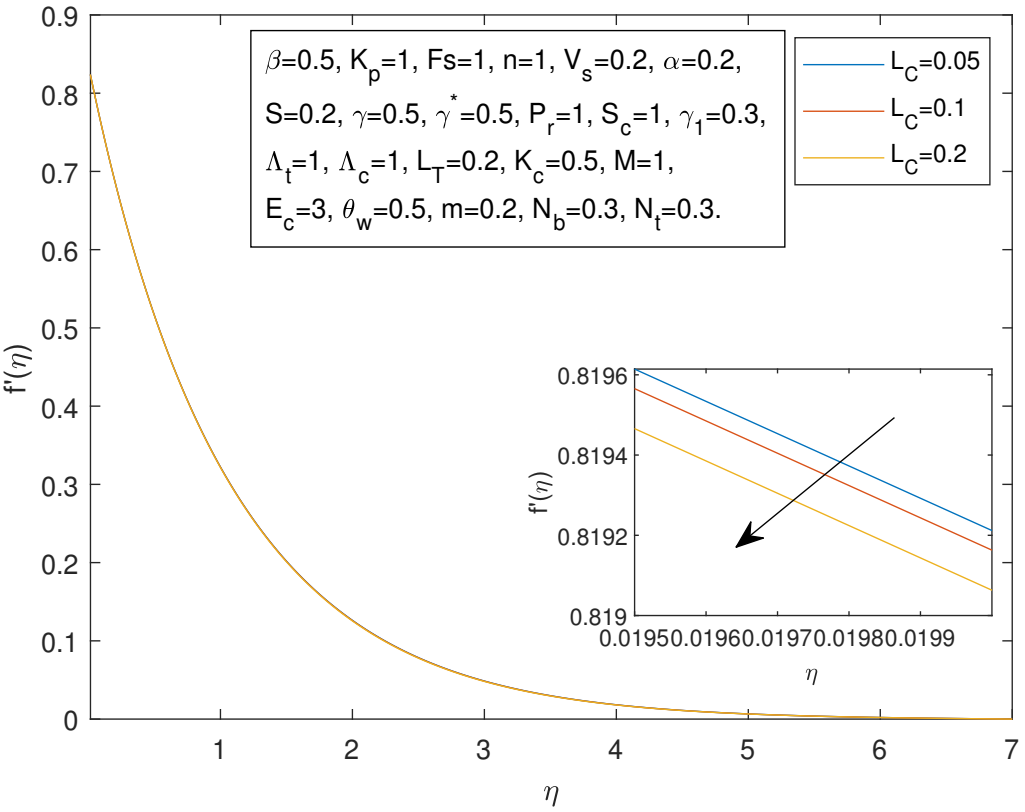

FIGURE 4.49: Velocity Profile $f'(\eta)$ and η against L_C

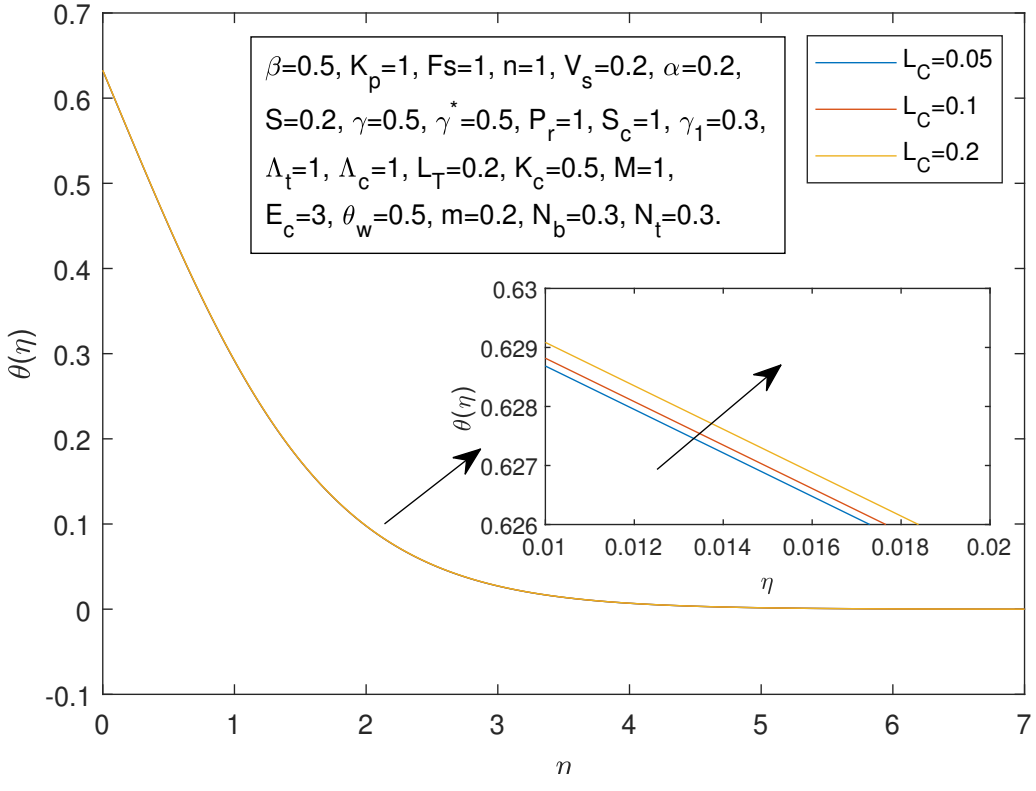

FIGURE 4.50: Temperature Profile $\theta(\eta)$ and η against L_C

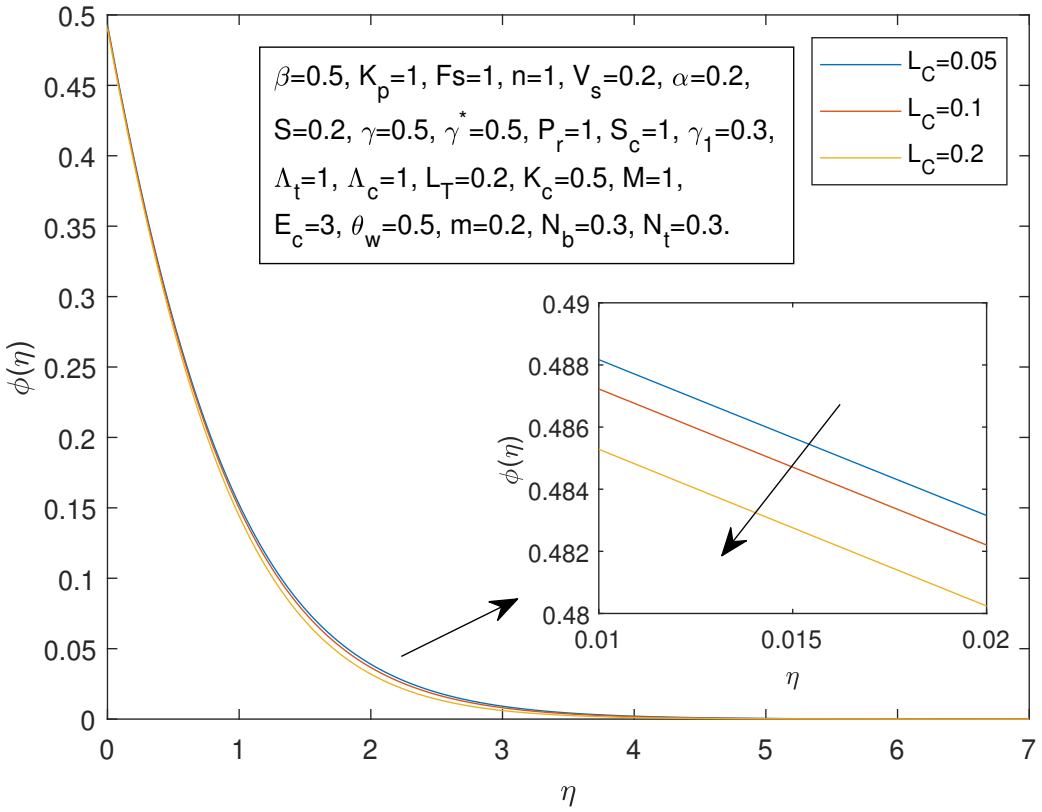

FIGURE 4.51: Concentration Profile $\phi(\eta)$ and η against L_C

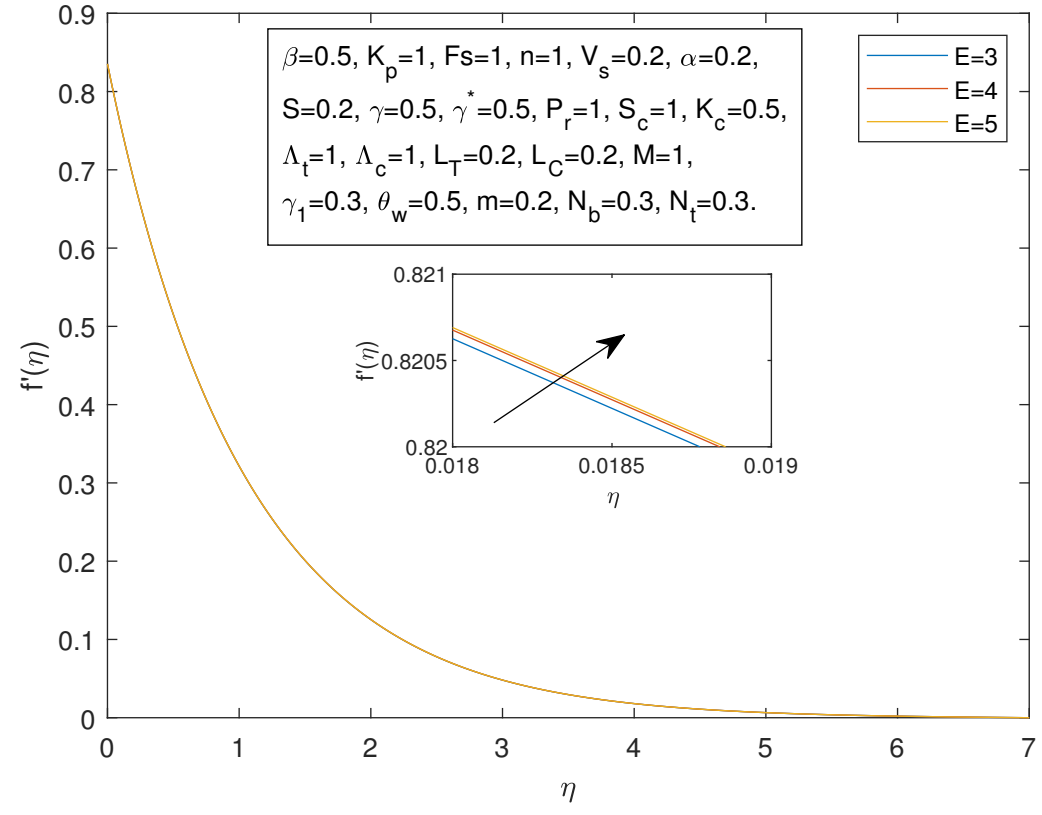

FIGURE 4.52: Velocity Profile $f'(\eta)$ and η against E

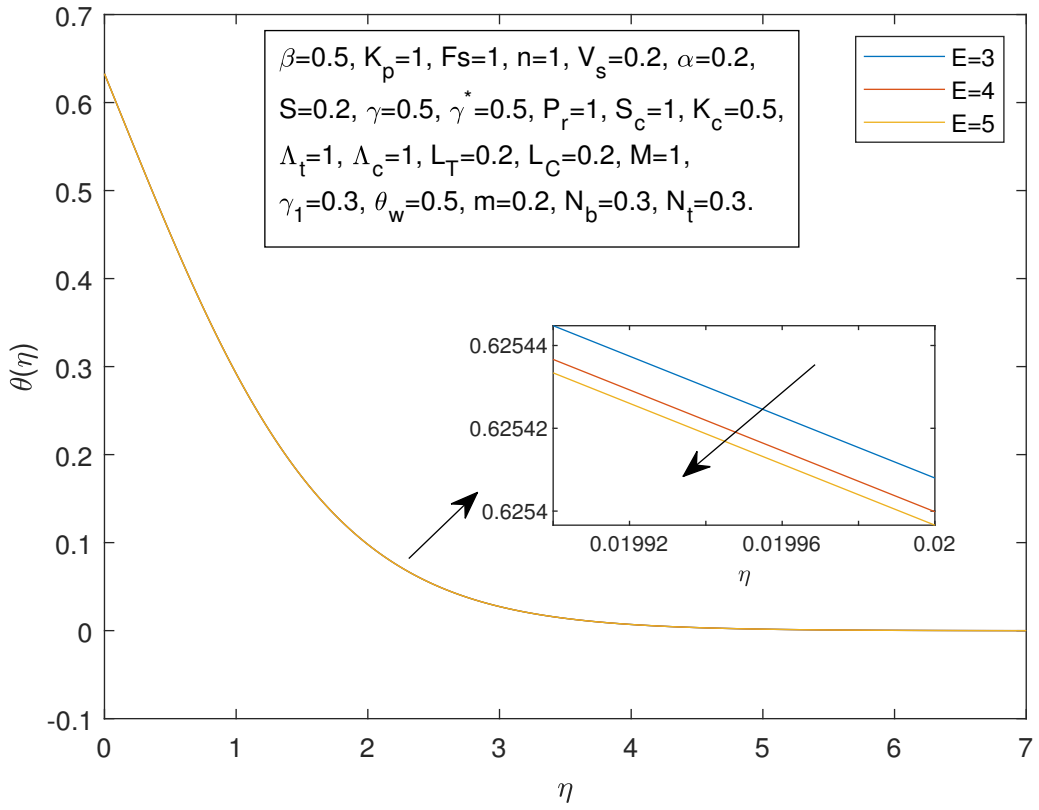

FIGURE 4.53: Temperature Profile $\theta(\eta)$ and η against E

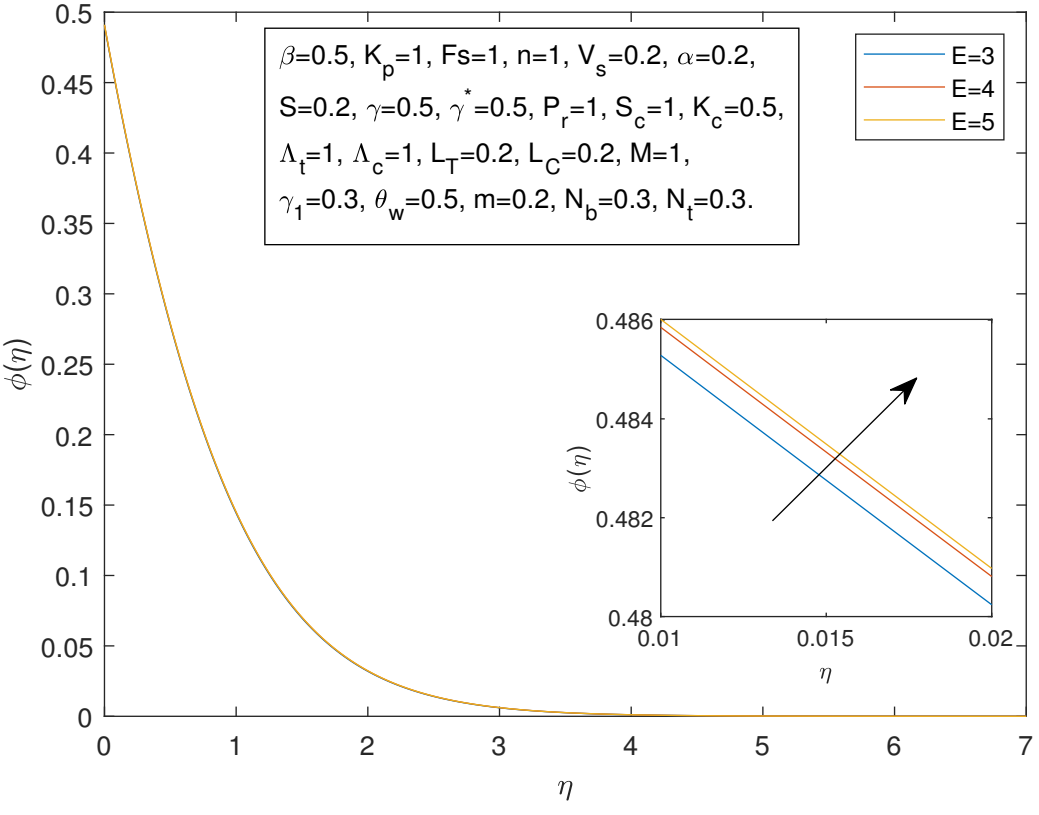

FIGURE 4.54: Concentration Profile $\phi(\eta)$ and η against E

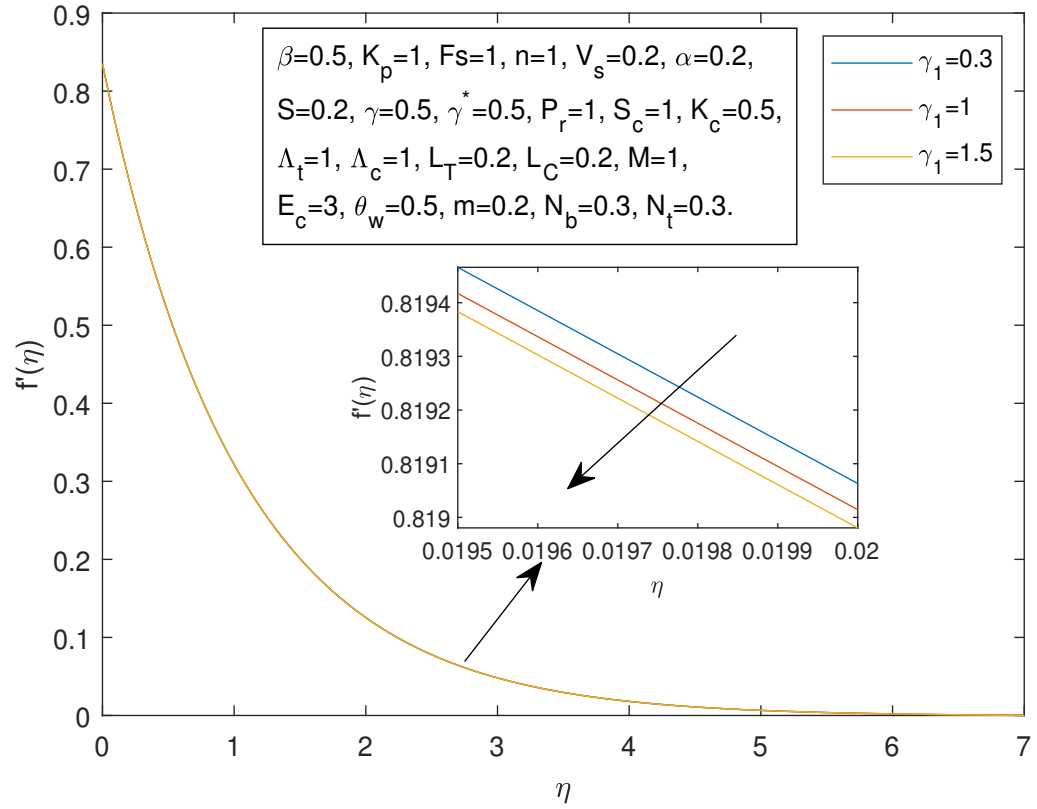

FIGURE 4.55: Velocity Profile $f'(\eta)$ and η against γ_1

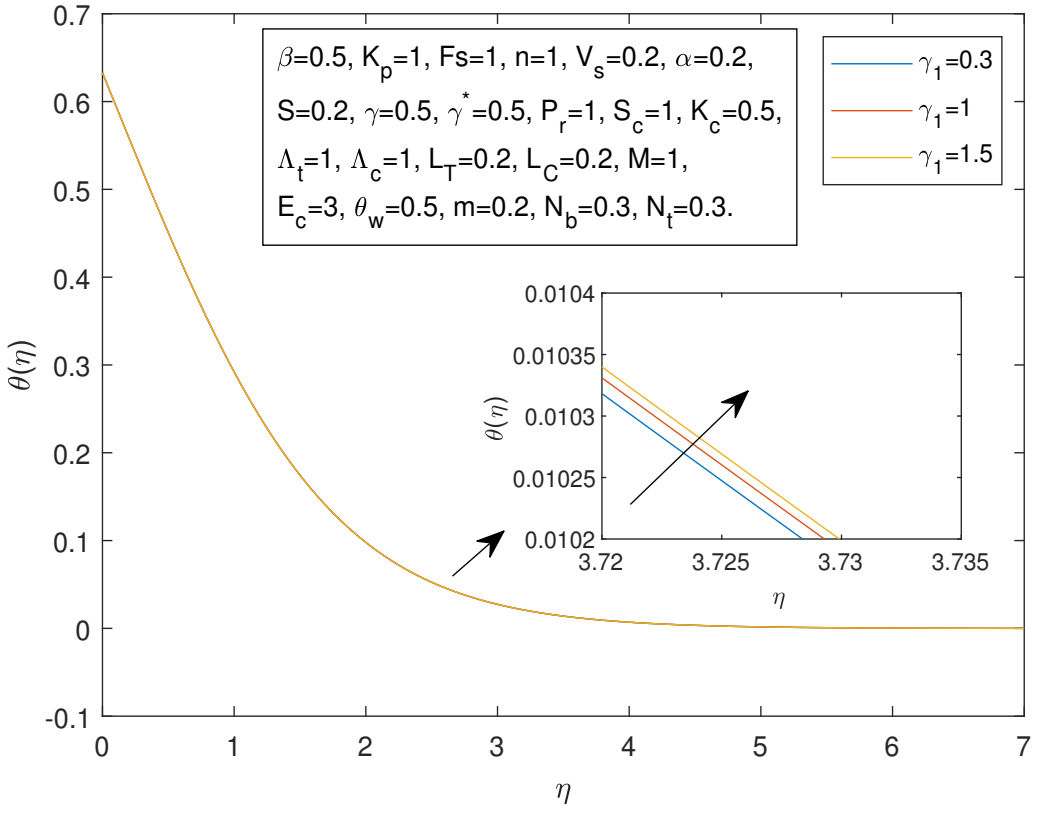

FIGURE 4.56: Temperature Profile $\theta(\eta)$ and η against γ_1

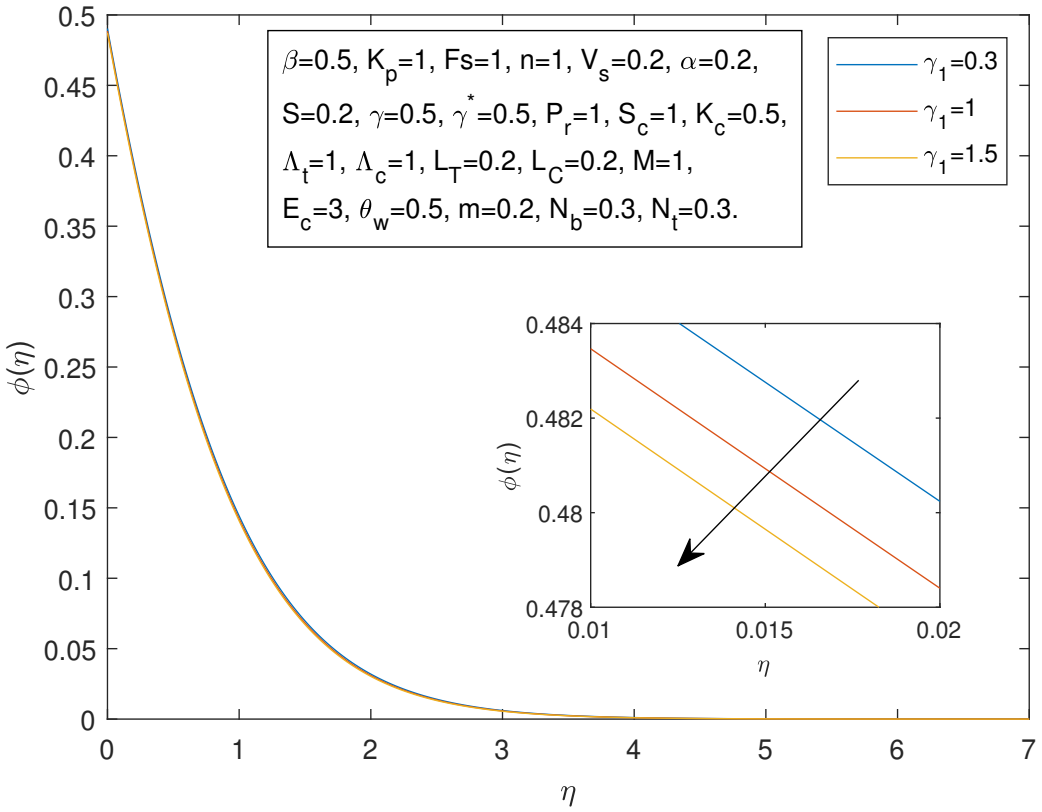

FIGURE 4.57: Concentration Profile $\phi(\eta)$ and η against γ_1

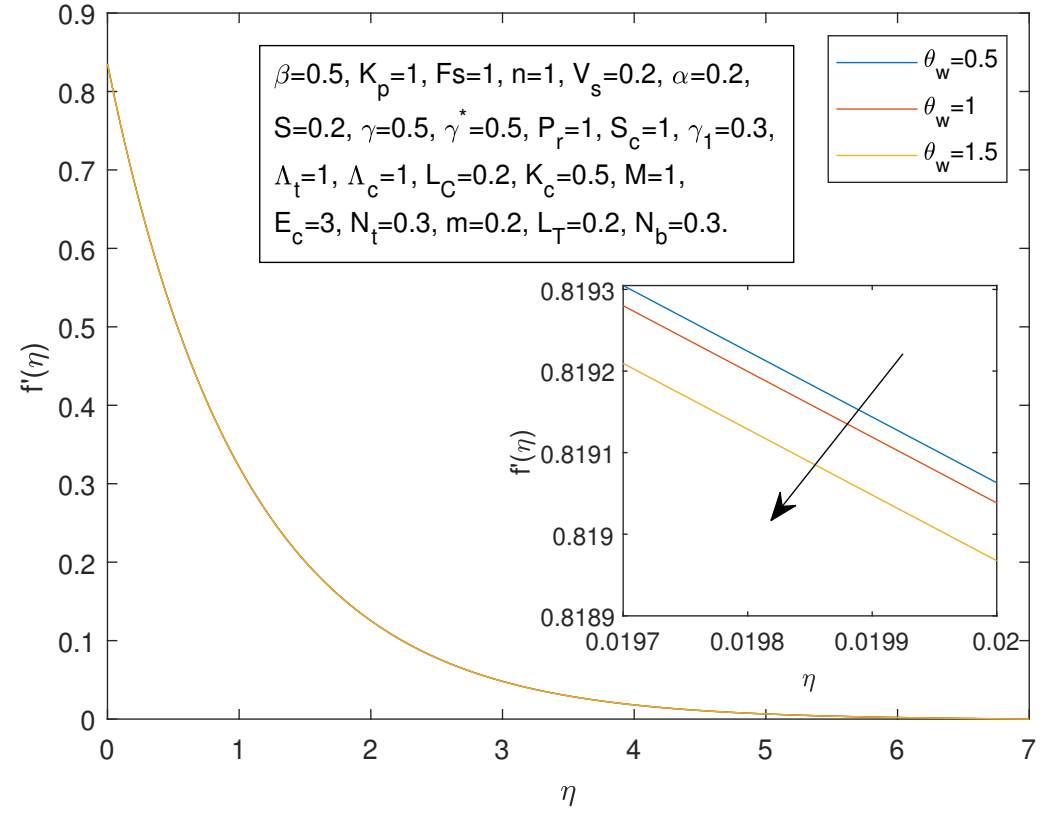

FIGURE 4.58: Velocity Profile $f'(\eta)$ and η against θ_w

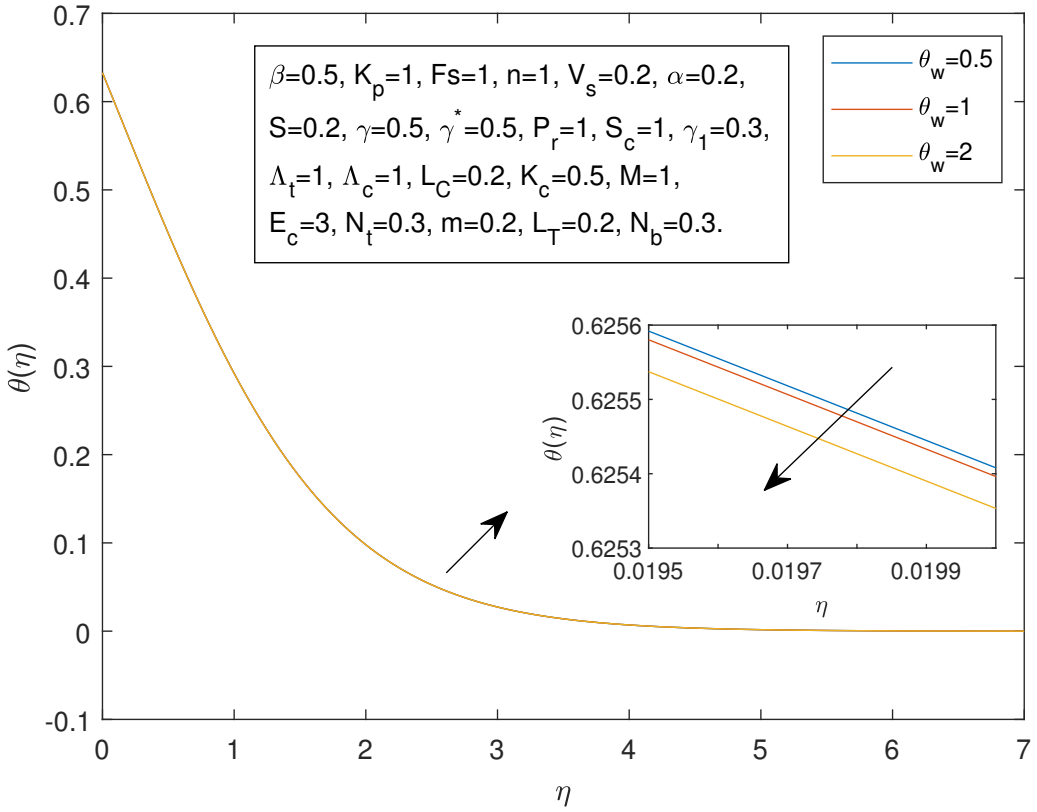

FIGURE 4.59: Temperature Profile $\theta(\eta)$ and η against θ_w

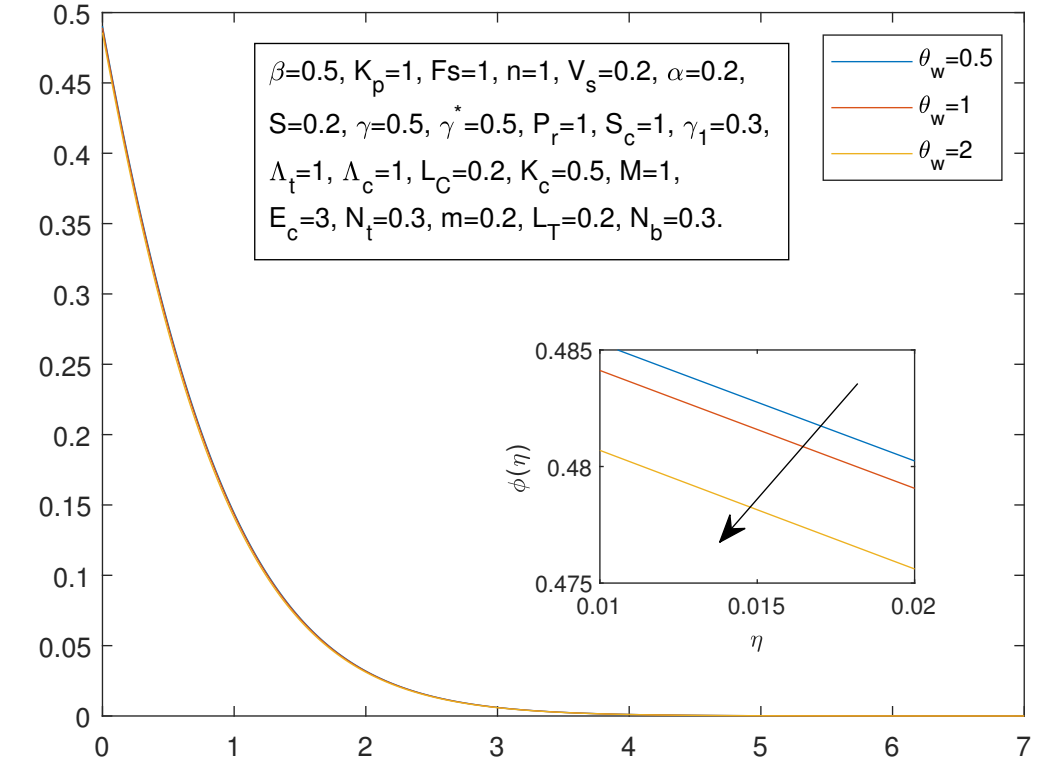

FIGURE 4.60: Concentration Profile $\phi(\eta)$ and η against θ_w

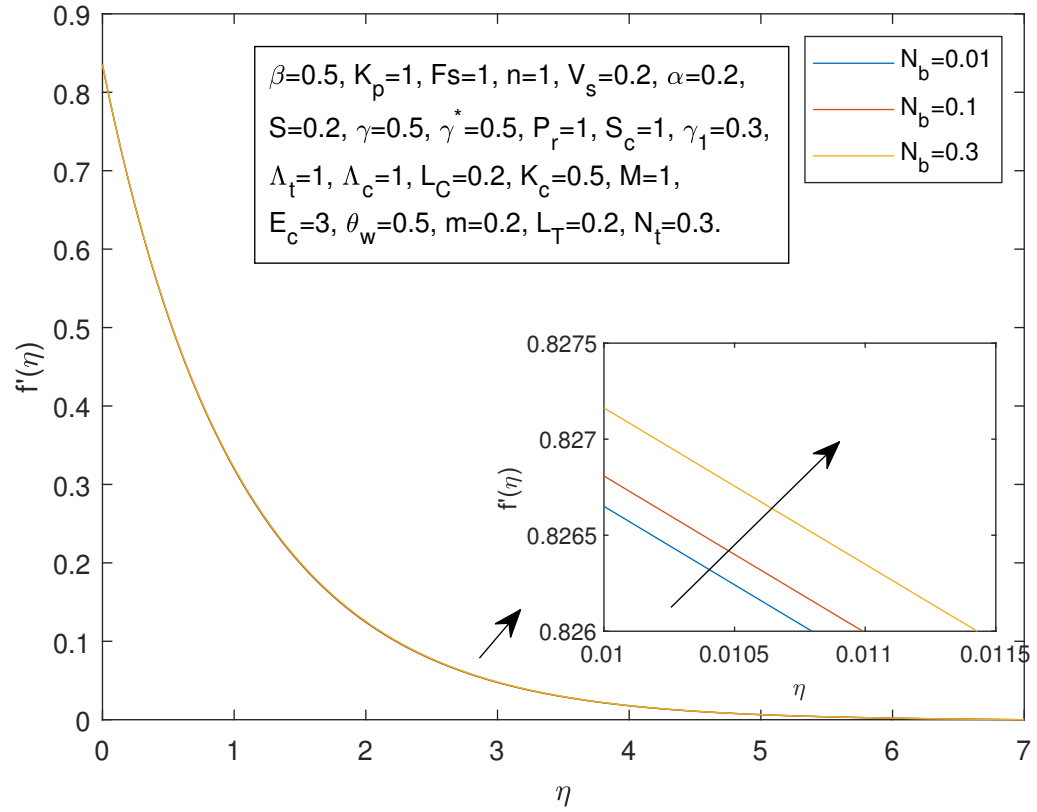

FIGURE 4.61: Velocity Profile $f'(\eta)$ and η against N_b

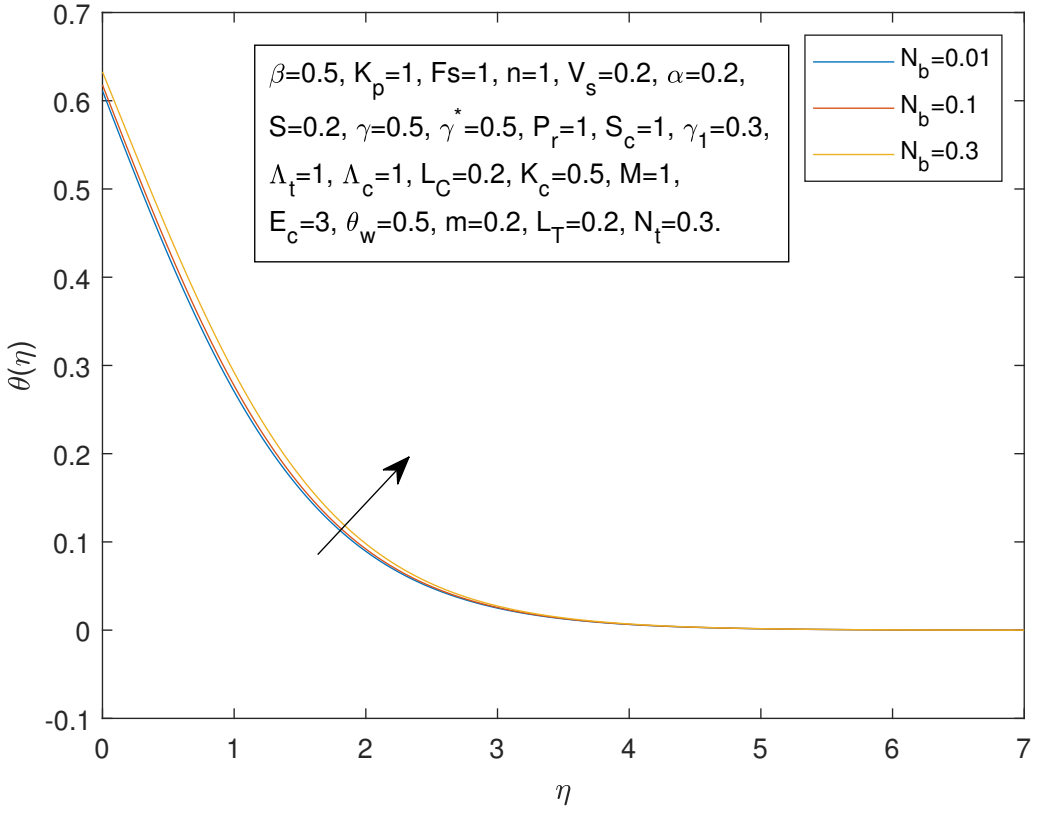

FIGURE 4.62: Temperature Profile $\theta(\eta)$ and η against N_b

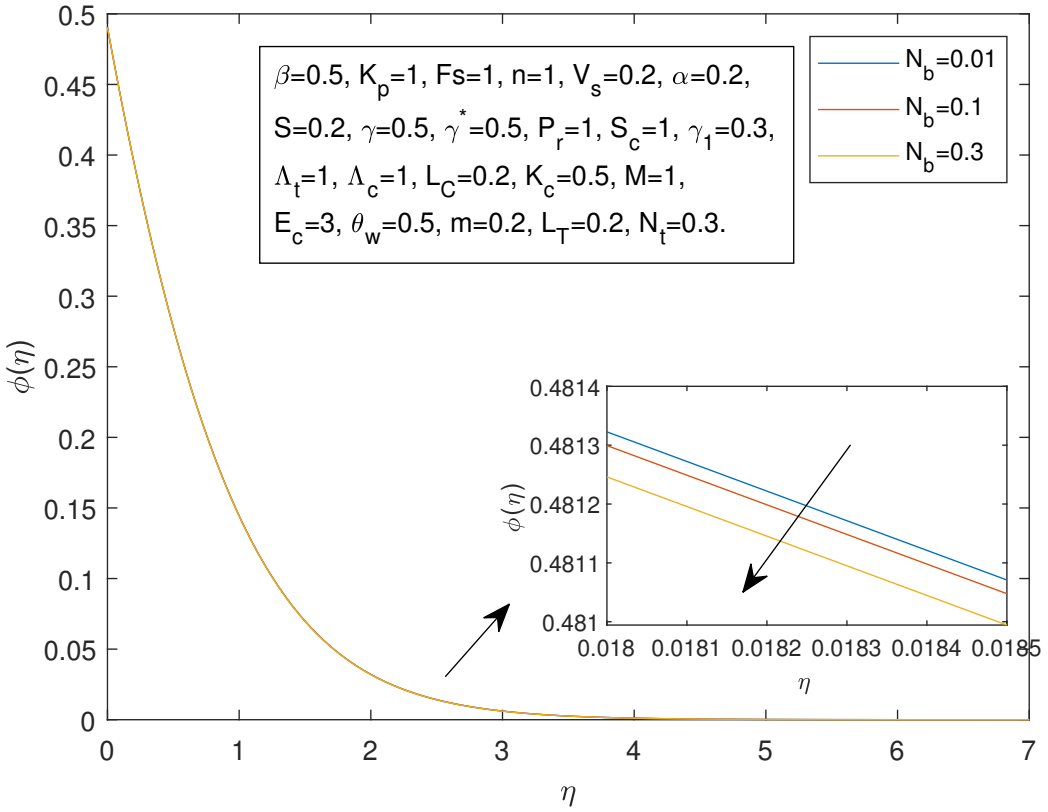

FIGURE 4.63: Concentration Profile $\phi(\eta)$ and η against N_b

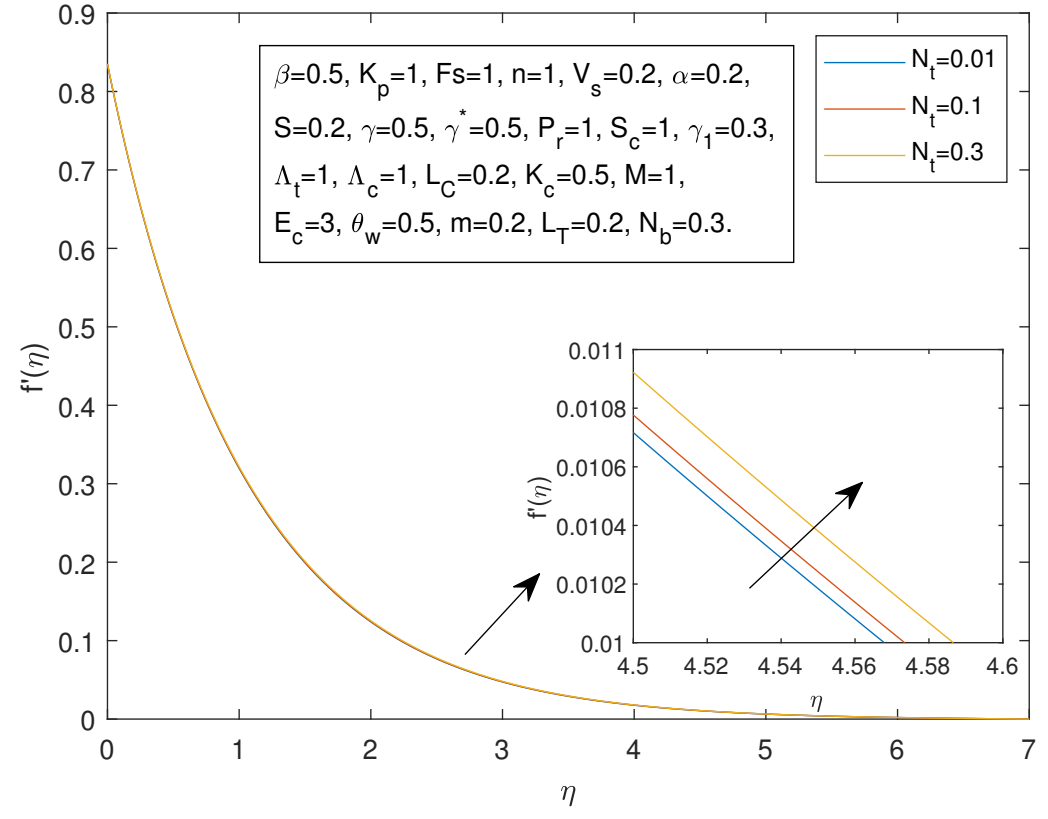

FIGURE 4.64: Velocity Profile $f'(\eta)$ and η against N_t

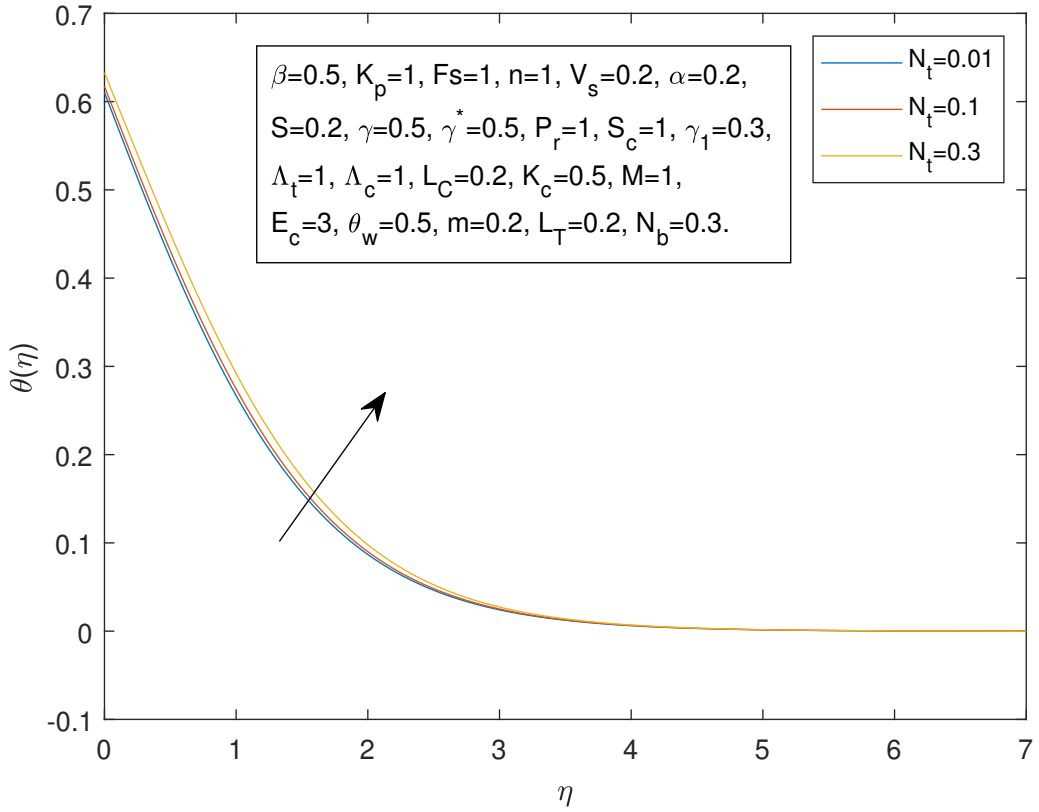

FIGURE 4.65: Temperature Profile $\theta(\eta)$ and η against N_t

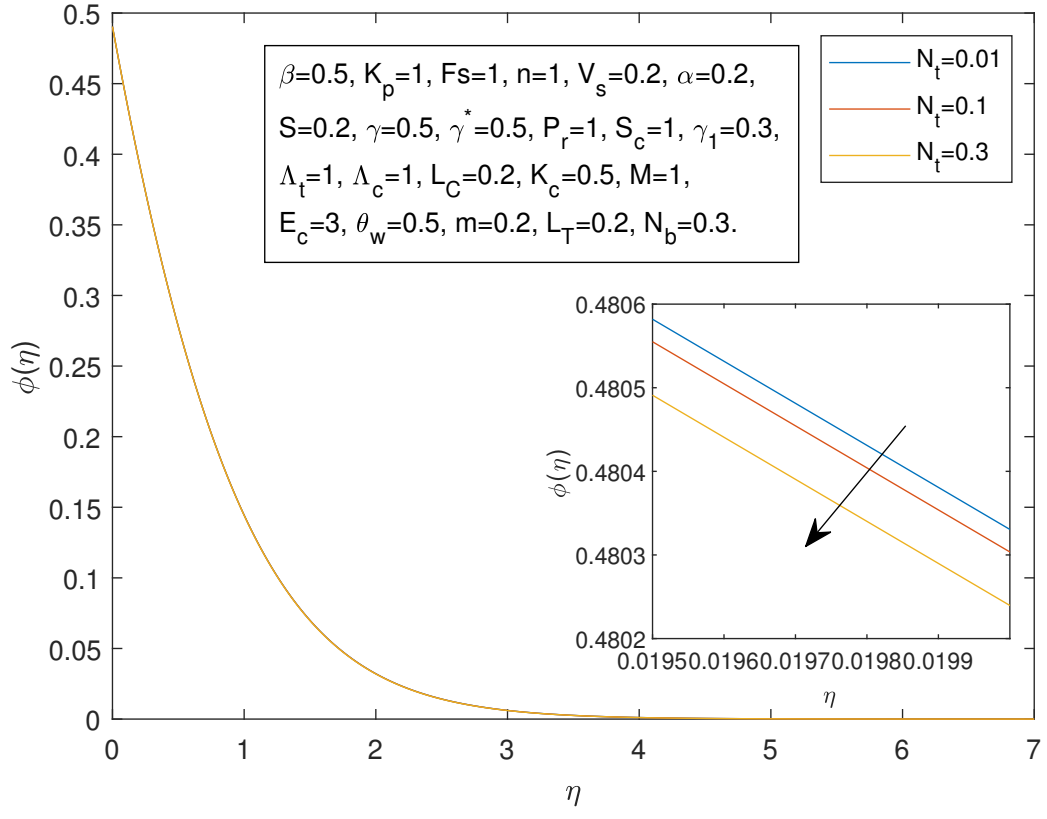

FIGURE 4.66: Concentration Profile $\phi(\eta)$ and η against N_t

Chapter 5

Conclusion

In this thesis, the work of Kala [40] is reviewed and extended by including the Cattaneo-Christov double diffusion in the temperature and concentration equations. Brownian and thermophoretic diffusion effects in temperature equation and activation energy in the concentration equation have also been incorporated. Firstly, by using the similarity transformation, the momentum, energy and concentration equations are altered into the ODEs. Through the application of the shooting technique, numerical solutions for the modified ODEs have been achieved. Utilizing the different values for the governing parameters, The results are presented in tables and graphs, illustrating the velocity, temperature, and concentration profiles. The following are the key findings of this study:

- As M increases, the velocity profile $f'(\eta)$ decreases, whereas the temperature distribution θ and concentration profile ϕ increase.
- The velocity distribution and temperature profile are showing decreasing trend by rising the Prandtl number while concentration distribution shows the increasing effects by rising Pr.
- As the Schmidt number S_c increases, a decreasing trend is observed in both the velocity profile and concentration distribution, while the temperature profile increases with increasing S_c.

- An increase in the Casson parameter β leads to a decline in the velocity profile $f'(\eta)$, whereas both the temperature profile $\theta(\eta)$ and concentration profile $\phi(\eta)$ increase with rising β values.

- As the activation energy parameter E increases, the velocity and concentration distributions exhibit an upward trend, while a rise in E leads to a decline in the temperature profile $\theta(\eta)$.

- An increase in the Forchheimer parameter F_s leads to a decline in the velocity profile $f'(\eta)$, whereas both the temperature profile $\theta(\eta)$ and the concentration profile $\phi(\eta)$ increase by rising F_s values.

- By increasing the values of Brownian parameter N_b and thermophoresis parameter N_t, the velocity and temperature profiles increase, while the concentration distribution shows a decreasing trend by rising the values of Brownian and thermophoresis parameters.

Bibliography

[1] L. Crane, "Flow past a stretch;ing plate," *Zeitschrift für angewandte Mathematik und Physik ZAMP*, vol. 21, pp. 645–647, 1970.

[2] K. Rajagopal, T. Na, and A. Gupta, "Flow of a viscoelastic fluid over a stretching sheet," *Rheologica Acta*, vol. 23, pp. 213–215, 1984.

[3] A. Ishak, R. Nazar, and I. Pop, "Falkner-skan equation for flow past a moving wedge with suction or injection," *Journal of Applied Mathematics and Computing*, vol. 25, no. 1-2, pp. 67–83, 2007.

[4] S. Mukhopadhyay, K. Bhattacharyya, and T. Hayat, "Exact solutions for the flow of Casson fluid over a stretching surface with tra;nspiration and heat transfer effects," *Chinese Physics B*, vol. 22, no. 11, p. 114701, 2013.

[5] A. Belhocine, N. Stojanovic, and O. I. Abdullah, "Numerical simulation of laminar boundary layer flow over a horizontal flat plate in external incompressible viscous fluid," *European Journal of Computational Mechanics*, vol. 30, no. 4-6, pp. 337–386, 2021.

[6] B. Siddappa and S. Abel, "Non-Newtonian flow past a stretching plate," *Zeitschrift für Angewandte Mathematik und Physik*, vol. 36, no. 6, p. 890–892, 1985.

[7] H. Andersson, "MHD flow of a viscoelastic fluid past a stretching surface," *Acta Mechanica*, vol. 95, no. 1-4, pp. 227–230, 1992.

[8] B. Dandapat, L. Holmedal, and H. Andersson, "On the stability of MHD flow of a viscoelastic fluid past a stretching sheet," *Acta Mechanica*, vol. 130, pp. 143–146, 1998.

[9] C. Mamaloukas, S. Spartalis, and Z. Manussaridis, "Similarity approach to the problem of second grade fluid flows over a stretching sheet," *Applied Mathematical Sciences*, vol. 1, no. 7, pp. 327–338, 2007.

[10] B. Jalili, A. Ganji, A. Shateri, P. Jalili, and D. Ganji, "Thermal analysis of non-Newtonian visco-inelastic fluid MHD flow between rotating disks," *Case Studies in Thermal Engineering*, vol. 49, p. 103333, 2023.

[11] T. Fang, F. Guo, and F. Chia-fon, "A note on the extended Blasius equation," *Applied Mathematics Letters*, vol. 19, no. 7, pp. 613–617, 2006.

[12] R. Bataller, "Numerical comparisons of Blasius and Sakiadis flows," *MATEMATIKA: Malaysian Journal of Industrial and Applied Mathematics*, pp. 187–196, 2010.

[13] A. Jannelli, "A finite difference method on quasi-uniform grids for the fractional boundary-layer Blasius flow," *Mathematics and Computers in Simulation*, vol. 215, pp. 382–398, 2024.

[14] S. Motsa, T. Hayat, and O. Aldossary, "Mhd flow of upper-convected Maxwell fluid over porous stretching sheet using successive Taylor series linearization method," *Applied Mathematics and Mechanics*, vol. 33, pp. 975–990, 2012.

[15] S. Motsa and P. Sibanda, "On the solution of MHD flow over a nonlinear stretching sheet by an efficient semi-analytical technique," *International Journal for Numerical Methods in Fluids*, vol. 68, no. 12, pp. 1524–1537, 2012.

[16] A. Rosca, "MHD boundary-layer flow over a permeable shrinking surface," *Acta Universitatis Apulensis*, vol. 36, pp. 31–38, 2013.

[17] S. Nadeem, S. Hussain, and C. Lee, "Flow of a Williamson fluid over a stretching sheet," *Brazilian Journal of Chemical Engineering*, vol. 30, pp. 619–625, 2013.

[18] S. Mukhopadhyay, "MHD boundary layer slip flow along a stretching cylinder," *Ain Shams Engineering Journal*, vol. 4, no. 2, pp. 317–324, 2013.

[19] N. Akbar, S. Nadeem, R. Haq, and S. Ye, "MHD stagnation point flow of Carreau fluid toward a permeable shrinking sheet: Dual solutions," *Ain Shams Engineering Journal*, vol. 5, no. 4, pp. 1233–1239, 2014.

[20] A. Khidir, "A note on the solution of general Falkner-Skan problem by two novel semi-analytical techniques," *Propulsion and Power Research*, vol. 4, no. 4, pp. 212–220, 2015.

[21] K. Sharada and B. Shankar, "MHD mixed convection flow of a Casson fluid over an exponentially stretching surface with the effects of Soret, Dufour, thermal radiation and chemical reaction," *World Journal of Mechanics*, vol. 5, no. 09, pp. 165–177, 2015.

[22] R. Biswas, M. Mondal, D. Sarkar, and S. Ahmed, "Effects of radiation and chemical reaction on MHD unsteady heat and mass transfer of Casson fluid flow past a vertical plate," *Journal of Advances in Mathematics and Computer Science*, vol. 23, no. 2, pp. 1–16, 2017.

[23] S. Ahmed, R. Biswas, and M. Afikuzzaman, "Unsteady Magnetohydrodynamic free convection flow of nanofluid through an exponentially accelerated inclined plate embedded in a porous medium with variable thermal conductivity in the presence of radiation," *Journal of Nanofluids*, vol. 7, no. 5, pp. 891–901, 2018.

[24] R. Biswas and S. Ahmed, "Effects of Hall current and chemical reaction on MHD unsteady heat and mass transfer of Casson nanofluid flow through a vertical plate," *Journal of Heat Transfer*, vol. 140, no. 9, p. 092402, 2018.

[25] N. Khan, S. Zuhra, Z. Shah, E. Bonyah, W. Khan, S. Islam, and A. Khan, "Hall current and thermophoresis effects on Magnetohydrodynamic mixed convective heat and mass transfer thin film flow," *Journal of Physics Communications*, vol. 3, no. 3, p. 035009, 2019.

[26] J. Raza, F. Mebarek-Oudina, and B. Mahanthesh, "Magnetohydrodynamic flow of nano Williamson fluid generated by stretching plate with multiple slips," *Multidiscipline Modeling in Materials and Structures*, vol. 15, no. 5, pp. 871–894, 2019.

[27] J. Raza, M. Farooq, F. Mebarek-Oudina, and B. Mahanthesh, "Multiple slip effects on MHD non-Newtonian nanofluid flow over a nonlinear permeable elongated sheet: numerical and statistical analysis," *Multidiscipline Modeling in Materials and Structures*, vol. 15, no. 5, pp. 913–931, 2019.

[28] S. Nadeem, R. Haq, and C. Lee, "MHD flow of a Casson fluid over an exponentially shrinking sheet," *Scientia Iranica*, vol. 19, no. 6, pp. 1550–1553, 2012.

[29] A. Lare, "Casson fluid flow with variable viscosity and thermal conductivity along exponentially stretching sheet embedded in a thermally stratified medium with exponentially heat generation," *Journal of Heat and Mass Transfer Research*, vol. 2, no. 2, pp. 63–78, 2015.

[30] H. Amlimohamadi, M. Akram, and K. Sadeghy, "Flow of a Casson fluid through a locally-constricted porous channel: a numerical study," *Korea-Australia Rheology Journal*, vol. 28, pp. 129–137, 2016.

[31] N. Vellanki, K. Hemalatha, and G. V. R. Reddy, "Radiation and chemical reaction effects on MHD Casson fluid flow of a porous medium with suction/injection," *International Journal of Mechanical Engineering and Technology (IJMET)*, vol. 2, no. 11, pp. 99–116, 2020.

[32] A. Ali, A. Fatima, Z. Bukhari, H. Farooq, and Z. Abbas, "Non-newtonian Casson pulsatile fluid flow influenced by Lorentz force in a porous channel with multiple constrictions: A numerical study," *Korea-Australia Rheology Journal*, vol. 33, pp. 79–90, 2021.

[33] S. Reddy, P. Valsamy, and D. Reddy, "Numerical solutions of Casson-nano fluid flow past an isothermal permeable stretching sheet: MHD, Thermal Radiation and Transpiration effects," *Journal of Nanofluids*, vol. 12, no. 6, pp. 1503–1511, 2023.

[34] A. Majeed, R. Mahmood, H. Shahzad, A. Pasha, Z. Raizah, H. Hosham, D. Reddy, and M. Hafeez, "Heat and mass transfer characteristics in MHD Casson fluid flow over a cylinder in a wavy channel: Higher-order FEM computations," *Case Studies in Thermal Engineering*, vol. 42, p. 102730, 2023.

[35] G. Buzuzi, "Unsteady MHD Casson fluid flow past an inclined surface subjected to variable magnetic field, Heat generation and effective Prandtl number.," *Engineering Letters*, vol. 31, no. 2, 2023.

[36] K. Rubab and M. Mustafa, "Cattaneo-Christov heat flux model for MHD three-dimensional flow of Maxwell fluid over a stretching sheet," *PLoS One*, vol. 11, no. 4, p. e0153481, 2016.

[37] T. Hayat, A. Aziz, T. Muhammad, and A. Alsaedi, "Three-dimensional flow of Prandtl fluid with Cattaneo-Christov double diffusion," *Results in Physics*, vol. 9, pp. 290–296, 2018.

[38] H. Upreti, S. Mishra, A. Pandey, and P. Bartwal, "Shape factor analysis in stagnation point flow of Casson nanofluid over a stretching/shrinking sheet using Cattaneo-Christov model," *Numerical Heat Transfer, Part B: Fundamentals*, pp. 1–17, 2023.

[39] B. Kala, "The numerical analysis of the effect of Grashof number, modified Grashof number and chemical reaction on the non-Darcy MHD flow of a Casson fluid over a nonlinearly stretching sheet in a porous medium," *International Journal of Scientific Research in Physics and Applied Sciences*, vol. 7, no. 3, pp. 49–70, 2019.

[40] B. Kala, M. Rawat, and A. Kumar, "Numerical analysis of the flow of a Casson fluid in magnetic field over an inclined nonlinearly stretching surface with velocity slip in a Forchheimer porous medium," *Asian Research Journal of Mathematics*, vol. 16, no. 7, pp. 34–58, 2020.

[41] R. W. Fox, A. McDonald, and P. Pitchard, "Introduction to Fluid Mechanics," 2006.

[42] R. Bansal, *A Textbook of Fluid Mechanics*. Firewall Media, 2005.

[43] J. N. Reddy and D. K. Gartling, *The Finite Element Methods in Heat Transfer and Fluid Dynamics*. CRC press, 2010.

[44] P. A. Davidson and A. Thess, *Magnetohydrodynamics*, vol. 418. Springer Science & Business Media, 2002.

[45] M. Gad-el Hak, *Advances in Fluid Mechanics Measurements*, vol. 45. Springer Science & Business Media, 2013.

[46] R. W. Lewis, P. Nithiarasu, and K. N. Seetharamu, *Fundamentals of the Finite Element Methods for Heat and Fluid Flow*. John Wiley & Sons, 2004.

[47] J. Kunes, *Dimensionless Physical Quantities in Science and Engineering*. Elsevier, 2012.